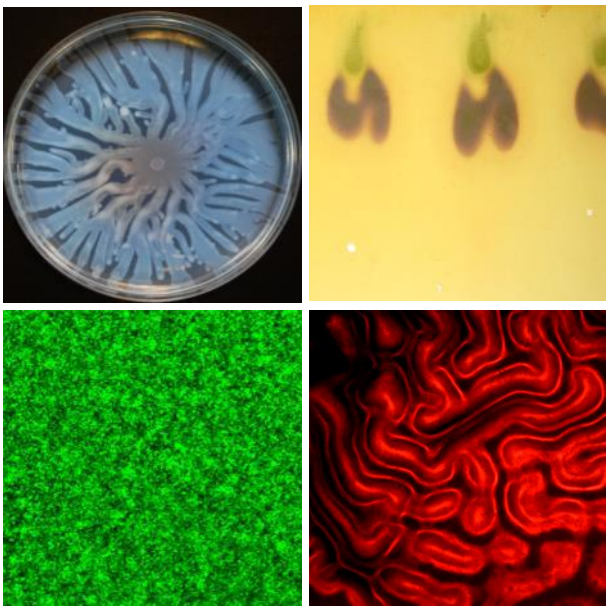
Linking fatty acid derivatives with signalling and cross-talk in *Pseudomonas aeruginosa*



Diana Palenzuela Bretones, MSc.

Thesis submitted to the University of Nottingham for the degree of Doctor of Philosophy

September 2016

DECLARATION

Unless otherwise acknowledged, the work presented in this thesis is my own. No part has been submitted for another degree at the University of Nottingham or any other institute of learning.

Diana Palenzuela, September 2016.

ABSTRACT

Xanthomonas campestris is a bacterial plant pathogen that produces diffusible signal factor (DSF), a signalling fatty acid mediating the regulation of important pathogenicity traits, such as protease production and biofilm formation. The production of DSF is dependent on the activity of an enoyl-CoA hydratase (ECH) enzyme. Chemically related long chain fatty acids, the DSF-type (DSF-T) molecules, have since been found to be produced by a large range of bacterial species including *Stenotrophomonas maltophilia* and *Burkholderia cenocepacia*, in which they have similar effects and are subject to a similar regulation. Interestingly, these molecules participate in inter-species signalling as well, as they can affect the behaviour of species that do not produce them.

Pseudomonas aeruginosa produces the DSF-T *cis*-2-decenoic acid (CDA), to disperse its biofilms and inhibit biofilm formation, but the extent of its effects, the regulatory network and the conditions leading to the production of this molecule are not yet understood. Whole transcriptome shotgun sequencing (RNA-seq) previously performed at The University of Nottingham on *P. aeruginosa* grown in the presence and absence of CDA was further analysed in **Chapter 3** to better understand the effects of this signalling molecule. The analysis of this transcriptomic approach and of other transcriptomic profiles performed with DSF-T molecules indicate that the effects of these signals are highly dependent on the conditions of growth. This chapter also investigates how non-cognate DSF-T affect the colonisation capacities of *P. aeruginosa.* It is of special interest that *X. campestris* DSF and *B. cenocepacia* BDSF limit the colonisation capacities of *P. aeruginosa* in *in vitro* experiments, which constitutes a starting point for future work on these communication networks in ecological settings.

Previous studies suggested that PA0744 and PA3426 encode enzymes which are involved in the metabolism of CDA, though further work was required in this direction. This line of work was continued in **Chapter 4** where it is shown that the regulation of CDA is especially complex and seems to involve other regulatory elements such as the intracellular second messenger cyclic diguanylate (c-di-GMP) and inter-cellular signalling by quorum sensing (QS). Although *P. aeruginosa* presents homologues of the sensor proteins and synthases of DSF-T, bioinformatic studies have not identified clear lead proteins that might perform these functions.

To get a broader view of small signalling molecules that affect the regulation of community behaviours, cultures of *P. aeruginosa* were treated with 2-tridecanone (2TDC) in **Chapter 5**. This molecule has been shown to affect biofilm formation and motility in *Sinorhizobium meliloti, Pseudomonas syringae* and *Salmonella enterica*, so the aim was to investigate what effects it might have in *P. aeruginosa.* Interestingly, this molecule inhibited the establishment of biofilms and swarming motility in *P. aeruginosa*. These two phenotypes are generally subjected to opposite regulations, thus 2TDC affects the behaviour of *P. aeruginosa* in a novel way.

In summary, various small molecules and their role in the regulation of colonisation mechanisms in *P. aeruginosa* were investigated in this study. Results give new perspectives to understand cell-to-cell communication in this bacterium and show that small molecules present overlapping yet distinct effects in the biology of *P. aeruginosa*, the knowledge of which could one day pave the way to new treatments against bacterial infections.

ACKNOWLEDGEMENTS

First and foremost, I would like to show my appreciation to my supervisors Miguel Cámara, Stephan Heeb and Paul Williams. This short experience in the world of research has been extremely challenging and intense, and I would have never been able to get this far without their valuable support. Miguel Cámara has mentored me throughout my thesis and has been pivotal with his enthusiasm and motivation, and he deserves an award for the fastest person to answer emails that I have ever encountered. Stephan Heeb has provided wonderful advice on molecular biology, and I have always enjoyed our discussions on cloning strategies. He has also given tips on nomenclature and IT which have been very useful for the completion of this thesis. Paul Williams has always been an approachable person, passing on his enthusiasm to all of us around him. I would also like to thank Nigel Halliday and Alex Truman for their help with analytical techniques and for providing me with DSF-T.

To my colleagues, I would like to thank you for making those long hours at work so much more enjoyable. Daniella, Chris, Manuel, Edu, I am glad to call you my friends and I hope this goes on far beyond the PhD life. It has been fantastic to meet you all and have an opportunity to work side by side with you. Special thanks go to Manuel for his handy tips on anything to do with laboratory work, and to Edu for his positive outlook on life (and his random playlists). Lorna, this last years would not have been the same without your house as the social hub! Chris, you have been the most unexpected gain out of this, who would have guessed we would meet again in such different circumstances. And to all those in the *Pseudomonas* group, a big thanks for always being there!

To the ladies back home, you have helped me get perspective on the important things in life. Madrid, Barcelona, Granada and Ibiza acquire special meanings to me knowing that you are there. To the Biotecs, everything started with your wanderlust, you are at the very origin of this journey.

To my orange man, whom I hope will proofread my English and will accompany me in this "scrumbly" journey for years to come.

And of course to my ever caring parents, who have supported every decision and brightened every dull moment.

This is to all of you.

TABLE OF CONTENTS

Declaration 1

Abstract 2

Acknowledgements 4

Table of contents 5

List of figures 10

List of tables 15

Abbreviations 18

1 Introduction 22

1.1 *Pseudomonas aeruginosa* overview 22

1.2 Relevance of studying *P. aeruginosa* 22

1.2.1 *P. aeruginosa* as a pathogen 22

1.2.2 *P. aeruginosa* as a biocontrol agent 24

1.2.3 *P. aeruginosa* in industry 25

1.3 Colonisation mechanisms 25

1.3.1 Motility 26

1.3.2 Biofilm 29

1.3.3 Pyocyanin and phenazines 32

1.3.4 Siderophores 33

1.3.5 Rhamnolipids 34

1.3.6 Proteases 36

1.3.7 Other colonisation factors 37

1.4 Global regulatory networks 38

1.4.1 Cyclic diguanylate (c-di-GMP) 38

1.4.2 cAMP and Vfr 39

1.4.3 Quorum sensing 39

1.4.4 Two-component systems and the Gac/Rsm pathway 45

1.5 2-Tridecanone as a bacterial signal molecule 47

1.6 Project overview and aims 48

2 Experimental procedures 50

2.1 Bacterial cell manipulation 50

2.1.1 Media and antibiotic concentrations 50

2.1.2 Culture growth 51
2.1.3 Bacterial storage 52
2.2 General chemicals 52
2.3 DNA manipulation 52
2.3.1 Strains and plasmids 52
2.3.2 Molecular procedures 55
2.3.3 Construction of biosensors 56
2.3.4 Microtiter plate assay 56
2.3.5 Reporter gene expression of strains grown on agar plates 57
2.3.6 Construction of deletion mutants and their complementation 57
2.4 Deep Sequencing analysis 60
2.4.1 Previous work 60
2.4.2 Representation of results and criteria 61
2.4.3 Functional database 61
2.5 Phenotypical assays 64
2.5.1 Growth assays 64
2.5.2 Addition of 2TDC to agar plates 65
2.5.3 Motility 65
2.5.4 Proteases 66
2.5.5 Biofilm formation 68
2.5.6 Production of secreted factors in semi-solid medium 69
2.5.7 Pyocyanin 70
2.5.8 Pyoverdine 70
2.6 Chemistry work 70
2.6.1 Chemical structures 70
2.6.2 Sample preparation 70
2.6.3 Solvent extraction 71
2.6.4 Thin layer chromatography 71
2.6.5 Detection of Rhamnolipids and HAAs by LCMS 72
2.7 Microscopy 73
2.7.1 Confocal laser scanning microscopy (CLSM) 73
2.7.2 Transmission electron microscopy (TEM) 73
2.7.3 Optical microscopy 74
2.8 Bioinformatics/structure determination 74
2.8.1 Prediction of domain organisation 74

2.8.2 Alignment of primary and secondary structures 74
2.8.3 Prediction of tertiary structures 75
2.8.4 Alignment of tertiary structures 75
2.9 Results analysis 75
2.9.1 Pixel integration analysis 75
2.9.2 Analysis of biofilms 75
2.9.3 Statistical analysis 76
3 Impact of diffusible signal factor-type molecules On the biology of *P. aeruginosa* 77
3.1 Introduction 77
3.1.1 Discovery and production of DSF-T molecules 77
3.1.2 Native production and metabolism of DSF-T 77
3.1.3 Impact of DSF-T in bacterial biology 78
3.1.4 Exploitation of DSF networks in infection 82
3.1.5 Aims of the chapter 83
3.2 Results 84
3.2.1 Whole transcriptome analysis 84
3.2.2 Comparison with Rahmani-Badi's microarray 90
3.2.3 Impact of DSF-T on *P. aeruginosa* growth 92
3.2.4 Effect of CDA on biofilm formation in *P. aeruginosa* 93
3.2.5 C-di-GMP 98
3.2.6 Motility 101
3.2.7 Analysis of rhamnolipid production 106
3.2.8 Proteases 111
3.2.9 Sensing of CDA 114
3.3 Discussion 116
3.3.1 General comparison on the effects of various DSF-T in PAO1 122
3.4 Conclusion and future directions 125
4 Enoyl-CoA hydratases and the biology of *P. aeruginosa* 126
4.1 Introduction 126
4.1.1 The *rpf* cluster 126
4.1.2 DSF-T in *P. aeruginosa* 130
4.1.3 Aims of the chapter 133
4.2 Results 134
4.2.1 *In silico* characterisation of ECH in *P. aeruginosa* 134

4.2.2 *In silico* characterisation of RpfC and RpfR homologues of *P. aeruginosa* 139
4.2.3 Phenotypical characterisation of PAO1 Enoyl-CoA Hydratases 143
4.3 Discussion 164
4.3.1 Bioinformatic analysis of enoyl-CoA hydratases in *P. aeruginosa* 164
4.3.2 Biological role of PA0744 and PA0745 in *P. aeruginosa* 167
4.3.3 Biological function and regulation of CbsA 171
4.3.4 Link between enoyl-CoA hydratases and CDA 172
4.4 Conclusion and future directions 175
5 2-tridecanone as a signalling molecule in *P. aeruginosa* PAO1 177
5.1 Introduction 177
5.1.1 2TDC synthesis and function 177
5.1.2 *P. aeruginosa* and environments with 2TDC 178
5.1.3 2TDC in bacteria 178
5.1.4 Aims of the chapter 179
5.2 Results 180
5.2.1 Impact of 2TDC on growth of *P. aeruginosa* 180
5.2.2 Impact of 2TDC on motility in *P. aeruginosa* 181
5.2.3 Impact of 2TDC on biofilms in *P. aeruginosa* 185
5.2.4 Impact of 2TDC on Rhamnolipids 193
5.2.5 Impact of 2TDC on pyoverdine production 195
5.2.6 Impact of 2TDC on *P. aeruginosa* regulatory pathways 197
5.3 Discussion 205
5.3.1 Impact of 2TDC on key switches of multiple gene expression 208
5.3.2 Possible conserved targets for 2TDC 210
5.4 Conclusion and future directions 212
6 General conclusion and future directions 214
7 Appendix 220
7.1 Additional general information 220
7.1.1 Functional database 220
7.1.2 Rationale for the assays in agar plates 225
7.1.3 Determination of rhamnolipids by thin layer chromatography 226
7.2 Additional information on Chapter 3 227
7.2.1 Summary of RNA-seq data with and without CDA 227

7.2.2 Biofilm disruption in M9-glucose 227
7.2.3 Detection of rhamnolipids by LC-MS/MS 228
7.2.4 Phenotypical characterisation of PA4982 229
7.3 Additional information on Chapter 4 230
7.3.1 Analysis of RNA-seq data CbsA 230
7.3.2 Interaction of PA0744 and PA0745 231
7.3.3 Pyoverdine in PA0744 and PA0745 mutants 233
7.3.4 IPTG does not affect rhamnolipid expression 234
7.4 Additional information on Chapter 5 234
7.4.1 Impact of 2TDC in *P. aeruginosa* chemotaxis 234
7.4.2 Determination of pyoverdine production from plates 235
7.4.3 Determination of pyocyanin from agar plates 235
7.4.4 Determination of AQ in *P. aeruginosa* cultures grown on agar plates 236
Bibliography 237

LIST OF FIGURES

Figure 1.1. Structure and regulation of the flagellum and type 4a pili (T4aP) in *P. aeruginosa.* 28
Figure 1.2. Factors affecting biofilm development stages in *P. aeruginosa*..... 31
Figure 1.3. Rhamnolipid biosynthesis in *P. aeruginosa.* 35
Figure 1.4. Phosphorelay systems in *P. aeruginosa.* 46
Figure 1.5. Gac/Rsm regulatory network in *P. aeruginosa.* 47
Figure 2.1. Schematic of the mutations introduced in the non-polar mutant for PA0745, 0745* 59
Figure 2.2. Reaction of rhamnose with orcinol during the detection of rhamnolipids following thin layer chromatography. 71
Figure 3.1. Differentially expressed genes in PAO1-L grown in the presence and absence of 100 μM CDA. 84
Figure 3.2. Volcano plot of genes differentially expressed in the RNA-seq of PAO1-L, in the absence and presence of 100 μM CDA..... 85
Figure 3.3. Functional annotation of genes differentially regulated in PAO1-L upon addition of MetOH control vs 100 μM CDA..... 86
Figure 3.4. Functional annotation of genes differentially regulated in PAO1-L grown upon addition of MetOH control vs 100 μM CDA. 89
Figure 3.5. Effect of DSF-T molecules in the growth of *P. aeruginosa* PAO1-L. .. 92
Figure 3.6. Attachment assay of *P. aeruginosa* PAO1-L in the presence and absence of 10 μM CDA. 93
Figure 3.7. Biofilm formation of PAO1-L tagged with GFP (PADP44), in the presence and absence of 10 μM CDA, in chamber slides. 94
Figure 3.8. Biofilm formation of PAO1-L tagged with GFP (PADP44) in the presence and absence of 10 μM CDA, at 30 ºC. 95
Figure 3.9. Biofilm formation of UCBPP-PA14 tagged with GFP (PADP326) in the presence and absence of 10 μM CDA, at 37 ºC. 95
Figure 3.10. Impact of CDA on the biofilm disruption of *P. aeruginosa* PAO1-L. 96
Figure 3.11. Effect of CDA on colony morphotypes. 97
Figure 3.12. Impact of DSF-T on c-di-GMP. 99
Figure 3.13. Impact of CDA on the expression of c-di-GMP regulators in PAO1. 100
Figure 3.14. Impact of DSF-T molecules on *P. aeruginosa* PAO1-L swimming motility. 102
Figure 3.15. Impact of DSF on *P. aeruginosa* PAO1-L swimming motility in a range of growth media. 103

Figure 3.16. Visualisation of PAO1-L swarmer cells with transmission electron microscopy (TEM), in the presence and absence of CDA 100 µM. 104
Figure 3.17. Impact of DSF-T on the swarming motility of PAO1-L. 105
Figure 3.18. Impact of DSF-T on the twitching motility of PAO1. 106
Figure 3.19. Impact of CDA on rhamnolipid expression. 107
Figure 3.20. Impact of CDA on rhamnolipid production in *P. aeruginosa* PAO1-L grown in liquid. 108
Figure 3.21. Impact of CDA on the rhamnolipid production of *P. aeruginosa* PAO1-L grown in swarming plates. 109
Figure 3.22. Rhamnolipid production of PAO1-L in the presence of 100 µM DSF. 110
Figure 3.23. Impact of CDA on rhamnolipid and HAAs production in PAO1-L, as determined by LC-MS/MS. 111
Figure 3.24. Impact of CDA on the proteolytic activity of PAO1-L. 112
Figure 3.25. Impact of DSF on proteases of PAO1-L. 113
Figure 3.26. Impact of BDSF on the proteolytic activity of PAO1-L. 114
Figure 4.1. Gene organisation of the *rpf* cluster in xanthomonads. 126
Figure 4.2. Crystal structure of $RpfF_{Xcc}$, as determined by Cheng et al. [405] . 127
Figure 4.3. Two broad mechanisms for DSF-T sensing and transduction. 128
Figure 4.4. Domain organisation of DSF-T receptors. 132
Figure 4.5. Two possible genomic contexts of CDA synthases in *P. aeruginosa.* 132
Figure 4.6. Growth of ECH mutants in various media. 144
Figure 4.7. Swarming motility of mutants for PA0745 (PADP135), PA0744 (PASC815), and the double mutant Δ0744 Δ0745 (PADP14). 145
Figure 4.8. Pyocyanin production of mutants of PA0744 and PA0745. 146
Figure 4.9. Effect of polar and non-polar mutation of PA0745 on the swarming motility of PAO1-L. 147
Figure 4.10. Effect of polar and non-polar mutations of PA0745 on the pyocyanin production of PAO1-L. 148
Figure 4.11. Effect of PA0744 and PA0745 expression in the double mutant PADP14, on the swarming motility of PAO1-L. 149
Figure 4.12. Effect of PA0744 and PA0745 expression in the double mutant PADP14 on pyocyanin production of PAO1-L. 149
Figure 4.13. Effect of PA0744 and PA0745 expression in the double mutant PADP14 on biofilm formation of PAO1-L. 150
Figure 4.14. Swarming of PADP14 (Δ0744 Δ0745) in the presence and absence of CDA and the expression of PA0744 and PA0745, in PAO1-L. 151

Figure 4.15. Biofilm formation of PADP14 (Δ0744 Δ0745) with and without CDA and the expression of PA0744 and PA0745, in PAO1-L. 152
Figure 4.16. Number of differentially expressed genes from the RNA-seq results of the conditional mutant for CbsA PASC315 without IPTG (mutant) compared to the wild-type PAO1. 153
Figure 4.17. Functional annotation of genes differentially regulated in PASC315 versus PAO1 from the Baggerly's test. 154
Figure 4.18. Functional annotation of genes differentially regulated in PASC315 versus PAO1 from the DESeq test. 155
Figure 4.19. Impact of the conditional mutation for CbsA (from PASC315) in LB. 156
Figure 4.20. Growth of PAO1 and PASC315 (conditional mutant for CbsA) in NB, with and without IPTG 1 mM. 157
Figure 4.21. Effect of CbsA expression on the motility of PAO1. 158
Figure 4.22. Effect of the expression of CbsA from the conditional mutant PASC315 on rhamnolipid production, in liquid cultures. 159
Figure 4.23. Effect of the expression of CbsA from the conditional mutant PASC315 on rhamnolipid production, in agar plates. 160
Figure 4.24. Effect of the conditional mutation of CbsA from PASC315 on protease secretion. 161
Figure 4.25. Effect of the expression of CbsA from the conditional mutant tagged with GFP (PADP305) as compared to the PAO1-L tagged with GFP (PADP44) on biofilm formation, in LB. 162
Figure 4.26. Biofilm formation of PADP305 (conditional CbsA, GFP) with and without CDA. 162
Figure 4.27. Analysis of possible interactions between the ECH PA0744 and PA0745, according to experimental data. 169
Figure 5.1. Impact of 2TDC on *P. aeruginosa* growth in liquid cultures. 180
Figure 5.2. Effect of 2TDC on PAO1-L growth in NB (A) and CAA (B). 181
Figure 5.3. Impact of 2TDC on PAO1-L swimming. 182
Figure 5.4. Visualisation of PAO1-L swarmer cells with transmission electron microscopy (TEM), in the presence and absence of 2TDC. 183
Figure 5.5. Swarming of PAO1-L in presence of various concentrations of 2TDC. 184
Figure 5.6. Impact of 2TDC on PAO1-L twitching in LB plates. 185
Figure 5.7. Effect of 2TDC on biofilm development under static conditions (A) and controlled flow conditions (B), and detail of growth in flow conditions (C). 187
Figure 5.8. Effect of 2TDC on colony morphotypes. 188

Figure 5.9. Effect of 2TDC on biofilm disruption using the chamber slides in LB. 189
Figure 5.10. Effect of 2TDC on biofilm disruption using the chamber slides in NB. 190
Figure 5.11. Evidence of physical disruption as a result of pipetting in chamber biofilms. 190
Figure 5.12. Effect of 2TDC on c-di-GMP levels using the P_{cdrA}-*gfp* fusion (pCdrA::*gfp*^{c}). 191
Figure 5.13. Effect of 2TDC on the expression from pSC855 (*pelA)* and pSC856 (*pslA*) translational fusions on agar plates. 192
Figure 5.14. TLC analysis of rhamnolipids production from liquid cultures in the presence of 2TDC. 194
Figure 5.15. TLC analysis of rhamnolipids production from cells grown on NB agar in the presence of 2TDC. 195
Figure 5.16. Effect of 2TDC on pyoverdine production in ion-depleted liquid media. 196
Figure 5.17. Impact of 2TDC on the pyoverdine production of PAO1-L in CAA plates. 197
Figure 5.18. Effect of 2TDC on the expression of the small RNAs RsmY and RsmZ. 198
Figure 5.19. Swarming of mutants for RsmY and RsmZ in the presence of 2TDC. 199
Figure 5.20. Effect of 2TDC on swarming in Δ*htpB* and Δ*gacA* mutants..... 200
Figure 5.21. Impact of 2TDC on the expression of quorum sensing regulatory genes..... 201
Figure 5.22. 2TDC does not affect the production of PQS or HHQ in NB plates. 202
Figure 5.23. Expression of transcriptional reporters pA2DA1L and pA1DA2L in the presence of 2TDC. 203
Figure 5.24. 2TDC does not impact pyocyanin production by swarmer cells.... 204
Figure 7.1. Impact on bacterial growth in motility plates. *P. aeruginosa* 225
Figure 7.2. Proof of concept for the determination of rhamnolipids by thin layer chromatography (TLC). 226
Figure 7.3. Impact of CDA in the dispersion of biofilms of *P. aeruginosa* PAO1-L, in M9 supplemented with glucose. 227
Figure 7.4. Detection of mono- and di-rhamnolipids, and HAAs by LC-MS/MS. 228
Figure 7.5. Chromatograms of standards for the rhamnolipid detection by LC-MS/MS. 228

Figure 7.6. Swarming and twitching motilities of PADP127 (Δ4982) as compared to PAO1-L. 229
Figure 7.7. Biofilm formation of PADP127 (Δ4982) as compared to PAO1-L. ... 229
Figure 7.8. Occurrence of PA0744 and PA0745 in genomes, as seen by the String database (consulted 10th May 2016). 231
Figure 7.9. Pyoverdine production from selected enoyl-CoA hydratase (ECH) mutants. 233
Figure 7.10. Impact of IPTG on the rhamnolipid production of PAO1. 234
Figure 7.11. Chemotaxis assay of *P. aeruginosa* PAO1-L in the absence and presence of 2TDC. 235
Figure 7.12. Determination of pyoverdine production on agar plates. 235
Figure 7.13. Determination of pyocyanin production on agar plates. 236
Figure 7.14. Determination of PQS and HHQ from *P. aeruginosa* grown on agar plates. 236

LIST OF TABLES

Table 1.1. Features of acute and chronic infections of *P. aeruginosa.* 23
Table 1.2. Structure and properties of diffusible signal factor-type (DSF-T) molecules. 43
Table 1.3. General features of the 2-tridecanone. 47
Table 2.1. Strains and plasmids used in this study. 52
Table 2.2. Primers used for reporter construction. 56
Table 2.3. Primer sequences to screen the in-frame deletion mutants in two-component systems. 58
Table 2.4. Primers used to construct enoyl-CoA hydratase deletion mutants. ... 59
Table 2.5. Primers used to construct the complementing plasmid pME6032::0745-0744. 60
Table 2.6. Functional categories present in the COG database. 62
Table 2.7. Functional categories from the COG database assigned according to listed functions in the *Pseudomonas* Genome Database. 62
Table 2.8. Additional categories created in the functional annotation database to respond to particular interests of this project. 63
Table 2.9. Hierarchy of COG categories. 63
Table 2.10. Molecular ions detected by LC-MS/MS for the quantification of rhamnolipids and rhamnolipid precursors produced by *P. aeruginosa* PAO1-L. .. 73
Table 3.1. Selected genes identified from the RNA-seq results of PAO1-L grown in the presence and absence of 100 µM CDA (i). 88
Table 3.2. Selected genes identified from the RNA-seq results of PAO1-L grown in the presence and absence of 100 µM CDA (ii). 89
Table 3.3. Selected genes from the microarray performed by Rahmani-Badi et al. 90
Table 3.4. Enzymes involved in the synthesis of c-di-GMP that were differentially expressed by CDA in the RNA-seq analysis. 98
Table 3.5. Impact of CDA on the expression of flagellum-associated genes. ... 101
Table 3.6. Expression of rod-shape genes in the presence and absence of CDA. 102
Table 3.7. Impact of CDA on the expression of rhamnolipid synthases. 107
Table 3.8. Selected genes for the screening of sensor kinases for CDA. 115
Table 3.9. Conditions used for the RNA-seq experiment and the microarray study that investigate the CDA regulon. 117
Table 4.1. Identity percentages of the BLASTP alignments between ECH of *P. aeruginosa* and RpfF proteins. 134

Table 4.2. Location of important catalytic residues as shown in [403, 405]in proteins annotated as ECH/Isomerase, in PAO1. 136
Table 4.3. Location of conserved residues within secondary structures in proteins annotated as ECH/Isomerase, in PAO1. 137
Table 4.4. Root mean square deviation (RMSD) numbers of RpfF proteins from *Xanthomonas* and *Burkholderia* aligned to ECH/Isomerases of PAO1. 138
Table 4.5. Top 10 hits of proteins from PAO1 found by BLASTP against RpfC from *Xcc*. 139
Table 4.6. Top 10 hits of the BLASTP with RpfR from *B. cenocepacia* H111. ... 140
Table 4.7. Domain organisation of BLASTP hits of RpfC against the PAO1 proteome. 141
Table 4.8. Candidate homologues to RpfC in PAO1, presenting the same domain organisation but lacking Hpt domains. 142
Table 4.9. Domain organisation of BLASTP hits of RpfR against the PAO1 proteome. 142
Table 4.10. Domain organisation of proteins of PAO1 presenting the same domains as RpfR. 143
Table 4.11. Summary of results from bioinformatic analysis of the described CDA synthases in *P. aeruginosa*. 165
Table 4.12. Summary of results with several combinations of PA0744 and PA0745 expression in PAO1. 170
Table 7.1. List of the genes assigned the additional category "o: Biofilm extracellular polymeric substances, formation and regulation". 220
Table 7.2. Genes assigned with the additional category "i: Two-component systems, probable two-component systems and Hpt proteins". 221
Table 7.3. Genes encoding small RNAs that were assigned the additional "%: Regulatory RNAs" category. 222
Table 7.4. Genes involved in T3SS in *P. aeruginosa* that were assigned category "U: Intracellular trafficking, secretion and vesicular transport" 222
Table 7.5. Genes involved in *P. aeruginosa* motility that were assigned category "N: cell motility". 222
Table 7.6. Genes containing GGDEF, EAL or HD-GYP motifs, which were assigned the additional category "a: c-di-GMP regulation". 223
Table 7.7. Genes which were not included in the functional annotation database. 224
Table 7.8. Overview of the number of genes differentially expressed according to two statistical tests, in the presence and absence of 100 μM CDA. 227

Table 7.9. Overview of the number of genes differentially expressed in the RNA-seq of CbsA. 230
Table 7.10. Gene expression profiles of various enoyl-CoA hydratases relevant to this thesis..... 232

ABBREVIATIONS

ºC	Degrees Celsius
2CS	Two-component system
2TDC	2-tridecanone
3OC12-HSL	*N*-(3-oxododecanoyl)-L-homoserine lactone
AHL	*N*-acyl-L-homoserine lactone
Ap	Ampicillin
AUC	Area under the curve
AQ	2-alkyl-4-quinolones
BDSF	*Burkholderia* diffusible signal factor
bp	Base pair
C4-HSL	*N*-butanoyl-L-homoserine lactone
CAA	Casamino acids-derived medium
Cb	Carbenicillin
CDA	*Cis*-2-decenoic acid
c-di-GMP	Cyclic diguanylate, formally bis-(3´-5´)-cyclic dimeric guanosine monophosphate
CF	Cystic fibrosis
cfu	Colony forming units
CLSM	Confocal laser scanning microscopy
Cm	Chloramphenicol
CRP	cAMP regulator protein
DCM	Dichloromethane
di-rhm	Di-rhamnolipids
DMSO	Dimethyl sulfoxide
DNA	Deoxyribonucleic acid
DSF	Diffusible signal factor
DSF-T	Diffusible signal factor-type
dyn	Dyne
ECH	Enoyl-CoA hydratase
eDNA	Extracellular DNA
EPS	Extracellular polymeric substances
EtOAc	Ethyl acetate

EtOH	Ethanol
f	Form
FDR	False discovery rate
g	Grams
GFP	Green fluorescent protein
Gm	Gentamicin
h	Hour
HAA	3-(3-hydroxyalkanoyloxy)alkanoate(s)
HAMP	Histidine kinases, adenylyl cyclases, methyl binding proteins, phosphatases domain
HATPase	Histidine kinase-like ATPase
HHQ	2-heptyl-4-quinolone
HK	Histidine kinase
Hpt	Histidine phosphotransfer
IPTG	Isopropyl-1-thio-(β-D-galactopyranoside)
ITC	Isothermal titration calorimetry
kb	Kilobase
Km	Kanamycin
kV	Kilovolts
LB	Lysogeny broth
LC-MS/MS	Liquid chromatography-tandem mass spectrometry
Mbp	Mega base pair
MetOH	Methanol
min	Minute
mL	Millilitre
mM	Millimolar concentration
mono-rhm	Mono-rhamnolipids
MOPS	3-(*N*-morpholino)propanesulfonic acid
MRM	Multiple reaction monitoring
MS	Mass spectrometer
Nal	Nalidixic acid
NB	Nutrient Broth medium
nm	Nanometre
OD	Optical density
ORF	Open reading frame

PAS	Per/Arnt/Sim domain
PAC	C-terminal to Per/Arnt/Sim domain
PCR	Polymerase chain reaction
PDB	Protein Data Bank
PHA	Polyhydroxyalkanoates
PIA	*Pseudomonas* isolation agar
PQS	*Pseudomonas* quinolone signal, 2-heptyl-3-hydroxy-4-quinolone
psi	Pounds per square inch
PTM	Post-translational modifications
pv	Pathovar
QS	Quorum sensing
QSSM	Quorum sensing signal molecules
Rf	Retention factor
REC	Receiver domain
RFU	Relative fluorescent units
rhm	Rhamnolipid
RLU	Relative luminescent units
RMSD	Root mean square deviation
RNA	Ribonucleic acid
RPKM	Reads per kilobase per million mapped reads
rpm	Revolutions per minute
RR	Response regulator
s	Second
SCV	Small colony variant
SK	Sensor kinase
Sm	Streptomycin
sv	Serovar
T1SS	Type 1 secretion system
T2SS	Type 2 secretion system
T3SS	Type 3 secretion system
T4aP	Type 4 a pillus/pili
T4P	Type 4 pillus/pili
T5SS	Type 5 secretion system
T6SS	Type 6 secretion system

Tc	Tetracycline
TDA	*Trans*-2-decenoic acid
TEM	Transmission electron microscopy
TLC	Thin layer chromatography
TLCK	*N*-α-tosyl-L-lysine chlotomethyl ketone hidrochloride
Tris-HCl	2-amino-2-hydroxymethyl-propane-1,3-diol
v/v	Volume per volume
w/v	Weight per volume
Xcc	*Xanthomonas campestris* pathovar *campestris*
µg	Microgram
µL	Microliter
µM	Micromolar concentration

1 INTRODUCTION

1.1 *Pseudomonas aeruginosa* overview

Pseudomonas aeruginosa is an ubiquitous Gram-negative rod-shaped bacterium, classified in the phylum Proteobacteria as a γ-proteobacterium. It presents a monotrichous flagellum. Generally, *P. aeruginosa* forms flat, transparent colonies on agar plates. It is able to grow in temperatures ranging from 5.5 to 45 ºC, with the majority of isolates growing in the range of 25-41 ºC, and at a pH 4-9. It is generally classified as aerobic, although it can survive under hypoxic conditions [1]; and it is non-fermentative, catalase positive and oxidase positive [2]. It can be identified for the production of the blue-green pigment pyocyanin, although other biochemical tests exist for the identification of apyocyanogenic isolates [3].

The pangenome of *P. aeruginosa* comprises nearly fourteen thousand genes [4]. From these, only a small subset represents the core genome of this bacterium, that is, the part of the genome shared by all isolates, and has been estimated to comprise between 4000 and 5316 ORFs. The rest of the genes, namely the accessory genome, represents between a 7 % and a 20 % of the total, which accounts for approximately 10000 genes. The genome size of this bacterium ranges between 6.26 and 7.4 Mbp [4-6].

8.4 % of genes in *P. aeruginosa* is involved in regulatory functions, which represents a much higher percentage than in other bacterial species, including 5.8 % in *E. coli* and 5.3 % in *B. subtilis* [7, 8]. This arsenal of adaptive mechanisms allows *P. aeruginosa* to colonise a large range of environmental niches.

1.2 Relevance of studying *P. aeruginosa*

1.2.1 *P. aeruginosa* as a pathogen

P. aeruginosa invades a vast range of hosts. It causes infections in various plant species, protozoa [9], and animals. Mammals affected by *P. aeruginosa* infections include dogs, bovines and small ruminants [10], and non-mammals comprise *Drosophila sp.* [11] and *Caernorhabditis elegans* [12], amongst others.

Perhaps one of the most studied colonisation sites of *P. aeruginosa* is the human body, where this bacterium is carried by healthy individuals in stool, urine, axilla and skin [13]. In humans, carriage of *P. aeruginosa* does not cause health issues

unless an underlying immunosuppression exists [14]. However, when the immune barriers are weakened or broken, this bacterium becomes a great hazard, causing both acute and chronic infections (**Table 1.1**). Community-acquired *P. aeruginosa* is rare, but it is found in cases of extreme immune suppression and, in some cases, even in healthy infants [15]. Because it can colonise an immunocompromised human host, *P. aeruginosa* is generally considered an opportunistic pathogen [16]. In fact, it is a prevalent cause of infections, and it is acquired by a large percentage of patients during their stay in the hospital. In an epidemiological study in France, 26 % of patients became colonised in the course of 8 months in the intensive care unit (ICU) [17]. Although the main cause of nosocomial infection is endogenous, various *P. aeruginosa* sources has been found in hospitals, such as water pipes, disinfectants, and even cosmetics [13, 18].

Table 1.1. Features of acute and chronic infections of *P. aeruginosa.* Acute and chronic infections are characterised by a vastly different expression of virulent determinants and a change in *P. aeruginosa* lifestyle. *P. aeruginosa* isolates presenting acute phenotypes are able to colonise new niches, where they sometimes establish a chronic infection. UTI, urinary tract infection; T4aP, type 4a pili; SCV, small colony variant; LPS, lypopolysaccharide; T#SS, Type # secretion system; QS, quorum sensing.

	Acute infection *short term, severe, extensive tissue damage*	**Chronic infection** *long term, refractory to treatment*	**References**
Lifestyle	planktonic, motile	sessile, biofilm-forming	[19, 20]
Infections caused	UTI, pneumonia, soft tissue infections (wound infections, ulcerative keratitis), bone and joint infections, bacteraemia and other systemic infections	UTI pneumonia chronic wounds	[16, 21, 22]
Iron uptake mechanism	pyoverdines	from haem groups	[23]
Bacterial factors	flagella, T4aP, proteases, pyocyanin, exotoxin A, phospholipase C, haemolysin	extracellular polysaccharides including alginate, SCV, higher levels of antibiotic resistance, modification of LPS and peptidoglycan	[16, 20, 24, 25]
Secretion systems	T1SS, T2SS, T3SS	T6SS	[26]
Key regulatory factors	QS, RsmA, Vfr	QS, c-di-GMP, GacSA, RsmY, RsmZ	[27, 28]

The establishment of a chronic infection by *P. aeruginosa* is virtually impossible to eradicate, due to the high intrinsic resistance of this bacterium to antibiotics [28, 29] and to the formation of biofilms that protect bacterial cells from antimicrobials and the immune system [30-32]. One of the best known chronic establishments caused by *P. aeruginosa* occurs in cystic fibrosis (CF) patients. Mechanical barriers play a crucial role in the defence against *P. aeruginosa,*

especially the mucociliary layer of the respiratory tract, which is impaired in CF and hence unable to physically remove pathogenic bacteria colonising the lung. Another key factor is the establishment of a neutrophil-mediated response against this opportunistic pathogen, which eventually promotes a chronic inflammation that destroys the lung architecture, contributing to bronchiectasis and respiratory failure [33]. In addition, CF patients often display a switch from a Th1 to a Th2-type response and the production of non-protective antibodies [25].

It has been proposed that the disease-causing strategies used by *P. aeruginosa* in both plants and humans share the same molecular basis [34]. In fact, a study in 2000 found that exotoxin A (ToxA), phospholipase C (PlcS) and the global transcriptional regulator GacA contributed to virulence in models of both *A. thaliana* and mice [35]. It is therefore important to study the colonisation of *P. aeruginosa* in an integrated way, accounting for the variety of settings in which this bacterium can establish itself in hosts.

Regarding the colonisation of plants, *P. aeruginosa* can establish itself in a vast range of hosts; including lettuce and *Arabidopsis* leaves [36], roots of *Arabidopsis* and sweet basil [37] and the rhizosphere of wheat and tomato, amongst others [38].

1.2.2 *P. aeruginosa* as a biocontrol agent

Infection by *P. aeruginosa* can be beneficial to plants, as it inhibits the growth of fungal pathogens and induces resistance mechanisms from the plant host [39, 40]. It is interesting to note that both the siderophore pyochelin and the redox-active pyocyanin, considered virulence factors produced by this bacterium when it colonises the human host, were important for the tomato plant defence against the fungal pathogen *Botrytis cinerea* [40]. Mechanisms induced by *P. aeruginosa* which are beneficial to plants also include the production of indole-3-acetic acid, nitrogen fixation and phosphate solubilisation [41] and the production of salicylic acid [42]. Siderophore secretion by bacterial strains is also beneficial to plants in the sense that these molecules scavenge iron, thus inhibiting fungal growth. Together with other beneficial factors, various strains of *P. aeruginosa* have shown to favour the growth of plants in pot studies, namely by an increase of dry weight, root length, germination, etc. [39, 43].

1.2.3 *P. aeruginosa* in industry

P. aeruginosa presents multiple industrial applications. The enormous metabolic potential of this bacterium is used in bioremediation to detoxify areas from heavy metals [44-46], hydrocarbons [47], and aromatic compounds [48, 49].

Furthermore, products from *P. aeruginosa* also present important industrial applications. Pyocyanin has been used in microbial fuel cells, for its role as an electron shuttle [50]. Polyhydroxyalkanoates (PHA) are used as biodegradable plastics and in the pharmaceutical industry as drug delivery vectors. *P. aeruginosa* accumulates PHA during growth for energy storage, up to a 75 % of the total dry weight, making this bacterium an excellent PHA producer [51, 52]. Rhamnolipids represent biodegradable agents with emulsifying, stabilising and antimicrobial properties. Rhamnolipids from *P. aeruginosa* have been exploited for detergent, oil, pharmaceutical and food industries [53, 54]. Interestingly, *P. aeruginosa* can be used for the simultaneous production of PHAs and rhamnolipids, increasing the cost-efficiency of the process [55, 56]. Alginates constitute another product of interest. These polysaccharides are composed of guluronic and mannuronic acids. They are used in the pharmaceutical industry (for drug and vaccine delivery, to treat wounds) and food and drinks industry (for the gelling and viscosifying properties), amongst others. Currently nearly all alginates are extracted from seaweeds, but *P. aeruginosa* presents a potential source of these molecules [57, 58]. Enzymatic products from *P. aeruginosa* have also been used in industry, such as lipases for application in cosmetics and metalwork [59, 60] or proteases in the textile and waste treatment industry [61-63].

1.3 Colonisation mechanisms

The paradigm of every life form is to colonise a niche, develop and give progeny, or in other words, to find mechanisms to survive. A strategy employed by *P. aeruginosa* is to scavenge nutrients, often from sites where they are unavailable; compete with other organisms for those nutrients, and avoid or inhibit defence mechanisms from the hosts that it invades [64, 65].

The term "colonisation niche" may apply to the well-researched human host, but it also refers to the establishment in the rhizosphere or in water pipes. In this sense, virulence factors are a specific term that describes molecules or structures used to colonise a living host, but they are more generally regarded as colonisation factors when they facilitate the survival of *P. aeruginosa* under

limiting conditions or the establishment of communities in inorganic settings, for example water pipes.

1.3.1 Motility

Bacteria present various motility strategies that serve to find new niches to colonise, and allow for the establishment of biofilms (see **1.3.2**). A survey conducted in 1972 determined various types of bacterial motility [66]. From those, swimming, swarming, twitching and sliding have been described in *P. aeruginosa.* Additionally, a recent study has identified surfing as another type of translocation. The different strategies employed by *P. aeruginosa* to move in the milieu will be revised in this section.

P. aeruginosa generally presents a single polar flagellum that can rotate to help this bacterium move in liquid and low-density media. Swimming motility depends on the presence and functionality of the flagellum, which is formed of more than 20 proteins (see **Figure 1.1**). In addition to their role in motility, flagella can also mediate adherence to epithelial cells and mucin [67], and are important for the initial establishment of biofilms [68, 69]. The flagellum of *P. aeruginosa* is therefore associated with the virulence of this bacterium. Indeed, mutants for *fliC,* coding for the filament protein, did not present virulence in a murine model of pneumonia [24]. Flagella are tightly regulated to allow for changes in rotation and for the switch between planktonic and sessile lifestyles. In particular, the transcriptional regulator FleQ controls the expression of most of the structural genes of the flagella, and is in turn negatively regulated by FleN. FleSR constitute a two-component system (2CS) that controls the transcription of *flgBCDEFGHIJKL* and *fliK;* and FliA, a sigma factor repressed by the anti-sigma factor FlgM, regulates the expression of the chemotactic genes [67]. The Che chemotaxis system is used to control flagellar rotation and hence the swimming direction, which allows *P. aeruginosa* to get closer to attractants and away from repellents. In particular, CheY proteins control changes in the rotation of the flagellum through direct interaction with FliM, a structural protein present in the C-ring (**Figure 1.1**). *P. aeruginosa* PAO1 presents more than 20 *che* genes which control the response to various stimuli [70].

Swarming is a more complex form of motility used by *P. aeruginosa,* which also depends on the flagellum. In addition, swarming uses biosurfactants, and presents characteristic dendritic patterns in *P. aeruginosa* [71]. The role of type 4a pili (T4aP) in the swarming motility of *P. aeruginosa* has been controversial. While studies show the importance of T4aP for swarming motility [72], genes

involved in T4aP biosynthesis were not differentially regulated in microarray analyses performed by comparing swimming and swarming cells grown in BM2 medium, and genes involved in pilus assembly were down-regulated [73]. In a recent study, the role of T4aP in swarming was shown to be dual, by slowing swarming progression and promoting cell-to-cell interactions of swarmers to orchestrate chemotactic movements [74]. Swarmer cells have shown properties that differentiate them from their planktonic counterparts [73, 75]. Kohler et al observed that swarmer cells at the edge of the tendrils are elongated and present hyperflagellation [72]. In fact, conditions that affect swarming do not always affect swimming, using the same media composition [76]. The regulation of swarming in *P. aeruginosa* reaches a high level of complexity, as a wide range of mutations has shown to affect this phenotype [77, 78]. Amongst the central regulators of swarming in this organism, both the Pqs and Rhl quorum sensing (QS) systems (see **1.4.3**) have been shown to control the expression of the genes required for the production of the rhamnolipid biosurfactants [79]. The regulation of swarming is also exerted at the post-transcriptional level via the RNA binding protein RsmA (see **1.4.4**) which positively influences swarming motility [80].

Twitching constitutes a distinct motility that does not depend on flagella or QS [81], but which requires functional pili. Specifically, T4aP is the only type of pilus involved in twitching and swarming motilities [82]. Twitching motility occurs on solid medium and is driven by the extension and retraction of T4aP, which promotes a worm-like movement [83, 84]. In *P. aeruginosa,* T4aP are composed by a multitude of genes belonging to the *pil* operon (**Figure 1.1**). Regulation of twitching depends on various 2CS including PilSR (which are in turn subjected to regulation from the alternative sigma factor RpoN), chemosensory systems (FimS/AlgR) and the global regulator Vfr [85, 86]. In turn, surface attachment mediated by T4aP results in the activation of the Pil-Chp chemosensory system, which resembles flagellar chemotaxis systems and results in the activation of c-di-GMP and cAMP/Vfr [87].

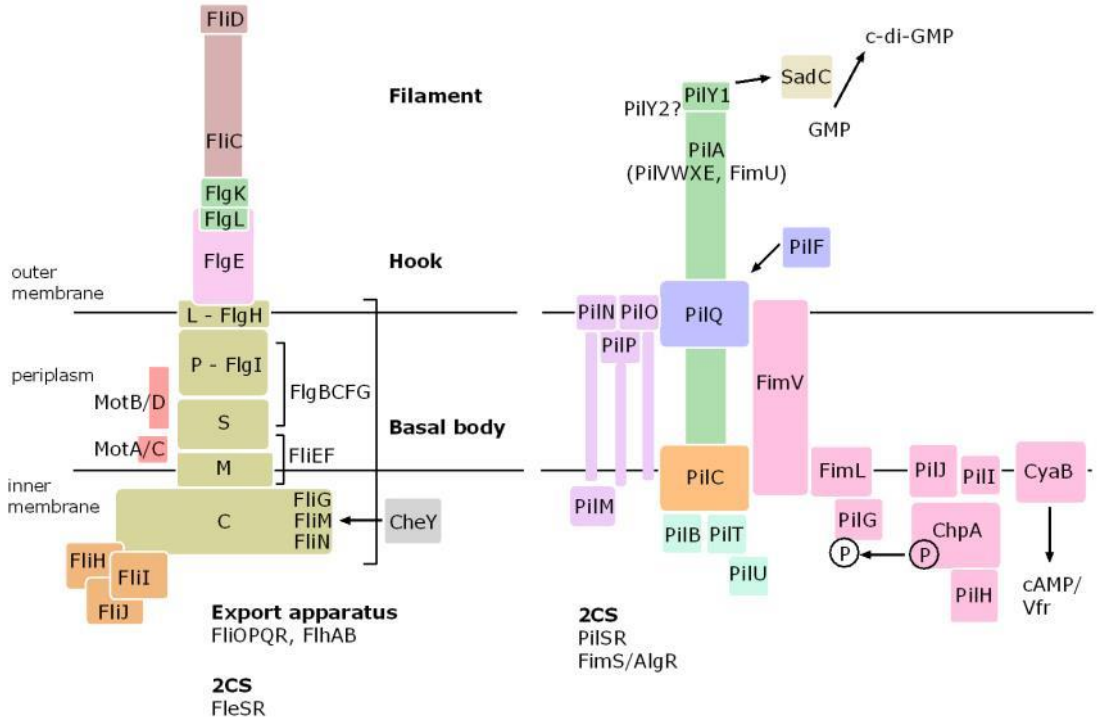


Figure 1.1. Structure and regulation of the flagellum and type 4a pili (T4aP) in *P. aeruginosa*. The flagellum of *P. aeruginosa* **(left)** is composed of three main complexes; the basal body, the hook and the filament. The basal body includes the L, P, S, M and C-rings and the stator proteins MotAB. CheY is the switch regulator from the Che system, and controls the direction of rotation by directly binding FliM. Figure adapted from [88], with information from [67, 89]. T4aP of *P. aeruginosa* **(right).** PilD is a pre-pilin peptidase that processes the pilins for their export to the cell surface. The helical filament is composed of the major pilin PilA and several minor pilins (PilVWXE and FimU). PilY1 is an adhesin which also functions as an anti-retraction protein, and which controls c-di-GMP levels through SadC. The function of PilY2 is not well determined. PilQ is a secretin, and PilF is a pilotin responsible for the assembly of PilQ. PilBTU are ATPases that promote the rotation of the motor, with PilB and PilT promoting the extension and retraction of the filament, respectively. The function of PilU has not been clearly defined. The Chp chemosensory system is activated upon surface binding with the methylation of PilJ. This triggers the autophosphorylation of the CheY-like protein ChpA, and subsequent phosphorylation of the response regulator PilG. PilG and PilH are CheY homologues, while PilI is a CheW homologue. The phosphorylation of PilG activates the adenylate cyclase CyaB, leading to the triggering of the cAMP/Vfr system. Adapted from [87, 88, 90-92]. 2CS, two-component system.

Other motilities employed by *P. aeruginosa* include sliding and surfing. Henrichsen defined sliding as a "spreading by expansion" motility [66]. In *P. aeruginosa*, sliding is observed in *fliC pilA* mutants that do not express flagella or pili, and depends on the secretion of rhamnolipids [93]. Surfing is a rapid motility observed on agar supplemented with surfactants such as mucin or detergents. It depends on QS and flagella, but not on rhamnolipids or T4aP. Surfing might be important in the CF lung, where mucin is produced by mucosal glands [94].

1.3.2 Biofilm

Biofilms are defined as "matrix-enclosed bacterial populations adherent to each other and/or to surfaces or interfaces" [95]. These structures are increasingly perceived to be the preferred mode of growth for bacteria, and are important for the colonisation of new niches, including human tissues [96] and plant tissues [97].

Biofilms comprise an extracellular matrix which helps enclose the bacterial cells and sustain the overall biofilm architecture. The composition of this matrix depends on the type of microorganism(s) involved in biofilm development and the environment in which this structure is formed; and may contain dead immune cells, extracellular DNA (eDNA), pieces of substrate such as catheters, proteins, carbohydrates and other products secreted from bacterial cells. *P. aeruginosa* uses several exopolysaccharides as components of the biofilm matrix: Pel, composed of N-acetylglucosamine and N-acetylgalactosamine [98]; Psl, composed of glucose, mannose and rhamnose [99]; and alginate, responsible for the mucoid phenotype of this bacterium, composed of guluronic and mannuronic acids [100].

Alginate can disrupt the immune response by inducing the production of mucin and lysozyme in tracheal cells, modulating neutrophil response and inhibiting complement activation [101, 102]. In addition to immune evasion, alginate facilitates water and nutrient retention in the bacterial biofilm [103]. Mucoid strains are often isolated from CF patients. However, they do not occur with high frequency in environmental isolates, and mostly arise after the initial colonisation of the CF lung [104]. The genetic basis for the biosynthesis of alginate has been the subject of extensive research. Alginate is synthesised from a 12 gene operon encoding *algD*, *alg8*, *alg44*, *algK*, *algE*, *algG*, *algX*, *algL*, *algI*, *algJ*, *algF* and *algA*. The transcription of this operon is driven by the alternative sigma factor AlgU, which is in turn regulated by the *mucABCD* operon. Mutations during the colonisation of the CF lung by *P. aeruginosa* usually inactivate the expression of the anti-sigma factor MucA, thereby switching the cells to a mucoid phenotype. Multiple additional regulators of *algD* transcription have been identified, including the 2CS KinB/AlgB and FimS/AlgR, the DNA-binding proteins AmrZ, AlgP and AlgQ, and the alternative sigma factor RpoN. Moreover, alginate biosynthesis is also subjected to post-translational regulation by c-di-GMP [103](see **1.4.1**).

Psl is the main polysaccharide component of the PAO1 biofilm matrix [105]. This polysaccharide serves as an important protection against the host immune

system in a similar way to alginate, as it also reduces phagocyte killing and the deposition of complement components in the bacterial cell surface [106]. Interestingly, Psl is important for biofilm establishment in mucoid populations, where an outer layer of alginate produced by mucoid strains may protect Psl-producing, antibiotic resistant isolates [107]. Psl is found in two forms; a low-molecular, soluble form and a high-molecular weight form, associated with the cell surface [99]. Psl is synthesised from 12 genes present in the *psl* operon, named *pslA-L* [99, 100], and is regulated by the alternative sigma factor RpoS [108].

Pel is responsible for the formation of pellicles in the air-liquid interface, and it is the main polysaccharide secreted by *P. aeruginosa* PA14 [109]. Pel is also responsible for the establishment of complex biofilm structures, particularly in PA14. In contrast, the loss of this polysaccharide does not cause a major disruption of biofilm in PAO1 [110]. Nevertheless, Pel might also perform functions that Psl cannot, such as the binding of eDNA [98]. Pel also serves a protective role in *P. aeruginosa* biofilm, by increasing antibiotic resistance [110]. Pel synthesis depends on the 7 gene operon *pelABCDEFG* [100].

Important factors for biofilm establishment include eDNA [111], which is involved in cell adherence and has an important structural function, allowing for the mushroom caps observed under flow cell conditions by cross-linking with Pel [98]. Proteins are also part of the biofilm matrix, notably lectins [112]. Additionally, biofilm establishment relies on the presence of adhesive structures in the surface of bacterial cells, such as the Cup fimbriae [113, 114], pili and flagella [115].

Biofilm development can be divided into distinct stages, according to the factors that regulate them and the phenotypic appearance of the biofilm [69] (**Figure 1.2**). Overall, biofilm formation and dispersion is a cyclic process where newly dispersed cells will serve as seeds which will establish biofilms in new niches [116]. Planktonic cells move to a favourable niche and use flagella and pili to adhere to surfaces, which constitutes the reversible attachment phase. Pili are upregulated by surface binding [117], which also leads to the production of virulence factors through Vfr [91]. Then, motility appendages together with adhesins promote an irreversible attachment phase. Microcolonies start developing, and then the biofilm matures. Finally, cells at the centre of the microcolony become motile again, in a process known as dispersion [69].

Dispersed cells present a distinct stage of growth, with marked differences to both sessile and planktonic cells [19, 118].

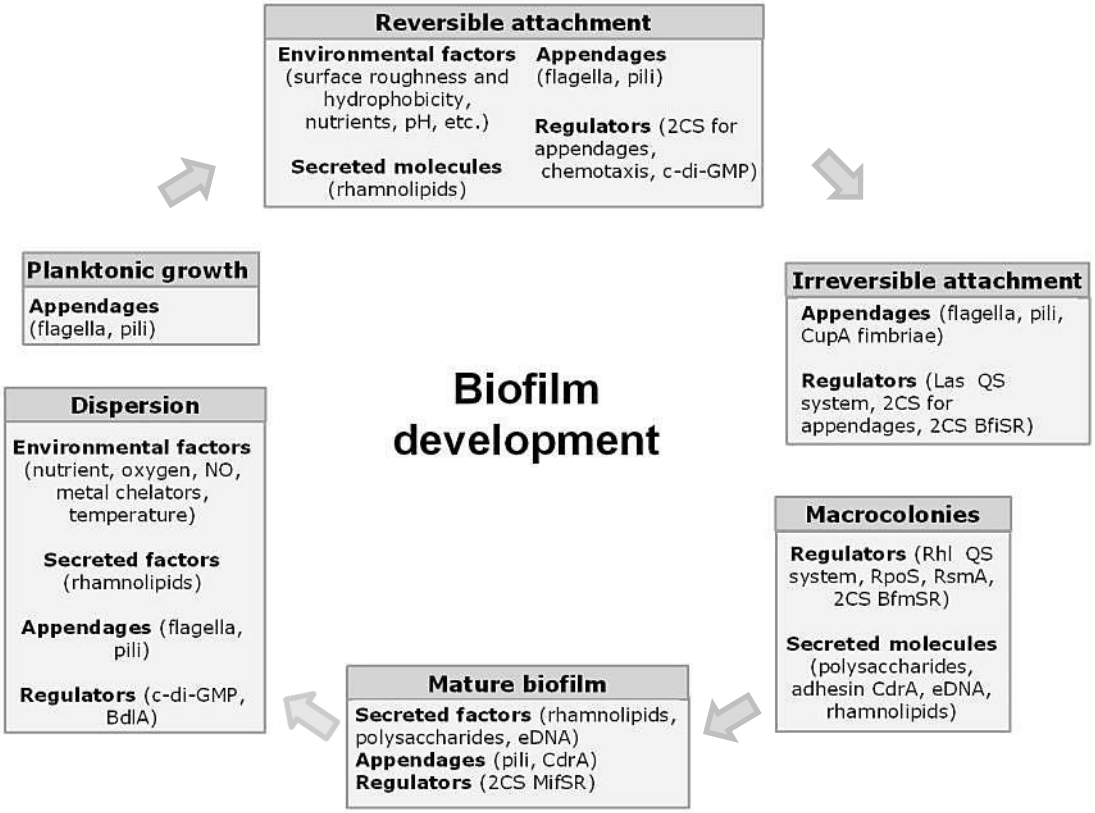


Figure 1.2. Factors affecting biofilm development stages in *P. aeruginosa*. Biofilm formation is a cyclic process that depends on a myriad of secreted factors, environmental conditions and regulators. Specific stages of biofilm development can be distinguished according to the factors that are essential for their establishment. With information from [69, 119-121]. 2CS, two-component system; QS, quorum sensing; eDNA, extracellular DNA; NO, nitric oxide.

An interesting autoaggregative phenotype happens when cultures of *P. aeruginosa* are allowed to grow in solid, rich medium. This is called "colony biofilm" or colony morphotype. Colonies are allowed to grow for several days and adopt a smooth or wrinkly phenotype, which depends on various factors. Pel is essential for wrinkle formation. As a result, PA14 wild-type is wrinkly, while PAO1, that uses mainly Psl as exopolysaccharide, forms smooth colonies [105, 109]. The redox state of the cell also determines colony morphogenesis: the increase of surface area, i.e. the formation of wrinkles, enables the cells to access oxygen [122]. Cells defective in phenazine production are not able to sense the redox imbalance, resulting in smooth morphotypes.

Another characteristic biofilm form of *P. aeruginosa* is observed in small colony variants (SCV). These isolates are characterised by a hyper-aggregative behaviour driven by the overexpression of both Pel and Psl polysaccharides, and

present high levels of c-di-GMP. SCV confer persistance and resistance to macrophages, and in consequence they are linked with poor lung function in CF [123].

Regarding the regulation of biofilm formation, multiple factors have been identified, including multiple 2CS, the sigma factor RpoS, the global post-translational regulator RsmA, and the secondary messenger c-di-GMP. These systems will be discussed in detail in section **1.4**.

1.3.3 Pyocyanin and phenazines

Phenazines are molecules with multiple roles produced by pseudomonads. *P. aeruginosa* produces several phenazines, including the precursor phenazine-1-carboxylic acid and three further modifications; pyocyanin, phenazine-1-carboxamide and 1-hydroxyphenazine [124]. The biosynthetic route of phenazine production involves two almost identical operons, *phzA1B1C1D1E1F1G1* and *phzA2B2C2D2E2F2G2*, which mainly differ in their promoter region [125].

The main characteristic of phenazines is that they can transfer electrons, which leads to various functions. First, phenazines serve as an important mediator of redox reactions under limiting conditions and facilitate niche colonisation by *P. aeruginosa*. As an electron donor, pyocyanin is able to provide electrons in an oxygen-depleted environment [126] and can also protect *P. aeruginosa* against toxics such as ionic silver [127]. As a virulence factor in the human host, pyocyanin can increase the glycosylation of mucin which facilitates the binding of this bacterium to airway epithelial cells [128]. Pyocyanin also increases mucus production in these cells [129] and induces neutrophil death [130], amongst other effects. The production of pyocyanin in clinical isolates of *P. aeruginosa* has been reported [131], and correlates with periods of pulmonary exacerbation [132]. In this sense, pyocyanin may be important during acute infections and only have a transient role in the first stages of chronic infections [133, 134].

Phenazines also interact with plants through the production of reactive oxygen species, with both positive and negative consequences for plant hosts [135]. Pyocyanin has been shown to have antibiotic effects on plants, helping *P. aeruginosa* to displace competitors [124, 136].

The link between pyocyanin production and biofilm formation is a complex one. Pyocyanin secretion seems important in the formation of wrinkly morphotypes and in flow cells biofilms [137]. Phenazine mutants of PA14 result in thinner

biofilms under flow, and also depict an increased swarming motility. Pyocyanin does not contribute to the adherence stage, but rather to later steps in biofilm establishment. At least one mechanism behind the increase of biofilm formation caused by pyocyanin is the binding of this phenazine to eDNA [138-140]. This is in disagreement with the observation that biofilm and pyocyanin show a negative correlation in a panel of *P. aeruginosa* strains [134].

1.3.4 Siderophores

Iron is essential for life, as it serves as a cofactor for important enzymatic functions. In particular, bacteria use iron in photosynthesis, respiration and nitrogen fixation, among others. However, iron is strongly chelated in the mammalian host by proteins such as lactoferrin, ferritin and transferrin; or present in haem groups. Living organisms have therefore developed a series of strategies to gain access to this micronutrient [141].

P. aeruginosa secretes two siderophores; pyoverdine, which has a high affinity to iron; and pyochelin, with a low affinity [142]. Three distinct pyoverdines have been found in *P. aeruginosa* strains which differ in the length of their peptide chains [143]. On the other hand, *P. aeruginosa* has been shown to use siderophores produced by other bacteria, such as enterobactin produced by *E. coli* or *S. enterica* [144]. In addition, this bacterium can also uptake iron from haem groups, and use phenazines together with the Feo system to reduce iron (III) to iron (II) and subsequently uptake it [23].

Pyoverdine is important for the establishment of biofilms during the colonisation of the CF lung, where iron is not readily available for bacteria to uptake [145]. However, mutants for QS systems, which are often found as a result of chronic infections, present reduced pyoverdine production [146]. Together with the fact that pyoverdine-negative mutants have been isolated from CF lungs [147], this suggests that the relevance of this molecule in infection mostly comprises acute stages of infection, while other iron-scavenging mechanisms can be used by *P. aeruginosa* to establish chronic infections [23]. As mentioned in **1.2.2**, siderophores have important roles in growth promotion in plants, as they can scavenge this limiting nutrient and hence inhibit the growth of fungi. Pyoverdine production leads to the activation of the sigma factor PvdS, which in turn controls a wide range or genes, including the virulence factors exotoxin A and the protease PrpL [148].

Research has shown that Pel and Psl exopolysaccharides, or rather cell aggregation, control the regulation of pyoverdine production through both c-di-GMP and the Gac/Rsm signalling system [149, 150]. In this sense, it appears that cell to cell contact is a signal that triggers pyoverdine production. Moreover, RsmA indirectly inhibits PvdS and PchR (a regulator of pyochelin) [151]. As mentioned above, pyoverdine production is dependent on QS, but in addition, the expression of QS signal molecules (QSSM) is activated under high iron conditions [152]. Interestingly, PQS (but not HHQ) can chelate iron, presumably to allow for siderophores to mediate iron transfer into the cell [153](see **1.4.3.1**).

1.3.5 Rhamnolipids

Rhamnolipids are amphipatic molecules produced by a variety of bacteria [154]. These glycolipids consist of one or various fatty acid moieties of 3-hydroxyfatty acids joined by a 3-glycosidic bond to one or two rhamnoses. They are produced by a variety of bacterial phyla; including Actinobacteria, Firmicutes and Proteobacteria [155]. *P. aeruginosa* has been extensively studied for its rhamnolipid production, and secretes a variety of rhamnolipids, containing one or two L-rhamnose moieties and one to three β-hydroxyfatty acids of 8 to 22 carbons.

The importance of rhamnolipids lies in the fact that these molecules have important biotechnological applications (see **1.2.3**), but also because these molecules are virulence factors. Rhamnolipids alter the respiratory epithelium, which then allows for the infiltration of bacterial cells [156-158]. Rhamnolipids also cause eukaryotic cell death, for instance in an amoeba virulence model [159], or in leukocytes. Rhamnolipids produced by *Burkholderia pseudomallei* and *P. aeruginosa* promote the death of neutrophils and macrophages, which is abrogated in rhamnolipid-deficient mutants [160-162].

The production of the different rhamnolipid species and their relative ratios are influenced by growth conditions. Particularly, Abdel-Mawgoud et al. identified 58 rhamnolipid species produced by various bacteria [155]. The production of rhamnolipid congeners is often complex. Déziel et al. showed 28 distinct rhamnolipids produced by *P. aeruginosa* grown in the presence of mannitol and naphthalene. Mono- and di-rhamnolipids were detected containing fatty acid chains of 10 carbons; though lengths of 8, 12 and 14 carbons were also observed. Most of the rhamnolipids presented 2 fatty acid chains with no insaturations [163]. Longer chains were produced by cultures of *P. aeruginosa*

grown in glycerol, ranging from 18 to 22 carbons [164]. Other bacteria, such as *Pseudomonas putida* or *Burkholderia sp.* also produce these biosurfactants, and the exact composition varies between species and growth conditions [165]. Rhamnolipids from *Burkholderia thailandensis* were found to contain fatty acid chains of 10 to 16 carbons [166].

The genetic basis for rhamnolipid production has been extensively studied. In *P. aeruginosa*, the core genes involved in rhamnolipids production are those from the *rhlAB* operon and the *rhlC* gene. RhlA is responsible for the biosynthesis of 3-(3-hydroxyalkanoyloxy) alkanoates (HAAs) [71], while RhlB transfers one rhamnose moiety to HAAs, giving rise to mono-rhamnolipids. The biosynthesis of di-rhamnolipids depends on RhlC, another rhamnosyltransferase which synthesises di-rhamnolipids from mono-rhamnolipids [167]. RhlG was thought to divert the flux of fatty acid moieties towards rhamnolipid biosynthesis [168], but it was later found that RhlA alone is sufficient for the conversion of HAAs to mono-rhamnolipids [169].

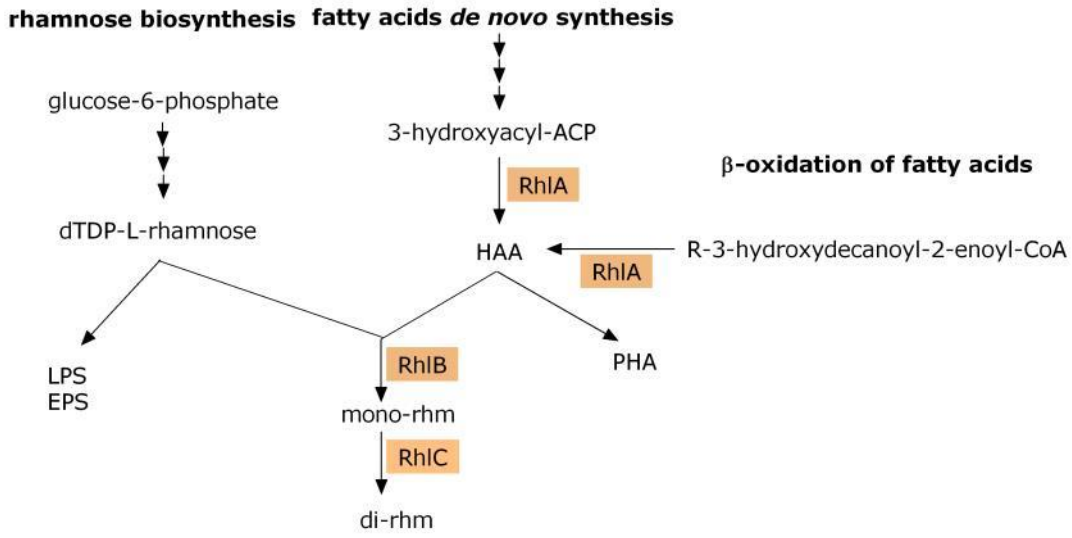


Figure 1.3. Rhamnolipid biosynthesis in *P. aeruginosa.* The synthesis of rhamnolipids components is shown, with emphasis on the steps catalysed by RhlA, RhlB and RhlC. Adapted from [170]. LPS, lipopolysaccharide; EPS, exopolymeric substances; mono-rhm, mono-rhamnolipid; di-rhm, di-rhamnolipid; HAA, 3-(3-hydroxyalkanoyloxy) alkanoates; PHA, polyhydroxyalkanoates.

The role of rhamnolipids within biofilm development has been greatly investigated. Rhamnolipids seem to play key roles in all the stages of biofilm formation, which suggests that a complex regulation is in place. Particularly, research has focused on the characteristic mushroom-like structures produced by *P. aeruginosa* in flow chambers. Under these conditions, rhamnolipids are paramount to the formation of macrocolonies, with *rhlA* expression coinciding with the formation of the stalks, and helping the translocation of twitching cells

towards the cap of the structure [171-173] help maintain the structural integrity of biofilms. On the one hand, these surfactants maintain channels within the biofilms that allow nutrient exchange and help avoid invasion from competitors [174]. In contrast, exogenous addition of rhamnolipids also impedes initial attachment of cells to surfaces [175], and the addition to mature biofilms promotes dispersion [176, 177]. In fact, rhamnolipids have been studied to counteract biofouling [178]. In this sense, it has been speculated that rhamnolipids have dual roles that depend on cell and rhamnolipid concentrations: at low concentrations, these glycolipids would favour cell aggregation, while at high cell densities they are induced by QS and produced at concentrations favouring cell migration and the maintenance of fluid channels [179].

In addition to biofilm formation, rhamnolipids also have a role in surface motility, together with their precursors, HAAs. These molecules have surfactant activity, which allows cells to rapidly move across surfaces [71, 72]. Interestingly, different molecules from the rhamnolipid biosynthetic pathways result in distinct effects in swarming. Rhamnolipids are important for the organization of swarming tendrils [180]. In addition, Tremblay et al. [76] showed that swarmers are repelled by HAAs and attracted by di-rhamnolipids, while mono-rhamnolipids only function as surfactants. Additionally, di-rhamnolipids diffuse faster than HAAs in agar, resulting in an elegant model in which increasing ratios of di-rhamnolipids/HAAs are established radial to the inoculation point. Motile cells are attracted by di-rhamnolipids in the edges of agar plates, while they are repelled by the HAAs produced in their vicinity, and this results in the formation of tendrils [76].

1.3.6 Proteases

P. aeruginosa produces a range of proteases, and four secreted proteases present major roles in virulence. Three of these are the metalloproteases LasA, LasB and AprA; and one serine protease named protease IV and coded by the *prpL* gene. Proteases are utilised to retrieve nutrients from the environment, and can affect a wide range of components of human tissues such as the extracellular matrix components collagen [181] and laminin [182]. Secreted proteases also interfere with the human immune system, including the effect on complement components [183, 184] and cytokines [185], amongst others. There are also studies suggesting the effect in the overall virulence of *P. aeruginosa* [186-189].

LasA presents elastase activity. Cleavage of elastin makes this substrate more available to LasB, resulting in a synergistic increase in activity [190, 191]. LasA

also presents a specific staphylolytic activity against the pentaglycine bridge in the peptidoglycan from *Staphylococcus aureus* [192]. AprA, the alkaline protease, is able to degrade casein and gelatin. It has an important role in disease, and can interfere with the complement factors C3b and C5a [193]. Protease IV belongs to the family of serine endoproteases, cleaving on the carboxyl side of lysine residues [194].

Secreted proteases are subjected to the regulation by the Las QS system [195-198]. In addition, other regulators are in place: notably, protease IV relies on the expression of the sigma factor PvdS [199]. Secretion systems differentially control the translocation of proteolytic enzymes: LasA, LasB and protease IV are secreted by the type 2 secretion system (T2SS) Xcp, while AprA is secreted by a type 1 secretion system (T1SS) [200].

1.3.7 Other colonisation factors

P. aeruginosa presents an arsenal of factors to ensure a successful colonisation in the environment. In addition to the molecules discussed so far, a number of other proteins have an important impact in *P. aeruginosa* niche establishment. Exotoxin A is a potent inhibitor of protein synthesis, which results in cell death by apoptosis [201]. Production of hydrogen cyanide inhibits aerobic respiration and chelates cofactors of metal-dependent proteins, affecting bacterial competitors [202]. *P. aeruginosa* also secretes the haemolytic (PlcH) and non-haemolytic (PlcN) phospholipases which can degrade host tissues to facilitate invasion [203].

Secretion systems constitute other important elements in *P. aeruginosa* virulence. *P. aeruginosa* presents one or more copies of type 1 (T1SS) to type 6 (T6SS) secretion systems, with the exception of type 4. T1SS are responsible for the secretion of the alkaline protease AprA and regulation under low-iron conditions. T2SS mediate the translocation of various proteases including LasA, LasB and PrpL, various phospholipases, a lipase and the exotoxin A. The T3SS forms a needle-like structure called injectisome that delivers up to 4 effectors in the cytoplasm of target cells. These effectors (ExoS, ExoT, ExoU and ExoY) then trigger cell death by necrosis and apoptosis. T5SS secrete an esterase, a protease and a haemagglutinin-like protein. During chronic infections, T6SS are the major secretion mechanisms in *P. aeruginosa* populations. Like T3SS, T6SS also form delivery structures to directly translocate effectors into neighbouring cells, which can be eukaryotic or bacterial. T6SS cause the down-regulation of toxicity and immune recognition [200].

1.4 Global regulatory networks

The regulatory network of *P. aeruginosa* has been extensively studied, and published data points to a high interconnection between global regulators [79], which allows it to respond to a large amount of environmental cues. The key systems controlling adaptation in this bacterium comprise networks regulated by small RNAs or nucleotides, 2CS and QS.

1.4.1 Cyclic diguanylate (c-di-GMP)

The cyclic nucleotide derivative cyclic diguanylate (c-di-GMP) is a secondary messenger in many bacterial species, including Gram-positives and Gram-negatives [204, 205]. It is structurally bis-(3′-5′)-cyclic dimeric guanosine monophosphate. The concentration of this signal is regulated by diguanylate cyclases (DGC) containing GGDEF motifs that synthesise it from two GTP molecules; and by phosphodiesterases (PDE) with EAL or HD-GYP motifs that convert it back to linear nucleotides [206]. Interestingly, *P. aeruginosa* PAO1 encodes 39 genes containing a c-di-GMP-binding domain, which highlights the importance of c-di-GMP in the regulatory network of this organism [207]. Regarding the existence of multiple c-di-GMP regulators, an idea is emerging of multiple, independently regulated pools of c-di-GMP within cells [208, 209].

C-di-GMP regulates many biological processes, but it has principally been studied for its role in the transition between motile and sessile, biofilm-forming cells; where high concentrations of this nucleotide promote biofilm formation while low concentrations activate cell motility [68, 206]. C-di-GMP activates genes encoding for the 3 main exopolysaccharides present in the biofilm matrix: Pel, Psl and alginate [121, 204]. SCV rise with the increase of c-di-GMP levels. Various regulators have been identified that modulate c-di-GMP levels promoting this switch, including the *yfiBNR* operon and the DGC *wspR* [210, 211]. With regards to antimicrobial susceptibility, c-di-GMP has been linked with increased resistance in both biofilm and planktonic cells [212].

This nucleotide also regulates motility in *P. aeruginosa*, where both flagella and pili production depend on c-di-GMP levels, and represents a link between motility and biofilm formation. In fact, FleQ, the transcriptional regulator for flagellum synthesis, is capable of activating the *pel* promoter in response to increased c-di-GMP levels and represses the *pel* operon in absence of the nucleotide [68, 207, 213]. C-di-GMP also offers control over the set of stators used for flagellum rotation, switching from MotCD (favourable to swarming motility) to MotAB [89].

BifA is a PDE that activates swarming and represses biofilm formation [214], while SadC is a DGC responsible for the opposite phenotypes [215]. Interestingly, SadC binds to PilY1, which offers a link between T4aP (and hence twitching motility), swarming and biofilm formation.

One of the phosphatases responsible for c-di-GMP degradation, PA3885, is activated by the Las system, showing the relationship between QS, c-di-GMP and biofilm formation [216]. Regarding cell-to-cell communication mechanisms, c-di-GMP controls the regulatory cascade of the diffusible signal factor (DSF) in *Xanthomonas campestris*, suggesting a possible role of this molecule into the regulation by *cis*-2-decenoic acid (CDA) in *P. aeruginosa* [217, 218].

Regarding plant infections, the overproduction of c-di-GMP enhanced aggregative phenotypes in species of *Pseudomonas* and *Rhizobium*, though it did not affect disease progression in *P. syringae* [219].

Overall, c-di-GMP favours aggregative phenotypes, which leads to a chronic growth state characterised by persistence, production of exopolysaccharides and the inhibition of acute phenotypes such as swarming motility. Further confirmation of this switch towards chronicity is given by the fact that c-di-GMP inhibits Vfr signalling, the archetypical regulator of acute phenotypes [220].

1.4.2 cAMP and Vfr

Vfr (for virulence factor regulator) is a homologue of the cAMP regulator protein (CRP) from *E. coli* produced by *P. aeruginosa*. This cAMP binding protein constitutes a major regulator of virulence in *P. aeruginosa*, where it affects the transcription of QS, twitching motility and exotoxin A production [85, 221, 222]. In addition, Vfr can repress the transcription of the global regulator *fleQ* [223].

Modulation of cAMP occurs through the Chp chemotaxis-like chemosensory system. Therefore, Chp indirectly affects Vfr activity and the activation of QS [91]. On the other hand, mucoid isolates of *P. aeruginosa* showed that the alternative sigma factor AlgU can inhibit the activity of Vfr. This constitutes part of the regulatory switch from acute to chronic lifestyle in *P. aeruginosa* [224].

1.4.3 Quorum sensing

Cell-to-cell communication systems allow cells to sense and respond to changes in their environment. One such system is termed quorum sensing (QS), a term first employed by Fuqua et al. [225] to define the mechanism by which cells

coordinate gene expression under certain cell densities. QS systems require the production of signal molecules to monitor the extracellular environment and to discriminate between high and low population densities (or high and low diffusion rates) [226]. A series of conditions have been proposed to define a molecule as a cell-to-cell signal and will be followed in this study [227]:

- The production of the molecule is restricted to certain physiological stages (including growth phase, nutrient availability…)
- The molecule accumulates extracellularly and is recognised by a specific receptor
- Accumulation of the signal results in a coordinated response, once a critical threshold is reached
- The response to the signal goes beyond the degradation or metabolic routes that directly respond to it. In this sense, toxic compounds or nutrients which activate or repress their own metabolic routes are not considered signal molecules.

In general terms, a pheromone, or signal molecule, is secreted by the bacterial cells. The signal molecule gets accumulated in the bacterial milieu as the number of cells increases, and once the levels of this molecule reach a threshold, the population gets *quorated*. The signal is sensed and triggers a cascade in the cells, resulting in changes of gene expression. When the synthesis of this molecule is subjected to a positive feedback loop, the pheromone is termed *autoinducer*. In these cases, the signal molecule triggers its own biosynthesis, resulting in a rapid activation of QS [79, 228, 229].

Signals involved in QS present various chemically distinct structures. In Gram-negatives, fatty acid molecules such as *N*-acyl-L-homoserine lactones (AHL) and diffusible signal factor-type (DSF-T) are found, together with 2-alkyl-4-quinolones (AQ) [229, 230]. Gram-positives usually employ autoinducing peptides, which they use to coordinate competence (in *Bacillus subtilis* and *Streptococcus pneumoniae*) [231, 232], and control virulence and biofilm formation (in *S. aureus*) [233], amongst others. Gram-positives can produce other cell-cell signals, such as γ-butyrolactones in *Streptomyces sp.* which regulate the production of antibiotics and spore formation [234].

1.4.3.1 AHL and AQ-based QS in *P. aeruginosa*

P. aeruginosa presents a complex QS system involving multiple signal molecules [28]. The better understood systems rely on the production of AHLs and AQ and are organised in a hierarchical manner. The Las system regulates the others: LasI synthetises *N*-(3-oxododecanoyl)-L-homoserine lactone (3OC12-HSL) early in the infection, which activates the Rhl and the PQS system. The Rhl system senses *N*-butanoyl-L-homoserine lactone (C4-HSL), while the PQS system depends upon two 4-quinolones, PQS (*Pseudomonas* quinolone signal, chemically 2-heptyl-3-hydroxy-4(1*H*)-quinolone) and its precursor HHQ (2-heptyl-4-quinolone) [230, 235].

QS in *P. aeruginosa* triggers the production of the secretion machinery, siderophores, proteases, exotoxins, lipases, rhamnolipids and hydrogen cyanide, amongst others [79, 230, 236-239]. Many of the molecules regulated by QS are known as virulence determinants, as the bacterial cells only activate their virulence once the population is sufficient to cope with the defence mechanisms of the host [238].

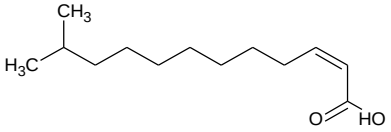
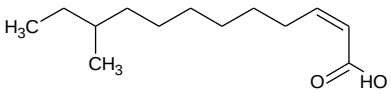
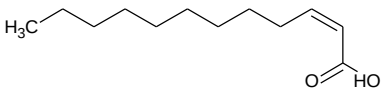
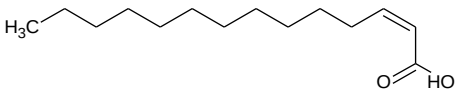
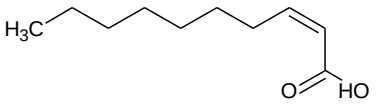
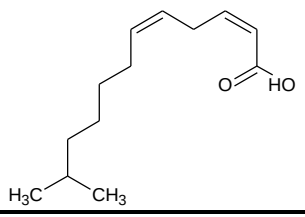
The contribution of QS to biofilm formation in *P. aeruginosa* is somewhat controversial. A study found that *lasI* mutants developed flat biofilms (unlike the mushroom cap structures formed by wild-type cultures). No difference was observed with *rhl* mutants [240]. Shrout et al suggested a model by which early swarming motility determined the overall biofilm structure – being flat in conditions favouring swarming; and mushroom-like, aggregative under low swarming. A direct relationship between QS and biofilm does not explain all studies, and the carbon source in growth media can allow for wild-type biofilms to be formed by a double mutant *lasI- rhlI-* [241]. Furthermore, *lasI* mutants are common in CF, but biofilms are thought to happen in the CF lung; which suggests that QS might be important for the establishment of biofilms but not the subsequent maintenance of these structures. On the other hand, many factors that are important for biofilm establishment are controlled by QS, including pyocyanin [139] and eDNA [242].

1.4.3.2 Diffusible signal factor-type family

Another QS system depends on the secretion of long chain fatty acids belonging to the diffusible signal factor-type (DSF-T) family. These molecules are thought to freely diffuse through the membranes due to their hydrophobic nature, and to

be sensed by various bacterial species, which results in pleiotropic effects, including the modulation of virulence, biofilm formation and motility [243, 244](**Table 1.2**).

Table 1.2. Structure and properties of diffusible signal factor-type (DSF-T) molecules. DSF-T molecules are produced by a variety of bacterial species and exert effects in both their cognate producers and in other organisms present in the environment. *Xcc*, *Xanthomonas campestris* pathovar *campestris.*

Name, abbreviation	Producer(s)	Formula	Effects	References
cis-11-methyl-2-dodecenoic acid, DSF	*Xanthomonas sp.* *S. maltophilia* *B. multivorans*		enzyme production, polysaccharide production, motility, biofilm dispersal, iron uptake, heavy metal tolerance, antibiotic resistance, virulence, polymyxin resistance of *P. aeruginosa,* inhibition of morphological transition in *C. albicans.*	[245-249]
cis-10-methyl-2-dodecenoic acid, DSF-II or IDSF	*Xcc*		biofilm dispersal, polysaccharide production	[250]
cis-2-dodecenoic acid, BDSF	*B. cepacia* complex *X. oryzae* pv. *oryzae* *Xcc*		biofilm formation, motility, virulence, inhibition of morphological transition in *C. albicans.*	[247, 248, 251, 252]
cis-2-tetradecenoic acid, *Xf*DSF	*X. fastidiosa* *Xcc*		blockage of virulence, adhesion to surfaces, enzyme production	[253, 254]
cis-2-decenoic acid, CDA	*P. aeruginosa*		biofilm dispersal, biofilm inhibition in Gram-positives, Gram-negatives and *C. albicans*, reversal of persisters to metabolically active cells	[255, 256]
cis, cis-11-methyldodeca-2,5-dienoic acid, CDSF	*B. cepacia* *X. oryzae* pv *oryzae* *Xcc*		biofilm dispersal, polysaccharide production, virulence, inhibition of morphological transition in *C. albicans.*	[247, 248]

There are discrepancies between authors on what constitutes a DSF-T molecule: Deng et al. consider that DSF-T comprise fatty acids with different side chains, double bonds and chain lengths, given that the presence or absence of a double bond does not affect the promotion of flagellar-independent translocation in *S. maltophilia* [257]. Furthermore, the structural requirements for DSF activity are variable, as while the presence of a *cis* double bond is important for the activity of DSF in *Xcc*, the *trans*-2 decenoic acid (TDA) acts as an interkingdom signal molecule in *Streptococcus mutans*, where it inhibits the yeast-to-hyphae transition in *C. albicans* [258]. Moreover, both *trans*- and *cis*-2-dodecenoic acids inhibit morphological transition, and thus biofilm in *C. albicans* [259]. On the other hand, Ryan et al. are more restrictive in their DSF-T classification, considering that only unsaturated fatty acids with *cis* double bonds are part of the DSF-T family and that TDA is another kind of signalling molecule [260]. As opposed to CDA, TDA only disrupts *P. aeruginosa* biofilms at millimolar concentrations, and it is not considered a signal molecule for this particular phenotype [255]. Other groups have reported similar effects with the *trans* isomers of DSF-T molecules [261, 262].

Using a previously developed bioreporter assay for DSF [263], Wang et al. identified DSF-like activity caused by a variety of closely related molecules. It is important to note that the *trans* isomer of DSF, *trans*-11-methyl-2-dodecenoic acid, was needed at a minimum concentration of 1000 μM for triggering the activation of the bioreporter, as opposed to DSF which activated the promoter of *engXCA* with 0.5 μM. This shows the importance of the *cis* insaturation for DSF-like activity [245]. Others have reported the same specificity in the bioreporter assay [264]. However, as mentioned before, *trans*-2-decenoic acid has an impact in *Candida* and was named SDSF; so *trans* isomers can still have important biological roles [258]. The double bond seems to be a key feature for signalling, as 11-methyldodecanoic acid, which does not present any insaturation, had a threshold of DSF-T activity of 10000 μM in the same bioreporter assay. In contrast, the presence of a methyl group had a minor importance; as BDSF, formally *cis*-2-dodecenoic acid, was required at a minimum concentration of 60 μM to promote activation of the bioreporter. The length of the fatty acid chain was also key, as *cis*-2-decenoic acid required a minimum concentration of 3000 μM [245].

DSF-T molecules, in particular DSF and BDSF, follow the requirements to be considered signal molecules: they are secreted to the extracellular milieu and mediate population behaviours, including biofilm formation and pathogenicity

[244]. They are taken up by specific receptors and trigger a regulatory cascade resulting in changes in gene expression [263, 265]. Furthermore, the production rate of DSF-T increases with cell density, reaching maximum levels in stationary phase, and then declines [243, 266]. A positive feedback loop has also been mentioned, as an increase in DSF production is observed when cells are grown in the vicinity of another DSF producer [267]. Though this is not a requirement for QS systems, it is often found.

For the purpose of this thesis, DSF-T are those who present the signature *cis* double bond at the second carbon, as described by Ryan et al. [260]. A summary of the key features of these molecules is presented in **Table 1.2**, and more information on the signalling pathways in which these molecules are involved will be discussed in **Chapter 4**.

1.4.4 Two-component systems and the Gac/Rsm pathway

Two-component systems (2CS) allow bacteria to sense external and internal stimuli. *P. aeruginosa* encodes approximately 127 2CS which contribute to its versatility [16, 268]. These regulatory systems can be classified according to their domain organisation (**Figure 1.4**). The *canonical* 2CS comprise a transmembrane sensor kinase (SK) and a response regulator (RR). A stimulus, such as a nutrient, is sensed by the SK which gets autophosphorylated in a conserved histidine residue and relays the phosphate group to an aspartate residue present in the RR. The phosphorelay will then lead to a differential gene expression as, in general, the RR contains a DNA-binding domain responsible for the binding to a target gene resulting in changes in transcription. Other strategies can be used to affect the bacterial phenotype, such as enzymatic domains which can regulate c-di-GMP levels, or domains that mediate the output by protein-protein binding [269, 270]. The RR is then dephosphorylated to return back to the initial state. *Hybrid* sensor kinases present a similar relay to their canonical counterparts; however in this case the SK contains an active aspartate in addition to the histidine. The histidine can therefore transfer the phosphate directly to the aspartate in the RR or, alternatively, to this second aspartate. If the phosphate group is transferred to the aspartate in the SK, it is then relayed onto an independent histidine phosphotransfer protein (Hpt) and then to the aspartate in the RR, as indicated by the arrows in **Figure 1.4**. A third domain organisation of SK is named *unorthodox*. In this case, the SK contains a REC domain and an Hpt domain. The phosphate is transferred from the SK histidine

catalytic domain to the REC domain, then to the Hpt domain, and then to the aspartate domain in the RR; in a multiple step phosphorelay [268].

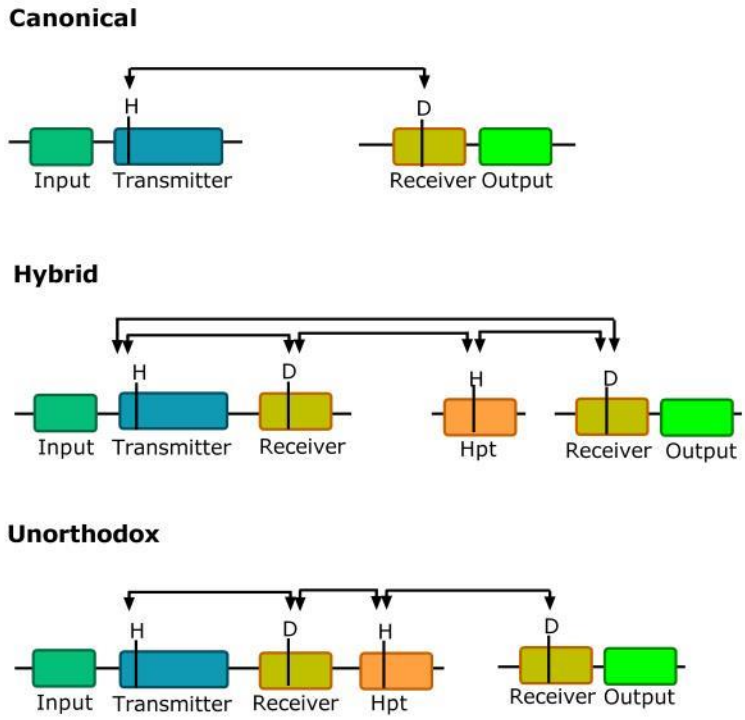


Figure 1.4. Phosphorelay systems in *P. aeruginosa*. This diagram depicts the canonical, hybrid and unorthodox systems employed by sensor kinases (SK). The phosphate groups are relayed from histidines (H) to aspartates (D), as shown by the arrows. In the hybrid SK, the phosphate groups can follow two paths: from the histidine in the transmitter domain of the SK directly to the aspartate in the receiver domain of the response regulator (RR) or in a multiple step relay from the transmitter to the receiver domain of the SK, then to a histidine phosphotransfer protein (Hpt) and to the receiver domain of the RR. The phosphorelay of unorthodox SK is similar to this second path, with the exception that the Hpt is located in a domain of the SK rather than being an independent protein. Adapted from [271].

Multiple 2CS have been identified in *P. aeruginosa*, such as those that regulate motility appendages (FleSR, PprAB, PilSR), and systems regulating specific stages of biofilm (BfmSR, MifR) [271].

Several 2CS converge into the central regulatory 2CS GacSA. GacS is a transmembrane, unorthodox SK that senses yet unknown signal(s) and transfers a phosphate group to GacA, the RR. In turn, GacA activates the small RNAs *rsmY* and *rsmZ,* which sequester the RsmA and RsmN proteins, resulting in a switch from phenotypes found in acute infection to those found in chronic infection [272]. The Gac system activates the small RNAs, and in fact, it has been published that the effects of GacSA depend almost completely on the upregulation of *rsmZ* and *rsmY* [273]. Activation of the Gac system affects a number of other 2CS playing an important role in *P. aeruginosa* infection [274].

The GacSA system is essential in *P. aeruginosa* pathogenesis, both in mammals and in *Caenorhabditis elegans* [35]. GacSA activates quorum sensing and virulence determinants. Specifically, GacSA exerts a post-transcriptional control of C4-HSL and virulence factors such as T6SS [275]. This system is also important in biofilm formation: it has been shown that GacS promotes biofilm development when dephosphorylated, but it has opposite effects in the phosphorylated state [120]. RsmA directly binds the *pel* mRNA and controls the production of Pel [276] and indirectly controls Psl [108].

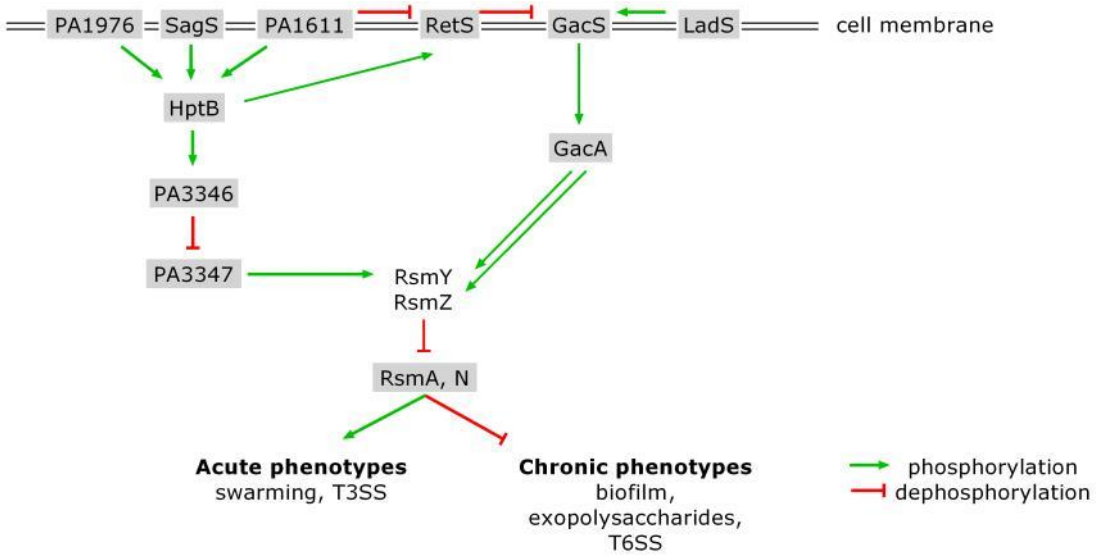
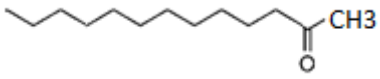


Figure 1.5. Gac/Rsm regulatory network in *P. aeruginosa*. Three sensor kinases (SK), PA1976, SagS and PA1611, activate the histidine phosphotransfer protein HptB. This leads to the activation of the response regulator PA3346, which dephosphorylates the anti-anti-sigma factor PA3347. RetS and LadS are sensor kinases that modulate the activity of GacS. The small RNAs RsmY and RsmZ can be activated by PA3347 and by GacA. In turn, these small RNAs sequester the global regulator RsmA, leading to a chronic phenotype. Adapted from [277], and with additional information from [278]. T3SS, type 3 secretion system; T6SS, type 6 secretion system.

1.5 2-Tridecanone as a bacterial signal molecule

The ketone 2-tridecanone (2TDC) is a compound produced by highly diverse organisms: it has been detected in plants including *Zanthoxylum alatum* and *Lycopersicon hirsutum* f. *glabratum*, the wild tomato [279], and animals like the deer *Odocoileus sp.*[280]. It is well known for its insecticidal activity [279, 281, 282].

Table 1.3. General features of the 2-tridecanone.

Name, abbreviation	Producer	Formula
2-tridecanone, 2TDC	various plant species animals (*Odocoileus hemionus columbianus*) *S. meliloti*	

This ketone has also been found in bacteria and it can accumulate in a Δ*fadD* mutant of *Sinorhizobium meliloti.* This mutated gene presents similarity to the *E. coli fadD*, as well as 55 % identity to *rpfB* from *X. campestris* [283], encoding a predicted long-chain fatty acyl-CoA ligase which has a role in the biosynthesis of DSF. The relationship between *rpfB* homologues and the synthesis of 2TDC requires further work.

The production of this molecule in *S. meliloti* raises the question of whether it is used as a signal molecule by bacteria. Research in this direction shows that 2TDC functions as a signalling molecule with inter-species effects [284]. However the mechanisms of sensing and the biological relevance are not yet understood.

1.6 Project overview and aims

Quorum sensing (QS) systems are used by bacteria to sense and respond to changes in population density. Although QS systems based in AQ and AHL have been extensively studied in *P. aeruginosa*, research in recent years has shown that they are far more complex than anticipated. Notably, a novel regulatory network based in DSF-T was identified, first in *X. campestris* and later on in multiple bacteria. In *P. aeruginosa,* the DSF-T CDA has shown to affect biofilm formation and development and shift persister cells to a metabolically active state. These are similar effects to those shown in other DSF-T networks, particularly with regards to biofilm formation and virulence. However, several key elements of the CDA network have not yet been investigated in depth. The full extent of effects that CDA promotes in *P. aeruginosa*, the particular growth conditions in which those effects are more critical for the biology of this bacterium, and the regulation behind the production and metabolism of this signal molecule have not been elucidated. Signal molecules involved in QS can also mediate cross-talk between different species and may therefore have a huge impact in the ecology of a particular niche. Inter-species communication can be mediated by many of the known DSF-T, and CDA is not an exception. In particular, CDA inhibits biofilm formation in several bacterial species and in the yeast *C. albicans* (albeit under specific conditions). **Chapter 3** analyses a transcriptomic study performed previous to this thesis, in the presence and absence of CDA, and characterises several processes in which this fatty acid affects the biology of *P. aeruginosa.* **Chapter 3** also studies the role of DSF and BDSF in *P. aeruginosa* phenotypes, to try to elucidate the effects of non-cognate DSF-T molecules in this bacterium.

Another key feature of CDA that has not been fully understood is the regulation and metabolism of this fatty acid. Research conducted in other bacteria has identified several DSF-T synthases. Homology studies of the primary, secondary and tertiary structure of RpfF in *Xcc* and in *B. cenocepacia* are presented in **Chapter 4** to identify candidates driving the metabolism of CDA in *P. aeruginosa.* Similarly, sequence homology and domain organisation are used to evaluate SK in *P. aeruginosa* and identify candidates for the sensing of CDA in this bacterium. Then, research of **Chapter 4** focuses on the characterisation of PA0744 and PA0745 for their potential roles in the biosynthesis of CDA, and in the characterisation of CbsA as a possible regulator of this fatty acid. Research in CbsA includes the analysis of an RNA-seq performed previous to this thesis, which compares the transcriptome of a wild-type PAO1 with an inducible mutant of CbsA in induced and uninduced conditions.

A natural occurring ketone named 2TDC has shown to modulate virulence and social interaction in an enormous variety of organisms, including deer and the tomato plant. The effects of 2TDC have been studied elsewhere in *S. meliloti*, *P. syringae* and *S. enterica*; but the effects on *P. aeruginosa*, sharing some of the same environments of these bacteria in nature, have not been elucidated yet. With the broad aim of better understanding cell-to-cell communication, inter-species communication and virulence in *P. aeruginosa*, **Chapter 5** focuses on the impact of this fatty acid-derived molecule in *P. aeruginosa*, especially with regards to niche colonisation.

Altogether, this study aims to better understand novel mechanisms of cell-to-cell interaction, and to set the basis for further ecological studies. The specific aims for this work are to:

- Understand the effects of CDA and other DSF-T molecules in *P. aeruginosa,* and how they compare to the effects in their cognate producers
- Get an insight into the metabolism and regulation of CDA in *P. aeruginosa*
- Understand the impact of 2TDC in *P. aeruginosa* and how this compares to the effects this molecule has on other bacterial species

2 EXPERIMENTAL PROCEDURES

2.1 Bacterial cell manipulation

2.1.1 Media and antibiotic concentrations

Lysogeny broth (LB) medium was used for general procedures. Where required, antibiotics were used at the following concentrations: for the culture of *E. coli,* ampicillin (Ap), 100 µg/mL; tetracycline (Tc), 25 µg/mL; gentamicin (Gm), 20 µg/mL; kanamycin (Km), 25 µg/mL. For the culture of *P. aeruginosa,* carbenicillin (Cb), 400 µg/mL; Tc, 100 µg/mL; Gm, 20 µg/mL. Plates were supplemented with nalidixic acid (Nal) at 15 µg/mL for the selection of transconjugants. Whenever IPTG was used to induce gene expression, the concentration was 1 mM, and sucrose was used at a concentration of 5-10 %. When using the highest concentrations of sucrose, a modified LB medium was used that did not contain NaCl to avoid cell lysis by osmosis.

2.1.1.1 Casamino acids medium

Casamino acids-derived medium (CAA) was used for pyoverdine assays, both in liquid cultures and agar plates, as described previously [285]. It contained 0.5 % casamino acids (Sigma), 3.3 mM K_2HPO_4 and 3 mM $MgSO_4$. For solid medium, 0.5 % D-glucose and 0.5 % Bacto Agar (BD) were added; whereas for liquid broth, it was supplemented with 2 % glycerol to allow for better growth of *P.* aeruginosa cells.

2.1.1.1 Chemically defined medium

Chemically defined medium (CDM) was used for growth assays and contained 3 mM KCl, 3 mM NaCl, 12 mM $(NH_4)_2SO_4$, 3.2 mM $MgSO_4$, 0.02 mM $FeSO_4$, 1.2 mM K_2HPO_4 and 50 mM 3-(N-morpholino)propanesulfonicacid (MOPS), pH 7.8 [286]. It was supplemented with 10 mM D-glucose.

2.1.1.2 M9 minimal medium

M9 medium was used for the growth of biofilms. It was comprised of 240.7 mg/L $MgSO_4$, 11.098 mg/L $CaCl_2$ and 0.4 % D-glucose, and a series of salts that were

prepared previously at a 5x concentration, with a final concentration of 1 g/L NH_4Cl, 6.78 g/L Na_2HPO_4, 3 g/L KH_2PO_4, and 0.5 g/L NaCl.

2.1.1.3 Nutrient Broth

Nutrient Broth (NB) was used for motility assays, rhamnolipid determination from liquid cultures and plates, biofilm formation in the presence of 2TDC and verification of the effect of ECH in pyocyanin.

The composition of this medium has been described elsewhere [287], with certain variations. It contains 0.8 % (w/v) Nutrient Broth No.2 (Oxoid) and 0.5 % (w/v) D-glucose. Whenever required, it was supplemented with Bacto Agar (BD).

2.1.1.4 *Pseudomonas* isolation agar

Pseudomonas isolation agar (PIA, BD) was used to select *Pseudomonas* transconjugants. This medium was prepared as stated in the manufacturer's instructions and consisted of 20 g/L enzymatic digest of gelatin, 1.4 g/L $MgCl_2$, 10 g/L K_2SO_4, 0.025 g/L 5-chloro-2-(2,4-dichlorophenoxy)phenol (irgasan), 13.6 g/L agar, and was made in distilled water with the addition of 2 % (v/v) glycerol.

2.1.1.5 Soft top agar

Soft top agar was used to overlay thin layer chromatography (TLC) plates with the AQ biosensor strain. This medium contains 1 % (w/v) tryptone, 0.5 % (w/v) NaCl, 0.65 % (w/v) and Technical Agar No. 3 (Oxoid).

2.1.2 Culture growth

Except otherwise stated, bacterial cultures were grown at 37 ºC with 200 rpm shaking. Conical flasks were filled to a 10 % of their total volume to allow for good oxygenation. Culture growth was monitored by measuring optical density at 600 nm (OD_{600}) with a Novaspec II Visible Spectrometer (Pharmacia LKB Ltd, Cambridge, UK), or an automated spectrometer (Tecan Infinite 200).

2.1.3 Bacterial storage

For long term storage of bacterial strains, overnight cultures were mixed with glycerol to a final concentration of 15 % and stored at -80 ºC.

2.2 General chemicals

Except otherwise stated, all chemical compounds were purchased from Sigma-Aldrich.

Cis-2-decenoic acid was purchased from Carbosynth (UK) and U-Chemo (China). *Trans*-2-decenoic acid was obtained from TCI Chemicals, (UK).

2.3 DNA manipulation

2.3.1 Strains and plasmids

Bacterial strains and vectors used in this study are listed in **Table 2.1**.

Table 2.1. Strains and plasmids used in this study. *, This study; **, The sequence of pEX19Gm is identical to pEX18Gm, except from the inversion in the multiple cloning site.

Name	Genotype	Reference
E. coli		
DH5α	F⁻ Φ80*lac*ZΔM15 Δ(*lac*ZYA-*arg*F) U169 *rec*A1 *end*A1 *hsd*R17 (rK^-, mK^+) *pho*A *sup*E44 λ– *thi*-1*gyr*A96 *rel*A1	[288]
S17-1 λ*pir*	*recA, thi, pro*, *hsdR*-M^+RP4: 2-Tc:Mu:Km Tn7 *λpir*, Tp^R Sm^R	[289]/ATCC 47055
P. aeruginosa		
ΔpqsA-L	PAO1-L, Δ*pqsA*	[290]
PADP116	PAO1-L P*phzA1-dsRed,* P*phzA2-luxCDABE* constructed from PA1DA2L	*
PADP127	PAO1-L Δ4982	*
PADP132	PAO1-L P*phzA2-dsRed,* P*phzA1-luxCDABE* constructed from PA2DA1L	*
PADP135	PAO1-L Δ0745	*
PADP14	PAO1-L Δ0744, Δ0745	*
PADP159	PAO1-L Δ*hptB*	*
PADP165	PAO1-L Δ*gacA*	*
PADP228	PAO1-L, pmini-CTX-lux, Tc^R	*
PADP236	PAO1-N, pmini-CTX-lux, Tc^S	*
PADP294	PAO1-L, P*mucR-luxCDABE* constructed from pDP293	*
PADP302	PAO1-L, P*bifA-luxCDABE* constructed from pDP296	*
PADP303	PAO1-L, P4929-*luxCDABE* constructed from pDP297	*
PADP305	PASC315 tagged with miniTn7-P*rrnA-gfp,* Tc^R Gm^R	*
PADP32	PAO1-L 0745*, non-polar mutant for 0745	*
PADP326	PA14, miniTn7-P*rrnA-gfp*	*

PADP33	PAO1-L, P*lecB-luxCDABE*, Tc^R	*
PADP44	PAO1-L::miniTn7-P*rrnA-gfp*, Gm^R	*
PADP93	PAO1-L, promoterless pmini-CTX1-*dsRed* control constructed from pDP51	*
PAO1-L	PAO1 Lausanne subline, wild-type	Dieter Haas, Université de Lausanne
PAO1-N	PAO1, Nottingham subline	Laboratory collection, derived from Holloway's isolate [291]
PAO6382	PAO1-L Δ*pvdF*	[292]
PAO6901	PAO1-L Δ*pvdS*::Gm^R	[293]
PAPD239	PAO1-L Δ4982 tagged with miniTn7-P*rrnA-gfp*, Gm^R	*
PASB05	PAO1-L Δ*rhlA*	Sebnem Bukavaz, University of Nottingham
PASB12	PAO1-N, Δ*rhlC*	Sebnem Bukavaz, University of Nottingham
PASC139	PAO1-L, P*rsmZ-luxCDABE* constructed from pKR121 (Karima Righetti), Tc^R	[294]
PASC141	PAO1-L, P*rsmY-luxCDABE* constructed from pKR26 (Karima Righetti), Tc^R	[294]
PASC203	PAO1-L Δ*cbsA*	[294]
PASC315	PAO1-L, *lacI^q,* P*tac-cbsA,* IPTG-inducible expression of CbsA, Sm^R Sp^R	[294]
PASC638	PAO1-N Δ*rsmY*	[294]
PASC659	PAO1-N ΔrsmY ΔrsmZ	[294]
PASC682	PAO1-L, P*rhlA'-'dsRed_express2* constructed with pSC274	[294]
PASC815	PAO1-L Δ0744	[294]
PASH12	PAO1-N, PPA2567-*luxCDABE* constructed from pSH12	Stephan Heeb, University of Nottingham
UCBPP-PA14	hypervirulent clinical isolate, generally referred to as PA14	[295]
Others		
SADP01	*Staphylococcus aureus* Newman strain for LasA assay	[296]/25904
Plasmids		
pA1DA2L	pminiCTX-P*phzA2-luxCDABE*, P*phzA1-dsRed2*	[297]
pA2DA1L	pminiCTX-P*phzA1-luxCDABE*, P*phzA2-dsRed2*	[297]
pBK-miniTn7-PrrnA-gfp	pUC19-derived miniTn7 delivery plasmid for constitutive GFP tagging, Gm^R	Birgit Koch, Newcastle University
pBS	pBluescript-II KS(+) cloning vector, Ap^R	[298]/X52329
pCdrA::gfp^C	pUCP22Not-P_{cdrA}-RBSII-*gfp* (Mut3)-T_0-T_1, Ap^R, Gm^R	[299]
pDP107	pME3087-based construct for PADP135 (Δ0745). Flanking regions of PA0745 were digested from pSC217 (with KpnI and EcoRI) and pSC218 (with EcoRI and XbaI)	*
pDP129	pEX18Gm construct for PADP32 (Δ0745*). Primers 0745*_UF and 0745*_UR, and primers 0745*_DF and 0745*_DR were used to amplify 2 genomic regions and introduce mutations	*

pDP146	pME3088-based construct for PADP14 (Δ0744 Δ0745). The upstream region of PA0745 was digested from pSC217 with XhoI and BamHI, and the downstream region of PA0744 was digested from pSC810 with BamHI and KpnI	*
pDP181	PA0744 and PA0745 inserted into pME6032, EcoRI and BglIII, amplified with primers PA0745_Fw and PA0744_Rv	*
pDP22	406 bp upstream *lecB* amplified using primers lecB_Fw and lecB_Rv, inserted into BamHI/PstI sites in pminiCTX-lux, Tc^R	*
pDP275	*dsRed_express2* cloned into pUCP18, promoterless reporter vector control	*
pDP293	568 bp upstream *mucR* amplified using primers mucR_Fw and mucR_Rv, inserted into XhoI/EcoRI sites in pminiCTX-lux, Tc^R	*
pDP296	521 bp upstream *bifA*, amplified using primers bifA_Fw and bifA_Rv, inserted into XhoI/EcoRI sites in pminiCTX-lux, Tc^R	*
pDP297	533 bp upstream PA4929 amplified using primers 4929_Fw and 4929_Rv, inserted into XhoI/EcoRI sites in pminiCTX-lux, Tc^R	*
pDP327	410 bp upstream PA2072 amplified using primers 2072_Fw and 2072_Rv, inserted into XhoI/PstI sites in pminiCTX-lux, Tc^R	*
pDP51	*dsRed_express2* cloned into pmini-CTX1, promoterless reporter vector control	*
pEX18/19Gm	gene replacement vector, $oriT^+$ $sacB^+$ Gm^R	[300]AF047518**
pEX19Gm::Δ4982	construct for deletion of PA4929 in *P. aeruginosa*	Steve Porter, University of Exeter
pEX19GmΔgacA	construct for deletion of *gacA* in *P. aeruginosa*	Steve Porter, University of Exeter
pEX19GmΔhptB	construct for the deletion of *hptB* in *P. aeruginosa*	Steve Porter, University of Exeter
pFlp2	site-specific excision vector, Cb^R	[300]/AF048702
pME3087	suicide vector for allelic replacement, Tc^R	[301]
pME3088	suicide vector for allelic replacement, Tc^R	[301]
pME6032	Δ*lacI*, P*tac* shuttle expression vector	[302]/DQ645594.1
pmini-CTX1	*P. aeruginosa* chromosome integration-proficient vectors	[303]
pminiCTX-lux	integration proficient vector with ΩFRT-*attP*, Tc^R, containing the *luxCDABE* operon downstream the multiple cloning site	[304]/AF251497
pminiCTX-PlasI-lux	transcriptional fusion of *lasI* upstream region to *luxCDABE* operon, in pminiCTX-lux	Giordano Rampioni, University of Nottingham
pminiCTX-PpqsA-lux	transcriptional fusion of *pqsA* upstream region to *luxCDABE* operon, in pminiCTX-lux	[153]
pminiCTX-PrhlI-lux	transcriptional fusion of *rhlI* upstream region to *luxCDABE* operon, in pminiCTX-lux	Giordano Rampioni, University of Nottingham
pSC217	pBluescript-II KS(+) containing a 512 bp insert upstream PA0745, amplified with primers PA0745_UF and PA0745_UR, XhoI and EcoRI	Ye Chen, University of Nottingham
pSC218	pBluescript-II KS(+) containing a 512 bp insert downstream PA0745, amplified with primers PA0745_DF and PA0745_DR, EcoRI and XbaI	Ye Chen, University of Nottingham

pSC3	PA0745 inserted into pME6032, EcoRI and ClaI, Tc^R	[294]
pSC323	PA0744 inserted into pME6032, EcoRI and XhoI, Tc^R	[294]
pSC58	PA3426 (*cbsA*) inserted into pME6032, EcoRI/MfeI and XhoI, Tc^R	[294]
pSC581	source of *dsRed_express2*	[294]
pSC810	pBluescript-II KS(+) containing a 410 bp insert downstream PA0744, amplified with primers PA0744.d.fw and PA0744.d.rv, BamHI and KpnI	Ye Chen and [294]
pSC855	495 bp upstream of *pelA* inserted with KpnI/HindIII, and *dsRed_express2* inserted with HindIII/EcoRI into pUCP18, Cb^R	[294]
pSC856	500 bp upstream of *pslA* with KpnI/HindIII, and *dsRed_express2* inserted with HindIII/EcoRI into pUCP18, Cb^R	[294]
pUCP18	shuttle vector for gene expression	[305]/U07164.1
pUX-BF13	helper plasmid for GFP tagging containing the transposase genes, Ap^R, mob^+	[306]

2.3.2 Molecular procedures

Standard molecular biology techniques were performed, as described elsewhere [307]. Plasmids were extracted with the GenElute Plasmid Miniprep Kit (Sigma-Aldrich). Chromosomal DNA extractions were performed using the GenElute Bacterial Genomic DNA Kit (Sigma-Aldrich).

PCR amplicons were cleaned from remaining reagents with the Geneclean turbo kit (MP Biomedicals). Unmodified primers were used for PCR amplification (Sigma-Aldrich). The PCR master mix contained the ready-to-use GoTaq Green Master Mix (Promega) and 1 µM of each primer, and was supplemented with DMSO (1-10 %) when necessary.

For plasmid and PCR amplicon digestions, Promega enzymes were used. The digestions were run in a 0.7 % agarose electrophoresis gel, and relevant bands were recovered when needed using the Genelute turbo kit (MP Biomedicals). For ligation reactions, 1 unit of T4 DNA ligase (Promega) was used as recommended by the supplier. When elevated concentrations of vector were required, the ligation reactions were dialysed using 0.025 µm membrane filters (Millipore).

Electrocompetent *E. coli* cells were prepared with 3 washes of glycerol 10 % in molecular water at 4 ºC. The resulting concentrated cell culture was aliquoted, and 50 µL were used for each electroporation. Electrocompetent *Pseudomonas sp.* were prepared similarly, taking cells grown overnight at 42 ºC. In both cases, the Bio-RAD MicroPulser delivered 12.5 kV/cm per pulse in a 0.2 cm electroporation cuvette.

During these procedures, DNA concentration and purity was assessed with the Nanodrop ND-1000 (Nanodrop Technologies).

DNA sequencing was performed by the DNA Sequencing Laboratory, Queen's Medical Centre (Nottingham), using the BigDye Termination v3.1 Cycle Sequencing Kit and the 3130xl Genetic Analyzer (Applied Biosystems).

For the transfer of genetical material by conjugation, overnight cultures grown at 37 ºC (for *E. coli*) or 42 ºC (for *P. aeruginosa*) were washed with fresh LB and mixed together. The mixture was concentrated by centrifugation and spotted on a dried LB agar plate. After 4-6 h incubation at 37 ºC, the cells were recovered and resuspended, then plated in selective media and incubated overnight at 37 ºC. Transconjugants were then restreaked into new plates in order to completely counterselect parental, sensitive cells.

2.3.3 Construction of biosensors

The pminiCTX-lux plasmid [304] was used for biosensor construction. Appropriate restriction sites were introduced by PCR into upstream regions of the genes of interest by using the oligonucleotides listed in **Table 2.2**, and cloned into pminiCTX-lux. The light output during bacterial growth was then measured with an automated luminometer/spectrometer (TECAN GENios Pro).

Table 2.2. Primers used for reporter construction. Restriction enzyme sites are underlined. Fw, forward primer; Rv, reverse primer.

Name	Sequence (5' → 3')	Restriction sites
2072_Fw	ATACTCGAGGTGATGAAGGTCGAGGTGGT	XhoI
2072_Rv	ATACTGCAGGGGCCTTGGTCACTGTCTTA	PstI
4929_Fw	ATACTCGAGGGACCTTGTCCTGCCAGTAG	XhoI
4929_Rv	ATAGAATTCCCTGGTGCCCGTGATG	EcoRI
bifA_Fw	ATACTCGAGCAAGAGCCTCGAAGAGATCG	XhoI
bifA_Rv	ATAGAATTCTTCCTGAGGGTAGACGATGG	EcoRI
lecB_Fw	TATGGATCCGGCAGGAAGGACGCATCG	BamHI
lecB_Rv	TATCTGCAGATAGCGACTTGAACCCAACG	PstI
mucR_Fw	ATACTCGAGATGGGTGGCATACATCACCT	XhoI
mucR_Rv	ATAGAATTCTAGCGGGAGAGAAGTGGTTG	EcoRI

2.3.4 Microtiter plate assay

The combined spectrophotometer/fluorimeter/luminometer Infinite F200 (TECAN) was used to measure the fluorescence of cultures growing in liquid. Briefly, overnight cultures were diluted 100 times and added to 96-well plates (Greiner),

previously sterilized by UV light. The unused wells of the plate were filled with medium to lower the evaporation of the samples. Plates were then incubated 12-36 h in a moisturised tank. The fluorescence (in relative fluorescent units, RFU) and the OD_{600} were then measured [308]. Excitation/emission wavelengths of 535 nm/595 nm and 485 nm/535 nm were used for the measurement of DsRed and GFP, respectively.

The luminescence of cultures from liquid cultures was determined similarly, by diluting overnight cultures 100 times and measuring relative luminescent units (RLU) and OD_{600}, every 30 min for 24 h.

2.3.5 Reporter gene expression of strains grown on agar plates

To measure the expression of reporter strains growing in solid media in the presence of 2TDC, plates were prepared with 1.5 % agar and 20 mL of either LB or NB were poured per plate. Once the plates were dried, overnight cultures were standardised at OD_{600}=1.0 and 3 µL were spotted on the agar. Then 20 µL of either EtOH (as a solvent control) or 2TDC were added to the lid of the plates, and plates were incubated statically at 37 ºC for a set time.

After the incubation period, the spots were recovered with a loop and diluted in 1 mL of distilled water. Then, 300 µL were added to each well of a 96-well plate (Greiner) and a single read was performed with a combined spectrophotometer/fluorimeter/luminometer (TECAN).

2.3.6 Construction of deletion mutants and their complementation

Mutants in sensor kinases

The suicide plasmid pEX19Gm was used to construct in-frame deletion mutants. This vector contains a gentamicin resistance selectable marker, and a counter-selection marker, *sacB* [309].

Mutants were constructed by double cross-over homologous recombination. The mechanism of deletion was as follows: the pEX19Gm-based construction was electroporated into *E. coli* S17-1 λ*pir* and then conjugated into *P. aeruginosa* (see **2.3.2**). The constructions in pEX19Gm were comprised of 150-200 bp fragments homologue to each extremity of the target gene. Constructions were verified by sequencing prior to performing the conjugations. By a single recombination event, the plasmids were inserted in PAO1-L chromosome. The transconjugants were subsequently grown in LB supplemented with sucrose,

selecting for the second cross-over event. The unmarked mutants were then checked by PCR, with primers annealing in the deleted region, and primers flanking said region. Primer sequences are shown in **Table 2.3**.

Table 2.3. Primer sequences to screen the in-frame deletion mutants in two-component systems. Fw, forward; Rv, reverse.

Name	Sequence (5' → 3')
PA4982_out_Fw	CGCAACTGATCATCACCATC
PA4982_out_Rv	GTGAGTTGCAGCCTTTCCTT
PA4982_in_Fw	TGCTGTTCAGCCTGTGTTTC
PA4982_in_Rv	GAAGTGGAGGACCTCGTTGA
hptB_out_Fw	GTGGTGTCCGTGGAGTTTTT
hptB_out_Rv	ACCGAAAACGTCTTTGAGGA
hptB_in_Fw	TATCCGGTCCTGCTGGATAC
hptB_in_Rv	ATAGCGCTGACGTTCCTGTT
gacA_out_Fw	CGAATGATGTTTCCATGACG
gacA_out_Rv	GGACTTGCGGAAATAGCTG
gacA_in_Fw	GGCCGACTGCGGTGAAGACT
gacA_in_Rv	GCCAGTTCCACGTCGCTGGT

Enoyl-CoA hydratase mutants

The in-frame deletion mutants for PA0745 (PADP135) and the double mutant Δ0744 Δ0745 (PADP14) were constructed using the following strategy: fragments of sequences flanking the targeted gene(s) were digested from previously constructed vectors [294] and cloned into the suicide vectors pME3087 and pME3088.

For the construction of PADP135 the vector pSC217, containing the upstream region of PA0745, was digested with KpnI and EcoRI; and the construct pSC218, containing the downstream region of PA0745, was digested with EcoRI and XbaI. The suicide vector pME3087 was digested with KpnI and XbaI and a triple ligation was then performed. The resulting construct, named pDP107, was electroporated into *E. coli* S17-1 λ*pir* and conjugated into PAO1-L. For the construction of PADP14, the upstream region of PA0745 was digested from pSC17 with XhoI and BamHI, and the downstream region of PADP0744 was digested from pSC810 with BamHI and KpnI. The suicide vector pME3088 was digested with XhoI and KpnI, and a triple ligation was then performed to construct pDP146. This vector was conjugated into PAO1-L. The primers used previous to this thesis for the construction of the vectors pSC17, pSC218 and pSC810 are listed in **Table 2.4**.

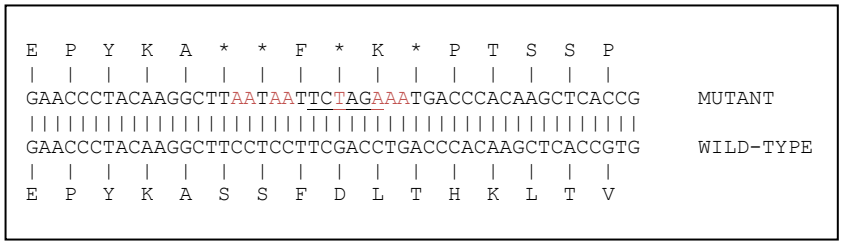
The selection procedure for mutants constructed with pME3087 or pME3088 is equivalent to the one employing pEX19Gm, except there is no counter-selection

procedure. In this case, the proportion of clones undergoing the second cross-over is increased using an enrichment protocol. Briefly, transconjugants were selected in LB plates supplemented with Tc 200 µg/mL. Resistant clones were cultured overnight in LB. Then, the cultures were restarted in fresh LB using a 1/100 dilution, and supplemented with bacteriostatic concentrations of Tc. The growing cells were killed with the addition of Cb, and the resulting culture was plated in LB.

Directed mutagenesis of PA0745

To construct a non-polar mutant of PA0745 (PADP32), flanking regions of PA0745 were amplified by PCR using the primers PA0745*_UF, PA0745*_UR (upstream region) and PA0745*_DF and PA0745*_DR (downstream region) (**Table 2.4**). The primers upstream reverse (PA0745*UR) and downstream forward (PA0745*DF) were modified to introduce an XbaI site and 4 stop codons, as well as a frameshift. **Figure 2.1** shows the resulting sequence.

Figure 2.1. Schematic of the mutations introduced in the non-polar mutant for PA0745, 0745* The mutated base pairs are shown in red, and the introduced XbaI site is underlined. *, STOP codon.



The suicide vector pEX18Gm was digested with KpnI and HindIII, and the PCR products were ligated by triple ligation. The resulting pDP129 construct was then electroporated into *E. coli* S17-1 λ*pir* and subsequently conjugated into PAO1-L cells. Potential mutants were amplified by PCR using PA0745*_UF and PA0745*_DR primers, and then screened in an XbaI digestion reaction.

Table 2.4. Primers used to construct enoyl-CoA hydratase deletion mutants. The restriction sites are underlined, and mutations are written in lower case. The non-polar mutant of PA0745 PADP135 is referred to as 'PA0745*".

Name	Sequence (5' → 3')	Restriction sites
PA0745_UF	ATACTCGAGATCGCCAGTTGTTCCCTGG	XhoI
PA0745_UR	ATAGAATTCGGCAGTGTTCATGAAGTCC	EcoRI
PA0745_DF	ATAGAATTCCGCAACTGCTGAGCCTTC	EcoRI
PA0745_DR	ATATCTAGAGGCCGATGCCGATCTCC	XbaI
PA0744.d.fw	ATAGGATCCGGGCTCTGATCCGCCGC	BamHI
PA0744.d.rv	ATAGGTACCATGGTCGAGCATTCCAGCA	KpnI

PA0745*_UF	ATAGGTACCGCTTCGTCTATGCCATGAAA	KpnI
PA0745*_UR	ATATCTAGAAttAttAAGCCTTGTAGGG	XbaI
PA0745*_DF	ATATCTAGAaaTGACCCACAAGCTCACC	XbaI
PA0745*_DR	ATAAAGCTTCGCTGTCCACCACCTGTT	HindIII

None of the promoters for these genes have been mapped. Therefore, the mutants were complemented by cloning the targeted genes into pME6032. This way, the transcription is controlled by the P*tac* promoter, resulting in a controllable expression of the corresponding genes by the adding IPTG to the media. Constructions pME6032::0744 and pME6032::0745 were made previously in Nottingham and named pSC323 and pSC3, respectively [294].

Primers PA0745_fw and PA0744_rv were used together to amplify by PCR both 0745 and 0744 and complement the double mutant PADP14. The primers used are stated in **Table 2.5**.

Table 2.5. Primers used to construct the complementing plasmid pME6032::0745-0744. Restriction enzyme sites are underlined. Fw, forward; Rv, reverse.

Name	Sequence (5' → 3')	Restriction sites
PA0745_Fw	ATAGAATTCATGAACACTGCCGTCGAAC	EcoRI
PA0744_Rv	ATAAGATCTTCAGAGCCCCGCCAGC	BglIII

2.4 Deep Sequencing analysis

Deep Sequencing is a methodology used to produce transcriptomic profiles from total RNA extractions. In summary, the reads are mapped to a reference genome and filtered to remove unwanted sequences, e.g. rRNA and tRNA. Then, the counts for each transcript are normalised by calculating the reads per Kb per million reads (RPKM) [310]. RPKM is a read count corrected against the total length of the mapped transcriptome and the length of the transcript, which facilitates the comparison between reads of different lengths.

2.4.1 Previous work

Two Deep Sequencing reactions were performed previously in Nottingham [294]. The first comprised *P. aeruginosa* PAO1-L cultures in middle log phase (4 h), grown in MetOH as a control, and in presence of CDA in a concentration of 100 μM. In the second sequencing, the PAO1-L conditional mutant for CbsA (PASC315) was grown 5 h under two conditions: in the absence of IPTG, this mutant behaves as a knock-out for CbsA; while in the presence of 1 mM IPTG, CbsA is overexpressed. PAO1-L grown in LB was used as a control in this second

extraction. Independent duplicates were used for each condition, in both assays. Sequencing of PAO1-L in the presence and absence of CDA was conducted with SOLiD (LifeTechnologies, USA), while the second sequencing used SOLiD 5500xl system [294]. In order for the experiments to be consistent, both datasets were mapped to PAO1-L, using LifeScope software version 2.5.1.

The data was analysed using two statistical tests in order to identify genes differentially expressed. The tests used were DESeq [311] and Baggerly's test [312]. The false discovery rate (FDR) was also calculated, and the threshold for relevance was set at 0.1 for both tests.

Both statistical tests take into account the biological variation of the data, and use a modified t-test statistic [313]. However, they rely on markedly different procedures. DESeq assumes a negative binomial distribution of the data. Baggerly's test assumes a binomial distribution of the data and compares the proportion of counts (against the total counts of the sample) between different datasets.

2.4.2 Representation of results and criteria

Venny was used to analyse data with Venn diagrams [314]. Microsoft Excel was used for the implementation of macros to call RPKM results, PA numbers, function of genes, and gene ID.

For the volcano plots, only statistically significant genes were plotted in order to facilitate the visualisation of results. The following data was plotted:

$$x\ axis = \log fold = \log_2 Condition1 - \log_2 Condition2$$
$$y\ axis = significance = \log_{10}(p - value)$$

In general, RPKM values were considered as valid when at least one of the statistical tests showed differential expression with an FDR of 0.1. However, when the majority of genes in an operon had a consistent trend, the results were also taken into account even if not significant. The *Pseudomonas* Genome Database was used as a search tool during this analysis [315].

2.4.3 Functional database

The database of clusters of orthologous groups of proteins (COG) takes into account a functional classification of the proteins encoded in 21 genomes, which classifies protein function according to 17 categories, listed in **Table 2.6**. COG accession numbers and categories were downloaded from NCBI (update 2014)

[316]. The PA numbers and related COG accession numbers were taken from the *Pseudomonas* Genome Database. Then, a macro was adapted to assign each PA number with its correspondent COG and category.

Table 2.6. Functional categories present in the COG database. These categories rationally classify proteins to aid functional studies.

Code	Category
A	RNA processing and modification
B	Chromatin structure and dynamics
C	Energy production and conversion
D	Cell cycle control, cell division, chromosome partitioning
E	Amino acid transport and metabolism
F	Nucleotide transport and metabolism
G	Carbohydrate transport and metabolism
H	Coenzyme transport and metabolism
I	Lipid transport and metabolism
J	Translation, ribosomal structure and biogenesis
K	Transcription
L	Replication, recombination and repair
M	Cell wall/membrane/envelop biogenesis
N	Cell motility
O	Post-translational modification, protein turnover, chaperones
P	Inorganic ion transport and metabolism
Q	Secondary metabolites biosynthesis, transport and catabolism
T	Signal transduction mechanisms
U	Intracellular trafficking, secretion and vesicular transport
Y	Nuclear structure
Z	Cytoskeleton
R	General function prediction only
S	Function unknown
V	Defence mechanisms
W	Extracellular structures
X	Mobilome: prophages, transposons

Approximately 900 genes did not have a function assigned in the database; a proportion of which were classified using the guidelines in **Table 2.7**.

Table 2.7. Functional categories from the COG database assigned according to listed functions in the *Pseudomonas* Genome Database. These guidelines were followed with an aim to assign COG categories to previously unclassified genes of the *P. aeruginosa* genome.

Function in *Pseudomonas* Genome Database	Category assigned
hypothetical protein	S: Unknown function
conserved hypothetical protein	S: Unknown function
tRNA	J: Translation, ribosomal structure and biogenesis
ribosomal protein	J: Translation, ribosomal structure and biogenesis

alginate	M: Cell wall, membrane, envelope
pvdP	P: Inorganic ion transport
type 3 export apparatus protein	U: Intracellular trafficking, secretion and vesicular transport
type 4 fimbrial biogenesis protein PilY2	N: Cell motility
pyocins	V: Defence mechanisms
transcriptional regulators	K: Transcription
regulatory RNAs	O: Post-translational modification, protein turnover, chaperones, and additional % sign

Categories that would be useful for subsequent analysis were then added to the existent list, and are listed in **Table 2.8** (for the complete list of genes, see **Appendix, section 7.1.1**).

Table 2.8. Additional categories created in the functional annotation database to respond to particular interests of this project.

Additional category	Functions
ᵒ: Biofilm formation and regulation	extracellular polymeric substances, including *pel* and *psl* operons, alginate biosynthesis, and regulators of biofilm formation.
ⁱ: Sensory pathways	two-component systems, probable two-component systems and histidine phophotransfer proteins
ᵃ: c-di-GMP regulation	genes containing either GGDEF and/or EAL motifs (from Kulesekara, Lee [207]) or HD-GYP (Stephan Heeb, personal communication)

As a result of these classifications, the functional database created currently comprises a total of 5563 ORFs annotated and 124 not annotated.

In a further step of complexity, some genes have more than one annotation in the COG database, so a hierarchy was put in place: those categories that were important for this thesis are shown in green and were considered in hierarchical order, starting from the top of **Table 2.9**. Those categories in salmon were considered secondary, and were added after the ones in green, if present. The "R" and "S" categories were only taken into account when no other category was annotated.

Table 2.9. Hierarchy of COG categories. A hierarchy was established COG categories together with the additional categories created. The categories were classified onto primary functions (in green), secondary functions (salmon) and others (burgundy), according to the interests of this thesis.

Code	Category
ᵒ	Biofilm formation and regulation
ᵃ	c-di-GMP regulation
N	Cell motility

i	Sensory pathways
%	Regulatory RNAs. Those are also part of category "O"
J	Translation, ribosomal structure and biogenesis
O	Post-translational modification, protein turnover, chaperones
K	Transcription
U	Intracellular trafficking, secretion and vesicular transport
I	Lipid transport and metabolism
V	Defence mechanisms
A	RNA processing and modification
B	Chromatin structure and dynamics
C	Energy production and conversion
D	Cell cycle control, cell division, chromosome partitioning
E	Amino acid transport and metabolism
F	Nucleotide transport and metabolism
G	Carbohydrate transport and metabolism
H	Coenzyme transport and metabolism
L	Replication, recombination and repair
M	Cell wall/membrane/envelop biogenesis
P	Inorganic ion transport and metabolism
Q	Secondary metabolites biosynthesis, transport and catabolism
T	Signal transduction mechanisms
Y	Nuclear structure
Z	Cytoskeleton
W	Extracellular structures
X	Mobilome: prophages, transposons
R	General function prediction only
S	Function unknown

2.5 Phenotypical assays

2.5.1 Growth assays

From liquid cultures

Two types of growth curves were performed: whenever possible, cells were grown in conical flasks and aliquots were taken every hour to assess the OD_{600}. When the volatile molecule 2TDC was studied, or when a minimal amount of compound had to be ensured, automated growth curves were performed by inoculating liquid cultures onto 96-well plates and measuring the OD_{600} with an automated spectrometer (TECAN).

From agar plates –viable count

Growth on agar plates was assessed by adding up to 10 mL of phosphate buffer saline (PBS) to bring swarming cells from the surface of the agar to the liquid phase. The resulting cellular suspension was then diluted accordingly to be measured in a spectrophotometer. Dilutions of this suspension were also plated onto LB plates, incubated at 37 ºC overnight, and the cfu/mL were subsequently counted.

2.5.2 Addition of 2TDC to agar plates

The methyl ketone 2-tridecanone (2TDC) is a volatile compound. To study the effects of this molecule as volatile, it was added onto the lids of Petri dishes after inoculation of the cells, and EtOH was used as a solvent control. No information on the partition coefficient is currently available for this molecule. Therefore, asterisks (*) are used in the figures to indicate that 2TDC was added as a volatile, and the numbers in this case represent the stock concentration that was used. Specifically, 20 µm of the stock solutions were added to the lid of agar plates containing 20 mL of medium.

In the cases were the addition of 2TDC as a volatile was not possible (e. g. biofilm assays in chamber slides or Bioflux), the molecule was added to liquid cultures. In this case, the final concentration is stated in the figures.

2.5.3 Motility

Media used for motility assays was prepared fresh on the day of the assay, autoclaved and allowed to cool down in a water bath at 50 ºC for 1 h. Temperature-sensitive compounds, such as glucose or IPTG, were then added, and 20 mL of molten medium were poured onto Petri dishes.

Exogenous fatty acids; namely CDA, DSF and BDSF, were added to the agar together with glucose or IPTG. The 2TDC was added to the lid of the plates as addressed in **2.5.2**. Pictures were taken at the end of the assay, using a black background and indirect illumination.

2.5.3.1 Swimming

Swimming assays were conducted in NB, LB and CAA media, supplemented with 0.3 % (w/v) Bacto Agar. Briefly, 1 µL of overnight cultures were inoculated at mid depth in the agar, and plates were then incubated at 37 ºC. For LB and CAA

media, plates were incubated to up to 16 h, while for NB, plates were only incubated for approximately 7 h. After this time swimming could not be accurately visualised due to the amount of surface motility observed.

2.5.3.2 Swarming

Swarming assays were performed on plates of NB with a 0.5 % (w/v) Bacto Agar (BD). 20 mL of medium were poured into Petri dishes, allowed to settle at room temperature and dried for 30 min under laminar flow. 3 µL of overnight cultures were spotted on the surface of the plate. The plates were incubated at 37 ºC for approximately 15 h.

CAA was also used to assess the differential motility in presence of DSF-T. This medium contained 0.5 % casamino acids, 2 % glycerol, 3.3 mM K2HPO4, 0.5 % D-glucose and 0.5 % Bacto Agar (BD).

A modification of this protocol was implemented when the amount of spiked compounds needed to be minimised: in this case, Petri dishes of 5 cm radius were used, with only 6.5 mL of medium and 9 min drying time.

2.5.3.3 Twitching

Twitching plates contained 1 % agar, 1 % tryptone, 0.5 % yeast extract and 1 % NaCl. 10 mL of medium were poured in plates and dried for 15 min under laminar flow. Washed overnight cultures were then stabbed to the bottom of the plates using a toothpick, and incubated at 37 ºC for 24-48 h, under high humidity. The medium was then removed and the twitching cells were stained with 1 % crystal violet.

2.5.4 Proteases

The protease activity of *P. aeruginosa* cultures was assessed in cultures of standardised OD_{600} grown in LB in flasks filled to 10 % of their total volume, for 16-24 h at 37 ºC and with 200 rpm shaking. Assays were performed as previously described, with modifications that will be addressed in the following sections [188, 194, 317].

2.5.4.1 Staphylolytic protease, LasA

LasA protease, also known as staphylolytic protease, is able to lyse boiled staphylococci. Overnight cultures of *S. aureus* Newman were boiled for 10 min, washed and standardised to OD_{600}=1 with Na_2PO_4 10 mM, pH 7.5. Then, 100 µL of *P. aeruginosa* supernatant were mixed with 900 µL of *S. aureus* suspension. The OD_{600} of the suspension was monitored manually for 1 h. The slope of the resulting curves corresponds to the LasA activity present in the supernatants; therefore the steeper the slope, the higher the activity of this protease.

2.5.4.2 Elastase, LasB

The ability of *P. aeruginosa* supernatants to cleave elastin was assessed by mixing 100 µL of culture supernatant with 1 mL of buffer composed of 100 mM Tris-HCl, 1 mM $CaCl_2$ at pH 7.5, and supplemented with 5 mg/mL elastin-Congo red (Sigma-Aldrich). The mixtures were incubated with 200 rpm shaking at 37 ºC, centrifuged to remove undissolved substrate and measured at OD_{495}. The blank was composed of 100 µL LB mixed with 1 mL of buffer and elastin-Congo red, and was incubated and centrifuged together with the samples.

2.5.4.3 Alkaline protease, AprA

To assess alkaline protease activity, 0.25 mL of *P. aeruginosa* supernatant were mixed with 0.75 mL of a buffer composed of 20 mM Tris-HCl, pH 8.0, 1 mM $CaCl_2$ and 10 mg of the substrate hide powder azure. The mixture was incubated at 37 ºC with 200 rpm shaking for 1 h. After incubation, samples were centrifuged at 13000 rpm to pellet undissolved substrate, and the OD_{595} was determined. The blank was a mixture of buffer and 0.25 mL fresh medium, to which the same treatment was applied.

2.5.4.4 Protease IV, PrpL

Protease IV activity was determined by mixing 0.02 mL of *P. aeruginosa* supernatants with 0.48 mL of a buffer consisting of 50 mM Tris-HCl, pH 8; 150 mM NaCl and 40 µg of the substrate chromozym PL, formally *N*-[6-amino-1-(4-nitroanilino)-1-oxohexan-2-yl]-1-[2-[(4-methylphenyl)sulfonylamino]acetyl]pyrrolidine-2-carboxamide. TLCK (*N*-α-tosyl-L-lysine chlotomethyl ketone hidrochloride) was added at 2 mM as a negative control. The blank was composed of 0.02 mL of fresh medium with 0.48 mL of buffer, and treated as an

additional sample. Samples were incubated for 30 min with 200 rpm shaking, after which the OD_{410} was determined.

2.5.5 Biofilm formation

2.5.5.1 Crystal violet determination

Quantification of initial stage biofilms were performed as described previously [318]. In summary, overnight cultures grown at 37 ºC were diluted to OD_{600}=0.05. Then, 100 µL were added to the bottom of polystyrene 96-well microtiter plates (Greiner), and allowed to grow at 37 ºC statically for 16 h. The supernatant, containing planktonic cells, was then removed and the wells were washed three times with water. Biofilms were stained with 1 % crystal violet for 30 min. The excess of crystal violet was washed three times with water, and the remaining stain was dissolved with 200 µL EtOH. The absorption of the EtOH was measured at 600 nm.

2.5.5.2 Colony biofilm

The morphologies of colony biofilms were assessed with a medium consisting of 1 % or 0.5 % agar, 1 % tryptone, 20 µg/mL Coomassie blue and 40 µg/mL Congo red. Petri dishes contained 20 mL of medium. After letting the agar set and dry, 3 µL of overnight cultures standardised to OD_{600}=1.0 were spotted onto the plates and incubated at room temperature for 10 days.

For plates containing CDA, the compound of the MetOH control were added onto the molten agar prior to pouring into the plates. For experiments involving 2TDC, 20 µL of compound or EtOH control were added to the lid of the Petri dishes.

Colonies were then visualised by optical microscopy.

2.5.5.3 Chamber slides for static biofilms

Fluorescent qualitative analysis was performed from biofilms in 8-well microchamber Lab Tek II 8-well glass slides (Nunc) [319]. This platform consists of a glass microscope slide with a coupled chamber that divides it into 8 wells, where assays can be performed in parallel.

Overnight cultures of strains tagged with the P_{rrnA}-miniTn7-*gfp*, that constitutively expresses green fluorescence, were standardised to OD_{600} 0.05.

Subsequently, 0.5 mL of cultures containing additional compounds where appropriate were inoculated into the wells and incubated statically at 37 ºC overnight. The supernatants, containing planktonic cells, were then removed; and biofilms were visualised using CLSM (see **2.7**). Alternatively, biofilms were stained with Syto 9 (Thermofisher scientific) by removing the supernatants and adding fresh medium with a 1/4000 dilution of Syto 9, incubating the mixture in the dark for 15 min, removing the medium and visualising the biofilms by CLSM.

2.5.5.4 Bioflux system for flow biofilms

Bioflux, a microfluidic system from Fluxion Biosciences, was used to study biofilms under shear flow [320]. Bioflux 200 48-well low-shear plates were used. This system allows fresh medium to go through capillaries under a low flow rate, which enables for laminar flow to occur. It works as a flow cell with low volume capacity.

Briefly, overnight cultures of *P. aeruginosa* PAO1 served as inoculum in a 1/100 dilution in fresh medium, and allowed to grow to exponential phase (approximately 7 h). They were then diluted to OD_{600} 0.05 for seeding into the plates.

Sterilised medium was re-filtered using a 0.2 µm filter to reduce the formation of micro-bubbles that would impair laminar flow, and was warmed up at 37 ºC prior to use. The capillaries of Bioflux plates were first wetted using 100 µL of fresh medium. Then, 70 µL of the diluted PAO1 cultures were seeded into the capillaries and allowed to attach for 45 min at 37 ºC, statically. Finally, 1 mL of fresh medium was allowed to flow at 0.5 dyn/cm^2 for approximately 13 h, prior to visualisation with CLSM.

2.5.6 Production of secreted factors in semi-solid medium

The determination of several extracellular factors (e.g. pyocyanin, pyoverdine, rhamnolipids) from semi-solid media was performed by adapting a protocol from [71]. The main aim of these assays was to understand the production of secreted factors under swarming conditions.

One notable difference was the observation that growth is impaired under conditions non-favourable for swarming motility (see **Appendix, Figure 7.1**). In consequence, the process was similar to a swarming assay, but instead of inoculating cells in the centre of the plate, 3 µL of overnight cultures were diluted

in 300 µL of water, and then spread onto swarming plates with the help of glass beads. This allowed for cells to grow independently from their motility capacities, and thus was used as a normalisation of secreted factors by the number of cells.

Each replicate was inoculated in 20 mL of agar and incubated overnight. The next day, the whole agar content was recovered and mixed with 20 mL of 1 % $KHCO_3$, pH 9, and the mixture was incubated 1-2 days at 4 ºC. The rest of the agar was removed by centrifugation and filtration, and the liquid phase was used for subsequent steps.

2.5.7 Pyocyanin

Pyocyanin production was quantified using an acid-base extraction procedure previously described [321]. Briefly, the pigment was first extracted from liquid cultures with chloroform and re-extracted from the solvent with 0.2 M HCl. The OD at 520 nm of the aqueous phase was then measured. In order to obtain quantitative data in µg/mL, the absorbance measurement was then multiplied by the extinction coefficient of the pigment, ε=17.072 m^2/mol. Pyocyanin was quantified in cultures grown in LB, at 37 ºC and 200 rpm shaking, for 16 h; and from cells grown in NB plates by using the procedure detailed in **2.5.6**, acidifying the liquid phase to pH 4 prior to the extraction steps.

2.5.8 Pyoverdine

To assess pyoverdine production, cells were grown in CAA, either in liquid or in agar plates. This medium contains low amounts of iron, allowing for the expression of pyoverdine genes in *P. aeruginosa*. The liquid phases resulting from the filtration of liquid cultures or from the removal of agar were measured at OD_{405} giving an estimate of the pyoverdine secretion.

2.6 Chemistry work

2.6.1 Chemical structures

Graphics containing organic molecules or reactions were drawn with ChemSketch [322].

2.6.2 Sample preparation

For extraction of components from liquid cultures, cells were removed by centrifugation and filtration through 0.2 µm pore filters (Sartorius) and the

supernatant was acidified to pH 3-4 using 1 M HCl, followed by solvent extraction.

For the extraction of rhamnolipids from swarming plates, liquid phases recovered following **2.5.6** were acidified to pH 4 previous to solvent extraction with acidified ethyl acetate (EtOAc), specifically 1/1000 glacial acetic acid into EtOAc.

2.6.3 Solvent extraction

Filtered supernatants from *P. aeruginosa* cultures were extracted with EtOAc to purify small organic molecules, i.e. rhamnolipids, HAAs, HHQ and PQS. Briefly, equivalent volumes of supernatant and solvent were mixed together for 30 s and vortexed for 1 min, followed by a 5 min centrifugation in order to separate the phases. The organic phase was then collected in scintillation vials (Fisher Scientific). This process was repeated 3 times, and the organic phases were evaporated in a Jouan RC1022 Vacuum concentrator coupled with a Jouan RCT90 Cold Trap (Thermofisher Scientific) for the non-halogenated solvent EtOAc.

2.6.4 Thin layer chromatography

Normal phase thin layer chromatography (TLC) was used to study rhamnolipid expression based on a previously published method [323], and AQ [324].

Briefly, rhamnolipids were extracted from 10 mL of liquid culture or 20 mL agar plates. Extracts were resuspended in 20 µl EtOH and 15 µl were spotted onto silica 60 TLC plates (Merck Millipore). The mobile phase consisted of chloroform: MetOH: glacial acetic acid in a 65: 15: 2 ratio. Once the samples were run, the plates were bathed with a detection agent comprised of 0.15 g orcinol monohydrate, 8.2 mL H_2SO_4 60 % (v/v) and 42 mL water, and subsequently incubated at 110 ºC for 10 min. During this procedure, rhamnoses are hydrolysed by the acidic conditions into methyl-furfural, which turns into a green-yellow colour when in contact with orcinol [325](**Figure 2.2**).

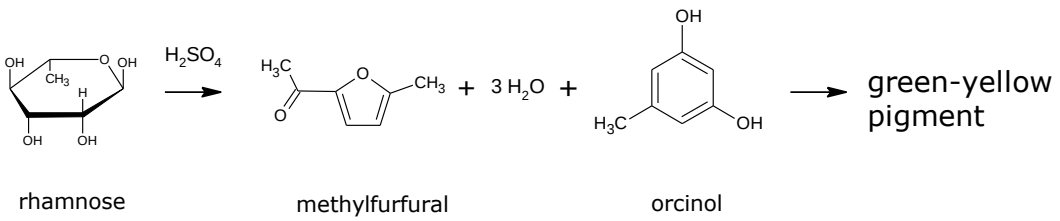


Figure 2.2. Reaction of rhamnose with orcinol during the detection of rhamnolipids following thin layer chromatography. Acid hydrolysis of rhamnoses results in the formation of methylfurfural, which reacts with orcinol to give rise to a green-yellow pigment. Adapted from [325].

For the detection of PQS and HHQ by TLC, silica 60 plates were incubated with 5 % KH_2PO_4 and then heated for 1 h at 100 ºC. Then, 20 mL of agar were extracted with acidified EtOAc. The extracts were subsequently resuspended in 50 µL of EtOH, and 5 µL were spotted onto TLC plates. The mobile phase consisted of 95: 5 DCM: MetOH. After running the TLC, the plates were allowed to dry and were then overlaid with soft-top agar containing the biosensor PAO1-L Δ*pqsA* CTX::P*pqsA-luxCDABE*. The resulting plate was incubated at 37 ºC. In contact with PQS and HHQ, this biosensor produces pyocyanin, which was visualised after overnight incubation. The light output from the biosensor was captured with a CCD camera (model C5405-51), an amplifier (C2741-3OH) and an intensifying unit (M4314, Hamamatsu Photonics K.K., Hamamatsu, Japan).

The retention factor (Rf) is defined as the distance travelled by a compound, relative to the distance travelled by the solvent. In the TLC determination of rhamnolipids, di-rhm show a lower Rf than the mono-rhm. In the determination of AQ, HHQ has a lower Rf than PQS.

2.6.5 Detection of Rhamnolipids and HAAs by LCMS

During this study, a semi-quantitative method for the extraction and detection of the major rhamnolipids and HAAs produced by *P. aeruginosa* was adapted to the in-house facilities. Method development and preparation of standards was performed by Nigel Halliday.

Standards were obtained from a culture of PAO1 grown in PPGAS. Briefly, rhamnolipids were extracted with EtOAc, and then a crude extract was obtained by normal phase column chromatography. Mono- and di-rhm were eluted with varying concentrations of chloroform in MetOH. Preparation of HAA standards was achieved with a dioxane-water reflux followed by EtOAc extraction as described previously [326].

For the preparation of samples, 0.5 mL were spiked with the internal standard 16-hydroxyhexadecanoic acid and brought to pH=4 prior to the extraction. After drying the liquid phase, they were reconstituted in MetOH in parallel with the standards.

The HPLC used was an Agilent Technologies 1200 Series LC system with an automatic injection and a column oven maintained at 50°C. The HPLC column was a Phenomenex Gemini C18 column (particle size 3.0 µm, 100 x 2 mm) with an appropriate guard column. Mobile phase A was and 0.1% (v/v) formic acid in water, and mobile phase B consisted of 0.1% (v/v) formic acid in MetOH. The

flow rate throughout the chromatographic separate consisted of 450 µL/min. Injection volume was 5 µL. The binary gradient started at 10 % phase B for 1 min, then rose to 99 % B in 9 min and maintained for 5 min, and finally lowered to 10 % B in 1 min and maintained for 4 min.

The MS system used was a Bruker HCT Plus ion trap mass spectrometer equipped with an electrospray ionisation interface. The electrospray settings were: nebuliser gas, 40 psi; drying gas, 10 L/min; drying temperature, 350 °C; capillary voltage, 4 kV. MS analysis was conducted with the MS operating in multiple reaction monitoring (MRM) mode, scanning the mass range 165-617 (m/z). The product ions used for the MRM detection are listed in **Table 2.10**.

Table 2.10. Molecular ions detected by LC-MS/MS for the quantification of rhamnolipids and rhamnolipid precursors produced by *P. aeruginosa* PAO1-L. The developed method allowed for the identification and quantification of the major species produced by *P. aeruginosa* [327]. Data extracted from [326]

Molecule detected	Pseudomolecular ion (m/z)	Major product ion (m/z)
$HO\text{-}(CH_2)_{15}\text{-}COOH$, Internal Standard	271	225
$C_{10}\text{-}C_{10}$ HAA	357	187
$Rha\text{-}C_{10}\text{-}C_{10}$ mono-rhamnolipid	503	339
$Rha\text{-}Rha\text{-}C_{10}\text{-}C_{10}$ di-rhamnolipid	649	479

2.7 Microscopy

2.7.1 Confocal laser scanning microscopy (CLSM)

Visualisation of biofilms was performed with a Zeiss LSM 700 confocal laser scanning microscope (Carl Zeiss, Ltd, Welwyn, UK), with a 5x objective. For the analysis of GFP expression, the confocal acquisition conditions were: acquisition wavelength 488 nm, pinhole 1.0, laser intensity 15 %. The gain was adjusted for each experiment in order to optimise the images, but they were kept constant within an experiment to facilitate comparison (500-700).

2.7.2 Transmission electron microscopy (TEM)

For the visualisation of individual *P. aeruginosa* cells by TEM, 0.5 mL of liquid cultures were pelleted 4 min at 5 krpm and fixed with 3 % glutaraldehyde in 0.1 M cacodylate buffer for 30 min. The fixative was subsequently washed twice

with a buffer consisting of 0.1 M sodium cacodylate buffer and twice again with distilled water.

Fixed cells were then added to 100Hex Formvar/Carbon coated grids (TAAB) and let to dry. Remaining water was removed with a filter paper (Millipore). The samples were finally stained with filter-sterilised 3 % uranyl acetate and left to dry for 1 min. Samples were visualised with a Tecnai G2 12 Biotwin microscope (FEI), using an accelerating voltage of 100 kV.

For the visualisation of swarmer cells, approximately 40 µL of NB were used to recover cells from the edge of swarming tendrils, which were then diluted in a total of 0.5 mL of medium. The procedure outlined above was then applied.

2.7.3 Optical microscopy

Colony biofilms were visualised every day for 10 days with an EVOS XL Core Cell Imaging System microscope (Thermofisher Scientific). Pictures of the biofilms were taken with the 10x objective.

2.8 Bioinformatics/structure determination

2.8.1 Prediction of domain organisation

Domain organisation was predicted using the SMART database (http://smart.embl-heidelberg.de/) [328, 329], which provides a comprehensive annotation of protein domains, retrieved from UniProt, Ensembl and STRING.

2.8.2 Alignment of primary and secondary structures

Alignment of amino acid sequences was mainly performed using BLASTP from NCBI (http://blast.ncbi.nlm.nih.gov/Blast.cgi), with the default parameters (BLOSUM-62 matrix, gap cost of 11, and gap extension cost of 1). This allowed for pairwise comparisons between CDA synthase candidates with known DSF-T synthases.

To deepen the analysis, multiple alignments were assessed with CLUSTALω (http://www.ebi.ac.uk/Tools/msa/clustalo/), with the default settings [330].

2.8.3 Prediction of tertiary structures

The prediction of 3D protein structures was determined with I-Tasser [331-333]. This prediction model is based on the use of previously described structures from Protein Data Bank (PDB) and from the protein-ligand database BioLiP.

2.8.4 Alignment of tertiary structures

Structures predicted from I-Tasser or described in PDB were aligned in PyMOL Molecular Graphics System, Version 1.1r1 Schrödinger, LLC.; following the guidelines of the program. The command `align` was used. This command gives a root mean square deviation (RMSD) number as an output, which is found with the following formula:

$RMSD = \sqrt{\sum(dii^2/N)}$, where dii is the distance between the i^{th} atom of structure 1 and the i^{th} atom of structure 2 and N is the number of atoms matched in each structure. Hence, the smaller the RMSD, the better the alignment between the two structures.

2.9 Results analysis

2.9.1 Pixel integration analysis

The areas corresponding to rhamnolipids on TLC plates, and the area colonised by cells in motility plates were quantified using GNU image manipulation program (GIMP) version 2.8.10. Briefly, the targeted area was selected and highlighted with a distinctive colour. The "histogram" tool allowed for counting of the number of pixels occupied by that colour.

For the analysis of motility, the total area of each plate was used to normalise, as different pictures may have slight differences in the zoom used by the camera.

2.9.2 Analysis of biofilms

Biofilms were analysed using Image J software version 1.49v [334], together with the plugin Comstat2 version 1.1 (www.comstat.dk) [335, 336]. At least 3 independent images were taken for each determination.

2.9.3 Statistical analysis

2.9.3.1 Analysis of phenotypical assays

All statistical analyses were performed with the use of GraphPad Prism version 6.05 for Windows, GraphPad Software, (La Jolla California, USA). Pair-wise comparisons were analysed with a two-tailed t-test, whereas when three or more data series were compared, one-way ANOVA was performed. Asterisks for single t-tests are used as follows:

$$NS\ if\ p > 0.05$$
$$*\ if\ p \leq 0.05$$
$$**\ if\ p \leq 0.01$$
$$***\ if\ p \leq 0.001$$
$$****\ if\ p \leq 0.0001$$

When multiple t-tests were calculated within the same data series, the Holm-Sidak method was used to account for multiple comparisons, using α=0.05. Using this method, p-values for each comparison are ordered from lower to higher, and then the significance is determined as:

$$p\ is\ significant\ if\ p < \frac{\alpha}{1-(1-\alpha)^{1/i}}, where \begin{array}{c} K = number\ of\ comparisons \\ i = K - j \\ j = cycle\ number - 1 \end{array}$$

So, on the first cycle, i=K. If the lowest p-value of the multiple comparisons is higher than the above expression, then there are no significant comparisons. Otherwise, the iteration continues and in the second cycle, i= K-1. For multiple t-tests, significance is only shown with one asterisk when $p < 0.05$. That is, no additional asterisks are shown, even when p is low.

3 IMPACT OF DIFFUSIBLE SIGNAL FACTOR-TYPE MOLECULES ON THE BIOLOGY OF *P. AERUGINOSA*

3.1 Introduction

The following chapter will mainly deal with the phenotypical effects of *cis*-2-decenoic acid (CDA) and other diffusible signal factor-type (DSF-T) signal molecules in *P. aeruginosa.* With a view to understand the role of DSF-T molecules in the biology of their producers and in cross-signalling, their impact in both their cognate producers and in inter-species communication will be considered.

3.1.1 Discovery and production of DSF-T molecules

A DSF involved in cell-cell communication was identified in *Xanthomonas campestris* pv. *campestris* (*Xcc*) [243]. It was later characterised as *cis*-11-methyl-2-dodecenoic acid [245]. In the following years, DSF-T molecules were identified in various *Xanthomonas* species, including *X. oryzae* [337], *X. axonopodis* [338] and *X. hortorum* [339], amongst others. Two closely related organisms, *S. maltophilia* and *Xylella fastidiosa,* also presented DSF-like activity [246, 340].

The production of DSF-T is not limited to γ-proteobacteria and has also been found in the *Burkholderia* genus of β-proteobacteria [251]. Furthermore, another DSF-T system was recently discovered in *Cronobacter sp.* [341]. This shows that DSF-based communication is a lot more widespread than previously thought, and that it may have a high level of conservation amongst bacteria.

P. aeruginosa produces a closely related molecule, which was identified as *cis*-2-decenoic acid (CDA). CDA is considered a DSF-T molecule, but although it is structurally related to other DSF-T molecules, it presents a much lower DSF activity with the P*engXCA-gusA* assay, a bioreporter that measures DSF activity through the production of endoglucanase in *Xcc* [263]. Additionally, CDA does not restore the phenotype of DSF-deficient *Xanthomonas* or *Burkholderia* [245, 255].

3.1.2 Native production and metabolism of DSF-T

The synthesis of DSF-T is driven by the activity of RpfF proteins. Interestingly, these proteins are non-specific and thus are responsible for the synthesis of

various DSF-T molecules. In *Xcc*, DSF, BDSF, CDSF and IDSF have been found, all depending on the activity of RpfF [250, 342]. Multiple members of the *Burkholderia cepacia* complex synthesise various DSF-T, including DSF, BDSF and CDSF (see **Table 1.2**). Seven structurally related, DSF-like molecules are produced by *S. maltophilia* [343].

Expression of Bcam0581 (the DSF-T synthase from *B. cenocepacia*) in *Xcc* shows that the production of several DSF does not differ between RpfF homologues but relies mainly in substrate availability and therefore in medium composition [251]. This hypothesis has been further investigated in *X. oryzae*, where results show that the proportion of different DSF-T changes greatly depending on the medium. In rich medium, DSF was the main molecule synthesised and smaller amounts of BDSF and CDSF were found, whereas BDSF was the main DSF-T produced in minimal medium [248]. This is in agreement with other studies suggesting that the production of one particular DSF-T molecule depends on the carbon source [344]. In particular, glucose has been suggested as one of the primary carbon sources leading to the production of this type of molecules [250]. In line with this, Huedo et al. found that *S. maltophilia* strains produce higher levels of DSF in rich medium [267]. This differential production, depending on environmental conditions, probably constitutes another layer in the complexity of regulation driven by these molecules.

3.1.3 Impact of DSF-T in bacterial biology

The biosynthesis and regulation of DSF in *Xanthomonas* has been extensively studied, and will be covered in **Chapter 4**. Briefly, *rpfF* is responsible for the synthesis of DSF, while the operon *rpfGHC* (*rpfH* not always present) is involved in DSF perception and signal transduction. These genes and the proteins that they encode are subjected to multiple regulations which tightly control the secretion levels of DSF-T.

In general, DSF affects a number of traits related to population adaptability and survival, which can also be regarded as colonisation factors. Similar effects of DSF-T have been reported in a range of bacterial species, and thus they constitute a starting point to study effects of DSF-T in *P. aeruginosa.*

Interestingly, DSF-T do not just affect their cognate producers but also intervene in inter-species communication. Indeed, *P. aeruginosa* is found in the rhizosphere and in the CF lung together with many other species such as *B. cepacia* or *S. maltophilia*, and this has led to the suggestion that these species interact with

one another in natural settings [34, 345]. Further evidence of cross-talk mediated by DSF-T will be reviewed in the following sections.

3.1.3.1 Extracellular proteins and polysaccharides

In *Xcc,* DSF controls the production of secreted enzymes and the exopolysaccharide xanthan, an important constituent of the extracellular biofilm matrix. Secreted enzymes controlled by DSF in this bacterium include protease, polygalacturonate lyase, endoglucanase and amylase [346]. DSF has similar roles in various other *Xanthomonas* such as *X. citri* and *X. oryzae* pv. *oryzicola* [243, 347-351]. Similar effects in protease secretion have been reported in *S. maltophilia* [246], and in *Cronobacter turicensis* [341].

In contrast with other *Xanthomonas*, DSF-negative *X. oryzae* is avirulent but produces wild-type levels of EPS or extracellular proteases, suggesting a different regulation in this bacterium [337]. The sensing deficient Δ*rpfC* in *X. oryzae* are reduced in EPS but not in protease production, which adds to the complexity of these regulatory mechanisms [352].

3.1.3.2 Motility

The role of DSF in the activation of cellular motility has been shown in *X. campestris, X. albiliensis* and *X. citri* [218, 349, 351, 353]. In *X. oryzae,* DSF-activated swimming is dependent on the orphan LuxR homologue OryR [354]. DSF deficient *S. maltophilia* isolates are impaired in swimming motility, which is restored by the exogenous addition of the signal molecule [246]. BDSF has a similar effect in its cognate producer *B. cenocepacia,* where it controls swarming [355, 356]. In *X. axonopodis* pv. *citri*, DSF activates both flagellar-dependent and flagellar-independent motility [357]. Consistent with these effects, swarming in *C. turicensis* is increased with the overexpression of *rpfF* [341].

3.1.3.3 Biofilm

The relation between DSF and biofilm is complex and often counter-intuitive. While DSF deficient mutants of *Xcc* have reduced amounts of exopolysaccharide, they present an aggregative phenotype, which can be abrogated by an endo-β-(1,4)-mannanase. DSF is thus involved in both biofilm dispersion and in EPS production. DSF-deficient mutants still have basal expression of xanthan,

and this component was found essential for aggregate formation [358]. An explanation for these apparent opposite phenotypes is that DSF positively controls xanthan production, while it negatively regulates the *xagABC* operon, potentially responsible for another exopolysaccharide [359]. The same results were obtained in *S. maltophilia,* where aggregates are found in *rpfF* mutants in L medium, but the *rpfF* mutation impairs microcolony formation in artificial sputum medium [246]. It seems therefore that DSF differentially regulates various forms of aggregative behaviours.

More definite results have been found in *B. cenocepacia* Δ*rpfF*, which shows reduced biofilm formation [355]. Studies in *X. albilineans* show that the triple mutant *rpfGCF* presents a reduction in attachment to sugarcane leaves, although the single mutations does not show this effect [351, 360]. *X. citri* presents reduced attachment to both leaves and abiotic surfaces in *rpfF, rpfC* and *rpfG* mutants, following the same trend [349].

In contrast, other species seem to behave in a completely opposite way. This is the case of *X. oryzae,* where DSF impairs swimming motility and activates adherence and biofilm formation [361]. Along with this idea, in *Xylella fastidiosa* *Xf*DSF is required for biofilm formation in plants, and DSF-T deficiency changes the architecture of the biofilm in the insect vector. Biofilm deficiency is, at least in part, related to the formation of outer membrane vesicles that impair the adherence to surfaces [362].

The more drastic effect shown in *P. aeruginosa* is the effect of CDA on biofilm formation. This fatty acid inhibits and disperses established biofilms, similarly to other DSF-T in *Burkholderia* and some *Xanthomonas sp.* More specifically, CDA is capable of disrupting biofilms of a range of bacterial species at nanomolar concentrations, and the effects of this molecule are observed after only 7 min of addition [255]. Furthermore, CDA can be combined with antibiotics and other compounds to boost the dispersion activity [363-365].

Interestingly, DSF-T molecules have been shown to affect *P. aeruginosa* biofilms; therefore these molecules could be involved in cross-talk between species. One example of this is that *P. aeruginosa* biofilms become filamentous in the presence of DSF [264]. On a related note, DSF-T molecules are structurally related to farnesoic acid and, like this pheromone, they can inhibit *C. albicans* yeast-to-hyphae transition, thereby affecting the adherence of *Candida* populations [245]. These effects have been reported for BDSF [251], CDA [255] and CDSF [247]. However, a later report showed no differences in *C. albicans*

biofilms after treatment with 10 μM CDA [366]. More promising results were found by Tian et al. in which urinary catheters treated with 90 μM BDSF were able to effectively reduce the adherence of *C. albicans* [252].

3.1.3.4 Iron uptake

A link has been found between DSF and the ability of cells to uptake iron. In *X. oryzae*, Δ*rpfF* mutants overproduce siderophores, but their growth is impaired under low iron conditions [337]. A Zur homologue, which functions as an iron uptake regulator, is responsible for this effect. This regulator is activated in the presence of DSF-T through the global regulator Clp and controls the transcription of genes encoding iron uptake proteins [367]. DSF in this species was later shown to regulate the uptake of ferric iron, and the supplementation of iron allowed for colonisation and survival in the host [368]. Therefore, DSF-T are not only responsible for the switch between motile and sessile lifestyles but also regulate the survival to harsh conditions through the modulation of metabolic routes.

3.1.3.5 Other survival strategies

Resistance to toxic compounds is also mediated by DSF-T, including oxidants such as hydrogen peroxide [347], antibiotics [356] and heavy metals [246]. This is also found in inter-species communication, as biofilms of *P. aeruginosa* grown in the presence of DSF present not only a filamentous structure, but also increased tolerance to polymyxins [264]. Production of BDSF and DSF in CF isolates has been experimentally proven and *P. aeruginosa* isolates exposed to these molecules show an increase in antibiotic resistance and persistence. Not only does PAO1 respond to these molecules, but this also shows that clinical strains retain the ability of communicating through DSF-T molecules [369]. In contrast, the opposite effect towards Gm and Km has also been reported [370].

Regarding the effects of DSF-T in persistence, CDA has been linked to the decrease of persister cells in *P. aeruginosa* [256]. CDA promotes the reversal of persisters to an antibiotic-susceptible state, which could be key in the development of new strategies against recalcitrant *P. aeruginosa* infections.

3.1.3.6 Effect of DSF-T in regulatory networks

Some of the effects that DSF-T produce in *Xcc* are, at least in part, explained by the finding that DSF induces the expression of *clp*, a global regulator with homology to the cAMP regulator protein (CRP), which results in a downstream cascade affecting iron intake, antibiotic resistance and flagellar synthesis [367].

Several of the phenotypes discussed above have been traditionally linked to AHL-based QS systems. While it has been reported that BDSF does not influence QSSM in *Burkholderia* [355], it is not surprising that subsequent publications which involved different genes showed an overlap of regulation between AHL and BDSF systems [266, 371]. Furthermore, AHL synthases are differentially expressed by BDSF [372]. Research also shows that *P. aeruginosa* responds to DSF by repressing QS and T3SS [373].

Interestingly, in *X. oryzae* pv. *oryzae* an RsmA homologue alters the production of DSF without affecting the expression of *rpfF* [374], suggesting that post-transcriptional regulation may be in place for DSF biosynthesis, and shedding light on a possible relation between the RsmA/Gac system and DSF synthesis.

3.1.4 Exploitation of DSF networks in infection

The pleiotropic effects of DSF-T in their cognate species lead to an overall adaptability, which in many cases results in a higher capacity of colonisation, whereas strains deficient in DSF-T production generally present an impaired virulence [246, 355]. In *Xcc*, DSF is able to inhibit stomatal closure of *Arabidopsis thaliana*; therefore facilitating the infection by this bacterium [353]. Similar results have been obtained in *X. oryzae* and in *C. turicensis,* where the loss of DSF production leads to a decrease in host colonisation [341, 349].

One exception is *X. fastidiosa*, in which Δ*rpfF* mutants are incapable of colonising the insect vector, but present more virulence if mechanically inoculated [375]. This is due to a reduced biofilm formation and increased motility in these mutants, which is key to the virulence in the plant xylem but prevents vector colonisation. So, in this sense, the DSF-T *Xf*DSF still controls the same phenotypes in *X. fastidiosa*; though resulting in different outcomes.

Due to the effects in colonisation, DSF-T networks can be targeted as a treatment against bacterial infections. RpfF from *X. fastidiosa* and from *X. campestris* has been expressed in grapes to at least 1 μM concentration, and it substantially lowers the infection by *X. fastidiosa* [376]. RpfF has also been

produced to limit the infection by *X. citri* [377]. On a different note, DSF-T also promote the colonisation of growth-promoting bacteria. For instance, a beneficial isolate of *S. maltophilia* was able to colonise oilseed rape, whereas the DSF negative mutant reduced the plant growth and germination rate of the seeds [378]

3.1.5 Aims of the chapter

This chapter aims to better understand the regulatory networks mediated by CDA in *P. aeruginosa* and the impact of DSF-T molecules in this bacterium. As more specific aims, work presented here is intended to:

- Use transcriptomics to elucidate potential targets of CDA
- Compare the role of CDA in *P. aeruginosa* with other DSF-T in their cognate species
- Compare the role of CDA and other DSF-T in *P. aeruginosa*

3.2 Results

3.2.1 Whole transcriptome analysis

Previous to this thesis, a transcriptomic approach (RNA-seq) was used to identify new targets for CDA in *P. aeruginosa.* The work in this chapter involves the general description of the results obtained and the analysis and identification of potential targets for this fatty acid. This RNA-seq was used as an iterative method, together with laboratory results and literature review, to better understand the CDA regulome.

RNA was extracted from cultures grown in LB for 4 hours, in the presence and absence of 100 μM of CDA. The statistical analysis was performed by the DeepSeq facility of the Queen's Medical Centre (Nottingham). Specifically, two statistical tests were performed, the Baggerly's test and the DESeq test.

3.2.1.1 Overview of results

An overview of the data was first performed with genes differentially expressed, and results show that the Baggerly's test is far less stringent than the DESeq test. In addition, few genes are statistically significant according to both tests (**Figure 3.1**).

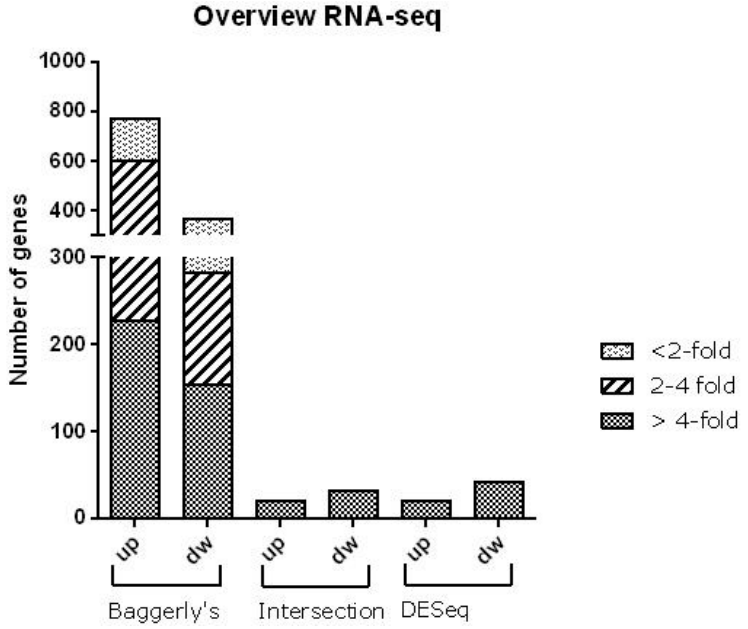


Figure 3.1. Differentially expressed genes in PAO1-L grown in the presence and absence of 100 μM CDA. Results from the RNA-seq were plotted to represent the number of differentially expressed genes according to the Baggerly's test, the DESeq test, or the intersection between both tests. up, up-regulated; dw, down-regulated. For additional information, see **Appendix, section 7.2.1**.

The results in **Figure 3.1** show that most of the genes differentially expressed presented a high fold change. To better understand the significance of these results, a modified volcano plot was then performed, using only the differentially expressed genes. Volcano plots show the fold change vs the significance, allowing for a quick overview of the data dispersion and for the identification of highly relevant targets [379].

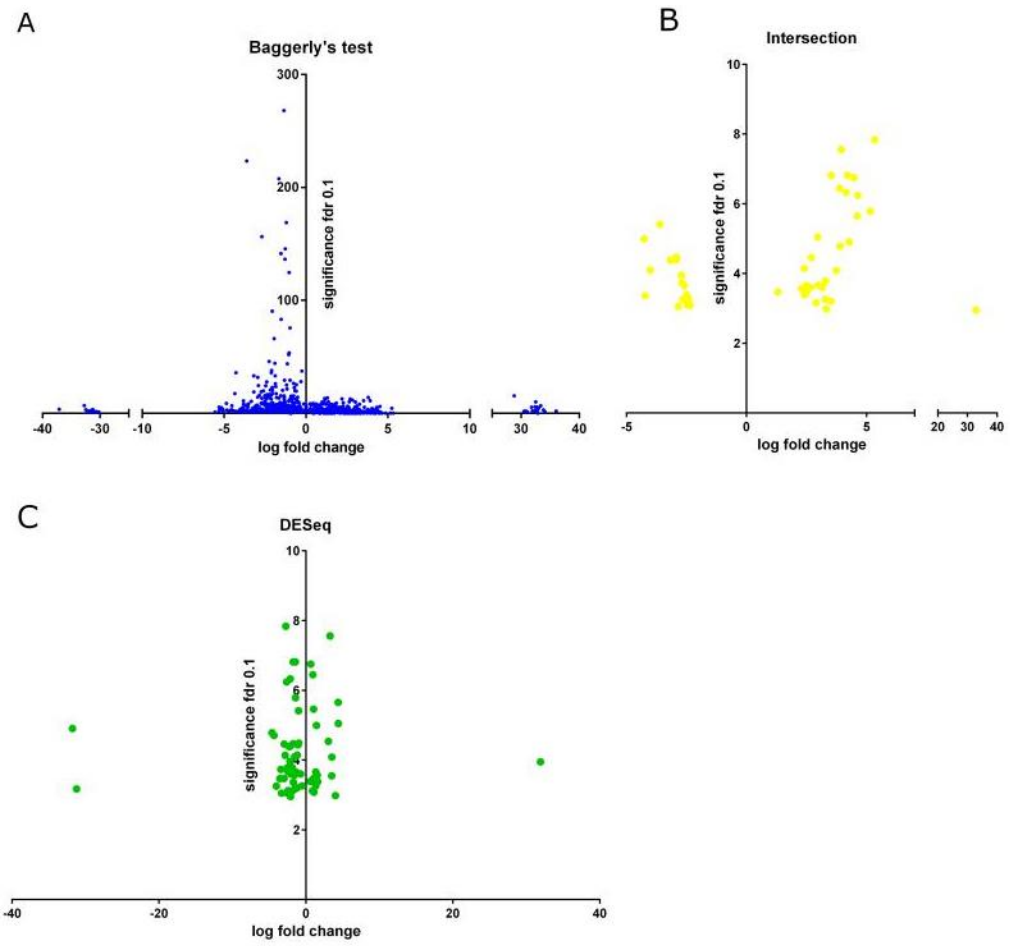


Figure 3.2. Volcano plot of genes differentially expressed in the RNA-seq of PAO1-L, in the absence and presence of 100 µM CDA. Genes identified as significant by the Baggerly's test **(A)**, the DESeq test **(C)**, or both **(B)** were used to generate volcano plots. *x* axis, log fold change [$\log_2$(RPKM(CDA))-$\log_2$(RPKM(MetOH))]; *y* axis, -$\log_{10}$(p-value). The genes represented here show FDR=0.1.

As can be observed in **Figure 3.2,** numerous genes presented both a high log fold change and a high p-value, which prompted us to look closely at the RNA-seq results. However, it should be noted that a number of genes showed very high log fold change due to the fact that the RPKM was 0 under one of the conditions. For the calculation of the fold change, 0 was approximated to 10^{-5}. Specifically, this anomaly happened for 21 out of 227 genes in Baggerly's test for up-regulated genes and 21 out of 154 in the down-regulated genes, in 1 out of

41 genes in the DESeq test, and in 1 out of 32 genes in the intersection of both tests (see **Appendix, section 7.2.1**).

3.2.1.2 Functional classification

Next, genes that changed transcriptional levels by at least 2-fold were classified in functional categories. A COG-based functional database was created and curated for genes of particular interest in this project (see **Chapter 2, section 2.4.3**).

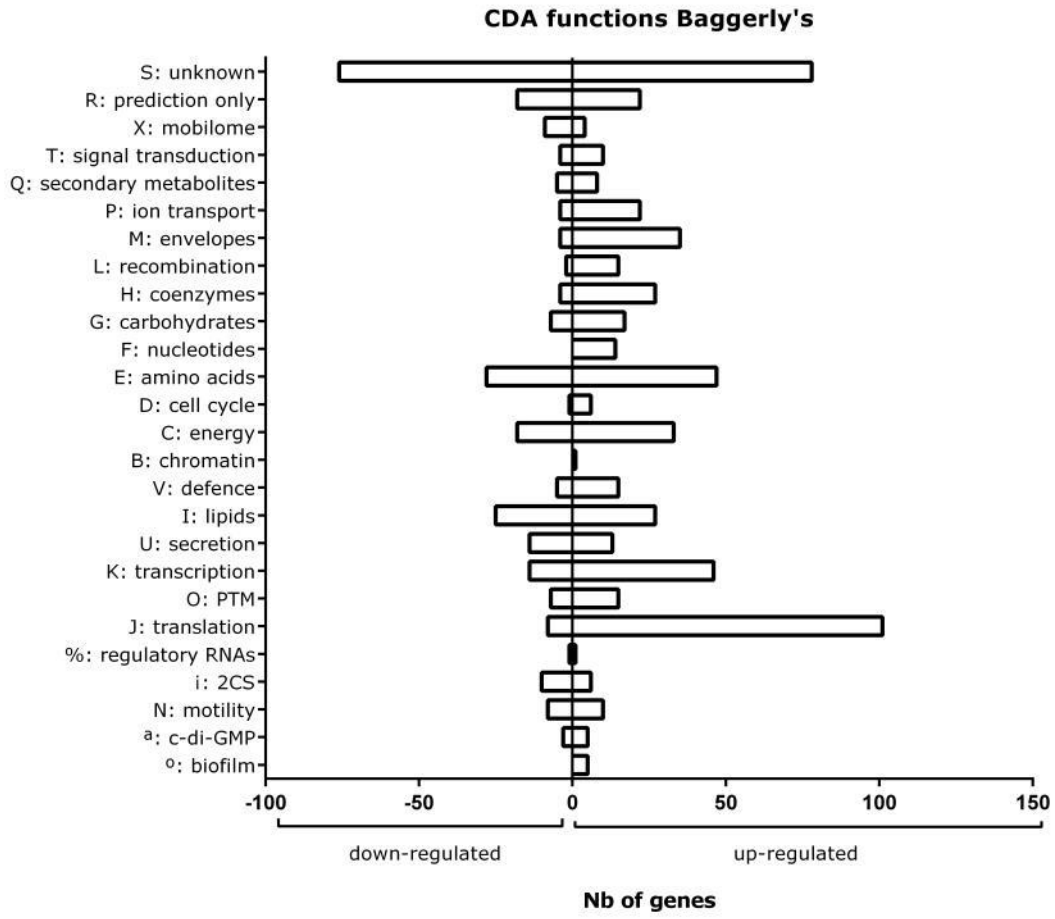


Figure 3.3. Functional annotation of genes differentially regulated in PAO1-L upon addition of MetOH control vs 100 µM CDA. A functional annotation database was created from the categories in the COG database and the *Pseudomonas* Genome Database. Genes differentially regulated from the Baggerly's test were classified according to this functional annotation. Negative values were assigned for genes down-regulated by CDA, while positive values correspond to up-regulated genes. PTM, post-translational modifications; 2CS, two-component systems.

Results from **Figure 3.3** show that relevant genes in the RNA-seq belong to various functional categories, with the most represented category being "J: Translation, ribosomal structure and biogenesis". Amongst those, most genes were related to ribosomal proteins and tRNAs, and thus were not of particular

interest for this work. A closer look led to the list of selected genes presented in **Table 3.1.** In particular, focus was put on genes related to the regulation of population behaviours including biofilm formation and genes involved in global regulation.

Table 3.1. Selected genes identified from the RNA-seq results of PAO1-L grown in the presence and absence of 100 µM CDA (i). Genes listed below were statistically significant according to the Baggerly's test, and differentially expressed at least 2-fold. Folds are indicated in brackets; positive numbers show an up-regulation driven by CDA while negative numbers show a down-regulation. *, *mucR* is also involved in c-di-GMP signalling. **, PA5364 presented 0.5 RPKM in MetOH and 0.0 RPKM in CDA; and *arsR* presented 7.6 RPKM in MetOH and 0.0 RPKM in CDA. T6SS, type 6 secretion system; 2CS, two-component systems; ECH, enoyl-CoA hydratase; QS, quorum sensing; T3SS, type 3 secretion system.

Gene ID	Function
Up-regulated	
bifA (2.5), PA3177 (2.9), *sadC* (2.7), *siaD* (3.7), *tpbB* (3.6)	c-di-GMP signalling
mucC (2.4), *pelA* (16.0), *pelF* (23.2), *pelG* (18.5), *pslD* (2.7)	exopolysaccharides
fliQ (2.8), *flgD* (2.0), *pilA* (2.3), *pilF* (2.6), *pilZ* (2.1), *tadG* (5.2)	motility
mreB (4.3), *mreC* (3.1), *rodA* (2.4)	shape
secB (2.5), *secE* (3.5), *secY* (3.0)	Sec secretion pathway
tssB1 (2.0), *tssC1* (2.5), *tssG1* (4.2), *tssJ1* (4.3), *tse6* (3.0)	T6SS
aauR (4.5), *arnB* (2.6), *colS* (2.1), *cprS* (5.1), *erdR* (2.4), PA1301 (7.1), PA4080 (3.1), PA4982 (2.0)	2CS and probable 2CS
PA1748 (5.2)	probable ECH/isomerase
P35 (3.8), *phrS* (2.1), *prrF1* (4.9)	regulatory small RNAs
lasI (2.0)	QS
femI (12.4), *rpoD* (2.1), *sigX* (2.4)	sigma factors
aguR (4.8), *dauR* (2.1), *dnr* (5.0), *metR* (23.1), *pcaQ* (4.4), *vqsM* (2.5)	transcriptional regulators
Down-regulated	
PA2072 (-7.1), PA4929 (-4.6)	c-di-GMP signalling
mucR (-2.5)*	exopolysaccharides
cupA1 (-3.5), *flp* (-2.2), *pilY2* (-2.2)	motility
pctA (-4.4)	chemotaxis
clpC (-7.9), *clpP2* (-4.9), *lasA* (-8.9)	proteases
rhlA (-17.7), *rhlB* (-5.4), *rhlC* (-16.8)	rhamnolipids
lecB (-35.6)	lectins
phzB1 (-14.9), *phzM* (-22.1)	phenazine biosynthesis and regulation
PA0178 (-9.8), PA0179 (-16.3), PA1397 (-2.6), PA2571 (-5.0), PA2572 (-5.9), PA3271 (-2.5), PA3462 (-3.3), PA4112 (-4.9), PA5364**, *pprA* (-4.5)	2CS and probable 2CS
exsC (-3.4), *popD* (-3.4), *pcrV* (-10.3), *pscI* (-9.6), *pscK* (-12.5)	T3SS
PA0746 (-7.8), PA2841 (-5.2)	probable ECH/isomerase
rsmY (-23.6)	regulatory small RNAs
pqsB (-11.5), *pqsC* (-6.5), *rhlI* (-2.3), *rhlR* (-2.9)	QS
arsR, *cdhR* (-3.7), *gbuR* (-3.2), *prtR* (-2.4)	transcriptional regulators

A functional annotation was then performed for genes identified in the DESeq test (**Figure 3.4**), followed by the identification of selected genes to use as starting point for further research (**Table 3.2**).

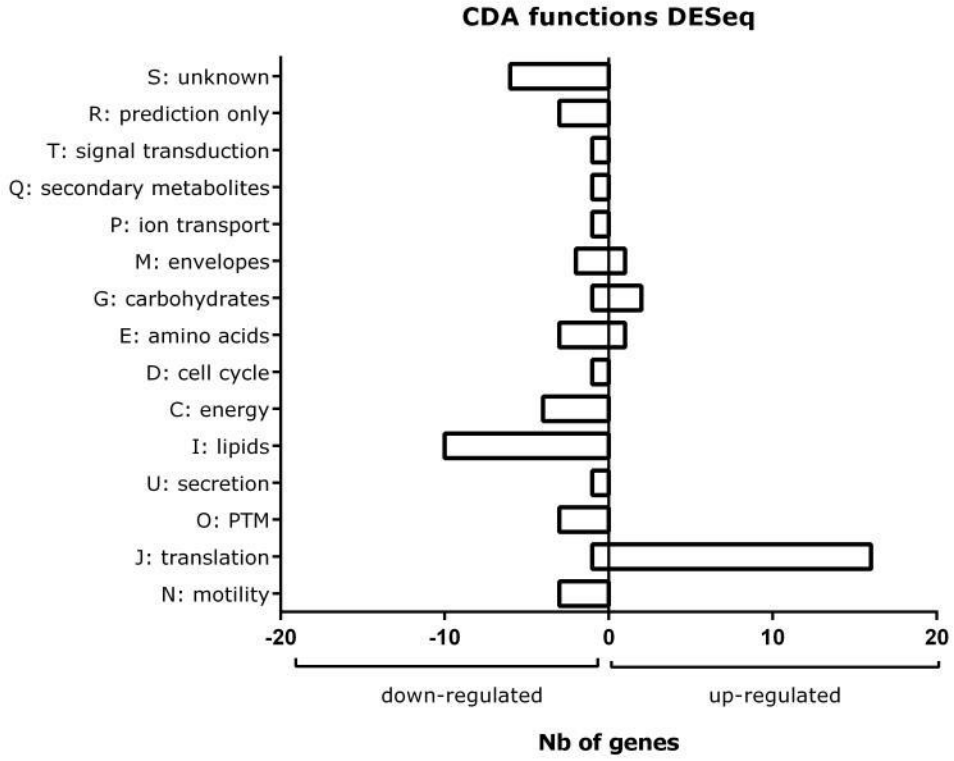


Figure 3.4. Functional annotation of genes differentially regulated in PAO1-L grown upon addition of MetOH control vs 100 µM CDA. A functional annotation database was created from the categories in the COG database and the *Pseudomonas* Genome Database. Genes differentially regulated from the DESeq test were classified according to this functional annotation. Negative values were assigned for genes down-regulated by CDA, while positive values correspond to up-regulated genes. PTM, post-translational modifications.

Table 3.2. Selected genes identified from the RNA-seq results of PAO1-L grown in the presence and absence of 100 µM CDA (ii). Genes listed below were statistically significant according to the DESeq test, and differentially expressed at least 2-fold. Folds are indicated in brackets; positive numbers show an up-regulation driven by CDA while negative numbers show a down-regulation. All genes of interest identified by DESeq were down-regulated by CDA. QS, quorum sensing.

Gene ID	Function
Down-regulated	
clpC (-7.9), *clpP2* (-4.9), *lasA* (-8.9), *lasB* (-7.0)	proteases and protease regulators
aer2 (-10.7), PA2573 (-9.7)	aerotaxis and chemotaxis
lecB (-35.6)	fucose-binding lectin PA-IIL
pqsC (-6.5), *pqsE* (-5.7)	QS
PA0178 (-9.8)	probable two-component sensor

Various interesting targets were identified from both statistical tests (**Table 3.1, Table 3.2**), and where subsequently used in *in vitro* assays. More specific RNA-

seq data regarding some phenotypes will be presented in the corresponding sections throughout this chapter.

3.2.2 Comparison with Rahmani-Badi's microarray

A microarray comparing the transcriptome of PAO1 grown in M9 medium with and without CDA was published during the development of this thesis [364]. Because of its similarities with the RNA-seq presented here, a formal comparison was next performed to evaluate the impact of experimental conditions in the effects of CDA and identify general trends in the effects caused by this fatty acid signal. First, a number of genes of interest were identified from the published results of the microarray, which are listed in **Table 3.3.**

Table 3.3. Selected genes from the microarray performed by Rahmani-Badi et al. Genes of particular interest were identified from the microarray analysis, following the same criteria as for the RNA-seq. These genes were all statistically significant according to ANOVA data with the Tukey's correction; and were differentially expressed by at least 2-fold in the presence of CDA. Folds are indicated in brackets; positive numbers show an up-regulation driven by CDA while negative numbers show a down-regulation. *, no information on the fold of *pvdD* was given in the publication by Rahmani-Badi et al. **, *pvdS* is involved in siderophore production and functions as a sigma factor. 2CS, two-component systems; ECH, enoyl-CoA hydratases; QS, quorum sensing; T3SS, type 3 secretion system

Gene ID	Function
Up-regulated	
fimX (5.0), PA0847 (4.4), PA5487 (12.3), *rocR* (6.1), *roeA* (2.8), *sadC* (10.1), *wspR* (4.4)	c-di-GMP signalling
pchD (18.2), *pchG* (3.1), *pchR* (3.1), *pvdD**, *pvdE* (16.4), *pvdF* (4.8), *pvdG* (9.3), *pvdJ* (10.9), *pvdL* (2.0), *pvdN* (11.9), *pvdO* (14.4), *pvdP* (15.5), *pvdS* (6.7)**	siderophores
fleN (12.2), *fleQ* (5.18), *flgB* (14.8), *flgC* (3.4), *flgD* (12.6), *flgG* (2.1), *flgH* (14.6), *flgI* (7.9), *flhB* (7.8), *fliC* (3.5), *fliD* (5.2), *fliF* (5.9), *fliG* (3.2), *fliM* (2.3), *fliO* (5.8), *fliQ* (28.5), *fliR* (4.1), *fppA* (2.1), *pilD* (2.7), *pilE* (7.8), *pilM* (8.7), *pilR* (3.1), *pilS* (10.5), *pilU* (3.3), *pilZ* (3.2)	motility
aauR (3.8), *bfiR* (5.6), *bfiS* (7.2), *copR* (2.9), *copS* (2.2), *crpR* (32.0), *cprS* (16.1), *czcS* (6.6), *fleS* (5.0), *gacA* (3.5), *mifS* (3.5), *ntrB* (9.2), PA0756 (7.0), PA1437 (11.0), PA1458 (4.0), PA2479 (36.1), PA2480 (6.4), PA3271 (3.1), PA4886 (9.5), PA4982 (2.8), PA4983 (4.3), *parS* (3.6), *pfeS* (5.3), *phoP* (5.6), *phoR* (6.4), *pmrA* (2.3), *pmrB* (15.8), *pprA* (7.9), *pprB* (388.4), *rocA1* (3.8), *rocS1* (7.5), *wspR* (4.4)	2CS and probable 2CS
PA1021 (15.9), PA1240 (9.9), PA2841 (13.9), PA3426 (2.9), PA3591 (2.2), PA4330 (7.2), PA4980 (2.6)	ECH/isomerases
foxI (5.4), *foxR* (13.6), *rpoD* (7.0), *rpoS* (4.9)	sigma and anti-sigma factors
lasI (21.4), *lasR* (2.5), *rhlI* (2.3), *rsaL* (4.9), *pqsB* (2.0), *pqsE* (7.0), *pqsR* (6.3), *qscR* (6.0), *vfr* (2.5)	QS
alg44 (3.1), *alg8* (4.8), *algB* (4.6), *algE* (4.4), *algF* (4.9), *algI* (30.8), *algU* (3.5), *algX* (4.0), *algZ* (11.8), *mucB* (11.2), *mucC* (3.1), *pslB* (2.4)	exopolysaccharides

aer (3.2), *aer2* (2.7), *cheY* (2.0), *motA* (6.4), *motB* (4.2), *motC* (3.3), *pctA* (2.3), PA5072 (2.1)	chemotaxis and aerotaxis
pcrD (2.1), *pscT* (2.3)	T3SS
clpP (9.1), *clpP2* (5.6), *clpX* (7.2), *lasB* (8.2), *prpL* (2.2)	proteases
mreB (2.4)	shape
phzD1 (2.8), *phzD2* (1.6), *phzM* (3.7)	phenazines
Down-regulated	
algC (-2.9)	exopolysaccharide

As can be observed, genes involved in phenotypes of particular interest for this work were differentially expressed in the microarray assay (**Table 3.3**), including additional c-di-GMP signalling genes to those identified in the RNA-seq (**Table 3.1, Table 3.2)**. The up-regulation of genes encoding biofilm matrix components and those related to motility appendages were consistent in both studies. In other cases, the amount of genes related to a particular phenotype was considered worthy of future work, such as those related to c-di-GMP signalling, and correspondent analysis will be presented in the relevant sections. Other phenotypes were exclusive to one of the assays, or were affected by CDA in opposite ways; which could be explained by the differences in growth conditions. All in all, the analysis of both transcriptomic assays was a starting point for the construction of a preliminary CDA network.

The effect of CDA in AHL and AQ-based QS systems was investigated in LB in a previous study and is consistent with the results of the RNA-seq [294]. More investigation in M9 would be required in the future to ascertain the results of the microarray.

Various ECH were differentially expressed in the microarray by Rahmani-Badi et al., including PA0745 (less than 2-fold induction) and PA4980 (**Table 3.3**). PA0745 had been identified as the CDA synthase and named *dspI* in a previous study. The authors stated that the expression levels of *dspI* were not affected by CDA [380]. However, Twomey et al. showed that the cluster PA0744-PA0747 is regulated by the presence of 50 μM DSF [369]. This discrepancy on whether synthases are affected by their cognate DSF-T molecules has been found elsewhere [263, 381], and will be covered in more detail in **Chapter 4**. PA4980 was defined as the synthase of CDA by Rahmani-Badi et al. following bioinformatic analysis.

Type 3 secretion system (T3SS) has been linked to acute phenotypes in *P. aeruginosa*; whereas type 6 secretion system (T6SS) is linked to chronic

infections [27, 200]. Results in LB show that T3SS is down-regulated by CDA and T6SS is up-regulated; this indicates that the cultures were switching from acute to chronic in the presence of this DSF-T (**Table 3.1**). In contrast, results in M9 show that T3SS is up-regulated (**Table 3.3**), suggesting an impact on acute phenotypes.

It is of note that there was a high amount of regulators differentially expressed by CDA in both studies, including transcriptional regulators, small RNAs and sigma factors. This indicates a global regulatory role for CDA in *P. aeruginosa.*

3.2.3 Impact of DSF-T on *P. aeruginosa* growth

The fatty acids DSF, BDSF and CDA were added to liquid cultures to assess the impact on bacterial growth in various growth media. The concentration used was 100 µM, as this is the maximum concentration used in subsequent assays, and a solvent control using MetOH was performed alongside. Growth was monitored by measuring OD at 600 nm, using an automated spectrophotometer. This method allows for a minimum use of DSF-T, given the limited availability of these compounds.

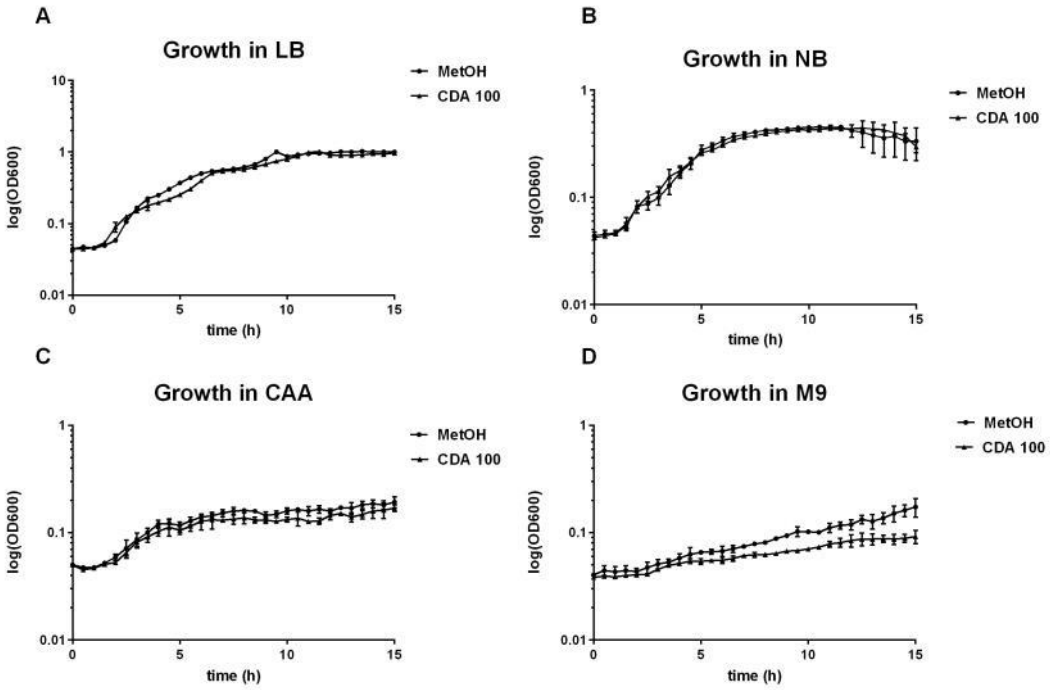


Figure 3.5. Effect of DSF-T molecules in the growth of *P. aeruginosa* PAO1-L. Liquid cultures of *P. aeruginosa* PAO1-L were spiked with 100 µM of DSF-T or MetOH as a solvent control. Growth was determined by the OD_{600} in an automated spectrophotometer. Readings were taken every 30 min. NB, Nutrient Broth medium; CAA, casamino acids-derived medium.

Results in **Figure 3.5** show that CDA does not cause cell toxicity or affects growth, under the conditions used. Next, a series of assays were used to assess the impact of these molecules in *P. aeruginosa* based on the targets identified in the RNA-seq data. LB was used as the main growth medium for consistency with the RNA-seq.

3.2.4 Effect of CDA on biofilm formation in *P. aeruginosa*

Previous to this thesis, the effects of CDA on *P. aeruginosa* were examined in biofilms grown in metal coupons, in RPMI medium. Under these conditions, treating grown biofilms with increasing concentrations of CDA showed that dispersion occurred in a dose-dependent manner. In particular, 30 min treatment with 50 nM and 10 μM CDA resulted in a loss of 50 % and 80 % loss of biofilm biomass, respectively. On the other hand, addition of 10 μM CDA to liquid LB cultures abrogated the formation of biofilms under flow in the Bioflux system [294].

During this chapter, alternative biofilm models were used to test whether the effect of CDA is reproducible under different growth conditions.

3.2.4.1 Crystal violet attachment model

Biofilm growth was first assessed in 96-well plates. A range of different conditions was used, including M9 supplemented with 1 μM succinate or 10 μM glucose, LB diluted to 10 % (v/v) in distilled water, and undiluted LB. The plates were either incubated statically at 37 ºC, or with 200 rpm shaking.

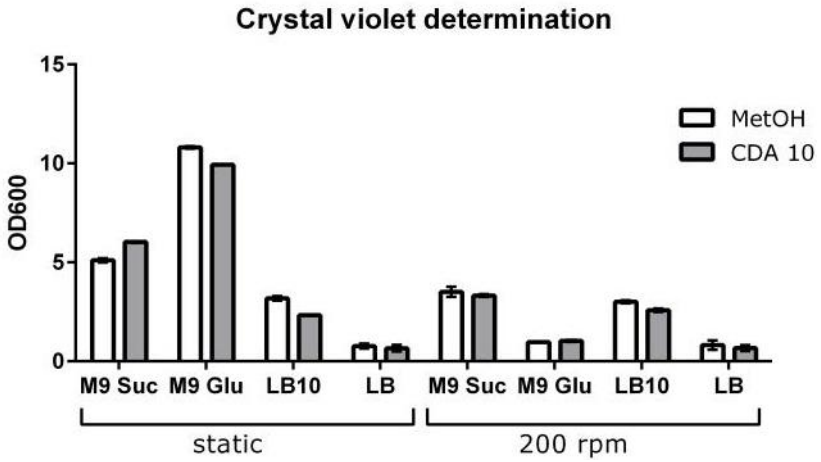


Figure 3.6. Attachment assay of *P. aeruginosa* PAO1-L in the presence and absence of 10 μM CDA. Biofilms of PAO1-L were grown in various media with and without CDA 10 μM in M9 supplemented with succinate (M9 Suc), M9 supplemented with glucose (M9 Glu), LB 10 % (LB10) or LB. Cells were incubated at 37 ºC for 16 h. The supernatants were then removed and the attached cells were stained with 1 % crystal violet.

The results presented in **Figure 3.6** sit in disarray with the current literature. It was hypothesised that CDA could be affecting local areas of the attached cells that would not result in substantial changes in absorption. Therefore, chamber slides were then tested, in LB and M9-glucose medium.

3.2.4.2 Biofilm chamber slide model

PAO1-L was tagged with a chromosomal fusion expressing GFP from the constitutive ribosomal promoter *rrnA* to enable visualisation using CLSM and the resulting strain was named PADP44. Biofilms of the GFP-tagged *P. aeruginosa* were grown for 16 h statically at 37 ºC on glass slides.

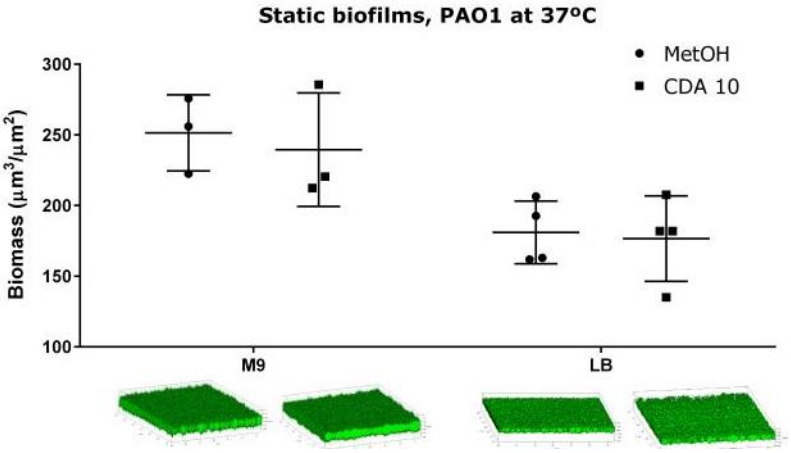


Figure 3.7. Biofilm formation of PAO1-L tagged with GFP (PADP44), in the presence and absence of 10 µM CDA, in chamber slides. Biofilms were grown statically at 37 ºC for 16 h in M9 supplemented with glucose and in LB. The supernatants were then removed and biofilms were visualised under CLSM. Representative micrographs are shown below. Quantification of biofilm biomass was performed with Image J and the plugin Comstat2.

As can be observed in **Figure 3.7**, the addition of 10 µM CDA did not affect biofilm growth under the conditions tested. It was next hypothesised that lowering the temperature of incubation would decrease the growth rate of PAO1, allowing more time for CDA to inhibit regulatory mechanisms of biofilm formation in PAO1. This is also in line with the original publication describing CDA in which biofilm studies were performed at 30 ºC [255]. Additionally, a transcriptomic study comparing the expression of genes at 22 ºC and 37 ºC in *P. aeruginosa* PAO1 found *pslC*, required for the production of the Psl exopolysaccharide involved in biofilm formation, to be upregulated at 37 ºC [382]. Hence, a lower temperature could result in a less robust biofilm structure, also making the effects of CDA in biofilm inhibition more evident.

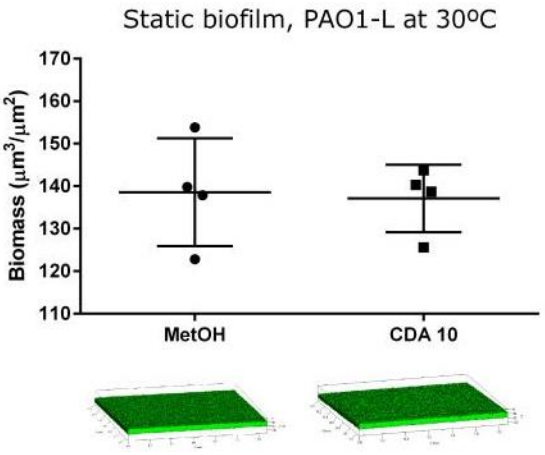


Figure 3.8. Biofilm formation of PAO1-L tagged with GFP (PADP44) in the presence and absence of 10 µM CDA, at 30 ºC. Biofilms were grown statically at 30 ºC for 16 h in LB. The supernatants were then removed and biofilms were visualised under CLSM. Representative micrographs are shown below. Quantification of biofilm biomass was performed with Image J and the plugin Comstat2.

Results in **Figure 3.8** show that CDA does not inhibit biofilm formation at 30 ºC. The effects of CDA on biofilm inhibition were next investigated in a different *P. aeruginosa* strain. A recent publication identifying *dspI* as the CDA synthase used PA14 as the wild-type strain [380]. PA14 is markedly different to PAO1, particularly as it uses Pel, and not Psl, as the major exopolysaccharide component of the biofilm matrix [105]. The chamber biofilm experiment was therefore performed in UCBPP-PA14.

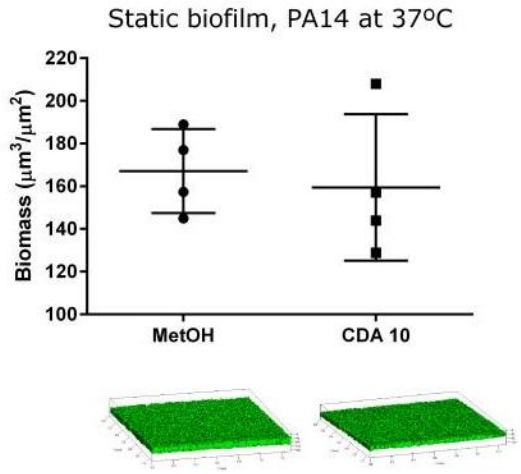


Figure 3.9. Biofilm formation of UCBPP-PA14 tagged with GFP (PADP326) in the presence and absence of 10 µM CDA, at 37 ºC. Biofilms were grown statically at 37 ºC for 16 h in LB. The supernatants were then removed and biofilms were visualised under CLSM. Representative micrographs are shown below. Quantification of biofilm biomass was performed with Image J and the plugin Comstat2.

As seen in **Figure 3.9**, biofilm formation in UCBPP-PA14 was not affected by the addition of 10 µM CDA. Results so far indicate that CDA may only inhibit biofilm formation under specific conditions that were not met in the chamber slide assay. To determine whether the GFP tagging was causing any metabolic changes that

could mask the effects of CDA, grown biofilms were stained with Syto9, but no differences were found in the biofilm formation of PAO1 in the presence of CDA (data not shown).

3.2.4.3 Biofilm disruption in chamber slides

It was then hypothesised that CDA might be degraded or converted into a different molecular species under the conditions tested. Therefore, the impact of CDA in biofilm disruption was investigated.

Assays were conducted in the chamber slide model, both in LB (**Figure 3.10**) and in M9 (see **Appendix, Figure 7.3**). Briefly, biofilms were grown overnight statically at 37 ºC. The supernatant was removed and visualised by confocal microscopy to obtain pre-treatment data. Then, media containing CDA or MetOH was added, and the biofilms were incubated for further 4 h or 8 h, after which the biofilms were visualised again.

The chamber slide biofilm model allows for easy visualisation and treatment of mature biofilms. However, biofilms formed under these conditions are not robust and can lose structural integrity after multiple rounds of pipetting (see **Figure 5.11**). Biofilm disruption was not quantified here and the data is only qualitative.

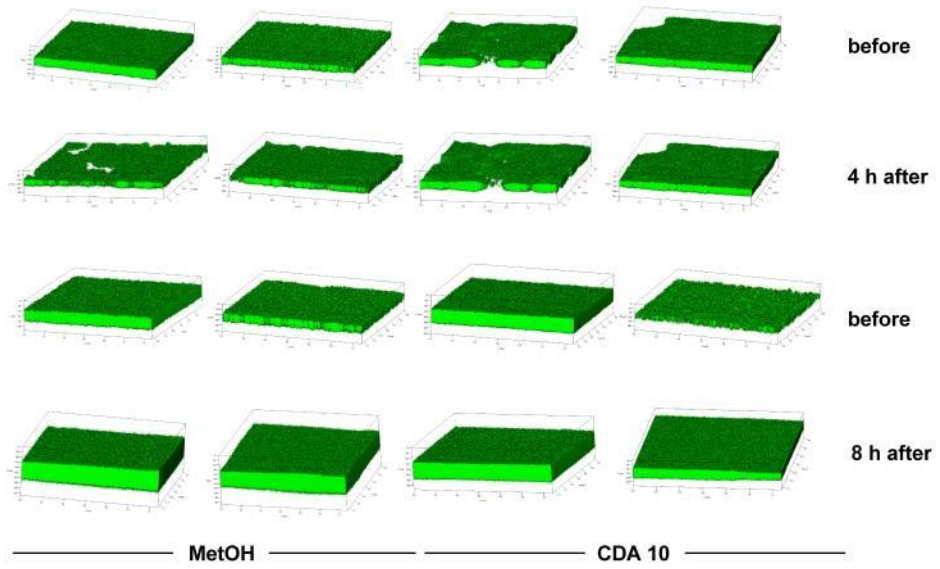


Figure 3.10. Impact of CDA on the biofilm disruption of *P. aeruginosa* PAO1-L. Biofilms were grown for 16 h, after which they were treated with CDA 10 µM or the carrier control (MetOH) for 4 h or 8 h. Biofilms were visualised before and after treatment with confocal laser scanning microscopy (CLSM).

Results in **Figure 3.10** show that CDA does not disrupt grown biofilms, under the conditions tested.

3.2.4.4 Impact of CDA on colony morphology

The assays presented above were conducted over a 13-16 h incubation time. One key factor during biofilm formation is the time of incubation, as longer times would allow for the maturation of the biofilms. Some of the publications on the dispersion of biofilms caused by CDA were performed in flow cells and in tube biofilms, which were kept over approximately a week [255, 380, 383].

The assessment of colony morphotypes was next performed. Briefly, PAO1 and UCBPP-PA14 (PA14) were grown in plates supplemented with Congo red and Coomassie blue. Under these conditions, PA14 forms wrinkly colonies to enhance surface area and therefore have better access to oxygen, whereas PAO1 remains smooth [105, 122]. Results show no differences in colony morphology caused by the exogenous addition of CDA (**Figure 3.11**).

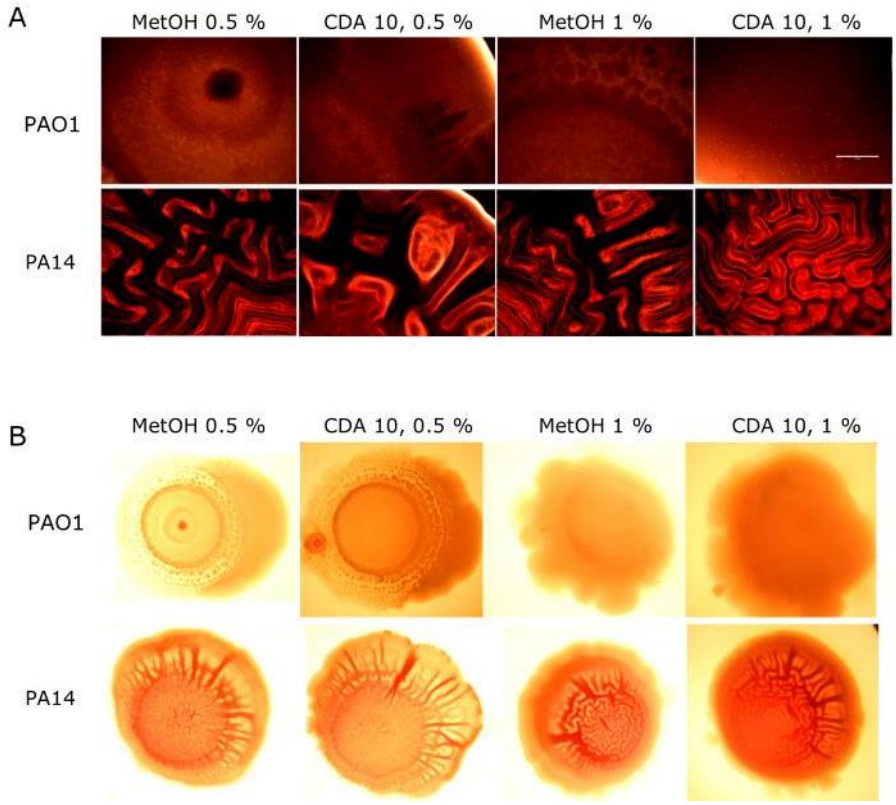


Figure 3.11. Effect of CDA on colony morphotypes. Colony morphologies of PAO1-L and UCBPP-PA14 were grown under different agar concentrations (0.5 % and 1 %) in the presence of Congo red and Coomassie blue, with and without 10 μM CDA. Images were taken by an EVOS optical microscope with a 10x objective **(A)** or a binocular **(B)**. The scale bar represents 1 mm.

3.2.5 C-di-GMP

C-di-GMP is a major contributor of biofilm formation in bacteria [205]. Given the dramatic reported effect of CDA on biofilm formation under conditions different to the ones presented above, the link between this fatty acid signal and c-di-GMP was assessed. C-di-GMP is synthesised by diguanylate cyclases (DGC) containing the GGDEF motif and is degraded by phosphodiesterases (PDE) carrying the motifs EAL or HD-GYP. Therefore, a search for enzymes containing these motifs was done using the RNA-seq data.

Table 3.4. Enzymes involved in the synthesis of c-di-GMP that were differentially expressed by CDA in the RNA-seq analysis. Results from transcriptomics data were assessed, with information from [207]. Reads per Kb per million reads (RPKM) have been listed. The genes shown are differentially expressed by 100 μM CDA according to the Baggerly's test. PDE, phosphodiesterase; DGC, diguanylate cyclase; CDA, *cis*-2-decenoic acid.

Gene ID	DGC/PDE motifs		MetOH	CDA
mucR	GGDEF	EAL	45	18
PA2072	GGDEF	EAL	11	2
PA2567	SPTRF	EAL	44	79
bifA	GGDQF	EAL	8	20
PA4929	GGEEF	-	13	3
PA5487	GGDEF	-	4	0

Results show that several c-di-GMP regulators are affected by the presence of CDA with some of them showing increased transcription whereas others showed the opposite effect (**Table 3.4**). If the presence of CDA results in c-di-GMP changes in the cells which lead to biofilm disruption, then this fatty acid would activate PDE and/or repress DGC. Insertions in PA4929 and in *mucR* result in less biofilm formation; hence the main activity of these enzymes is the DGC. In contrast, an insertion in *bifA* brings about a hyperbiofilm phenotype and is therefore a PDE [207]. PA2567 presents an aberrant GGDEF motif, and functions as a PDE [217]. Interestingly, these observations fit with the results of the RNA-seq analysis. No information was found on the main activity of PA2072.

As a first step, experiments were conducted to assess the effect of CDA on general c-di-GMP levels. First, the pCdrA::gfp^{C} reporter fusion [299] was used to evaluate the general pool of c-di-GMP. The DSF-T molecules DSF and BDSF were included alongside, together with the negative control *trans*-2-decenoic acid (TDA).

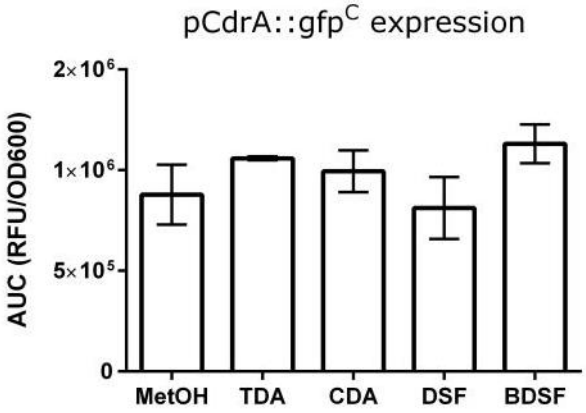


Figure 3.12. Impact of DSF-T on c-di-GMP. PAO1-L/pCdrA::gfp^C was grown in microtiter plates in LB supplemented with 100 µM of either DSF-T molecules, TDA or the solvent control MetOH. GFP fluorescence and OD_{600} were measured every 30 min for 24 h. The area under the curve (AUC) of the normalised relative fluorescent units (RFU) was calculated. Error bars represent one standard deviation of the means.

As can be observed in **Figure 3.12**, none of the molecules tested affect the general pool of c-di-GMP in *P. aeruginosa*. However, current literature has shown that c-di-GMP exists in distinct pools within bacterial cells, which are independent from each other [208, 209, 384]. The overall levels of c-di-GMP expression could be masking more subtle changes.

Hence, to confirm the results of the RNA-seq and evaluate whether specific pools of c-di-GMP may have been affected by CDA, transcriptional *lux*-based reporters were constructed. PA5487 is located in an operon, and the gene upstream was not differentially regulated, so the correspondent reporter was not constructed.

The P2567-*luxCDABE* reporter (pSH12) was available from the laboratory strain collection, while the others were constructed using the vector pminiCTX-lux. Briefly, the upstream regions of *bifA*, PA4929 and *mucR* were cloned in pminiCTX-lux, inserted in the PAO1-L chromosome, and named PADP302, PADP303 and PADP294; respectively. Since CDA seems to interfere with luciferase activity [294], strains containing the *lux* operon without a promoter were used as background controls, as these strains still show luciferase activity. Strain PADP236 was used in experiments with PASH12; they were both constructed in a PAO1-N background, while strain PADP228 was used for the rest of the biosensors, and has a PAO1-L background.

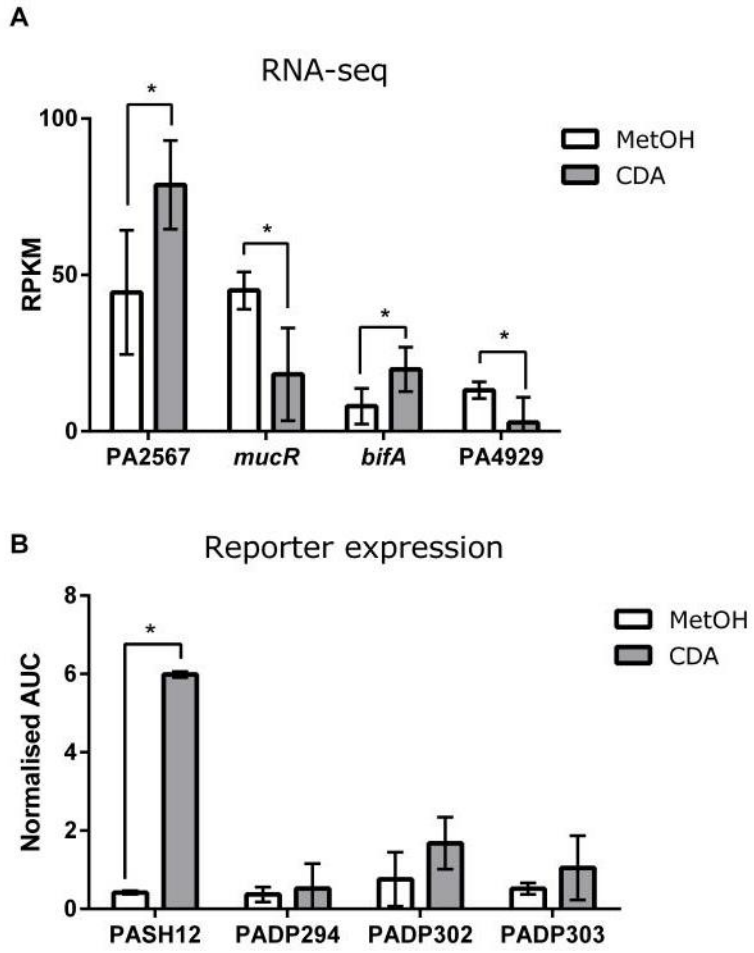


Figure 3.13. Impact of CDA on the expression of c-di-GMP regulators in PAO1. A, Reads per Kb per million reads (RPKM) of selected c-di-GMP regulators, from the RNA-seq analysis. These genes were differentially regulated in the Baggerly's test. Error bars represent one standard deviation from the means from two independent replicates. **B,** Strains containing biosensors for PA2567 (PASH12), *mucR* (PADP294), *bifA* (PADP302) and PA4929 (PADP303) were grown in LB in microtiter plates, and the luminescence and OD_{600} were measured every 30 min for 24 h. The relative luminescent units (RLU) were then normalised by the OD600, and the area under the curve (AUC) was determined. This was divided by the AUC(RLU/OD600) of the promoterless controls PADP236 (for PASH12) or PADP228 (for the rest) to give the normalised luminescence per cell. Error bars represent one standard deviation of the means from 3 independent replicates. The luminescence from PASH12 was activated by CDA, $p=6\cdot10^{-8}$ in a multiple t-test assay with $\alpha=0.05$, and the Holm-Sidak correction.

Results show that the transcription of the phosphodiesterase gene PA2567 was activated in the presence of 100 μM CDA, both from the RNA-seq and from the biosensor assay (**Figure 3.13**). It is possible that this leads to decreased biofilm formation in the presence of CDA, under conditions that were not tested in this chapter. The fusion to *bfiA* (PADP302) presents a similar trend to that of the RNA-seq. However, *mucR* and PA4929 do not show the same effects in the RNA-seq and in the reporters, which might be due to post-transcriptional regulations controlling those genes.

3.2.6 Motility

3.2.6.1 Swimming and cell morphology

Expression of flagellar genes

CDA, as well as other related molecules, has been described in the literature as an inhibitor of biofilm formation. A possible underlying mechanism for this is the activation of motility [68].

It is noteworthy that gene expression in liquid cultures and in biofilms differs greatly. As the deep sequencing data derived from liquid cultures, the impact of CDA on planktonic cells may not have reflected the real scenario in established biofilms. Nevertheless, many of the genes identified in the RNA sequencing study support the hypothesis of CDA playing a key role in the transition between biofilm and planktonic states. Amongst these are genes involved in flagellum biosynthesis and function which were clustered together. Only operons where at least one gene was statistically relevant are shown.

Table 3.5. Impact of CDA on the expression of flagellum-associated genes. The reads per Kb per million reads (RPKM) from the RNA-seq are shown for genes related to flagellum. Statistically relevant genes are shown in bold letters. Lines separate different predicted operons.

Gene ID	MetOH	CDA	Gene ID	MetOH	CDA	Gene ID	MetOH	CDA
fleQ	**159**	**215**	*flgF*	46	71	*fliL*	245	280
fleS	**16**	**27**	*flgG*	43	57	*fliM*	68	112
fleR	**13**	**21**	*flgH*	21	36	*fliN*	81	130
fleN	103	119	*flgI*	47	37	*fliO*	32	23
fliA	104	112	***flgJ***	**41**	**61**	*fliP*	47	58
cheY	**149**	**184**	*flgK*	27	49	***fliQ***	**21**	**59**
cheZ	243	223	***flhA***	**21**	**29**	*fliR*	14	17
flgB	13	31	*flhF*	56	49	*flhB*	10	9
flgC	70	81						
flgD	**80**	**160**						
flgE	**44**	**71**						

Results show that the genes related to flagella are activated by CDA, with few exceptions (**Table 3.5**). Interestingly, genes related to flagellar function were generally activated, such as the 2CS FleS and FleR [385], and the master transcriptional regulator for flagellar expression, FleQ [68, 213].

Expression of rod-shape genes

The results related to flagella prompted us to investigate if other features of cell morphology might be regulated by the presence of CDA. Genes related to pili

synthesis were not found differentially expressed, but interestingly, a number of rod-shape determining genes were activated by CDA (**Table 3.6**).

Table 3.6. Expression of rod-shape genes in the presence and absence of CDA. The reads per Kb per million reads (RPKM) from the RNA-seq show that a set of shape-determining genes is activated by the presence of CDA. Statistically significant genes are shown in bold. Lines separate different predicted operons. Most of the genes in an operon with *rodA* presented higher RPKM with CDA, but they are not involved in cellular morphology, and hence those were not added to the table.

Gene ID	MetOH	CDA
rodA	54	130
mreD	8	15
mreC	11	34
mreB	21	89

Swimming assay

The activation of flagellar genes suggests that CDA might be potentiating the biosynthesis of flagellar appendages; therefore facilitating motility in *P. aeruginosa*. Hence, swimming motility was assessed in the presence of this fatty acid. DSF-T molecules have shown to affect bacterial motility in their cognate producers [246], but the effects of these molecules in *P. aeruginosa* has not been fully described. Hence, the motility of *P. aeruginosa* PAO1 in the presence of DSF and BDSF was also addressed.

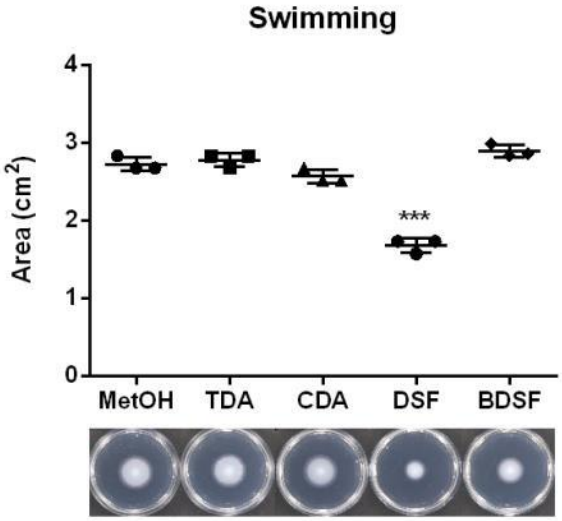


Figure 3.14. Impact of DSF-T molecules on *P. aeruginosa* PAO1-L swimming motility. Swimming in the presence of 100 µM DSF-T was performed in LB. Cells were inoculated to mid-depth in 0.3 % agar plates, and incubated for approximately 14 h at 37 ºC. Pictures show representative results. Swimming is impaired in the presence of DSF as compared to the MetOH control, p=0.0001.

Results show that swimming is reduced by DSF, while the other DSF-T molecules (CDA and BDSF) do not impact swimming motility, under the conditions tested (**Figure 3.14**).

Next, a more in depth analysis was performed to unravel the effects of DSF in *P. aeruginosa* motility. Briefly, swimming was assessed in 3 different media; namely LB, NB and CAA. A number of cells remain on the surface of the agar when inoculating cultures, and therefore swarming occurs in those media in which surface motility is promoted, such as CAA. In order to accurately observe the swimming patterns, CAA plates were only evaluated at 5 h post-inoculation.

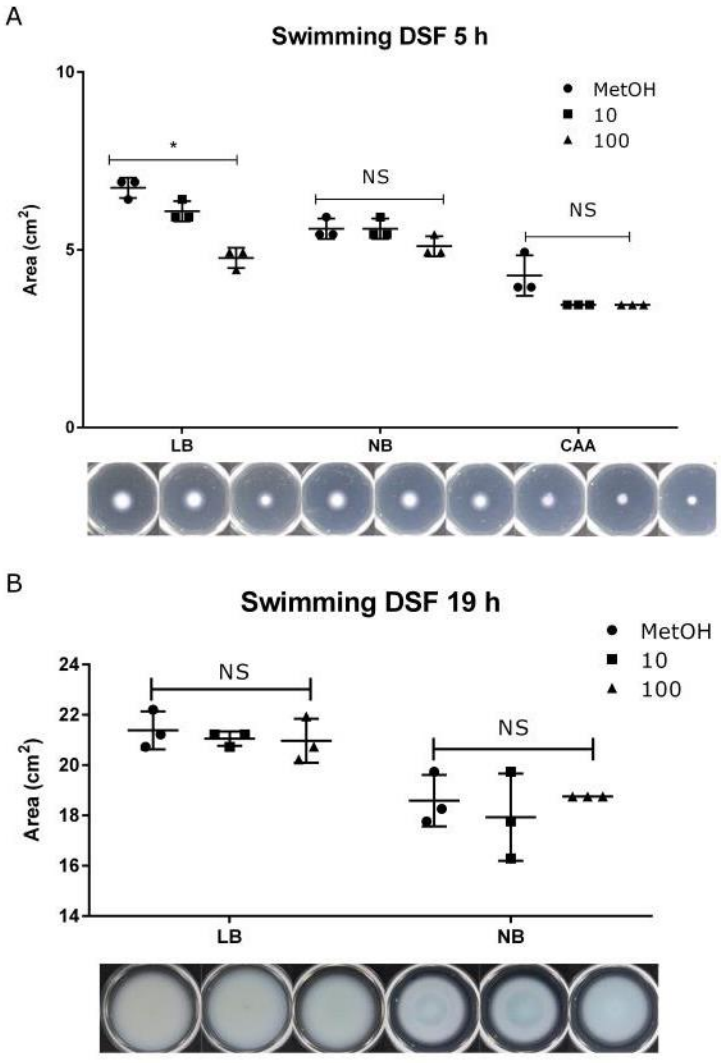
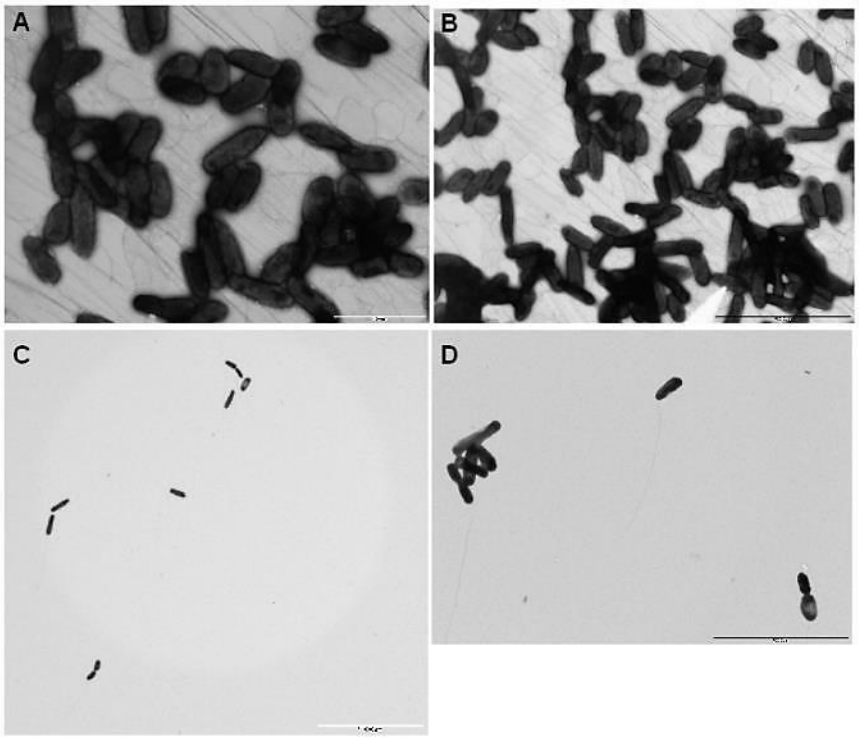


Figure 3.15. Impact of DSF on *P. aeruginosa* PAO1-L swimming motility in a range of growth media. Swimming in the presence of 10 μM and 100 μM DSF-T was performed in LB, NB and CAA. Cells were inoculated to mid-depth in 0.3 % agar plates, and incubated for 5 h **(A)** and 19 h **(B)** at 37 ºC. Pictures show representative results. Swimming is delayed in the presence of DSF after 5 h of incubation, in LB (p=0.015), but reaches wild-type levels at longer incubation times.

Results show that DSF delays swimming in LB, though this effect is reduced in NB and CAA. In addition, swimming reaches wild-type levels at longer incubation times, where no difference can be observed due to the presence of DSF (**Figure 3.15**).

Visualisation of cell morphology

Next, cells grown in the presence of CDA were visualised to study effects of this fatty acid on cellular morphology. The study of cell morphology would shed light onto major effects of CDA, and potentially validate results of the RNA-seq (**Table 3.5, Table 3.6**). On the other side, this analysis would represent a preliminary description of swarmers in the presence of CDA. Therefore, swarming cells were grown in confluent in the presence of CDA 100 µM, recovered from swarming plates, and then visualised by transmission electron microscopy (TEM).



E

Length of MetOH cells (n=20)	Length of CDA cells (n=13)
1.47 µm ± 0.23	1.50 µm ± 0.30

Figure 3.16. Visualisation of PAO1-L swarmer cells with transmission electron microscopy (TEM), in the presence and absence of CDA 100 µM. PAO1-L cells were recovered from swarming plates, fixed with glutaraldehyde in cacodylate buffer, and stained with uranyl acetate, then visualised under a Tecnai G2 12 Biotwin (FEI). **A and B,** cells incubated with the solvent control MetOH, magnification x9900 and x6000; respectively. **C and D,** cells incubated with 100 µM CDA, and visualised under x1700 and x6000 magnification; respectively**. E,** average length of the cells, as measured with GIMP v. 2.8.10.

Results show that the presence of CDA does not affect the overall morphology of PAO1-L cells, in terms of cell length, shape or presence of flagella (**Figure 3.16**).

3.2.6.2 Swarming

Next, surface motility was investigated. Swarming is a rapid movement generated in semi-solid medium that depends on flagella and the secretion of rhamnolipids [386]. Some authors consider that T4aP also play a role in swarming motility [72]. This movement is dependent on both the Rhl and Las QS systems.

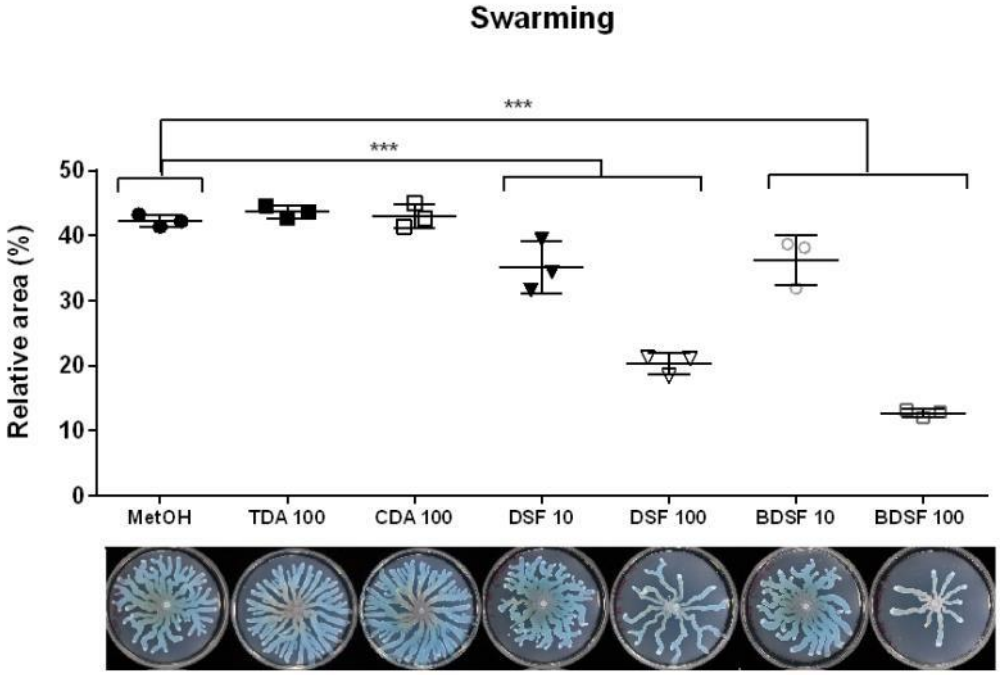


Figure 3.17. Impact of DSF-T on the swarming motility of PAO1-L. Plates of NB were supplemented with 0.5 % agar and 10 µM or 100 µM of DSF-T. MetOH and TDA were used as controls. Overnight cultures of PAO1-L were inoculated in the surface of the plates, which were then incubated at 37 ºC for 16 h. The swarming area was quantified relative to the total area of the plates. Error bars represent one standard deviation of the means. One-way ANOVAs were used to assess statistical significance, $p=0.0001$ for DSF and $p<0.0001$ for BDSF. Pictures depict representative results.

Interestingly, as can be observed in **Figure 3.17**, the diameter occupied by swarming tendrils did not drastically change with the addition of DSF-T, but the density of tendrils was reduced with DSF and BDSF, which can indicate an impairment of the infection spread potential of *P. aeruginosa* caused by these fatty acid signals. The addition of CDA did not affect swarming motility, under the conditions tested.

3.2.6.3 Twitching

Twitching represents another form of collective motility, in which cells are propelled by their pili to move across solid surfaces [86]. Twitching was assessed in the presence of DSF and BDSF, in LB plates supplemented with 1 % agar.

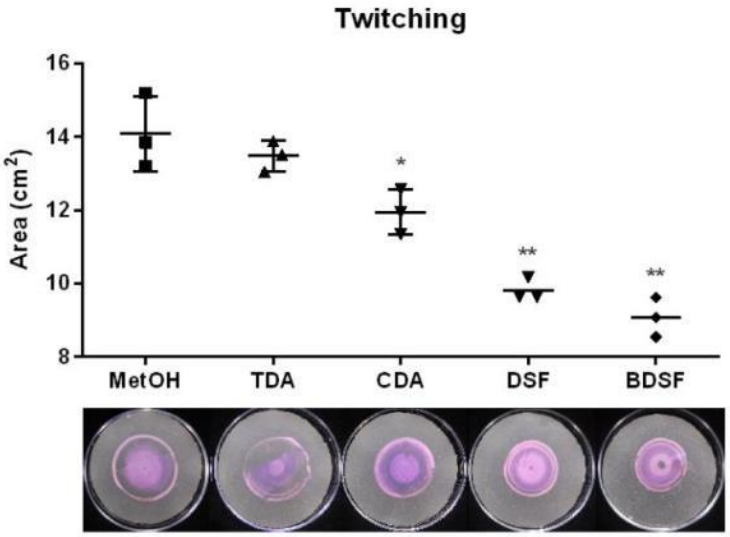


Figure 3.18. Impact of DSF-T on the twitching motility of PAO1. Overnight cultures of PAO1-L were inoculated at the bottom of 1 % agar plates supplemented with 100 µM DSF-T, or MetOH or TDA as controls. They were then incubated statically under high humidity conditions, at 37 ºC, for 48 h. The agar was subsequently taken out from the plates and cells were stained with 1 % crystal violet. Error bars represent one standard deviation from the means. T-tests were performed to assess statistical significance, CDA vs MetOH, p=0.036; DSF vs MetOH, p=0.0023; BDSF vs MetOH, p=0.0017. Pictures depict representative results.

Figure 3.18 shows that all DSF-T tested cause a reduction in *P. aeruginosa* twitching. DSF-T molecules, therefore, may impair the functionality of pili, or the adherence to solid surfaces, in *P. aeruginosa.* This does not follow the trend of the major T4aP, which was mostly up-regulated in the RNA-seq (**Table 3.1**).

3.2.7 Analysis of rhamnolipid production

A well-known factor that activates swarming motility is the production of rhamnolipids, which act as biosurfactants to facilitate bacterial motility in semi-solid surfaces [72]. Interestingly, rhamnolipids have also been linked to biofilm formation, and seem to be important components for the structure and function of biofilms [172, 174].

DSF-T molecules affect biofilm formation, both in their cognate species and in interspecies communication [244]. To gain a further insight in the mechanisms behind the impact in motility and biofilm caused by these signals, the production of rhamnolipids was next assessed.

3.2.7.1 RNA-seq

An overview of the RNA-seq results showed that the rhamnolipid synthases *rhlABC*, as well as the regulators *rhlIR*, are highly repressed by CDA (**Table 3.1**). **Table 3.7** shows the RPKM values for these genes.

Table 3.7. Impact of CDA on the expression of rhamnolipid synthases. Reads per Kb per million reads (RPKM) from the RNA-seq are shown for genes related to rhamnolipids. All the genes listed below were statistically significant in the Baggerly's test. Lines separate different predicted operons.

Gene ID	MetOH	CDA
rhlI	169	75
rhlR	585	205
rhlA	187	11
rhlB	27	5
rhlC	10	1

3.2.7.2 Reporter expression

To verify the results of the RNA-seq, the expression of *rhlAB* was studied with a biosensor strain of PAO1-L containing a translational fusion of P*rhlA-dsRed* (PASC682).

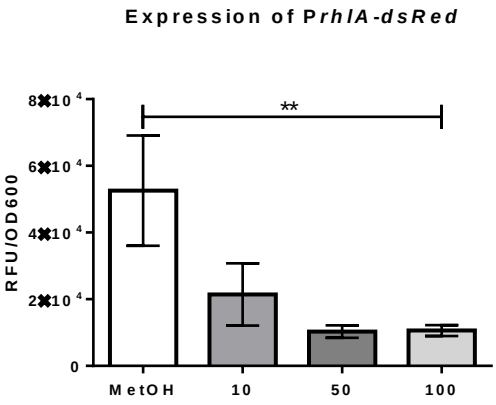


Figure 3.19. Impact of CDA on rhamnolipid expression. The biosensor strain PASC682, containing a fusion of *rhlA* with *dsRed_express2*, was grown in LB supplemented with 10, 50 or 100 µM CDA; or with the solvent control MetOH. Single reads of fluorescence and OD_{600} were taken after 16 h of incubation at 37 ºC. Error bars represent one standard deviation of the means. One-way ANOVA was used to assess statistical significance, p=0.0020.

Results show that CDA represses *rhlA* in a dose-dependent manner (**Figure 3.19**). These results are consistent with the RNA-seq (**Table 3.7**), and therefore prompted us to further investigate the effect of DSF-T, and in particular CDA, in rhamnolipid expression.

3.2.7.3 TLC analysis

Mono-rhamnolipids and di-rhamnolipids function as surfactants that help bacteria swarm across surfaces; however different signalling roles have been described for these families of chemicals. While mono-rhamnolipids only have a surfactant function, di-rhamnolipids attract swarming tendrils to one another, and HAAs (rhamnolipid precursors) repel the tendrils [76]. In addition to their impact on motility, rhamnolipids also contribute to biofilm formation. The supplementation of CDA to LB cultures was shown to decrease the expression of a translational *rhlAB* fusion (**Figure 3.19**) which prompted us to study the link between rhamnolipids and CDA. First, PAO1-L cultures were grown in NB, and rhamnolipids were extracted and run on TLC.

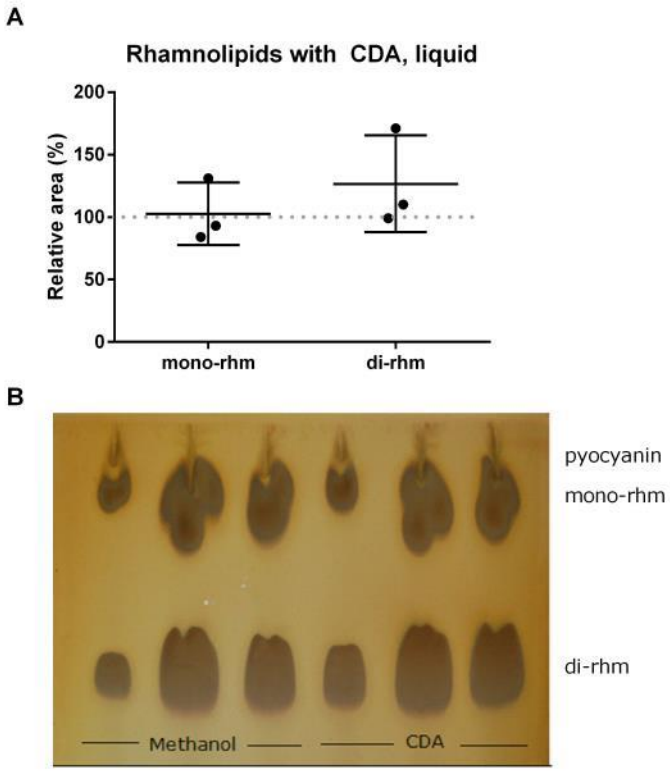


Figure 3.20. Impact of CDA on rhamnolipid production in *P. aeruginosa* PAO1-L grown in liquid. Bacterial cultures were grown in NB with and without 100 µM for 16 h and the rhamnolipids were extracted with EtOAc. **A,** the area occupied by mono- and di-rhamnolipid (mono-rhm and di-rhm, respectively) was determined by pixel integration analysis and plotted relative to the area of spots from the cultures grown with the solvent control MetOH. Error bars represent one standard deviation of independent triplicates. **B,** Picture of TLC plate after the detection of spots with an acidic solution of orcinol. The upper spots correspond to mono-rhm, the lower spots correspond to di-rhm. No statistically significant differences were found in plates supplemented with CDA.

Results show that the addition of CDA to *P. aeruginosa* PAO1-L does not affect rhamnolipid secretion, under the conditions tested (**Figure 3.20**). Given that CDA has shown to inhibit biofilm formation in other studies, the production of rhamnolipids was studied in surface-grown bacterial cells. *P. aeruginosa* cultures

were spread on swarming plates and incubated for 16 h, and rhamnolipids were then extracted.

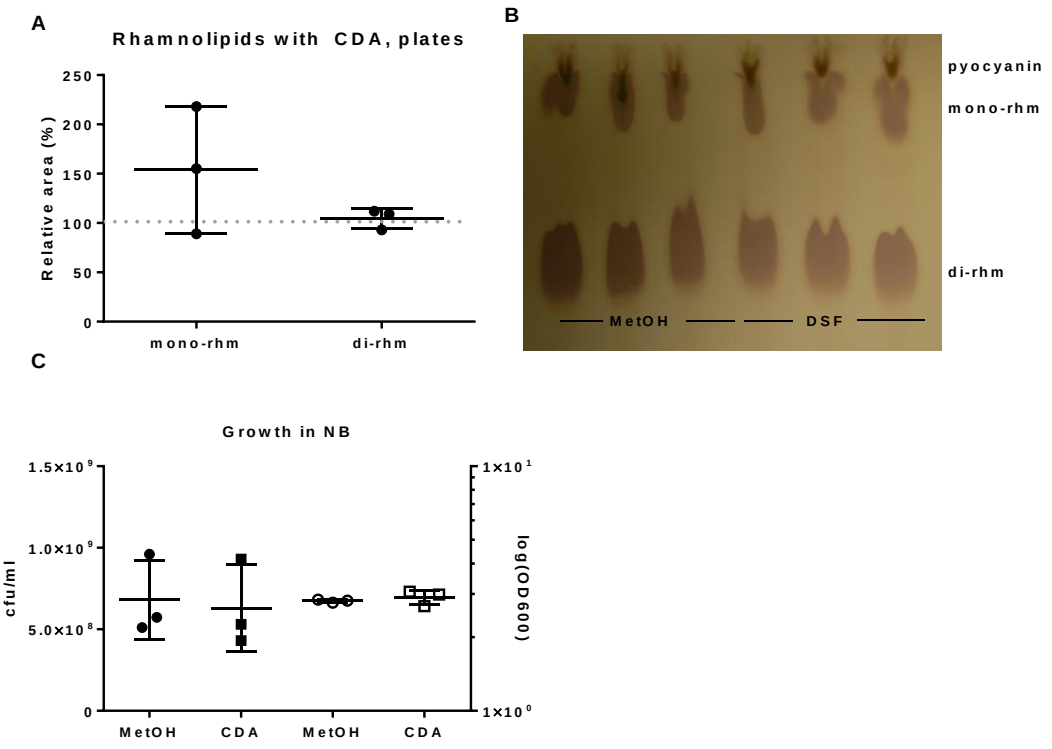


Figure 3.21. Impact of CDA on the rhamnolipid production of *P. aeruginosa* PAO1-L grown in swarming plates. Bacterial cultures were grown in NB supplemented with 0.5 % agar, in the presence and absence of 100 µM CDA for 16 h and the rhamnolipids were extracted with EtOAc. **A,** the area occupied by mono- and di-rhamnolipid (mono-rhm and di-rhm, respectively) was determined by pixel integration analysis and plotted relative to the area of spots from the cultures grown with the solvent control MetOH. Error bars represent one standard deviation of independent triplicates. **B,** Picture of TLC plate after the detection of spots with an acidic solution of orcinol. The upper spots correspond to mono-rhm, the lower spots correspond to di-rhm. No statistically significant differences were found in plates supplemented with CDA. **C,** Growth of *P. aeruginosa* in agar plates supplemented with CDA. Filled symbols represent the cfu/ml, open symbols represent the OD_{600}. Growth was assessed from 0.5 % agar plates by recovering cells with phosphate buffer saline (PBS) from the surface of the agar.

Results show that CDA does not affect rhamnolipid production in agar plates (**Figure 3.21**).

Previous results show that DSF and BDSF cause the reduction of surface colonisation in swarming assays (**Figure 3.17**). Therefore it was hypothesised that these molecules would reduce the ratio di-rhm: HAAs and cause the reduction of swarming tendrils. Due to time constraints, the effects of BDSF were not assessed with this technique and only DSF was studied.

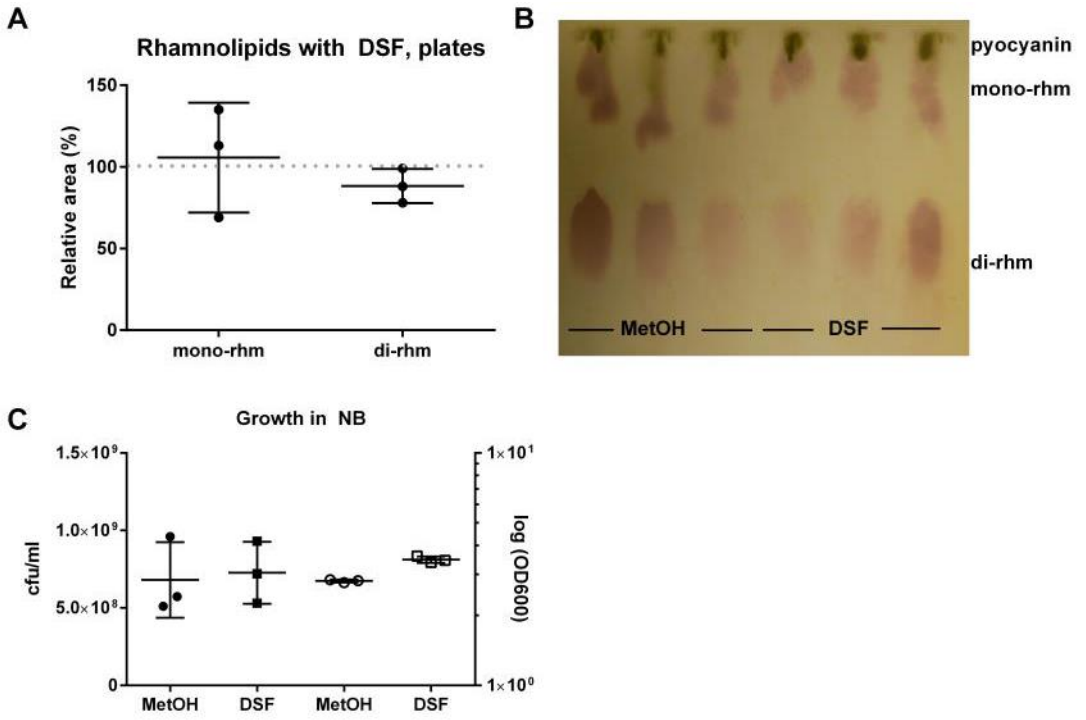


Figure 3.22. Rhamnolipid production of PAO1-L in the presence of 100 µM DSF. A, the area occupied by mono- and di-rhamnolipid (mono-rhm and di-rhm, respectively) was determined by pixel integration analysis and plotted relative to the area of spots from the cultures grown with the solvent control MetOH. **B,** Picture of TLC plate after the detection of spots with an acidic solution of orcinol. The upper spots correspond to mono-rhm, the lower spots correspond to di-rhm. No statistically significant differences were found in plates supplemented with DSF. **C,** Growth of *P. aeruginosa* in agar plates supplemented with DSF. Filled symbols represent the cfu/ml, open symbols represent the OD_{600}. Growth was assessed from 0.5 % agar plates by recovering cells with phosphate buffer saline (PBS) from the surface of the agar.

As can be seen from **Figure 3.22**, DSF does not affect the rhamnolipid production of PAO1-L in swarming plates. More sensitive or specific techniques could potentially reveal small shifts in rhamnolipid secretion that would not be detected here. Another shortcome of the TLC assays is that HAAs are not detected. Nevertheless, dramatic shifts in rhamnolipid production were not observed here. Hence, there might be other mechanisms responsible for the observed effects of DSF in swarming.

3.2.7.4 LC-MS/MS analysis

The use TLC with orcinol detection to study rhamnose-rich species does not allow the identification of HAAs nor an accurate quantitation of the biosurfactants. In order to obtain more quantifiable data, and to study the effect of signalling molecules on HAAs production, an LC-MS/MS method was developed (see **Chapter 2, section 2.6.5** and **Appendix 7.2.3**). For the TLC analysis, rhamnolipid extraction was performed from cultures grown 16 h in NB whereas the RNA-seq and the biosensor studies were performed in liquid LB cultures (at

4 h and 16 h, respectively). Therefore, for a better comparison with the transcriptional studies, the impact of CDA on HAA and rhamnolipid production was studied by LC-MS/MS on extracts from cultures grown in LB, for both 4 h and 16 h.

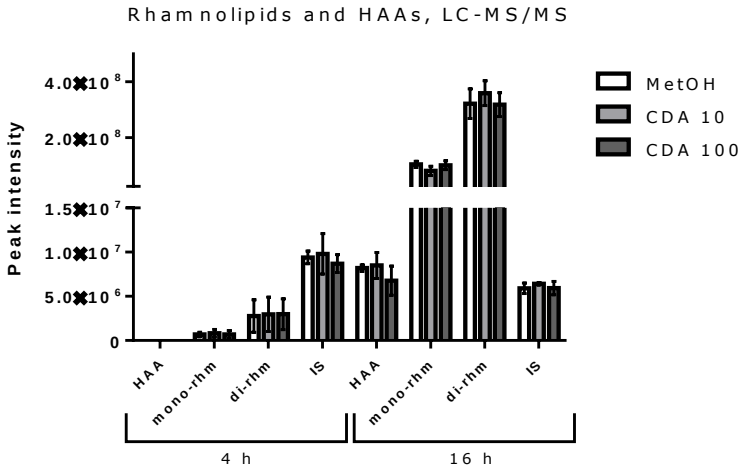


Figure 3.23. Impact of CDA on rhamnolipid and HAAs production in PAO1-L, as determined by LC-MS/MS. *P. aeruginosa* cultures were grown in LB supplemented with 10 µM and 100 µM CDA (or the solvent control MetOH) for 4 h and 16 h. EtOAc extractions were performed from the filter-sterilised supernatants. The major HAA (C_{10}-C_{10}), mono-rhamnolipid (mono-rhm, Rha-C_{10}-C_{10}) and di-rhamnolipid (di-rhm, Rha-Rha-C_{10}-C_{10}) were detected with this method. The internal standard (IS) 16-hydroxyhexadecanoic was used to validate the results. Error bars represent one standard deviation from the means.

Results show that the major rhamnolipids and HAAs were not affected by CDA (**Figure 3.23**). Together with previous results, this shows that the effect of CDA on the promoter of *rhlAB* is only transient and likely to be subjected to post-translational regulation.

3.2.8 Proteases

Proteolytic enzymes are virulence determinants that facilitate nutrient availability and degrade components of the host immune system. Therefore, proteases contribute to *P. aeruginosa* virulence [194]. The DSF-T regulatory network is responsible for protease secretion in *Xcc* and other bacterial species [246, 346]. In addition, *lasA* and *lasB* were differentially expressed by CDA (**Table 3.1, Table 3.2**). Given the importance of proteolytic enzymes, their production in the presence of DSF-T molecules was further investigated.

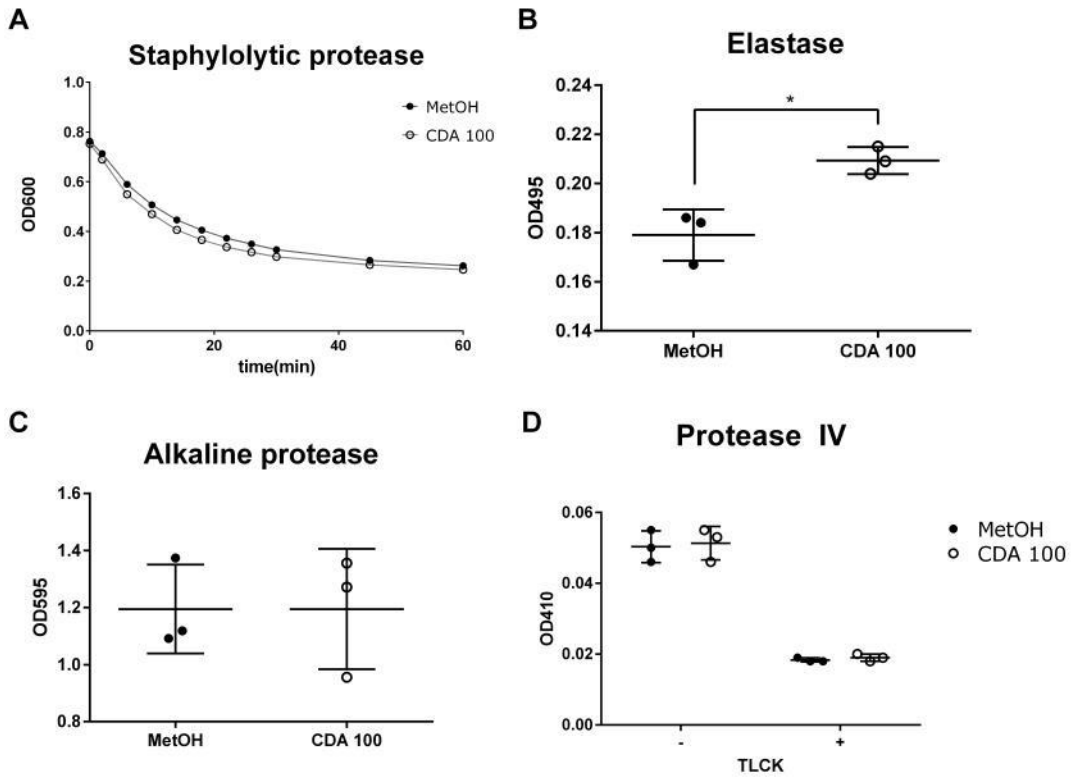


Figure 3.24. Impact of CDA on the proteolytic activity of PAO1-L. A series of protease assays were conducted in the presence and absence of 100 µM CDA, after incubation of cultures for 16 h at 37 ºC. **A,** Staphylolytic assay. Supernatants of cultures were put in contact with a suspension of *S. aureus* Newman, and the decay in OD_{600} was monitored over 1 h. **B,** Elastase assay. Supernatants were mixed with a suspension of elastin-Congo red, incubated at 37 ºC with 200 rpm shaking for 2 h and centrifuged. The OD of the suspension was then measured at 495 nm. A t-test was used to assess significance, p=0.011. **C,** Alkaline protease assay. Supernatants mixed with hide powder azure were incubated for 1 h at 37 ºC with 200 rpm shaking, and the OD_{595} of the resulting suspension was determined. **D,** Protease IV assay. Chromozym PL were mixed with culture supernatants and the OD_{410} was determined. TLCK is a serine protease inhibitor used as a negative control.

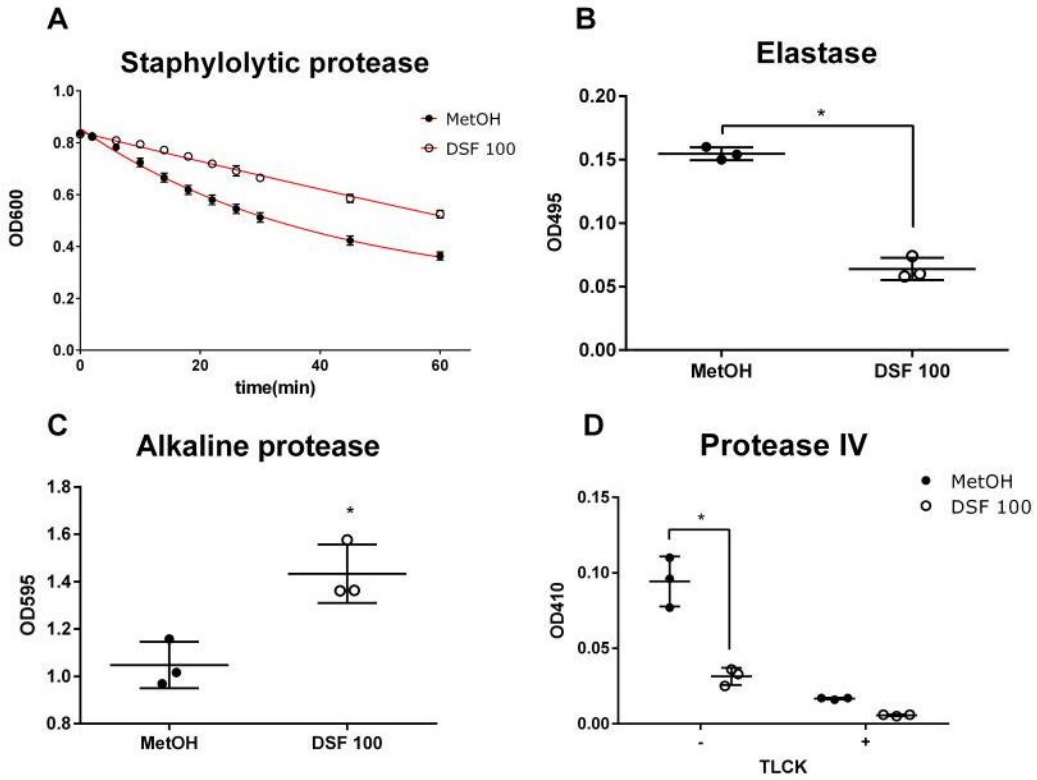


Figure 3.25. Impact of DSF on proteases of PAO1-L. A series of protease assays were conducted with PAO1-L in the presence and absence of 100 µM DSF, after incubation of cultures for 16 h at 37 ºC. **A,** Staphylolytic assay. The decay of absorbance in a *S. aureus* suspension was monitored. A one phase decay fit was used to assess statistical significance, p<0.0001. **B,** Elastase assay. Supernatants were mixed with a suspension of elastin-Congo red, and the OD was then measured at 495 nm. A t-test was used to assess significance, p=0.028. **C,** Alkaline protease assay. Supernatants were mixed with hide powder azure and the OD_{595} of the resulting suspension was determined. A t-test was used to assess statistical significance, p=0.013. **D,** Protease IV assay. Chromozym PL was mixed with culture supernatants and the OD_{410} was determined. TLCK is a serine protease inhibitor used as a negative control. A t-test was used to assess significance, p<0.0001.

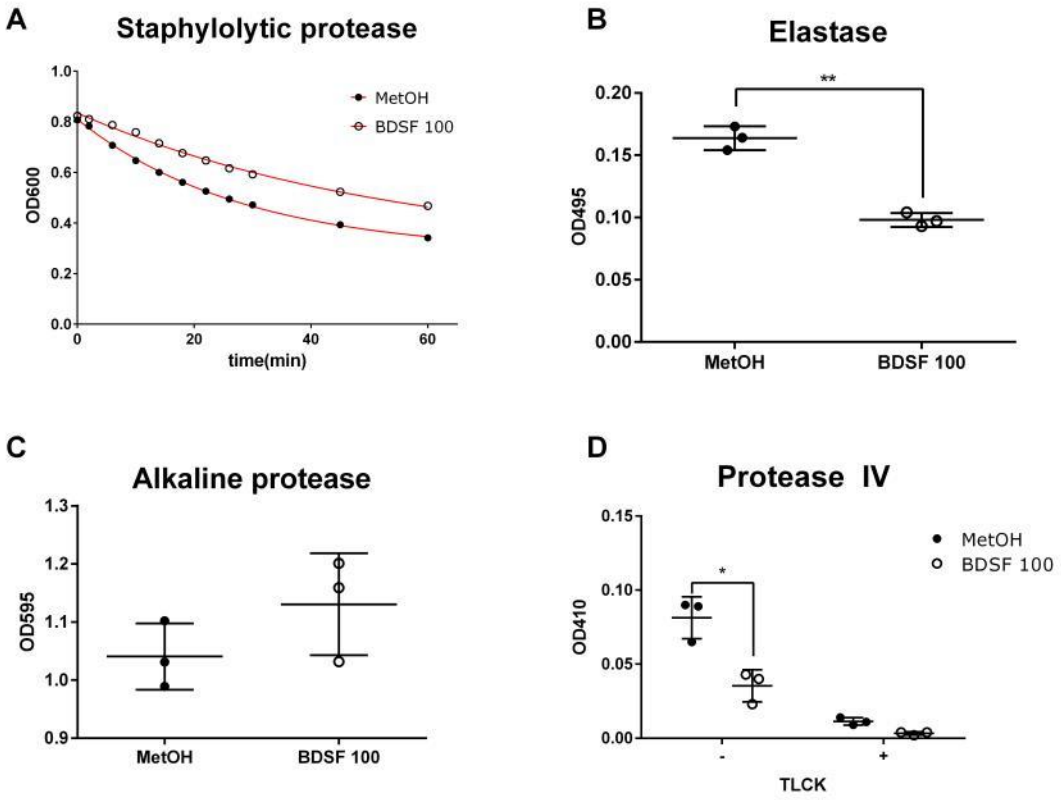


Figure 3.26. Impact of BDSF on the proteolytic activity of PAO1-L. A series of protease assays were conducted in the presence and absence of 100 µM BDSF, after incubation of cultures for 16 h at 37 ºC. **A,** Staphylolytic assay. Supernatants of cultures were put in contact with a suspension of *S. aureus* Newman, and the decay in OD_{600} was monitored over 1 h. A one phase decay was used to assess statistical significance, $p<0.0001$. **B,** Elastase assay. Supernatants were mixed with a suspension of elastin-Congo red, incubated at 37 ºC with 200 rpm shaking for 2 h and centrifuged. The OD of the supernatants was then measured at 495 nm. A t-test was used to assess significance, $p=0.001$. **C,** Alkaline protease assay. Supernatants mixed with hide powder azure were incubated for 1 h at 37 ºC with 200 rpm shaking, and the OD_{595} of the resulting suspension was determined. **D,** Protease IV assay. Chromozym PL was mixed with culture supernatants and the OD_{410} was determined. TLCK is a serine protease inhibitor used as a negative control. T-test was used to assess for statistical significance, $p=0.0002$.

Protease assays showed a range of effects caused by DSF-T molecules. On one hand, CDA does not seem to affect proteolytic activity in a dramatic way, albeit there appears to be a small increase in elastase activity (**Figure 3.24**). DSF and BDSF produce similar effects on the proteases of PAO1-L, by generally repressing their activity, with some exceptions (**Figure 3.25, Figure 3.26**). These results show that the presence of DSF-T molecules can have consequences in the colonisation capacity of *P. aeruginosa*.

3.2.9 Sensing of CDA

PA1396 has been identified as the sensor kinase responding to DSF and BDSF in *P. aeruginosa* [264]. Interestingly, it does not respond to CDA, which suggests the presence of one system for inter-species communication through DSF, and

an independent signalling pathway for intra-species communication. A preliminary analysis was conducted to identify potential sensor proteins for CDA.

Table 3.8. Selected genes for the screening of sensor kinases for CDA. The following genes have been selected for being differentially expressed according to the RNAseq data. Expected value (e-value) was found from BLASP alignments to RpfC, the sensor kinase for DSF-T molecules in *X. campestris.* No significant alignments were found between these sensor proteins and RpfR from *B. cenocepacia*. BLASTPs were used with the default settings, in the *Pseudomonas* Genome Database. MetOH, methanol; CDA, *cis*-2-decenoic acid.

Gene ID	MetOH	CDA	e-value RpfC
colS	6	12	1e-06
cprS	1	6	-
fleS	16	27	-
PA0178	37	4	-
PA1458	242	195	-
PA2571	27	5	2e-09
PA3271	28	11	1e-30
PA3462	6	2	5e-09
PA3771	4	1	-
PA4112	15	3	0.0
PA4982	1	3	0.0
pprA	5	1	-

A number of genes coding for sensor kinases were found differentially expressed by CDA. A protein BLAST was performed with the primary amino acid sequence of the translated proteins, and results show that some of the candidates presented high similarities to RpfC (**Table 3.8**). Furthermore, the microarray conducted by Rahmani-Badi et al. identifies a high number of sensor kinases differentially expressed (**Table 3.3**). Further information and an in-depth analysis of RpfC and RpfR homologues can be found in **Chapter 4, section 4.2.2**.

Interestingly, PA4982 was differentially expressed by CDA and predicted as the sensor protein for CDA by Rahmani-Badi et al. [364]. A PA4982 mutant was constructed in PAO1-L and various assays were conducted; however no phenotypical differences were observed with the addition of CDA (see **Appendix**, **section 7.2.4**).

3.3 Discussion

During this chapter, an RNA-seq analysis was used to set up starting points for a better understanding of CDA regulation in *P. aeruginosa.* Although RNA-seq results suggested multiple targets differentially regulated by this fatty acid, validation studies were unable to verify some of these data.

CDA was added at a concentration of 100 μM for the majority of assays with the exception of biofilm assays, in which CDA was added to a final 10 μM concentration. These concentrations were chosen for a number of reasons: the previous RNA-seq on which this research was based was performed in LB with 100 μM; therefore the work here was meant to resemble those conditions. Moreover, 100 μM was chosen to mimic an "overproduction" of CDA status which could show clear effects well above those expected by the endogenous production of this molecule and therefore better identify targets genes for CDA. This was performed in part because the synthase for CDA had not been clearly identified (see **Chapter 4**), so a CDA deficient strain was unavailable. Additionally, the effects reported to date for CDA and other DSF-T molecules were dose-dependent, and thus a higher concentration would have provided clearer results. DSF and BDSF were added at 100 μM, mainly to control for physical interactions of these molecules (e. g. possible surfactant effect in motility assays). A concentration of 10 μM was also used in some cases, to observe a dose-dependent effect.

While the endogenous production of these molecules is believed to be lower than 100 μM (Davies et al. reported 2.5 nM) [255], previous work with DSF producers was performed with similar concentrations, ranging from 5 μM [250, 266] to up to 100 μM [261], and even as high as 500 μM [373]. In *Xcc*, the concentrations of DSF used range from 1-2 μM [267] to 100 μM [261]. It was estimated that *B. cenocepacia* secretes about 0.5 μM of BDSF [251], and the concentration of both DSF and BDSF in CF samples was estimated at 250 nM [369].

Two statistical tests were used to assess transcriptomic data. As can be observed in **Figure 3.1**, these two approaches identified an extremely different number of targets. Because the Baggerly's test is based on the proportion of counts aligned to an ORF, this may result in an over-estimate of highly expressed genes, and therefore be one possible explanation for the differences found [311, 312]. Moreover, the DESeq test was found to retrieve a low number of positive targets

in comparison to other tests for the analysis of transcriptomics data, which fits the results found here [387].

During the course of this project, a microarray comparing the transcriptome of *P. aeruginosa* cells grown with and without CDA was published [364]. There are various differences in the conditions of the RNA-seq and this microarray analysis; therefore the comparison needs to be taken as a preliminary step towards understanding CDA regulation (**Table 3.9**). In particular, nutrient availability is of high importance to the proportion of DSF-T produced [344], and therefore changes in medium composition could greatly impact CDA production.

Table 3.9. Conditions used for the RNA-seq experiment and the microarray study that investigate the CDA regulon. Various conditions differ between the two assays, including growth conditions and the subsequent analysis of the data.

	This study	**Rahmani-Badi et al.**
technique	RNA-seq	microarray
temperature	37 ºC	25 ºC
medium	LB	M9 + 20 mM glucose
type of cell	planktonic	sessile
CDA concentration	100 µM	100 nM
CDA addition	beginning of assay	5 days post-inoculation
statistical analysis and distribution	Baggerly's test (binomial), DESeq test (negative binomial)	ANOVA (normal)

A microarray performed with a wild-type and an Δ*rpfF* mutant of *Xcc* showed a series of up-regulated genes, including genes for flagellar synthesis and protease production [347]. In contrast, flagellar functions are inhibited by DSF in *X. oryzae* pv. *oryzae* and *X. oryzae* pv. *oryzicola* [350, 361]. In consequence, the same DSF-T molecule can play different roles depending on the genomic context; however functions such as flagellar motility, proteolytic enzymes and biofilm seem to be a common target for these molecules.

Lectins represent an important structural and functional component of biofilms, [112, 388]. From the RNA-seq, *lecB* is highly repressed by the presence of CDA, presenting RPKM of 142 (for MetOH) and 42 (for CDA). These results were statistically significant in both the DESeq and the Baggerly's test (**Table 3.1, Table 3.2**). However, CDA did not affect biofilms in this study, so the effect in lectins was not investigated in detail.

Regarding secretion systems, results from the RNA-seq in LB show that T3SS is down-regulated whereas T6SS is up-regulated, suggesting a switch from acute to chronic infection caused by CDA [200, 389] (**Table 3.1**). Moreover, specific

markers of chronic infection include the genes *tssB1, tssC1, tssG1* and *tssJ1,* which were up-regulated by CDA [276]. Unexpectedly, the small RNA *rsmY* was down-regulated by CDA, which sits in disarray with a chronic state of the cells [277] (**Table 3.1**). It has recently been shown that dispersed cells present a specific phenotypic status which has characteristics of both biofilm and planktonic cells. Dispersed cells grown in ABTG medium presented increased T2SS and T3SS as compared to planktonic cells, and were more virulent in a *C. elegans* model [19]. Chua et al*.* also investigated the role of the Sec secretion pathway, and found that *secB, secD* and *secF* were up-regulated in dispersed cells. Interestingly, this pattern is also found in the presence of CDA (**Table 3.1**). Overall, it is possible that CDA, like other dispersion agents, promotes a distinct state which does not fit with the classical conceptions of acute or chronic phenotypes.

Tse6 is a T6SS effector, also up-regulated in the presence of CDA (**Table 3.1**). This protein was found to promote fitness of wild-type *P. aeruginosa* in competition experiments against the Δ*tse6* Δ*tsi6* mutant (deficient in effector and immunity protein, respectively) [390]. Transcript levels of *tsi6* were similar to *tse6*, though not statistically significant (mean RPKM of MetOH vs CDA: *tsi6*, 12 vs 57; *tse6*, 19 vs 56). CDA could be mediating effects in *P. aeruginosa* through this T6SS; specifically to compete against other bacterial cells.

In this study no clear evidence for an effect of CDA on biofilms was found. Previous research has found that EPS is differentially expressed during biofilm development [69], and that the centre of microcolonies is devoid of Psl prior to biofilm dispersion [391]. In contrast, this thesis shows that both Pel and Psl biosynthetic genes are up-regulated by CDA (**Table 3.1**). Furthermore, Psl genes are also up-regulated in the microarray performed by Rahmani-Badi et al*.* (**Table 3.3**). Regulation of alginate by CDA did not follow a clear trend either. Hence the previously described effect of CDA on biofilm dispersal did not seem to function through the regulation of EPS under the conditions tested. A series of experiments were therefore performed to verify the effects of CDA in biofilms.

As mentioned above, the addition of CDA to *P. aeruginosa* cultures did not inhibit biofilm formation. Assays were performed in 96-well plates, under a variety of conditions (**Figure 3.6**). Given those results, further biofilm assays were performed using chamber slides and agar plates (**Figure 3.7, Figure 3.8, Figure 3.9, Figure 3.11**). Research has shown that growth conditions greatly influence the establishment and structure of biofilms. For instance, an increase in

carbon and nitrogen content resulted in increased biomass and the formation of a porous biofilm structure, in mixed-species biofilms formed mainly by *K. pneumoniae* and *P. aeruginosa* [392]. Klausen et al. showed that biofilm architecture is dependent on the carbon source, and that flagella and pili and necessary for biofilm establishment in medium supplemented with glucose and casamino acids, but not when citrate is used as the carbon source [393]. Together with the differences in regulation found in the comparison between the RNA-seq and the microarray from Rahmani-Badi et al. (see **3.2.2**), It was therefore believed that the effects of CDA in biofilm occur only under certain specific conditions that were not met during this study. Consequently, the characterisation of other phenotypes in the presence of CDA was next investigated.

The general pool of c-di-GMP did not present significant differences in the presence of CDA or other DSF-T (**Figure 3.12**). It is possible that the sensitivity of the biosensor is not sufficient to detect small changes in the overall c-di-GMP content of the cells. Alternatively, the reported effects of DSF-T molecules in biofilm formation may not result from changes in c-di-GMP, but may rather rely on other pathways. Indeed, although the secondary messenger has been linked to biofilm changes; to the best of our knowledge several biofilm dispersion mechanisms have not yet been elucidated. One such example is the effect of amino acids, where tryptophan has been shown to disperse *P. aeruginosa* established biofilms [394]. Other amino acids promote biofilm formation, and while the c-di-GMP levels increased in the presence of phenylalanine, tyrosine and ornithine; only the addition of tyrosine resulted in statistically significant changes on the levels of this nucleotide, showing that other pathways distinct to c-di-GMP might be involved in biofilm development in the presence of amino acids [395]. Metal chelators such as EDTA have shown to kill and disperse *P. aeruginosa* biofilms, and a connection to c-di-GMP has not been established [396].

Several genes selected from the RNA-seq results were used to further investigate the link between CDA and c-di-GMP (**Table 3.4**). Assays performed with translational reporters for those genes show that the phosphodiesterase PA2567 is highly activated with 100 µM CDA, in a PAO1-N background (**Figure 3.13**). PAO1-N is a substrain of PAO1 used in our laboratory, derived from Holloway's isolate [291]. This substrain presents differential phenotypes when compared to PAO1-L; notably, it better responds to the presence of AQ (Stephan Heeb, personal communication). Therefore, it is possible that PA2567 is showing a

higher induction than other c-di-GMP regulators because it was tested in PAO1-N rather than PAO1-L. PA2567 is a phosphodiesterase capable of cleaving c-di-GMP, which can complement phenotypes in *Xcc rpf* mutants [217]. The accumulation of c-di-GMP in bacterial cells strongly promotes biofilm formation [206, 208, 397]. Therefore, activation of a phosphodiesterase by CDA would decrease c-di-GMP levels, and may therefore lead to a decreased biofilm formation or to the dispersion of established biofilms in *P. aeruginosa.* The mechanism behind PA2567 activation and the impact of this in the overall phenotype of *P. aeruginosa* requires further investigation.

Several genes involved in cell morphology were differentially regulated by CDA (**Table 3.6**). However, no differences were observed following TEM analysis, both in terms of cell lengths and general morphology (**Figure 3.16**). This indicates that there might be artefacts in the RNA-seq results, that these genes might be subjected to post-transcriptional regulation, or that CDA might result in subtle changes that are not observed with the methodology employed.

Flagellar functions are generally up-regulated by CDA in LB (**Table 3.5**) and in M9 (**Table 3.3**). An activation of motility would explain the effect of CDA on biofilms; however the addition of CDA to biofilms did not have any impact during this study. In addition, swimming was not affected by CDA (**Figure 3.14**); hence the effects of flagellar genes need to be further investigated. DSF delays swimming motility in PAO1, but no effects were found with the addition of BDSF, which shows that DSF-T molecules, although similar in both chemical structure and function, do not always present matching effects (**Figure 3.14**).

Pili are also motility appendages that appear differentially regulated. Specifically, *pilA, pilF* and *pilZ,* which are involved in T4aP biosynthesis, are up-regulated. However, *pilQ*, another component of the T4aP, was down-regulated by 1.4-fold. On the other hand, type 4b pili genes did not follow a clear trend, as *tadG* is up-regulated while *flp* is down-regulated (**Table 3.1.**). Interestingly, all the DSF-T molecules studied here promoted a decrease in twitching motility (**Figure 3.18**). Moreover, *trans*-2-decenoic acid was used as a control and does not affect twitching; therefore the effect is specific to the *cis* configuration.

Swarming motility was not affected by the addition of CDA (**Figure 3.17**), but the swarming area was decreased upon addition of DSF and BDSF in a dose-dependent manner. This points to a specific regulation of collective behaviour [76]. One of the factors that affect swarming motility is the secretion of the surfactants rhamnolipids [72]. RNA-seq results show that the rhamnolipid

biosynthetic operon *rhlAB* is repressed in the presence of CDA, together with *rhlC* and the QS regulators *rhlI* and *rhlR* (**Table 3.7**). While a translational reporter shows the same effect in *rhlA* and *rhlB* (**Figure 3.19**), TLC analysis revealed that this pathway is most probably subjected to post-translational regulation and that rhamnolipid secretion is not affected by CDA (**Figure 3.20, Figure 3.21, Figure 3.23**).

HAA and di-rhamnolipids cause the repulsion and attraction of *P. aeruginosa* swarming tendrils, respectively [76]. Additionally, rhamnolipids have been linked with biofilm dispersion as well as maintenance of biofilm structure [174, 176]. It was therefore hypothesised that the non-cognate molecules DSF and BDSF could affect the ratios of rhamnolipid and HAA species, causing a decrease in the swarming areas of *P. aeruginosa* and potentially explaining the impact of these fatty acids in biofilm formation. The effect of DSF in rhamnolipid secretion of PAO1 was investigated, and results show that neither mono-rhamnolipids nor di-rhamnolipids were affected by this molecule (**Figure 3.22**). Due to time constraints, the effect of DSF in HAAs could not be studied; it is therefore possible that an up-regulation of HAAs would explain the decrease of swarming areas.

Results from the DESeq test point towards a repression of protease genes caused by CDA (**Table 3.2**). Various proteases, along with amino acid transporters, have been reported to be expressed in CF patients by *P. aeruginosa* for nutrient acquisition [398]. The down-regulation of proteases could cause a lower availability of nutrients, leading to the activation of an acute, planktonic state in *P. aeruginosa* cells and therefore the inhibition or disruption of biofilm formation. Interestingly, results from Rahmani-Badi et al. suggest that proteases are up-regulated by CDA (**Table 3.3**).

Several protease assays were performed in LB, and did not show a drastic effect caused by the addition of CDA (**Figure 3.24**). The only activity tested in which CDA promoted statistical difference in protease was the elastase assay, albeit with just a slight increase. LasA, LasB and AprA present elastolytic activity [190]; therefore this might be a cumulative effect that is not perceived in the individual staphylolytic or the alkaline protease assays. Secreted proteases are regulated, amongst others, by QS systems [195, 197, 198], and therefore their activation depends on the population densities and diffusion rates. More specifically, *aprA* is mainly secreted during the early stationary phase, in LB [399]. However,

samples for RNA-seq were processed at 4 h of growth, and therefore they might not be representative for these particular enzymes.

In contrast to CDA, DSF and BDSF had an important impact in the protease secretion of PAO1. Both DSF-T decrease the activities of LasA, LasB and protease IV. Alkaline protease had a different trend, being activated by DSF and not affected by the presence of BDSF (**Figure 3.25, Figure 3.26**). The mechanisms behind this selective decrease of proteolysis remain to be fully elucidated; however previous studies showed a general down-regulation of *P. aeruginosa* virulence caused by non-cognate DSF-T that partially explains the effects observed ([373], see **section 3.3.1**). Furthermore, secretion systems controlling proteases represent scope for future work; as the T2SS Xcp promotes the secretion of LasA, LasB and PrpL while T1SS secretes AprA [200]. It has been pointed out that, although the primary function of secreted proteases is probably nutrient acquisition, other important functions such as the interference with host defence mechanisms are also performed by these enzymes [400]. The general reduction of proteolytic activity caused by DSF and BDSF could also result in an increased susceptibility in *P. aeruginosa* to the immune system of animal and plant hosts.

3.3.1 General comparison on the effects of various DSF-T in PAO1

The complexity of DSF-T regulation has been studied during this chapter. Multiple DSF-T molecules have been identified over the last decades [244] which present highly similar structures; however they do not necessarily exert the same impact in living organisms. On one hand, the same molecule can produce different outcomes. DSF is secreted by multiple bacterial species, but the effects only partially overlap. On the other hand, BDSF and DSF present a similar regulon as BDSF can complement phenotypical defects in a DSF-deficient mutant of *Xcc* [251]. Similarities in DSF and BDSF were also observed during this chapter: DSF and BDSF presented very similar roles on the biology of *P. aeruginosa*, including the decrease in pyocyanin production and proteolytic activity (with the exception of alkaline protease) and a decrease in swarming area (**Figure 3.17, Figure 3.25, Figure 3.26** and data not shown).

A general decrease in *P. aeruginosa* virulence was observed upon addition of the non-cognate molecules BDSF and DSF. A previous study found that BDSF interferes with AQ and AHL QS systems and with the T3SS, which causes the inhibition of pyocyanin, biofilm, proteases, motility and toxicity in HeLa and zebrafish [373]. This study validates the effects of BDSF in pyocyanin, proteases

and motility (**Figure 3.17, Figure 3.26**). According to these results, DSF and BDSF could be important signals in both intra- and inter-species communication by simultaneously promoting virulence in their cognate species while inhibiting virulence in competitors such as *P. aeruginosa*. C4-HSL is a major regulator of rhamnolipid secretion [327] but, surprisingly, rhamnolipids were not affected by DSF (**Figure 3.22**). This suggests that the levels of C4-HSL are still sufficient for a wild-type production of rhamnolipids in NB.

While *Burkholderia* and *Xanthomonas* species share a similar regulon mediated by DSF-T, *Pseudomonas* utilises different processes. The effects of CDA were studied previously in Nottingham and results show that this fatty acid decreases the secretion of C4-HSL, PQS and HHQ, while it increases 3OC12-HSL [294]. Results from the RNA-seq reveal a pattern of regulation similar to that of the transcriptional regulator PtxR. This regulator decreases levels of C4-HSL and PQS while it increases 3OC12-HSL, and this results in the decrease of *rhlA* expression and pyocyanin production and the increase of *lasB* [401]. The *ptxR* gene presents very low RPKM that are not statistically significant (0.0 for MetOH vs 0.9 for CDA) and the addition of CDA did not affect pyocyanin production (data not shown), rhamnolipid secretion (**Figure 3.23**), or LasA, AprA and PrpL activities (**Figure 3.24**). Nevertheless, investigating the link between CDA and PtxR could be of future interest.

Nevertheless, despite a high number of relevant genes identified in the RNA-seq analysis, very few effects were observed in cultures supplemented with CDA. Given that the supplementation of DSF and BDSF shows effects in *P. aeruginosa* in both liquid cultures and agar plates (**Figure 3.17, Figure 3.25, Figure 3.26**), these molecules are likely soluble and remain stable throughout the duration of the assays, under the conditions tested. CDA is similar in structure to DSF and BDSF; hence the lack of results with this molecule is not likely due to a degradation or unavailability of CDA.

RpfF presents a degree of non-specificity, which allows bacteria to produce a range of DSF-T molecules using only one protein [250]. This led to the hypothesis that results obtained in other studies with the addition of CDA or with the mutants in *dspI*$^{-}$, described as the CDA synthase [380], were driven by another, more active DSF-T molecule, and not CDA. In this sense, it is possible that CDA is only a minor regulator of DSF-T targets, and another DSF-T molecule is what majorly controls DSF-T phenotypes in *P. aeruginosa*. Different strains of

P. aeruginosa might offer differential sensitivity towards DSF-T molecules, or might produce different proportions of DSF-T.

Another possibility is that the system is saturated by the endogenous production of CDA. Indeed, Barber et al*.* found that the amount of DSF could not be enhanced by the addition of multiple copies of the *rpf* cluster, and that the addition of DSF did not enhance the expression of *rpfF* [243]. This suggests that DSF-T work at maximum capacity in wild-type strains, or, alternatively, the existence of additional regulators that ensure the homeostasis of the system. In contrast, work with *X. fastidiosa* showed the induction of gene expression in wild-type cultures spiked with 10 μM of *Xf*DSF [254], so possible interferences with endogenous DSF-T require further work.

3.4 Conclusion and future directions

This chapter investigates the effects of DSF-T molecules in *P. aeruginosa* PAO1. Communal behaviours were the main focus of this work; namely biofilm, motility, rhamnolipids and proteolytic enzymes.

DSF and BDSF cause a dramatic switch in the virulence of PAO1. The ecological significance of these findings is yet to be tested; however DSF-T molecules have been found in the CF lungs, and it has been proven that *P. aeruginosa* responds to them *in vivo* [369]. This is indicative of a potentially great impact on *P. aeruginosa*, and requires further work to fully elucidate the shift in regulatory networks mediated by non-cognate DSF-T.

Unexpectedly, despite the large number of differentially expressed genes, few phenotypical assays showed an effect caused by CDA. Some hypotheses are suggested that could explain this lack of impact, including possible interferences with endogenous CDA and artefacts caused by other DSF-T synthesised in *P. aeruginosa*.

Multiple species co-colonise niches with *P. aeruginosa*, such as *S. maltophilia* and *Burkholderia sp.* in the CF lung. Common goods such as proteases could benefit the whole community, whereas motility or biofilm could either benefit, or compete with, other species present in the same niche. Results presented in this chapter suggest that DSF and BDSF compete with *P. aeruginosa* for niche colonisation; however DSF increases polymyxin resistance of PAO1 [264]. Therefore, this fatty acid signal can also have beneficial effects in *P. aeruginosa.* Regarding CDA, only minor effects were observed during this study. The potential of CDA as an inter-species signal is yet to be elucidated.

Overall, this chapter has led to a better understanding of the role of DSF-T in *P. aeruginosa*, with a high number of starting points for further research.

4 ENOYL-COA HYDRATASES AND THE BIOLOGY OF *P. AERUGINOSA*

4.1 Introduction

4.1.1 The *rpf* cluster

Enoyl-CoA hydratase (ECH) is an enzyme that intervenes in fatty acid metabolism, specifically during the second step of the β-oxidation. The catalytic mechanism of ECH results in the hydration of a 2-double bond which produces hydroxyacyl-CoA thioesters. The reference ECH, or crotonase, is found in rat mitochondria. It hydrates *trans*-2 double bonds, although this reaction is easily reversible [402]. Given the similarity to the rat mitochondrial ECH, the synthases involved in the biosynthesis of DSFs have been designated as putative ECHs. However, the most likely reaction that these proteins catalyse *in vivo* is a dehydration between the α and β carbons in a fatty acid chain to generate a *cis*-double bond [403].

The genes responsible for the regulation of DSF production were first identified in *X. campestris* pv *campestris (Xcc)*. They form a cluster named *rpf* for "regulation of pathogenicity factors" [346]. A number of species present homologues of the *Xanthomonas rpf* cluster, albeit with different gene organisations (**Figure 4.1**). Notably, this cluster is found in species closely related to *Xanthomonas*, like *Xylella fastidiosa* and *Stenotrophomonas maltophilia* [404]. All in all, RpfF and RpfB are involved in the synthesis of DSF, while RpfG, RpfH and RpfC regulate perception and the downstream signalling cascade. The remaining genes of the originally identified cluster, *rpfADEI*, are of unknown function and have been reported to only have a minor impact in DSF production [263].

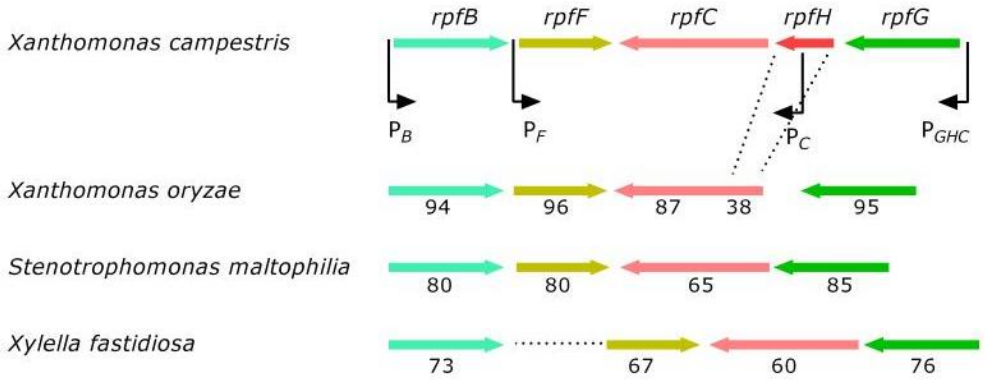


Figure 4.1. Gene organisation of the *rpf* cluster in xanthomonads. *rpfF* and *rpfB* encode proteins related to diffusible signal factor-type (DSF-T) synthesis and are well conserved in xanthomonads. RpfCHG participate in the sensing and signal transduction of DSF-T. *rpfG(H)C* form an operon, but *rpfC* has an additional internal promoter located within the ORF of *rpfH*. Numbers represent the percentage of identity of the corresponding proteins, as compared to the *X. campestris* cluster, from BLASTP searches. RpfH presents homology to the N-terminal domain of RpfC (38 % identity against RpfC from *X. oryzae*). Adapted from [244].

Homologous *rpf* clusters are also found in distantly related species such as *Burkholderia* and *Cronobacter*. However, no homologues of the RpfCHG proteins are found in these species, which present a different strategy for the signalling and transduction of DSF-T molecules. This suggests two broad mechanisms orchestrating the regulation of DSF-T molecules (see **section 4.1.1.2**).

4.1.1.1 Synthesis of DSF-T

RpfF was reported as the DSF synthase in *Xcc* soon after the discovery of the *rpf* cluster [243], and it was later crystallised as a homotrimer [405](**Figure 4.2**). This enzyme presents the characteristic features of the crotonase superfamily, with two conserved glutamate residues (E141 and E161) important for the thioesterase activity of this enzyme, an overall α/β N-terminal region and an α C-terminal region [405].

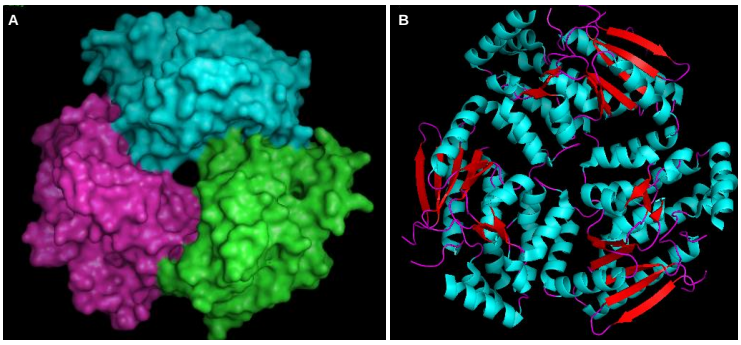


Figure 4.2. Crystal structure of RpfF$_{Xcc}$, as determined by Cheng et al. [405] A, Surface disposition of the three chains of RpfF$_{Xcc}$. **B,** Ribbon view of the three chains of RpfF$_{Xcc}$, with the secondary structures coloured. In cyan are the α-helix, in red the β-sheets and in purple the loops or unstructured regions. This crystal structure corresponds to the code 3m6n in the Protein Data Bank (PDB) and was visualised using PyMOL Molecular Graphics System, Version 1.1r1 Schrödinger, LLC.

The *Burkholderia* RpfF has been characterised in detail. This protein intervenes in two catalytic reactions, comprising a dehydratase and a thioesterase activity. For the synthesis of BDSF, RpfF$_{Bc}$ first dehydrates the precursor 3-hydroxydodecanoyl-ACP to *cis*-2-dodecenoyl-ACP, and also cleaves the thioester bond between the acyl and the ACP to release the free *cis*-2-dodecenoic acid [251, 403]. Two conserved glutamate residues, E138 and E158, are important for the thioesterase activity, and together with G83 and G135, they drive the dehydratase reaction [403].

The thioesterase activity of RpfF affects a wide range of activated fatty acids, which may result in the disturbance of fatty acid biosynthesis. To avoid potentially toxic effects of RpfF, RpfB is an acyl CoA ligase that counteracts the thioesterase activity of RpfF [406].

4.1.1.2 Perception and transduction of DSF-T signalling

So far, two general mechanisms for sensing and transduction of DSF-T signals have been characterised. The classical one depends on the expression of RpfCHG and is found in *Xanthomonas* and closely related organisms. Another system, depending on RpfR and less well characterised is found in *Burkholderia* species, and bioinformatic analysis suggests that it could be widespread amongst Proteobacteria (**Figure 4.3**).

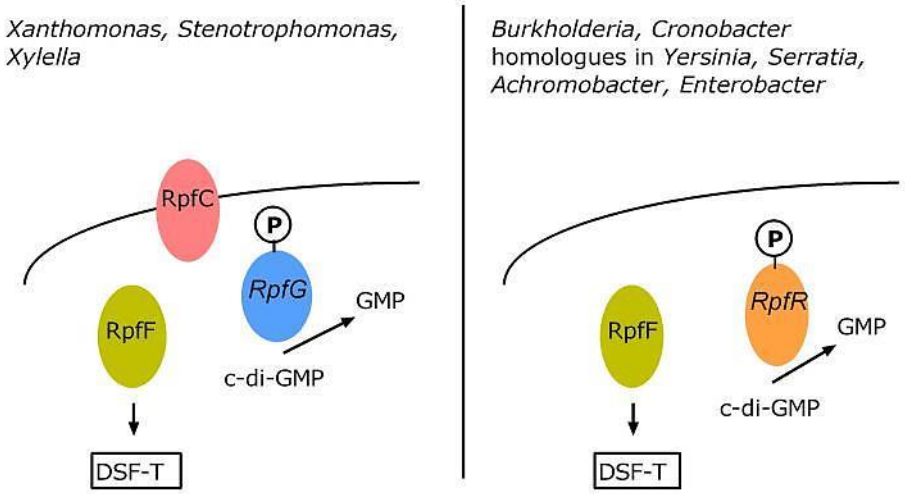


Figure 4.3. Two broad mechanisms for DSF-T sensing and transduction. Original idea from [265]. In the xanthomonads mechanism, RpfC is a transmembrane sensor which relays the signal to the cognate transducer protein RpfG. RpfG is responsible for c-di-GMP turnover. RpfF synthesises DSF-T when dissociated from RpfC. In the *Burkholderia sp.* system, RpfR is a cytosolic receptor which also presents phosphodiesterase activity.

RpfCHG system

Xanthomonas, Stenotrophomonas and *Xylella* present a 2CS which responds to the presence of DSF-T molecules. RpfC is an unorthodox sensor kinase presenting a receiver (REC) and a histidine phosphotransfer (Hpt) domain (**section 4.1.2.2** and **Figure 4.4**). RpfG constitutes the cognate response regulator (RR) of RpfC, and contains an HD-GYP domain which degrades c-di-GMP leading to the characteristic phenotypes driven by DSF such as biofilm dispersal, protease production, xanthan secretion, etc. [217, 218]. Additionally, RpfG can control phenotypes by protein-protein interaction. In particular, the interaction between the GYP motif of RpfG and GGDEF domains of other proteins has been shown to control pili modulation. DSF increases these protein-protein interactions [218, 407].

The gene coding for RpfH is found only in some species. It has moderate similarity to the 5' of *rpfC* (39 % identity to *rpfC* of *Xcc*, 38 % to that of *X. oryzae*, as seen by BLASTP). This suggests a possible common origin for *rpfH* and *rpfC*. RpfH does not present a sensor kinase (SK) domain, and is probably an accessory protein to RpfC [263]. In RNA-seq analysis, only 4 genes were found 4-fold differentially regulated by an in-frame deletion of *rpfH* [381], which points to a minor regulatory role of the encoded protein.

Interestingly, RpfC also participates in the inhibition of RpfF, probably as a way to maintain stable levels of DSF [263]. The REC domain of RpfC interacts with RpfF. Crystallisation of this interaction shows that the substrate pocket is too small to accommodate DSF or its substrate, and therefore suggests that the RpfF-RpfC complex blocks the entry of the precursor, and that the dissociation of these two proteins results in a conformational change that allows for DSF biosynthesis [405, 407, 408].

It has been reported that the levels of *rpfF* mRNA are constant and are not influenced by the addition of DSF [248, 263]. In contrast, *rpfF* levels increase 6-fold in *Xcc* Δ*rpfC*, at least under certain experimental conditions [381]. This overexpression of *rpfF* has also been shown in *X. fastidiosa* [409]. In addition to a possible transcriptional regulation of DSF production under certain conditions, the complex RpfF-RpfC drives a post-translational regulation of DSF. In this latter case, the autoinduction of DSF production is driven by a de-repression. Cheng et al. suggested that, under low cell/high diffusion conditions, most of RpfF is sequestered by RpfC, allowing for a basal expression of DSF. Under high cell density, DSF binds RpfC and drives its autophosphorylation, leading to the release of RpfF and hence the induction of DSF synthesis [405]. This model is yet to be proven experimentally. On the other hand, transcriptomic analysis shows that RpfF, RpfG and RpfC control a subset of common targets, but also independent targets, which suggests the existence of additional sensors and response regulators [381]. Other publications have hinted to the possibility of secondary sensor proteins [409, 410]. RpfS has been identified as an alternative sensor for DSF, and controls chemotaxis and type 4 secretion in *Xcc*, but not biofilm formation or production of extracellular enzymes [411].

Furthermore, RpfF in *X. fastidiosa* is involved in a different regulation of DSF-T, as not only is it responsible for the production of the signal molecule, but also affects the downstream transduction of the signal by repressing RpfC activity. In this organism, binding to the DSF-T signal results in the dissociation of RpfC from

RpfF [254]. This is possibly a different evolutionary consequence of the RpfF-RpfC interaction, which in this case results in the repression of RpfC rather than RpfF.

RpfR system

Burkholderia sp. does not present homologues to RpfC, thus the identification of sensor proteins responding to BDSF was not straightforward. Early work showed a minor protein responsible for the perception of BDSF, encoded by Bcam0227. However, only a subset of BDSF-regulated phenotypes is controlled by this sensor protein [356]. RpfR, encoded by Bcam0580, was later reported as the major sensor for BDSF (**Figure 4.3**). This protein is not homologous to the *Xcc* RpfC, and constitutes a one component system. Nevertheless, this sensor contains both GGDEF and EAL domains, so although the sensor mechanism is not the same, both xanthomonads and *Burkholderia sp.* have converged in their strategy and modulate c-di-GMP levels as a result of DSF-T sensing. Specifically, BDSF binds to the PAS domain of RpfF, which stimulates the phosphodiesterase activity of this receptor, probably through conformational changes. A wide range of bacterial species present homologues for RpfR, which seems to suggest the existence of two broad DSF regulatory systems (**Figure 4.3**) [265].

4.1.2 DSF-T in *P. aeruginosa*

4.1.2.1 Synthesis of CDA

P. aeruginosa encodes 15 predicted ECH/isomerases, which are good candidates for CDA synthesis. A recent publication describes PA14_54640 (PA0745 in PAO1) as a CDA synthase, as the biofilm dispersal observed in wild-type microcolonies was abrogated in the insertional mutant for this gene [380]. This protein, named DspI, has a high similarity to RpfF (**Table 4.1**) and similar tertiary structure to RpfF proteins (**Table 4.4**). On the other hand, bioinformatics analysis of protein-protein interactions suggests that the cluster of genes PA4978, PA4979, PA4980, PA4982 and PA4983 is involved in the biosynthesis and signal transduction of CDA in this bacterium [364]. PA4980 is one predicted ECH that would drive the synthesis of DSF, while PA4982 and PA4983 constitute a potential 2CS.

In addition, data from Nottingham suggests that the gene downstream *dspI*, PA0744, has a role in the synthesis of CDA. The PA0744 mutant presents a marked decrease in CDA production, which is restored by complementation from an expression plasmid. However, the CDA production is still detectable in this

mutant, suggesting that PA0744 is not the sole enzyme involved in CDA synthesis [294].

Multiple DSF-T synthases present in one organism have not been described so far. However, the existence of more than one mechanism for CDA synthesis is a possibility that cannot currently be discarded based on experimental data. It is possible that, under different experimental conditions, *P. aeruginosa* drives the synthesis of CDA by using different strategies. As a result, the roles of PA4980, PA0744 and PA0745 in CDA synthesis are not mutually exclusive.

Regarding potential mechanisms of autoinduction, the expression levels of *dspI* were not influenced by the addition of exogenous CDA [380]. In contrast, Rahmani-Badi et al. [364] reported a differential expression of *dspI* caused by the addition of CDA. It is possible that transcriptional regulation occurs under specific experimental conditions.

On the other hand, PA3426, named CbsA for controls the biofilm and swarming, is suggested to have a role in CDA catalysis, as the overexpression of this gene results in a reduced CDA production [294]. CbsA is, additionally, a regulator of swarming motility and biofilm formation. CbsA might constitute a link between DSF regulation and the Gac/Rsm system, which prompted us to further investigate the function of this ECH.

4.1.2.2 Perception and transduction of CDA signalling

Regarding the sensing of extracellular CDA, PA1396 is a SK responding to DSF and BDSF, but not to CDA [264]. PA1396 is an orthologue of RpfC, and the cognate RR is encoded by the gene downstream, PA1397 (**Figure 4.4**).

Sensing of CDA in *P. aeruginosa* has not been proven experimentally, but bioinformatic analysis of protein-protein interactions suggests that PA4982 could code for a sensor protein, in a system similar to that of *Xanthomonas* [364].

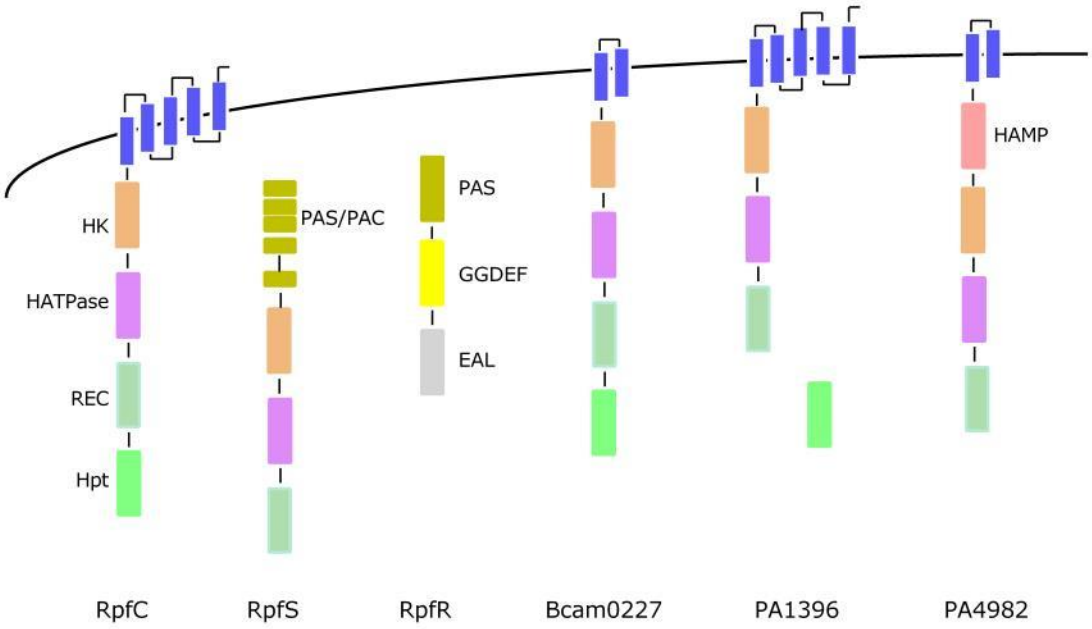


Figure 4.4. Domain organisation of DSF-T receptors. RpfC is the major sensor protein of DSF in xanthomonads. RpfS is a secondary sensor found in *X. campestris*. RpfR is the major sensor in *Burkholderia sp.,* constituting a one-component system. Bcam0227 is a secondary sensor in *Burkholderia.* PA1396 is a sensor highly similar to RpfC found in *P. aeruginosa,* but does not mediate the sensing of CDA and rather responds to DSF and BDSF. PA1396 is thought to relay the phosphate to orphan Hpt proteins. PA4982 is a predicted sensor for CDA in *P. aeruginosa.* HK, histidine kinase domain; HATPase, histidine kinase-like ATPase; REC, receiver domain; Hpt, histidine phosphotransfer; PAS, Per/Arnt/Sim domain; PAC, C-terminal to PAS; GGDEF, diguanylate cyclase domain; EAL, c-di-GMP phosphodiesterase domain; HAMP, histidine kinases, adenylyl cyclases, methyl binding proteins, phosphatases domain. Adapted from [244] and with information from the SMART database [328, 329].

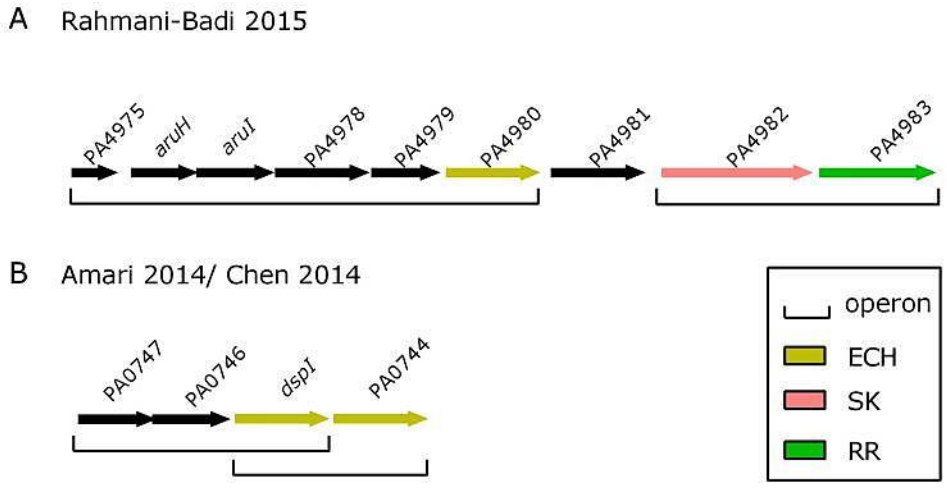


Figure 4.5. Two possible genomic contexts of CDA synthases in *P. aeruginosa.* **A,** Rahmani-Badi et al.[364] reported the involvement of PA4978, PA4979, PA4980, PA4982 and PA4983 in CDA synthesis and signal transduction, based on bioinformatic analysis of protein-protein interactions. Predicted operons from the *Pseudomonas* Genome Database are shown with brackets [315]. PA4975 is an oxidoreductase which protects *P. aeruginosa* against H_2O_2 challenge [412]. *aruH* and *aruI* are involved in arginine catabolism [413]. PA4978 is a hypothetical protein. The following are predicted functions from the *Pseudomonas* Genome Database: PA4979, acyl-CoA dehydrogenase; PA4980, ECH/isomerase; PA4981, amino acid permease; PA4982, two-component sensor; and PA4983, response regulator. **B,** Experimental data from [380] shows that DspI is involved in the synthesis of CDA, and that *dspI* is transcribed together with the two genes located upstream, PA0747 and PA0748. The *Pseudomonas* Genome Database shows a predicted operon including genes *dspI* and PA0744. The predicted functions encoded by these genes, according to the *Pseudomonas* Genome Database, are as follows: PA0747, aldehyde dehydrogenase; PA0746, acyl-CoA dehydrogenase; *dspI,* ECH/isomerase; PA0744, ECH/isomerase.

Research in *Burkholderia* and *Xanthomonas* has identified multiple sensor proteins linked to the signal transduction of DSF-T molecules [263, 265, 356, 411]. Additionally, a number of sensor kinases were found differentially regulated both by Rahmani-Badi et al. [364] and in RNA-seq data from Nottingham (see **Chapter 3**). It is thus possible that *P. aeruginosa* uses multiple sensor/transduction mechanisms to respond to the presence of CDA.

4.1.3 Aims of the chapter

This chapter is aimed to validate the data mentioned above and to unravel the role of the ECH in CDA metabolism. More specifically, this chapter comprises 3 main objectives:

- To study the regulation of PA0747-PA0743 in *P. aeruginosa*
- To see the effect of PA3426 (CbsA) in *P. aeruginosa*
- To determine the link between ECHs and CDA regulation

4.2 Results

4.2.1 In silico characterisation of ECH in *P. aeruginosa*

According to its annotated genome, *P. aeruginosa* strain PAO1 presents 13 "Enoyl-CoA hydratase/Isomerase" proteins. Additionally, PA2890 is predicted as an "Isohexenylglutaconyl-CoA hydratase", and PA1846 as a "*cis/trans* isomerase". All these proteins were characterised to better identify regulators of CDA.

4.2.1.1 Sequence alignments of ECH in *P. aeruginosa* and RpfF proteins

To get a general overview of the potential synthases for CDA, BLASTP were performed comparing the PAO1 proteins with both the RpfF present in *Xcc* and the homologue from *B. cenocepacia* H111 ($RpfF_{Xcc}$ and $RpfF_{Bc}$, respectively) (**Table 4.1**).

Table 4.1. Identity percentages of the BLASTP alignments between ECH of *P. aeruginosa* and RpfF proteins. The percentages of identity and query cover are given as a means to compare the amino acid sequence of ECH homologues. $RpfF_{Xcc}$ corresponds to the DSF synthase in *Xanthomonas campestris* pv. *campestris* ATCC 33913. $RpfF_{Bc}$ refers to the BDSF synthase in *Burkholderia cenocepacia* H111. N/A is given when BLASTP did not produce significant alignments.

PAO1 protein ID	PA14 protein ID	Identity to $RpfF_{Xcc}$ /query cover (%)	Identity to $RPfF_{Bc}$ /query cover (%)
0744	54660	25/33	26/57
0745	54640, DspI	28/94	27/66
1021	51110	31/60	27/51
1240	48200	28/44	23/32
1629	43440	28/74	33/31
1748	41950	N/A	37/70
1821	40980	23/51	22/37
1846, Cti	40640	32/12	N/A
2767	28310	36/34	35/44
2841	27360	25/31	23/47
2890, AtuE	26690	34/32	37/15
3426, CbsA	19740	28/58	32/34
3591	17850	26/83	34/33
4330	56250	25/67	N/A
4980	65840	29/57	29/31

Most of the proteins listed in **Table 4.1** present very small coverage to either of the RpfF proteins, and even within the short alignments, little identity is found. These results suggest that *P. aeruginosa* does not present clear orthologues for DSF-T synthases. From the candidates found with experimental data (PA0744,

PA0745, CbsA and PA4980), the highest coverage is given by PA0745 (94 %), however there is only a 28 % identity to $RpfF_{Xcc}$. The similarities between RpfF from *Xcc* and from *Bc* are also limited (37 % identity, with a 97 % coverage), so further analysis was required to better define the ECH candidates in PAO1.

To this end, the primary sequences of these proteins was analysed in detail. A number of conserved residues have been linked to the enzymatic activity of DSF-T synthases. Two catalytic glutamates, E141 and E161, where identified in $RpfF_{Xcc}$ [405], and correspond to E138 and E158 of $RpfF_{Bc}$ [403]. To verify essential residues located in the active site, Bi et al. [403] created the subtitutions G83P and G135P in $RpfF_{Bc}$, and showed that the resulting mutated proteins did not present thioesterase activity. The equivalent of G135 ($RpfF_{Bc}$) in *Xcc* was also identified by Cheng et al. [405], together with additional residues located in the oxyanion hole of $RpfF_{Xcc}$, namely G85, L136, G137, and M170. Interestingly, the other glycine identified in [403], G83, is not mentioned in [405], but rather the glycine located upstream. Both residues were considered.

The first step in the analysis of this proteins was to use BLASTP against ECH and $RpfF_{Xcc}$. To verify the output, a multiple alignment with all the proteins listed in **Table 4.1** was performed in CLUSTALω, which showed several additional alignments, and some different ones. As shown in **Table 4.2**, out of 8 identified residues, 2 of them are clearly variable, i. e. G86 ($RpfF_{Xcc}$) and M170 ($RpfF_{Xcc}$). Notably, in both cases the ECH from rat mitochondria does not present the same residues, but rather two alanines.

Table 4.2. Location of important catalytic residues as shown in [403, 405]in proteins annotated as ECH/Isomerase, in PAO1. BLASTP against the rat mitochondrial ECH and $RpfF_{Xcc}$ were performed, together with CLUSTALω multiple alignments. Conservative changes are highlighted in yellow, while non-conservative changes are highlighted in red. In all the alignment with the exception of PA1748, PA2767 and PA3426; the two conserved glutamates were 20 bp apart.

Protein ID								
ECH	E115	E135	A69	G68	L110	G111	G112	A143
$RpfF_{Xcc}$	E141	E161	G86	G85	L136	G137	G138	M170
$RpfF_{Bc}$	E138	E158	G83	G82	L133	G134	G135	M167
0744	G123	E143	Y308/D69/G68	E307/G67	M118	G119	G120	V152
0745	E126	E146	A78	G77	M121	G122	G123	A155
1021	S111	F131	G63	G62	V106	G107	A108	L140
1240	E119	E139	L70	G69	W114	T115	A116	L147/G148
1629	E115	E135	A69/A219	G68/G218	L110	G111	G112	A144
1748	F108	E129	Y61	G60	V103	A104	K105	H138
1821	D124	E144	I66	G65	L119	G120	G121	V153
1846, Cti	Q672	N690	A185	G184	L669/L482	R670/F483	gap/E484	T698/D529
2767	E150	E174	F67	H66	L145	G146	G147	G183
2841	E117	E137	L68	G67	Y112	T113	I114	G146
2890, AtuE	G119	E139	G68	G67	L114	G115	G116	Q148
3426, CbsA	E110	L137	A62	G61	V105	A106	G107	I138/D139
3591	E119	E139	A73	G72	L114	G115	G116	A148
4330	T109	F129	T107/N64	G107/G63	V104	G105	I106	F138
4980	D117	Y137	A56	G55	V112	G113	A114	A146

Table 4.3. Location of conserved residues within secondary structures in proteins annotated as ECH/Isomerase, in PAO1. Secondary structure predictions were performed in I-Tasser. The structure of $RpfF_{Xcc}$ was described by [405] and retrieved from the Protein Data Bank (PDB: 3m6n). Residues within α-helices are shown in turquoise, β-sheets in red, and loops in purple.

Protein ID							
$RpfF_{Xcc}$	E141	E161	G85	L136	G137	G138	M170
$RpfF_{Bc}$	E138	E158	G82	L133	G134	G135	M167
0744	G123	E143	E307/G67	M118	G119	G120	V152
0745	E126	E146	G77	M121	G122	G123	A155
1021	S111	F131	G62	V106	G107	A108	L140
1240	E119	E139	G69	W114	T115	A116	L147/G148
1629	E115	E135	G68/G218	L110	G111	G112	A144
1748	F108	E129	G60	V103	A104	K105	H138
1821	D124	E144	G65	L119	G120	G121	V153
1846, Cti	Q672	N690	G184	L669/L482	R670/F483	gap/E484	T698/D529
2767	E150	E174	H66	L143	G144	G145	G183
2841	E117	E137	G67	Y112	T113	I114	G146
2890, AtuE	G119	E139	G67	L114	G115	G116	Q148
3426, CbsA	E110	L137	G61	V105	A106	G107	I138/D139
3591	E119	E139	G72	L114	G115	G116	A148
4330	T109	F129	G107/G63	V104	G105	I106	F138
4980	D117	Y137	G55	V112	G113	A114	A146

Amino acid sequence can relate to protein function and help identify conserved residues as well as functional motifs. However, secondary and tertiary structures generally retain more similarity than primary sequences, and structure-to-function analysis is a usefull tool to identify functional homologues [414, 415].

In order to deepen the analysis, the predicted secondary structures of ECH/Isomerases were assesssed and are listed in **Table 4.3**. G86 ($RpfF_{Xcc}$) was not analysed at this point, as results from **Table 4.2** show poor conservation of this residue in ECH, and suggest that this is unlikely essential for catalytic activity. Briefly, protein structures were predicted with I-Tasser, and the crystal structure of $RpfF_{Xcc}$ was retrieved from the Protein Data Bank (PDB: 3m6n) [405].

In $RpfF_{Xcc}$, the two conserved glutamates E141 and E161 are present within α-helices. G85 is in a loop, and L136 is part of a two-amino acids β-sheet. G137 and G138 are part of a α-helix, and M170 is in a loop. As expected, the putative structures of the other proteins show similar secondary arrangements (**Table 4.3**). Next, alignments of 3D structures were performed.

4.2.1.2 Structure alignment of ECH of *P. aeruginosa* with RpfF proteins

For the alignment of predicted tertiary structures, protein structures were aligned in PyMOL using the `align` command. This algorithm aligns two proteins in a structure-dependent manner, and gives a root mean square deviation (RMSD) number as output, which relates to the distances between aligned atoms (see **2.8.4**).

Table 4.4. Root mean square deviation (RMSD) numbers of RpfF proteins from *Xanthomonas* and *Burkholderia* aligned to ECH/Isomerases of PAO1. RMSD values were determined with the `align` command in PyMOL and are inversely proportional to the quality of the alignment.

		RMSD to $RpfF_{Xcc}$	RMSD to $RPfF_{Bc}$
	$RpfF_{Bc}$	2.6	N/A
PAO1 ID	PA14 ID		
0744	54660	5.1	4.7
0745	54640, DspI	2.8	1.4
1021	51110	2.0	2.6
1240	48200	2.9	10.5
1629	43440	3.4	6.0
1748	41950	7.8	2.5
1821	40980	4.4	2.6
1846, Cti	40640	19.3	11.4

2767	28310	2.1	15.8
2841	27360	3.0	2.9
2890, AtuE	26690	2.5	10.5
3426, CbsA	19740	2.2	2.4
3591	17850	2.5	5.2
4330	56250	5.1	2.5
4980	65840	9.5	3.7

Results from **Table 4.4** show that some of the proteins from PAO1 had smaller RMSD numbers than the alignment between $RpfF_{Xcc}$ and $RpfF_{Bc}$, particularly DspI vs $RpfF_{Bc}$ and CbsA vs $RpfF_{Xcc}$, showing the similarity between the predicted 3D structures of these proteins.

Overall, bioinformatic analyses were useful to determine to get a general understanding of the extent of ECH-like proteins found in *P. aeruginosa*, and to segregate various strong candidates for the synthesis of DSF-T molecules. However, results did not allow for the identification of a lead candidate. Instead, it seems that PA0744, PA0745, CbsA and PA4980 are all potential synthases for CDA.

4.2.2 *In silico* characterisation of RpfC and RpfR homologues of *P. aeruginosa*

P. aeruginosa belongs to the class of γ-proteobacteria. One could therefore assume that the receptor(s) of CDA should be more closely related to the xanthomonads RpfC, rather than to the β-proteobacteria *Burkholderia* RpfR. However, homologues for RpfR have been found in other γ-proteobacteria such as *Yersinia* or *Serratia*. A bioinformatic analysis was therefore performed to have an overview of potential receptors in *P. aeruginosa*.

4.2.2.1 Primary sequence

BLASTP searches were conducted to determine whether *P. aeruginosa* presents homologues to either RpfC or RpfR, using the *Pseudomonas* Genome Database.

Table 4.5. Top 10 hits of proteins from PAO1 found by BLASTP against RpfC from *Xcc*. Default settings were used. Identity and query cover percentages are shown as a mean to compare the hits to RpfC.

Protein ID	Identity (%)	Query cover (%)
4982	37	58
0928, GacS	46	33
1611	34	55

3974, LadS	33	55
3946, RocS1	31	70
4112	34	54
3044, RocS2	31	68
3462	43	33
4856, RetS	33	57
2583	32	61

It is of note that PA4982, predicted as a CDA sensor, is the first hit for RpfC homologues. Even then, the percentage identity is only of 37 %. As seen in **Figure 4.4**, this sensor protein presents a histidine kinase (HK), histidine kinase-like ATPase domain (HATPase), and a REC domain, which are also found in RpfC and account, at least partially, for the similarities in amino acid sequence. On a different note, this particular BLAST was performed against the proteome of strain PAO1, and PA1396 came as the 11th hit, showing that it presents high similarity to RpfC. Indeed, PA1396 has a similar domain organisation to RpfC (**Figure 4.4**), but this protein is not involved in sensing CDA.

The same procedure was repeated for RpfR from *B. cenocepacia* and shows similar results, with identity percentages around 30-40 %. Interestingly, the query cover is much higher for the hits of RpfR than it is for the hits of RpfC (**Table 4.5, Table 4.6**). It is thus worth of consideration whether *P. aeruginosa* may present a similar strategy to *Burkholderia* for DSF-T signal transduction.

Table 4.6. Top 10 hits of the BLASTP with RpfR from *B. cenocepacia* H111. Default settings were used. Identity and query cover percentages are shown as a mean to compare the hits to $RpfR_{Bc}$.

Protein ID	Identity (%)	Query cover (%)
4601, MorA	37	84
0285	35	81
5442	36	83
1727, MucR	42	66
0575	33	84
5017, DipA	36	84
3311, NbdA	37	66
2072	37	65
4367, BifA	35	66
5295	37	64

4.2.2.2 Domain organisation

Next, two strategies were followed to retrieve putative homologues for RpfC and RpfR. First, the hits to RpfC obtained with the primary sequence (**Table 4.5**) were checked for domain organisation using SMART.

Table 4.7. Domain organisation of BLASTP hits of RpfC against the PAO1 proteome. SMART was used to determine the domain organisation of the top 10 hits of BLASTP of RpfC against PAO1 [328]. transmb, transmembrane domain; HK, histidine kinase; HATPase, histidine kinase-like ATPase; REC, receiver domain; Hpt, histidine phosphotransfer; HAMP, histidine kinases, adenylyl cyclases, methyl binding proteins, phosphatases domain; PBPb, periplasmic substrate-binding protein; PAS, Per/Arnt/Sim domain; CHASE, cyclases/histidine kinases associated sensory extracellular; PAC, C-terminal to PAS. Numbers in brackets are used to specify the number of domains of the same kind.

Protein ID	**Domains (N to C-ter)**							
RpfC	transmb (5)	HK	HATPase	REC	Hpt			
4982	transmb (2)	HAMP	HK	HATPase	REC			
0928, GacS	transmb (2)	HAMP	HK	HATPase	REC	Hpt		
1611	transmb	HAMP	HK	HATPase	REC			
3974, LadS	transmb (6)	HK	HATPase	REC				
3946, RocS1	transmb	PBPb (2)	transmb	PAS	HK	HATPase	REC	Hpt
4112	transmb	CHASE	PAS/PAC (6)	HK	HATPase	REC (2)	Hpt	
3044, RocS2	transmb (2)	PAS	HK	HATPase	REC	Hpt		
3462	transmb (6)	HK	HATPase	REC				
4856, RetS	transmb (7)	HK	HATPase	REC (2)				
2583	PBPb (2)	transmb	HK	HATPase	REC			

Results in **Table 4.7** show a variety of domain organisations, characteristic of most sensor proteins. Again, PA4982 seems like a good candidate in terms of the domains that it presents.

Another approach was taken by searching for similar domain organisations to RpfC with SMART. Two options are given, search for similar "domain organisation" allows to find proteins containing all the domains of the query and in the same organisation (additional domains may be present). Only 2 results were given against the proteome of PAO1, PA4112 and PA3946 (RocS1). The other option, "domain composition", finds proteins with at least one copy of each of the domains in the query (not necessarily in the same order). The same proteins were found.

P. aeruginosa contains a number of orphan hybrid sensor kinases, which sometimes need to relay the phosphate through an Hpt protein. It is possible

that, similarly to PA1396, the sensor for CDA would not present an Hpt domain, and instead relay to an orphan Hpt. In consequence, the search was also conducted for proteins presenting HK, HATPase and REC domains only. The output, shown in **Table 4.8**, includes several of the proteins mentioned above and 3 new hits: PA2177, PA1992 (ErcS) and PA1976 (ErcS'). ErcS' and ErcS are both involved in ethanol oxidation [416].

Table 4.8. Candidate homologues to RpfC in PAO1, presenting the same domain organisation but lacking Hpt domains. transmb, transmembrane domain; HK, histidine kinase; HATPase, histidine kinase-like ATPase; REC, receiver domain; Hpt, histidine phosphotransfer. Numbers in brackets are used to specify the number of domains of the same kind.

Protein ID	**Domains (N to C-ter)**				
RpfC	transmb (5)	HK	HATPase	REC	Hpt
1976, ErcS'	PAS/PAC (4)	HK	HATPase	REC	
1992, ErcS	PAS (8)	HK	HATPase	REC	
2177	PAS/PAC (4)	HK	HATPase	REC	

The same procedure was followed for RpfR. Given the relative simplicity of the domain organisation of RpfR, most of the hits shown in **Table 4.9** contain all of the domains present in RpfR.

Table 4.9. Domain organisation of BLASTP hits of RpfR against the PAO1 proteome. PAS, Per/Arnt/Sim domain; GGDEF, diguanylate cyclase domain; EAL, c-di-GMP phosphodiesterase domain; transmb, transmembrane domain; PAC, C-terminal to PAS; PBPb, periplasmic substrate-binding protein; GAF, domain present in phytochromes and cGMP-specific phosphodiesterases. Numbers in brackets are used to specify the number of domains of the same kind.

Protein ID	**Domains (N to C-ter)**						
RpfR	PAS	GGDEF	EAL				
4601, MorA	transmb (2)	PAS/PAC (7)	GGDEF	EAL			
0285	transmb (2)	PAS/PAC (4)	GGDEF	EAL	PAS/PAC (4)	GGDEF	EAL (2)
5442	transmb (5)	PAS/PAC (4)	GGDEF	EAL			
1727, MucR	transmb (7)	GGDEF	EAL				
0575	PBPb	transmb	PAS/PAC (8)	GGDEF	EAL		
5017, DipA	PAS	GAF	PAS/PAC (2)	GGDEF	EAL		
3311, NbdA	transmb (7)	GGDEF	PAS				
2072	transmb (2)	PAS/PAC (2)	GGDEF	EAL			
4367, BifA	transmb (2)	GGDEF	EAL				
5295	GGDEF	EAL					

Then, RpfR "domain organisation" found an additional 2 proteins, listed in **Table 4.10**. The option "domain architecture" did not give further hits.

Table 4.10. Domain organisation of proteins of PAO1 presenting the same domains as RpfR. PAS, Per/Arnt/Sim domain; GGDEF, diguanylate cyclase domain; EAL, c-di-GMP phosphodiesterase domain; MASE, membrane-associated sensor; PAC, C-terminal to PAS; transmb, transmembrane domain. Numbers in brackets are used to specify the number of domains of the same kind.

Protein ID	**Domains (N to C-ter)**			
RpfR	PAS	GGDEF	EAL	
1181	MASE	PAS/PAC (6)	GGDEF	EAL
0861, RbdA	transmb (2)	PAS/PAC (2)	GGDEF	EAL

4.2.3 Phenotypical characterisation of PAO1 Enoyl-CoA Hydratases

Based on previous data from Nottingham and New York [380], one aim of this study was to better understand the regulation of PA0744 and PA0745; and that of CbsA. The mutants of PAO1-L Δ0744 (PASC815) and Δ*cbsA* (PASC203) were available from Nottingham, and the mutant for Δ0745 (PADP135) and the double mutant Δ0744 Δ0745 (PADP14) were constructed during this work. A range of phenotypical assays was conducted to characterise them.

4.2.3.1 Impact of Enoyl-CoA Hydratases in growth

Growth curves were performed in the media used for subsequent phenotypical assays. Additionally, to identify possible autotrophies in the ECH mutants that would not be obvious in rich media, a growth curve was also performed in CDM minimal medium. The results show that all the mutants grow at the same rate as the wild-type control (**Figure 4.6**). The mutant PASC203 (Δ*cbsA*) was added to these assays despite the fact that it was not used in further analysis, to ascertain that the mutation of *cbsA* does not impair the viability of *P. aeruginosa*.

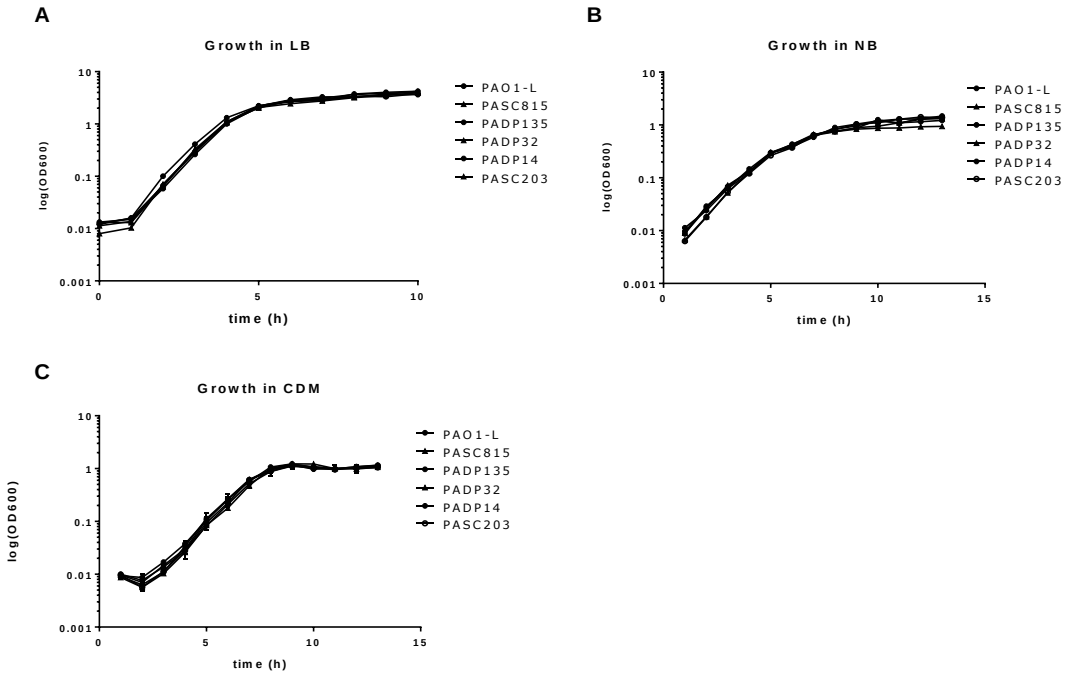


Figure 4.6. Growth of ECH mutants in various media. Cultures of PASC815 (Δ0744), PASC135 (ΔPA0745), PADP32 (0745*), PADP14 (ΔPA0744 ΔPA0745) and PASC203 (Δ*cbsA*) were grown in conical flasks, and incubated at 37 ºC with 200 rpm shaking. Samples were taken every hour for 12 h. Results represent the average of three independent replicates. Error bars represent one standard deviation of the means. Results show that mutations in these ECH do not affect growth under the conditions tested.

4.2.3.2 Characterisation of PA0745 and PA0744

Characterisation of in-frame deletions

Swarming

DSF-T molecules are involved in the activation of cellular motility, and in particular, BDSF is key for swarming in *B. cenocepacia* [355](see **Chapter 3, section 3.1.3.2**). Therefore, as a first step to characterise the roles of PA0744 and PA0745, swarming motility was assessed. In-frame mutants of these genes were used (PASC815 and PADP135, mutants in PA0744 and PA0745 [*dspI*], respectively), together with the in-frame double mutant PADP14. pME6032-based constructions harbouring PA0744 (pSC323), PA0745 (pSC3) and both ORFs together (pDP181) were used to complement the mutations.

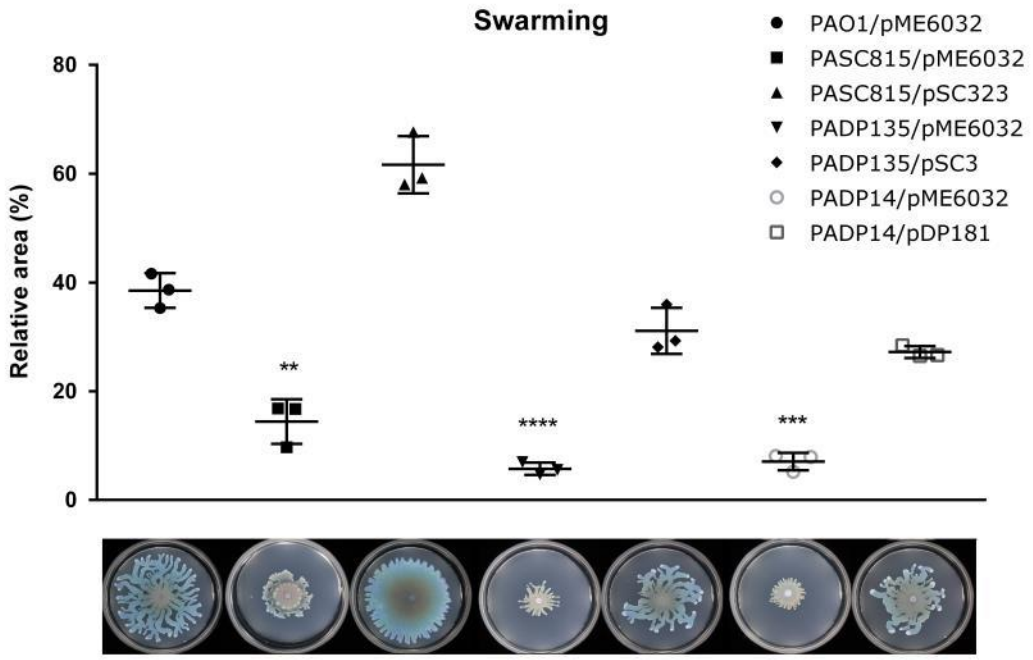


Figure 4.7. Swarming motility of mutants for PA0745 (PADP135), PA0744 (PASC815), and the double mutant Δ0744 Δ0745 (PADP14). Independent triplicates of each mutant were grown overnight and spotted on swarming plates supplemented with 1 mM IPTG, then incubated at 37 ºC statically. The total area of swarming was quantified and normalised against the area of the plates. Error bars represent one standard deviation of the means. T-test were used to compare between strains, PAO1/pME6032 vs PASC815/pME6032, p=0.0013; PAO1-L/pME6032 vs PADP135/pME6032, p<0.0001. PAO1-L/pME6032 vs PADP14/pME6032, p=0.0001. Pictures show representative results of the assay.

All the mutants tested present reduced swarming motility as compared to the isogenic wild-type, and this phenotype was restored by complementation from the expression vector pME6032. The morphology of swarming tendrils was modified in the case of the PASC815 expressing PA0744 from pSC323, which may be an effect of the multiple copies of the gene being expressed from the pME6032 construction (**Figure 4.7**).

Pyocyanin

Pyocyanin production is lost from *P. aeruginosa* cultures grown in the presence of DSF or BDSF [265]. To help elucidate the link between ECH and the production of DSF-T, pyocyanin production was subsequently studied in ECH mutants. Briefly, pyocyanin was extracted from cultures of PA0744 and PA0745 mutants and then measured by spectroscopy.

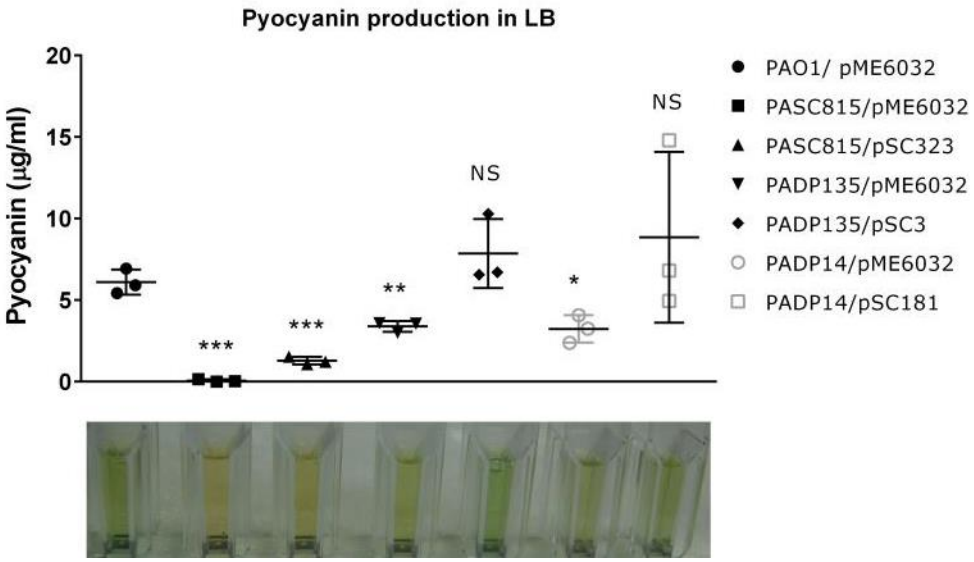


Figure 4.8. Pyocyanin production of mutants of PA0744 and PA0745. Independent cultures of PASC815, PADP135 and PADP14 (Δ0744, Δ0745 and the double mutant Δ0744 Δ0745, respectively) were grown in conical flasks for 16 h at 37 ºC with 200 rpm shaking. Pyocyanin was subsequently extracted with chloroform from filter-sterilised supernatants. T-tests were used to assess statistical significance, PAO1/pME6032 vs PASC815/pME6032, p=0.0002; PAO1/pME6032 vs PASC815/pSC323, p=0.0005; PAO1/pME6032 vs PADP135/pME6032, p=0.005; PAO1/pME6032 vs PADP14/pME6032, p=0.0123.

Pyocyanin secretion followed a similar trend to swarming motility, with the exception of the mutant of PA0744, PASC815; which was not restored by complementation (**Figure 4.8**). This phenotype was lost by long-term usage of the strain during this work, as pyocyanin was complemented in the first experiments performed (data not shown).

The effects of the mutations on PA0744 and on PA0745 are similar. It is thus possible that both genes code for proteins with similar functions, or involved in the same metabolic pathways. On the other side, PA0744 and PA0745 could encode subunits of a heterodimeric protein or interact together to perform their biological function, resulting in loss of function when either of the genes is mutated.

Characterisation of a PA0745 non-polar mutant

PA0745, also known as *dspI*, is located immediately upstream PA0744 (see **Figure 4.5**). In order to prevent possible polar effects caused by the mutation of PA0745, site-directed mutagenesis was used to introduce 4 STOP codons and a frameshift into the ORF of PA0745, thus preventing the expression of the protein and still allowing for wild-type expression of PA0744 (see **Chapter 2, section 2.3.6**). Next, swarming motility and pyocyanin production were compared from the in-frame and the non-polar mutants.

Swarming

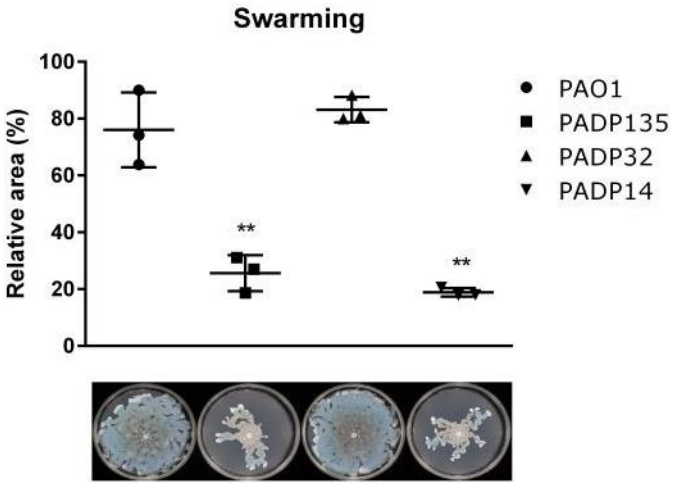


Figure 4.9. Effect of polar and non-polar mutation of PA0745 on the swarming motility of PAO1-L. Swarming motility of an in-frame mutant of PA0745 (PADP135) was compared to a non-polar mutant of PA0745 (PADP32) and the double mutant Δ0744 Δ0745 (PADP14); alongside a wild-type control of PAO1-L. The total area of swarming, relative to the area of the plates, was quantified from independent triplicates. Error bars represent one standard deviation of the means. Pictures show representative results. T-test were used to assess for statistical significance, PAO1 vs PADP135, p=0.0039; PAO1 vs PADP14, p=0.0017.

Results from **Figure 4.9** show that the non-polar mutant PADP32 presents wild-type levels of swarming motility. In contrast, the PADP135 in-frame deletion causes polar effects which result in a loss of swarming, similar to the behaviour of the double mutant PADP14.

Pyocyanin

Pyocyanin production was assessed in parallel to swarming motility. Results show a similar trend, where the polar mutant behaves as the double mutant PADP14 (**Figure 4.10**).

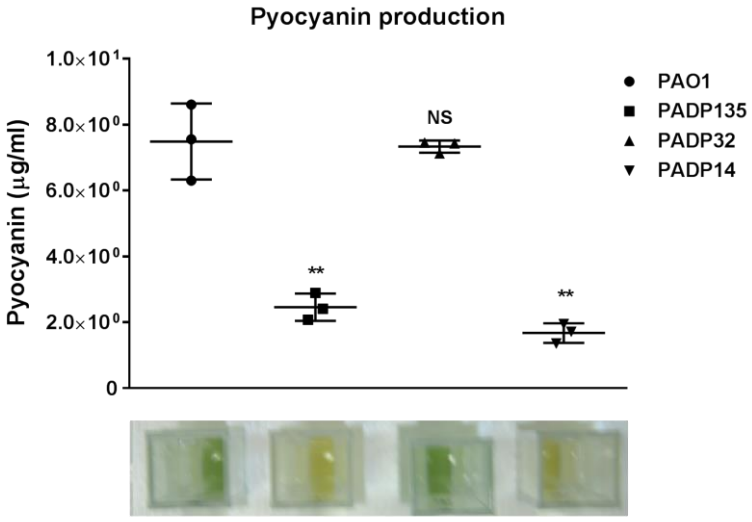


Figure 4.10. Effect of polar and non-polar mutations of PA0745 on the pyocyanin production of PAO1-L. Pyocyanin extracted from an in-frame mutant of PA0745 (PADP135) was compared to that of a non-polar mutant of PA0745 (PADP32) and the double mutant Δ0744 Δ0745 (PADP14); alongside with a wild-type control of PAO1-L. Pictures show representative results. T-test were used to assess for statistical significance, PAO1 vs PADP135, p=0.0021; PAO1 vs PADP14, p=0.0011.

Results so far show that the PASC815 failed to restore pyocyanin production by complementation from the pSC323 construction, which suggests that secondary mutations occurred during this work. On the other hand, the mutant PADP135 presents polar effects that possibly alter the expression of PA0744. Thus, to better characterise these possible CDA synthases, a different approach was taken by using the double mutant PADP14 complemented with PA0744 and PA0745.

Characterisation of PA0744 and PA0745 from a double mutant background

In the following experiments, the in-frame double mutant PADP14 was transformed with pSC323 (expressing PA0744), pSC3 (PA0745, *dspI*) and pDP181 (PA0745-PA0744). This way, the contribution of PA0744 and PA0745 was assessed separately, using the double mutant as a baseline.

Swarming

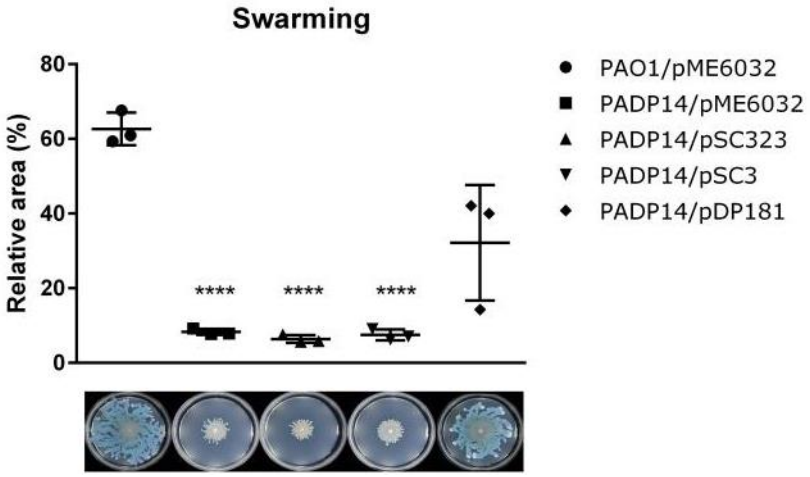


Figure 4.11. Effect of PA0744 and PA0745 expression in the double mutant PADP14, on the swarming motility of PAO1-L. The double mutant for PA0744 and PA0745, PADP14, was complemented with pSC323, pSC3 and pDP181 (pME6032 expressing PA0744, PA0745 and both PA0745-PA0744, respectively). The total area of swarming was quantified relative to the area of the plates, in independent triplicates. Error bars represent one standard deviation from the means. T-tests were used to assess for statistical significance, $p<0.0001$. Pictures show representative results. Swarming is only restored to wild-type levels when both genes are expressed.

As shown in **Figure 4.11**, the double mutant PADP14 is only complemented by both PA0744 and PA0745, indicating that both genes are needed for swarming motility.

Pyocyanin

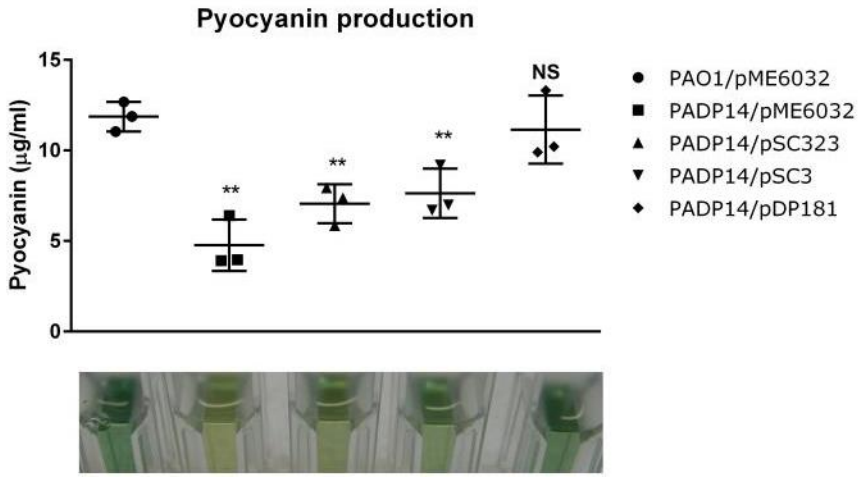


Figure 4.12. Effect of PA0744 and PA0745 expression in the double mutant PADP14 on pyocyanin production of PAO1-L. PADP14 (Δ0744 Δ0745) was complemented with pSC323, pSC3 and pDP181 (containing PA0744, PA0745 and both PA0745-PA0744). Pyocyanin was extracted from filter-sterilised supernatants with chloroform. Error bars represent one standard deviation of the means. T-tests were used to assess for statistical significance. PAO1 vs PADP14, p=0.0009; PAO1 vs PADP14/pSC323, p=0.0001; PAO1 vs PADP14/pSC3, p=0.0002. Pictures show representative colourations of the supernatants.

Results in **Figure 4.12** show a similar trend to those in **Figure 4.11**, albeit with a higher background of pyocyanin production in the double mutant expressing

either PA0744 or PA0745 alone. In parallel with swarming results, full restoration of pyocyanin production was only accomplished when both genes were expressed from pDP181.

Biofilm

One of the most drastic phenotypes found elsewhere in cultures spiked with CDA is the dispersion of biofilms and biofilm inhibition [255, 380]. Hence, the double mutant PADP14 was used in a static biofilm experiment.

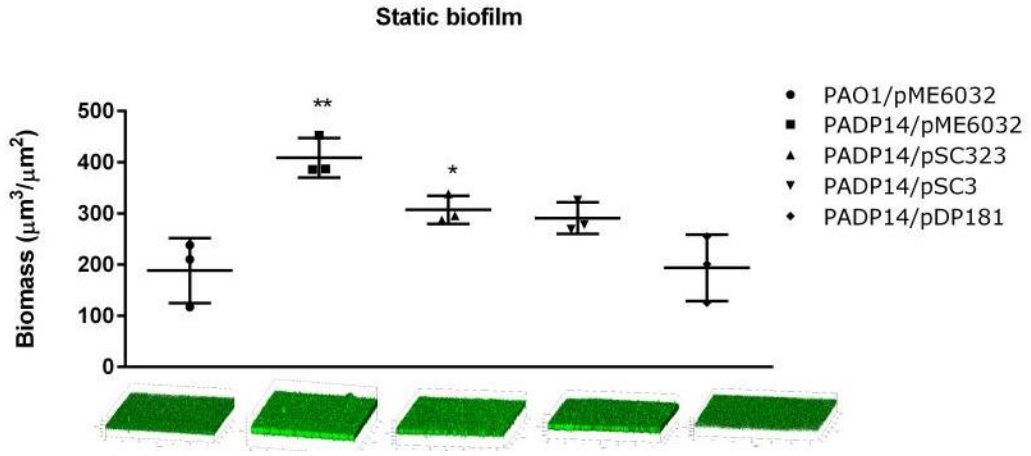


Figure 4.13. Effect of PA0744 and PA0745 expression in the double mutant PADP14 on biofilm formation of PAO1-L. PADP14 was complemented with pSC323, pSC3 and pDP181 (expressing PA0744, PA0745 and both PA0745-PA0744 respectively). Biofilms were grown in chamber slides statically, at 37 ºC for 16 h, then stained with Syto 9, prior to being visualised with confocal microscopy and quantified in Comstat2. Error bars represent one standard deviation from the means. T-tests were used to assess for statistical significance. PAO1 vs PADP14, p=0.0068; PAO1 vs PADP14/pSC323, p=0.0411; PAO1 vs PADP14/pSC3, p=0.0653. Pictures show representative results.

Interestingly, the same trend of complementation from PADP14 was found for pyocyanin production (**Figure 4.12**) and for biofilm formation (**Figure 4.13**). In both cases, PADP14 is partially complemented by PA0744 and also by PA0745, the latter having a stronger effect. In addition, both genes are needed to get restoration to wild-type levels.

Link with CDA

Results so far seem to suggest a complicated regulation involving PA0744 and PA0745. One major challenge faced during this thesis was the fact that wild-type PAO1-L presents endogenous production of CDA, which may mask the effects of exogenously added CDA. To better determine the role of this fatty acid, a series of assays were performed on the double mutant PADP14 spiked with CDA. This mutant is expected to lack endogenous production of this DSF-T, and might therefore show strong effects when spiked with this molecule.

Swarming

The impact of CDA in swarming motility of PA0745 and PA0744 mutants with pME6032-based construction was tested by adding 1 mM IPTG in all the swarming plates, which were additionally spiked with 100 µM CDA or the solvent control MetOH.

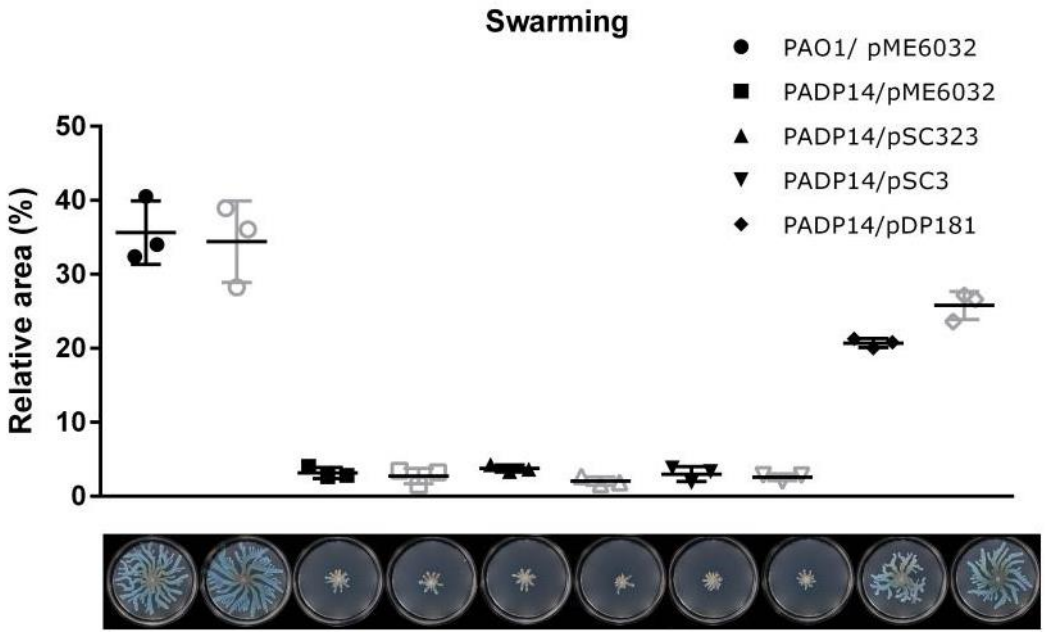


Figure 4.14. Swarming of PADP14 (Δ0744 Δ0745) in the presence and absence of CDA and the expression of PA0744 and PA0745, in PAO1-L. Swarming plates were supplemented with 1 mM IPTG and 100 µM CDA or the solvent control (MetOH). After inoculation, plates were incubated statically at 37 ºC for 15 h approximately. Total area, relative to the area of the plates, was quantified from independent triplicates. Filled symbols, MetOH; grey open symbols, CDA. T-tests were used to assess statistical significance, no differences were found caused by the addition of CDA. Pictures show representative results.

The addition of CDA to the plates did not result in drastic differences in swarming motility, either in tendril morphology or in spread throughout the agar surface (**Figure 4.14**).

Biofilm

Next, a similar approach was taken to evaluate whether CDA changes the biofilm formation of ECH mutants: PADP14 with and without CDA and expressing PA0744 and PA0745 was grown in the static chamber slides model. Only 10 µM CDA was used for this assay, as opposed to 100 µM used in the swarming assay, for consistency with other biofilm assays and given the strong effects caused by CDA in this phenotype, as reported in the literature.

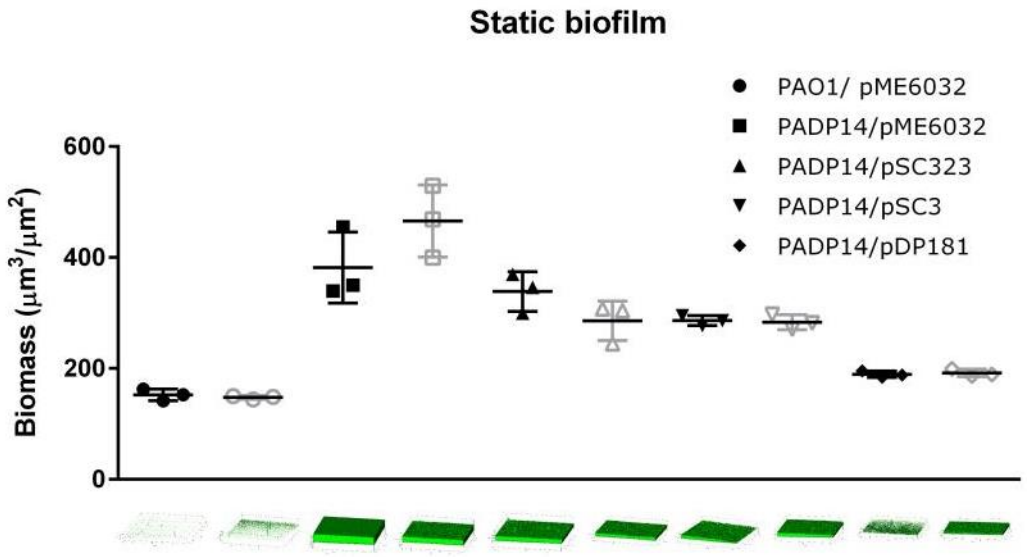


Figure 4.15. Biofilm formation of PADP14 (Δ0744 Δ0745) with and without CDA and the expression of PA0744 and PA0745, in PAO1-L. LB was supplemented with 1 mM IPTG and 10 μM CDA or the solvent control MetOH. After inoculation, chamber slides were incubated statically at 37 ºC for 16 h. The supernatants were subsequently removed and biofilms were stained with Syto 9 and visualised by CLSM. Filled symbols, MetOH; grey open symbols, CDA. T-tests were used to assess statistical significance, no differences were found caused by the addition of CDA. Pictures show representative results.

Despite the reported effect of CDA in biofilms, no differences were found after the addition of this fatty acid to chamber slides (**Figure 4.15**).

4.2.3.3 Characterisation of CbsA

Previous investigation conducted in Nottingham revealed a global role for PA3426 (CbsA) in the biology of *P. aeruginosa* PAO1. The overexpression of CbsA results in an attenuation of swarming motility and total rhamnolipid secretion, and an increase in biofilm formation, eDNA and exopolysaccharides [294].

In particular, experiments were mainly performed using the conditional mutant PASC315, in which the endogenous gene is replaced for a construction controlled by the inducible P*tac* promoter.

Transcriptomic approach (RNA-seq)

PASC315 with and without IPTG, and the wild-type PAO1-L were used on a transcriptomic study. Here, results from Deep Sequencing were analysed with an aim to identify interesting targets for future phenotypical assays.

One observation made during previous assays was that the overexpression of CbsA (i.e. PASC315 with IPTG) resulted in drastic phenotypical changes, whereas the mutation of CbsA (i.e. PASC315 without IPTG) showed mild or no effects on

the biology of *P. aeruginosa*. Therefore, the analysis of the RNA-seq was mainly performed by comparing the wild-type PAO1 vs PASC315 in the absence of IPTG.

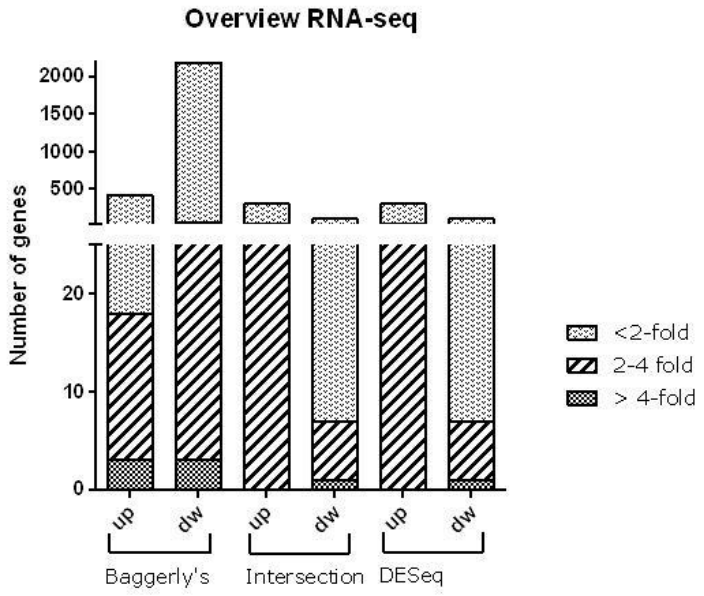


Figure 4.16. Number of differentially expressed genes from the RNA-seq results of the conditional mutant for CbsA PASC315 without IPTG (mutant) compared to the wild-type PAO1. Columns show the number of genes differentially expressed according to the Baggerly's test, the DESeq test, or the intersection between both tests. up, up-regulated; dw, down-regulated. For additional information, see **Appendix, section 7.3.1**.

As shown in **Figure 4.16**, the Baggerly's test identified a high number of differentially expressed genes, whereas the DESeq test was more stringent. Indeed, all genes found with the DESeq test were also present in the Baggerly's test. However, most of those genes presented a low fold change as compared to the PAO1 wild-type expression.

Next, to gain a more in-depth understanding of the transcriptomic results, genes differentially expressed at least 2-fold were classified according to a functional annotation, based in the COG database, with modifications (see **Chapter 2, section 2.4.3**).

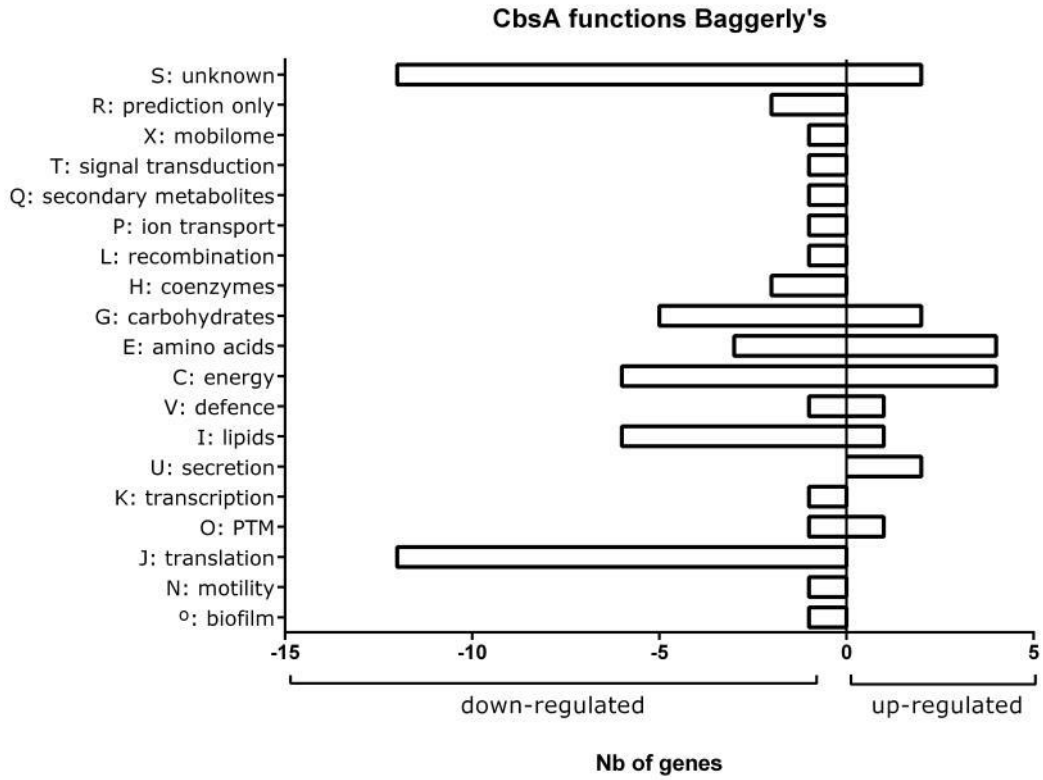


Figure 4.17. Functional annotation of genes differentially regulated in PASC315 versus PAO1 from the Baggerly's test. A functional annotation database was created from the categories in the COG database and the *Pseudomonas* Genome Database. Genes differentially regulated from the Baggerly's test were classified according to this functional annotation. Negative values were assigned for genes down-regulated in the PASC315 mutant and positive values correspond to up-regulated genes. PTM, post-translational modifications.

Results from **Figure 4.17** show that relevant genes in the RNA-seq belong to various functional categories, with the most represented categories being "J: Translation, ribosomal structure and biogenesis","G: Carbohydrate transport and metabolism" and "E: Amino acid transport and metabolism". All genes classified into category J encoded tRNAs, and thus were not of particular interest for this work.

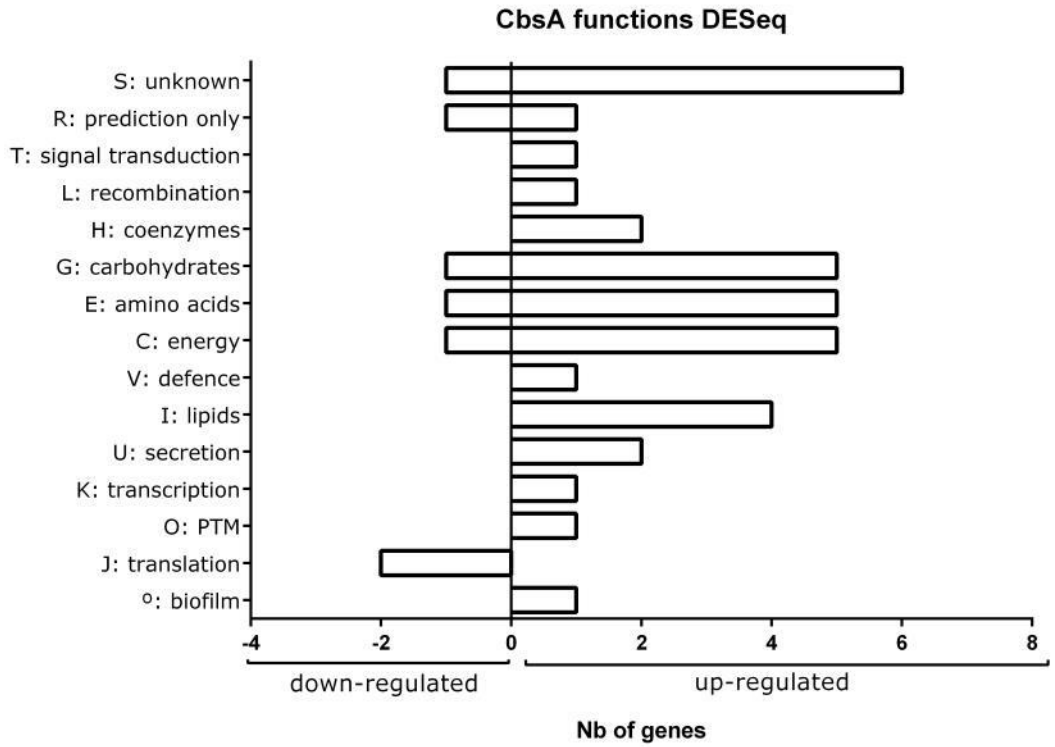


Figure 4.18. Functional annotation of genes differentially regulated in PASC315 versus PAO1 from the DESeq test. A functional annotation database was created from the categories in the COG database and the *Pseudomonas* Genome Database. Genes differentially regulated from the DESeq test were classified according to this functional annotation. Negative values were assigned for genes down-regulated in the PASC315 mutant, while positive values correspond to up-regulated genes. PTM, post-translational modifications.

The most represented categories from the DESeq test, listed in **Figure 4.18**, were "G: Carbohydrate transport and metabolism", "E: Amino acid transport and metabolism" and "C: Energy production and conversion".

All in all, transcriptomic analysis did not lead to strong hypotheses on pathways regulated by CbsA, and thus phenotypical characterisation was carried out mainly based on previous results and in the available literature.

Phenotypical characterisation

Impact of CbsA on growth

Growth of the in-frame mutant of CbsA, PASC203, was tested in a variety of media which did not reveal any changes as compared to the wild-type (see **Figure 4.6**). The effect of the conditional mutation was further tested under the conditions used for subsequent assays.

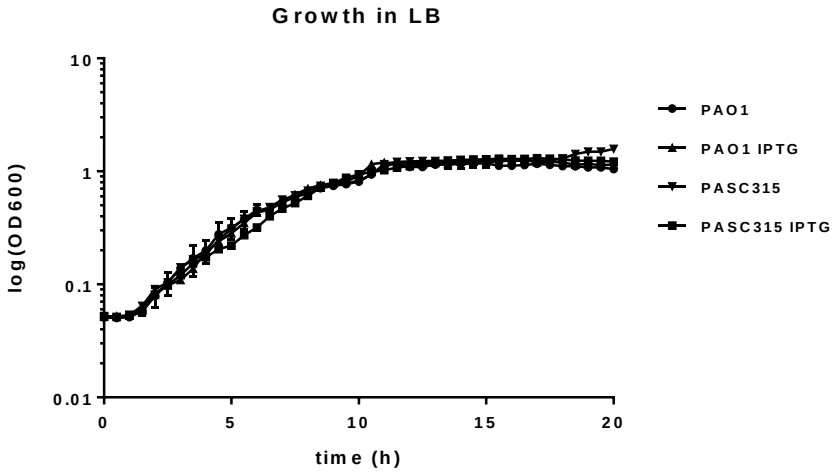


Figure 4.19. Impact of the conditional mutation for CbsA (from PASC315) in LB. Cultures of PAO1-L were incubated at 37 ºC for 24 h in 96-well plates, with IPTG added at 1 mM when appropriate. Results represent the average of three independent replicates. Error bars represent one standard deviation of the means.

Growth in LB was not affected by mutation or overexpression of CbsA (**Figure 4.19**). Growth in NB was slightly delayed in PASC315 with IPTG, but this strain reached the same OD as the isogenic wild-type after 6 h of growth, and no defect in growth was observed in NB agar plates (**Figure 4.20**).

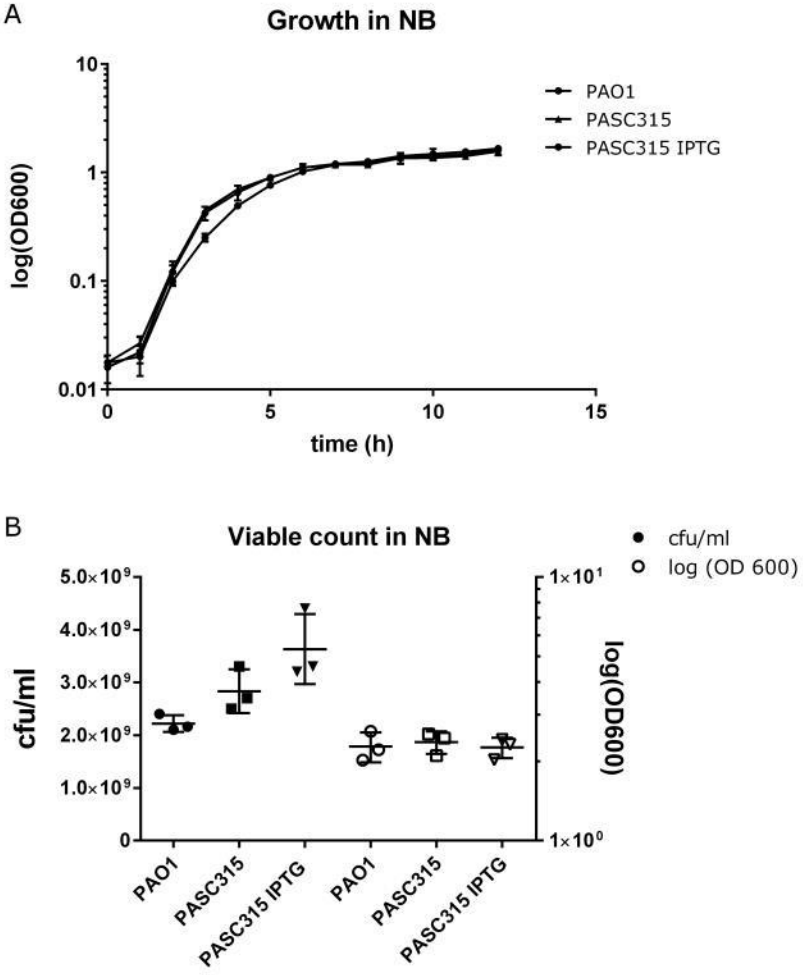


Figure 4.20. Growth of PAO1 and PASC315 (conditional mutant for CbsA) in NB, with and without IPTG 1 mM. A, Cultures were grown in conical flasks, at 37 ºC with 200 rpm shaking; and aliquots were taken every hour for the determination of the OD_{600}. **B,** Overnight cultures were spread onto NB agar plates and allowed to grow for 16 h at 37 ºC statically. Cells were then recovered and both the OD_{600} and cfu counts were performed.

Impact of CbsA on bacterial motility

CbsA was first identified in a swarming screen of strains overexpressing ECH, performed with a broader aim to discern potential CDA regulators [294]. Strains overexpressing CbsA, either from a plasmid-based construction or from the chromosomal construction of PASC315, show an attenuation of swarming motility.

Therefore, swimming and twitching motilities were assessed in addition to swarming to ascertain if flagella and pili are affected by the overexpression of CbsA. PAO1 with and without IPTG was used as a control, and compared to the conditional mutant PASC315, with and without IPTG.

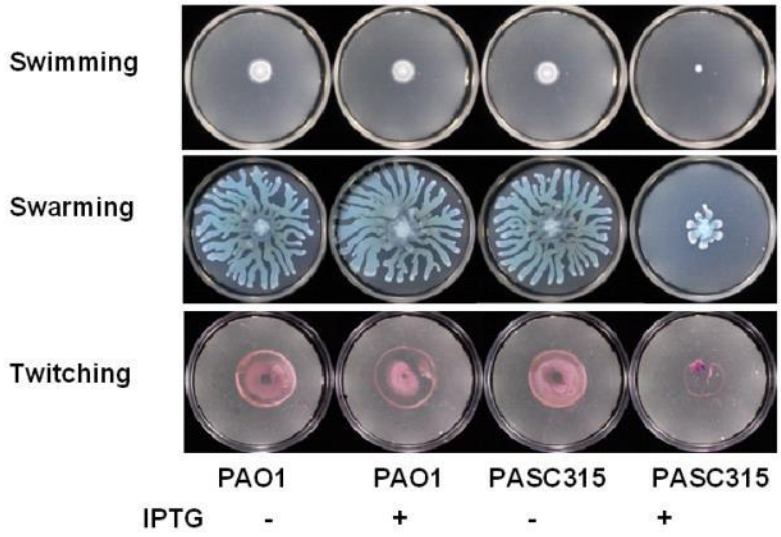


Figure 4.21. Effect of CbsA expression on the motility of PAO1. Swimming, swarming and twitching assays were performed in NB, with 0.3 %, 0.5 % and 1 % agar, respectively. Cells were inoculated in the centre of the plates and incubated at 37 ºC statically for 5 (swimming), 16 h (swarming) and 48 h (twitching). For twitching, the agar was removed and plates were stained with 1 % crystal violet. Pictures were taken with indirect light and depict representative results. The overexpression of CbsA results in a reduction of motility.

Results show that overexpression of CbsA from PASC315 results in a reduction of all three forms of motility assayed; including swimming, swarming and twitching (**Figure 4.21**).

Impact of CbsA on rhamnolipid secretion

Rhamnolipids are biosurfactants that, amongst other functions, allow bacteria to move across surfaces by reducing surface tension [417]. Mutation in CbsA was shown to increase total rhamnolipid secretion (as seen by a liquid orcinol assay and the expression of a translational fusion P*rhlAB-dsRed*), whereas the overexpression of CbsA results in a decrease of rhamnolipids [294]. Mono- and di-rhamnolipids have different roles in swarming motility, where mono-rhamnolipids only act as surfactants while di-rhamnolipids result in an increase in swarming tendrils [76]. Therefore, and with an aim to better understand the link between CbsA, motility and rhamnolipid production; a TLC assay was performed by extracting rhamnolipids from liquid cultures and agar plates. First, the addition of IPTG to PAO1 cultures was studied and results showed that it did not affect the expression of rhamnolipids (see **Appendix, Figure 7.10**).

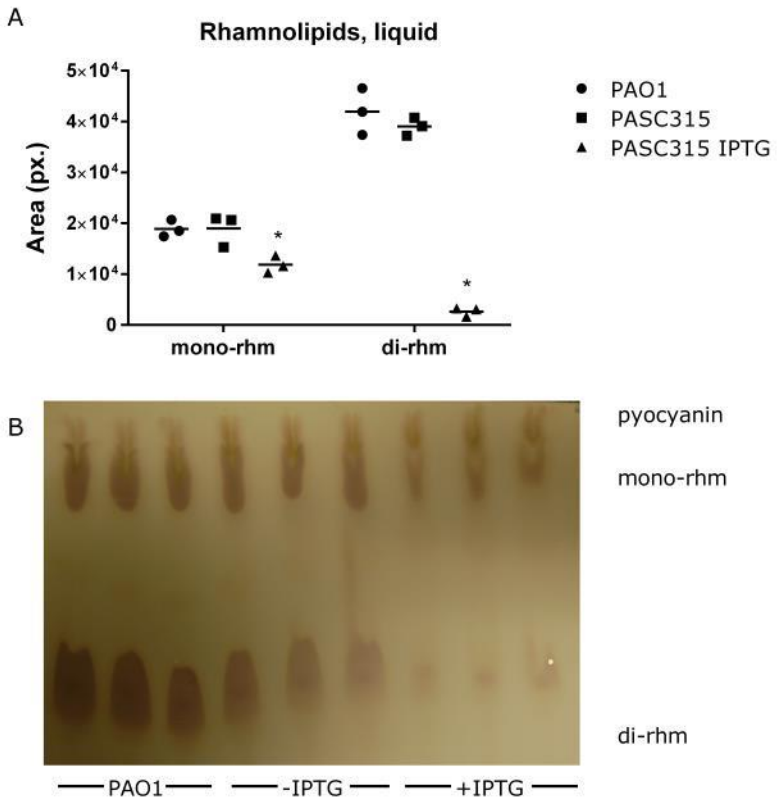


Figure 4.22. Effect of the expression of CbsA from the conditional mutant PASC315 on rhamnolipid production, in liquid cultures. Cells were grown at 37 ºC for 16 h with 200 rpm shaking in NB. Rhamnolipids were extracted from filter-sterilised supernatants with EtOAc, and the extracts were run on normal phase silica plates. **A,** the area occupied by mono- and di-rhamnolipid (mono-rhm and di-rhm, respectively) was determined by pixel integration analysis. Error bars show one standard deviation of the means, from independent triplicates. Multiple t-tests were used to assess statistical significance, using the Holm-Sidak correction and a threshold value of 0.05. PASC315 IPTG vs PAO1, p-value mono-rhm=0.011; p-value di-rhm=$7.96 \cdot 10^{8}$. **B,** Picture of TLC plate after detection of the spots with an acidic solution of orcinol. The upper spots correspond to mono-rhm; the lower spots correspond to di-rhm. Overexpression of CbsA results in a reduction of rhamnolipid production.

As can be observed in **Figure 4.22**, the overexpression of CbsA from PASC315 results in a reduction of both mono-rhamnolipids and di-rhamnolipids. The same results were found when rhamnolipids were extracted from agar plates (**Figure 4.23**).

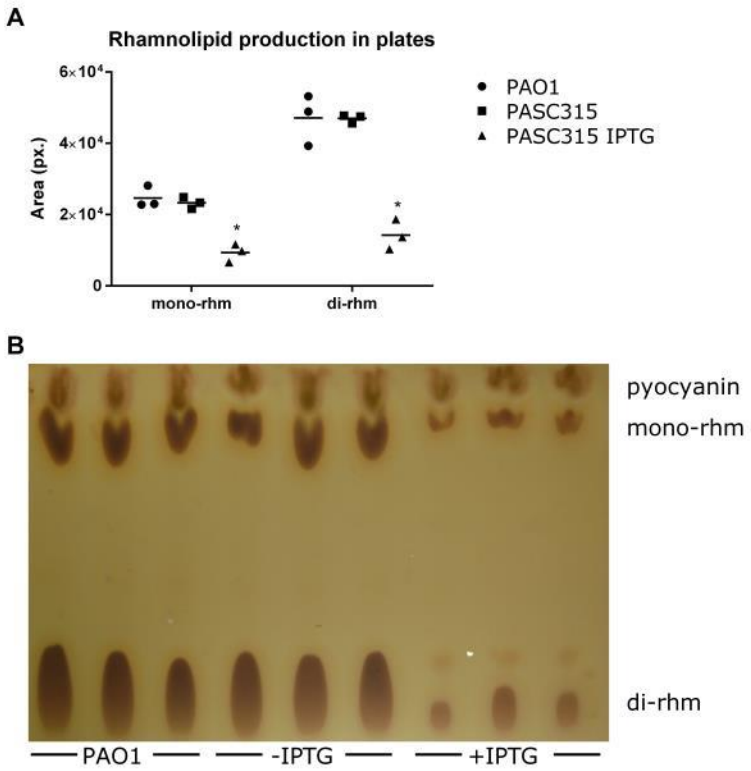


Figure 4.23. Effect of the expression of CbsA from the conditional mutant PASC315 on rhamnolipid production, in agar plates. Cells were spread on NB agar plates and incubated at 37 ºC for 16 h. Rhamnolipids were extracted with EtOAc, and the extracts were run on normal phase silica plates. **A,** the area occupied by mono- and di-rhamnolipid (mono-rhm and di-rhm, respectively) was determined by pixel integration analysis. Error bars show one standard deviation of the means, from independent triplicates. Multiple t-tests were used to assess statistical significance, using the Holm-Sidak correction and a threshold value of 0.05. PASC315 IPTG vs PAO1, p-value mono-rhm=0.0002; p-value di-rhm=$3.68 \cdot 10^{7}$. **B,** Picture of TLC plate after detection of the spots with an acidic solution of orcinol. The upper spots correspond to mono-rhm; the lower spots correspond to di-rhm. Overexpression of CbsA results in a reduction of rhamnolipid production.

Impact of CbsA on proteases

Previous research showed that CbsA is a positive regulator of RsmY and RsmZ, which results in a negative regulation of RsmA. Indeed, cells overexpressing CbsA show some of the phenotypes of RsmA mutants, such as reduced motility and increased biofilm [294]. Overexpression of RsmA results in a reduction of proteases [418]. Additionally, the secretion of DSF-T molecules is linked to the production of proteases in various *Xanthomonas sp.* and in *S. maltophilia* [244]. To better understand the regulation of CbsA in relation to the Rsm system and to CDA production, a range of protease assays were performed from supernatants of PASC315.

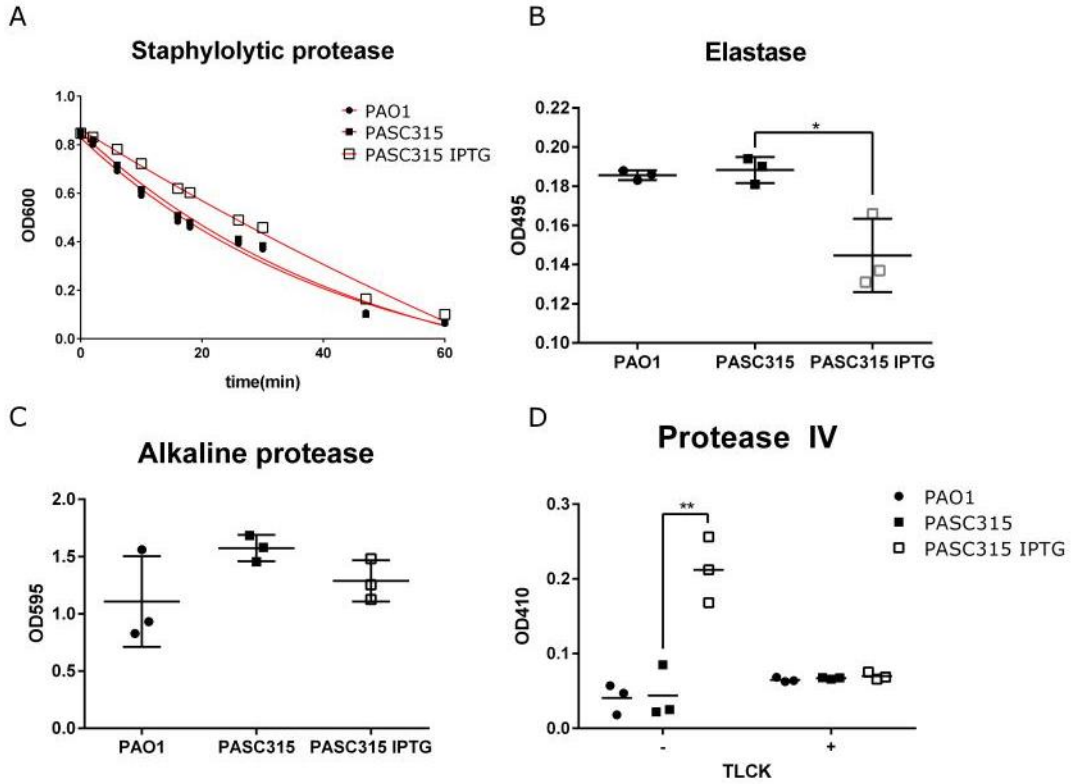


Figure 4.24. Effect of the conditional mutation of CbsA from PASC315 on protease secretion. A series of protease assays were conducted with PASC315 in the presence and absence of 1 mM IPTG, after incubation of cultures for 16 h at 37 ºC. **A,** Staphylolytic assay. Supernatants of cultures were put in contact with a suspension of *S. aureus* Newman, and the decay in OD_{600} was monitored over 1 h. A one phase decay fit was used to assess statistical significance, $p<0.0001$. **B,** Elastase assay. Supernatants were mixed with a suspension of elastin-Congo red, incubated at 37 ºC with 200 rpm shaking for 2 h and centrifuged. The OD of the suspension was then measured at 495 nm. A t-test was used to assess significance, $p=0.019$. **C,** Alkaline protease assay. Supernatants mixed with hide powder azure were incubated for 1 h at 37 ºC with 200 rpm shaking, and the OD_{595} of the resulting suspension was determined. **D,** Protease IV assay. Chromozym PL was mixed with culture supernatants and the OD_{410} was determined. TLCK is a serine protease inhibitor used as a negative control. A t-test was used to assess significance, $p=0.0036$.

Figure 4.24 shows that the mutation of CbsA (PASC315 without IPTG) results in a slight, negligible decrease in alkaline protease activity. The overexpression of CbsA (PASC315 with 1 mM IPTG) shows a decrease in protease activity, including staphylolytic and elastase activities; and an increase in protease IV.

Impact of CbsA on biofilm formation

As CbsA triggers the Gac/Rsm pathway, mutation in CbsA results in a reduction of biofilm. This was previously assessed in RPMI medium, with biofilms grown in metal coupons for up to 7 days [294]. As a further validation and for consistency, static biofilms were grown statically in chamber slides, in LB.

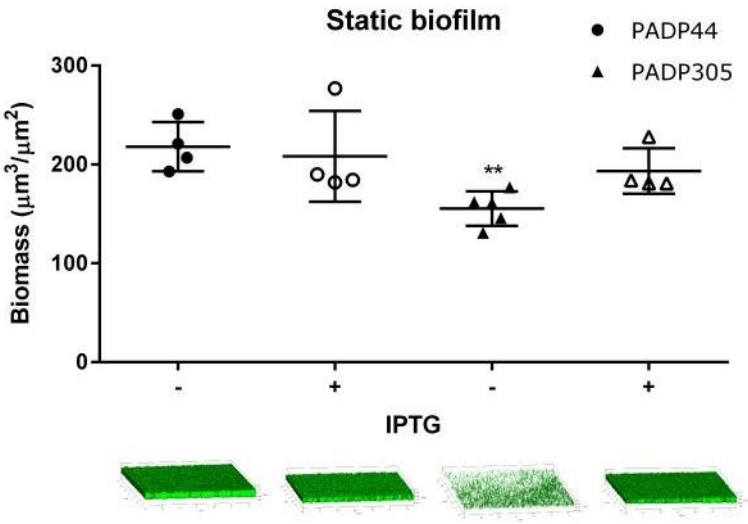


Figure 4.25. Effect of the expression of CbsA from the conditional mutant tagged with GFP (PADP305) as compared to the PAO1-L tagged with GFP (PADP44) on biofilm formation, in LB. Biofilms were grown in chamber slides for 16 h at 37 ºC, statically. Supernatants were subsequently removed and biofilms were visualised with CLSM and quantified with Comstat2. Error bars represent one standard deviation of the means. T-tests were used to assess statistical significance; PADP305 vs PADP44, p=0.0030.

Results in **Figure 4.25** show that CbsA indeed affects biofilm formation, consistent with the link of this regulator to the Gac/Rsm system and with previous results from The University of Nottingham [294].

Link with CDA

Biofilm formation in chamber slides revealed a statistical difference between the phenotypes of PAO1-L wild-type and PASC315 without IPTG (**Figure 4.25**). Therefore, static biofilms were used as a model to study possible links between CbsA and the production of CDA by PAO1.

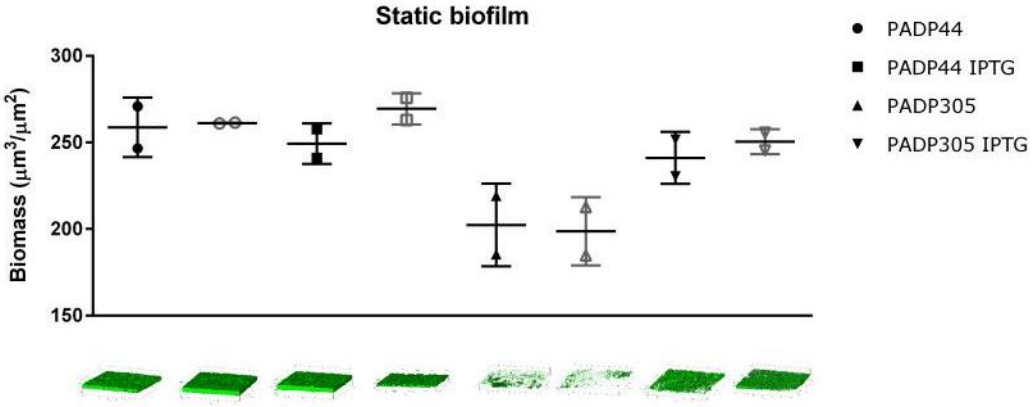


Figure 4.26. Biofilm formation of PADP305 (conditional CbsA, GFP) with and without CDA. LB was supplemented with 1 mM IPTG and 10 µM CDA or the solvent control MetOH. After inoculation, chamber slides were incubated statically at 37 ºC for 16 h. The supernatants were subsequently removed and biofilms were visualised by CLSM. Filled symbols, MetOH; grey open symbols, CDA. T-tests were used to assess statistical significance, no differences were found caused by the addition of CDA. Pictures show representative results.

Results show that CDA did not change the biofilm formation of the conditional mutant of CbsA tagged with GFP (PADP305) (**Figure 4.26**). This is in line with the results in **Chapter 3**, in which CDA did not affect biofilms of PAO1; and with **Figure 4.15**, in which CDA did not change the biofilm of various mutants expressing combinations of PA0744 and PA0745.

4.3 Discussion

4.3.1 Bioinformatic analysis of enoyl-CoA hydratases in *P. aeruginosa*

P. aeruginosa contains a set of putative enoyl-CoA hydratases (ECH) which are potentially involved in the metabolism of CDA. Previous work at The University of Nottingham suggests that PA0744 has a partial role in the synthesis of CDA, while PA3426 is involved in the degradation of this molecule [294]. In addition, PA0745 and PA4980 have been identified elsewhere [364, 380](**Figure 4.5**).

A preliminary, sequence-to-function approach was first conducted. Primary sequence alignments showed that none of the proteins from *P. aeruginosa* has high similarity to the RpfF of either *B. cenocepacia* H111 or *Xcc* (**Table 4.1**). All alignments presented less than a 40 % similarity, which does not allow for the inference of protein function [419]. Indeed, Feinbaum et al. pointed out that PA0745 is homologous to *paaF* in *X. campestris,* with 65 % sequence identity and 95 % coverage; which is significantly higher than the alignment to RpfF and suggests that PA0745 might have a primary function unrelated to CDA synthesis [420].

A detailed analysis of key residues was next conducted, and shows that some of the conserved residues in these proteins are found in *P. aeruginosa* ECH (**Table 4.2**). In particular, E141, E161, G85, L136, G137 and G138 ($RpfF_{Xcc}$) were well conserved amongst the ECH candidates. Regarding the conserved glutamates, some degenerated sequences were found. In particular, PA0744, which is one of the strong candidates for CDA biosynthesis according to our experimental data, presents a glycine in the first position. Other proteins such as PA1021 and PA4330 do not present either of the glutamates, suggesting that the enzymatic activity of these is not related to the synthesis of DSF-T.

Bi et al. and Cheng et al. suggested two different glycines to be essential for the catalytic activity of RpfF [403, 405]. According to these data the conserved residue is G85, and not G86 ($RpfF_{Xcc}$) (**Table 4.2**). In addition to being better conserved in general, G85 is also present in the rat mitochondrial ECH, as opposed to G86. With the exception of somewhat more complex results in PA0744, G85 ($RpfF_{Xcc}$) is very well conserved in PAO1 ECH/Isomerases. It is of note that, during that study, the glycines were subtituted by prolines to avoid the presence of available peptidic nitrogens. The analysis presented here, together with the conserved residues suggested by [405], rather suggest that G82 is required for catalysis. The substitution of G83P likely impeded the correct conformation for G82 to contribute to the oxyanion hole.

Regarding PA0744, BLASTP against $RpfF_{Xcc}$ showed only short alignments, and in particular, G85 ($RpfF_{Xcc}$) was aligned with E307 (PA0744), at the very end of the protein sequence. In constrast, both BLASTP against ECH and CLUSTALω analysis showed longer alignments, and G67 (PA0744) was identified. This latter result seems to have a stronger basis, given the location of the residues in the protein and the validation of CLUSTALω analysis.

The residues present in the oxyanion hole; L136, G137 and G138 ($RpfF_{Xcc}$); are also highly conserved. The first leucine is substituted by similar residues, namely methionine and valine. Only two exceptions were found, in PA1240 and PA2841, were the leucine was not conserved. The following two glycines were also conserved, however some annotated ECH/isomerases are unlikely to catalyse the synthesis of DSF-T based on these results, such as PA1240, PA1748, PA1846 (Cti) and PA2841.

Finally, a M170A mutation in $RpfF_{Xcc}$ resulted in a total loss of DSF production [405]. Some of the PAO1 proteins present similar residues, such as PA0744, whereas others present an alanine, as found in ECH, PA0745, and PA4980.

Predicted secondary structures presented a high degree of conservation (**Table 4.3**), whereas the tertiary, folded structures ranged from very similar to RpfF protein(s), to very distant (**Table 4.4**), with the structural alignment between $RpfF_{Bc}$ and PA0745 having the lowest RMSD. A summary of the results of this *in silico* analysis for the best candidates for CDA synthases is found in **Table 4.11**.

Table 4.11. Summary of results from bioinformatic analysis of the described CDA synthases in *P. aeruginosa*. Numbers of conservative and non-conservative changes relate to the following amino acid residues: E141, E161, G85, L136, G137, G138 and M170 ($RpfF_{Xcc}$). For secondary structures, both RpfF proteins are considered, and the minimum number of changes is listed on the table. α, alpha helix; β, beta-sheet; l, loop. Root mean square distance (RMSD) is given as a measure for the alignment between 3D structures. The RMSD of $RpfF_{Xcc}$ vs. $RpfF_{Bc}$ is 2.6.

Protein ID	**Primary seq. identity**	**αα changes, (conservative, non-conservative)**	**Secondary structure**	**3D structure (RMSD) ($RpfF_{Xcc}$, $RpfF_{Bc}$)**
PA0744	<30	1,2	conserved	5.1, 4.7
PA0745, DspI	<30	1,2	α → l α → l	2.8, 1.4
PA3426, CbsA	32 vs $RpfF_{Bc}$	2,2	α → l α → l α → β	2.2, 2.4
PA4980	<30	2,3	l → β	9.5, 3.7

In silico analysis involving the study of conserved residues and structural alignment has proven to be an effective strategy to identify functional homologues [421]. However, the variety of ECH present in *P. aeruginosa,* together with the evolutionary distance between this bacterium and the *Burkholderia* and *Xanthomonas* genus make this analysis complex, and therefore this only constitutes a first step towards the identification of CDA regulators.

Regarding signal sensing and transduction of DSF-T, two broad mechanisms have been identified so far (**Figure 4.3**). Bioinformatic analysis performed in this chapter was unable to identify which, if any, is employed by *P. aeruginosa* for the sensing of CDA. Instead, it seems that this bacterium contains multiple candidates for both RpfGHC-like and RpfR-like systems. However, query coverages for putative homologues of the *Burkholderia cenocepacia* RpfR were much higher than the coverage of alignments against RpfC (**Table 4.5, Table 4.6**), which suggests that *P. aeruginosa* might be using the *Burkholderia* strategy for the sensing of CDA.

Interestingly, a number of sensor proteins homologous to either RpfC or RpfR are involved in biofilm regulation (**Table 4.5, Table 4.6, Table 4.8, Table 4.10**). Biofilm regulators homologous to RpfC include RocS1 and RocS2, two sensors involved in the assembly of Cup fimbriae, which are adhesins that influence biofilm formation in *P. aeruginosa* [114, 422, 423]. LadS and RetS are sensors that modulate the signalling of the Gac system, a global regulatory system controlling the switch between acute and chronic lifestyle in *P. aeruginosa* [424]. Alignments of BLASTP against RpfR were expected to show biofilm regulators, given that this protein presents a GGDEF and an EAL domain (**Figure 4.4, Table 4.9**). The top hit of this alignment was MorA, whose mutant presents less biofilm in *P. aeruginosa* PAO1 [425]. MucR is the main regulator of alginate production [426], and together with NbdA, RbdA and DipA, regulates biofilm dispersion [427, 428]. BifA is important in biofilm establishment, and also regulates swarming in PA14 [214]. The sensing of CDA coupled with an alteration of c-di-GMP levels could constitute one possible mechanism behind the reported effects of CDA, leading to biofilm inhibition and dispersion. Further research is needed in this area to better understand the role of CDA in the biofilm dispersion of *P. aeruginosa.*

4.3.2 Biological role of PA0744 and PA0745 in *P. aeruginosa*

Previous results showed that PASC815 (mutant for PA0744) presented reduced swarming motility due to a repression of rhamnolipid genes, and an increased biofilm formation in LB. Additionally, this mutant secreted reduced amounts of HHQ and PQS [294]. During this thesis, phenotypical characterisation of PA0744 was further researched, together with the effects of a mutation in PA0745. Both proteins were shown to positively regulate swarming motility and pyocyanin production, and to be negative regulators of biofilm (**Figure 4.7, Figure 4.8, Figure 4.13**). These effects are consistent with an involvement of the Rsm/Gac system, where RsmA activates acute phenotypes while repressing chronic phenotypes [80]; however due to time restrictions the link between ECH and Rsm/Gac was not investigated.

On the other hand, DSF-T molecules positively regulate bacterial motility [353], and CDA is described as a biofilm inhibitor [255]. Therefore, the above-mentioned phenotypes also fit with these ECH being involved in CDA synthesis. This role was investigated by spiking ECH mutants with CDA, but results are inconclusive (for more information and discussion, see **4.3.4**).

During this thesis, the regulation of PA0744 and PA0745 was researched. Swarming attenuation by PASC815 was validated (**Figure 4.7**), and the effects of ECH mutants in pyocyanin were additionally assessed (**Figure 4.8**). Then, various mutant backgrounds including a non-polar mutant of PA0745 and a double mutant Δ0744 Δ0745 were used to understand the regulation of these genes.

One interesting point about these proteins is that they are encoded by genes located side by side in PAO1 genome (**Figure 4.5**). The question then rises of whether PA0744 and PA0745 interact together, or are involved in the same processes.

A feature that the String database takes into account to predict protein-protein interactions is the occurrence of two proteins in genomes, and indeed PA0744 and PA0745 are present together in multiple Proteobacteria, and more distantly related organisms (see **Appendix, section 7.3.2**).

Regarding a possible co-expression of PA0744 and PA0745, Amari et al. showed by RT-PCR that PA0745 (*dspI*) is transcribed together with two genes upstream, PA0747 and PA0746 [380]; whereas the *Pseudomonas* Genome Database predicts that PA0745 and PA0744 constitute an operon. Furthermore, both genes

appear to be induced by QSSM, at least under certain conditions. In a microarray analysis, both PA0744 and PA0745 were induced (7 and 8-fold, respectively) by 3OC12-HSL and C4-HSL [429].

Furthermore, a search of expression profiles from the Gene Expression Omnibus (GEO, http://www.ncbi.nlm.nih.gov/geo/, [430, 431]) showed that PA0744 and PA0745 are often co-regulated, together with PA0746 and PA0747 to a lesser extent (see **Appendix, section 7.3.2**). Of particular relevance for this thesis is the fact that PA0747-PA0744 were induced by the addition of 50 μM DSF to PAO1 [369]. The addition of 100 μM CDA to PAO1 resulted in the repression of these genes, ranging from PA0746 with an 8-fold reduction (see **Chapter 3, Table 3.1**) to PA0744 (7-fold) and PA0747 and PA0745 (1.5-fold) (data not shown). PA0746 was the only gene statistically relevant in the operon.

Results during this work reveal that the regulation of PA0744 and PA0745 is indeed highly complex. Firstly, differential results with the in-frame deletion mutant PADP135 and the non-polar mutant PADP32 show the existence of regulatory sequences within the PA0745 ORF that result in polar effects in PADP135 (**Figure 4.9, Figure 4.10**). The polar PADP135 mutant lacks swarming motility and pyocyanin production, phenotypes that are found in the PA0744 mutant PACS815 and also in the double mutant PADP14. In contrast, PADP32 presents wild-type levels of both phenotypes. Interestingly, mutations in PA0745 have been reported to attenuate virulence in *C. elegans* in PAO1 [432] and in PA14, together with reduced pyoverdine and twitching motility levels, and increased swimming motility [420]. These phenotypes could be a consequence of polar effects and a result to altered levels in the expression of PA0744. Pyoverdine was assessed during this work and both PADP32 and PADP135 presented reduced levels of the pigment. While none of them was statistically significant, levels of the in-frame mutant PADP135 were lower to those of PADP32 (see **Appendix, section 7.3.3**).

PA0745 seems to be required for swarming and pyocyanin, as shown in the complementation of the double mutant, where only the expression of both PA0744 and PA0745 was able to restore these phenotypes to wild-type levels (**Figure 4.11, Figure 4.12**). Results in static biofilms were similar, though in this case the complementation of the double mutant with only PA0745 (from pSC3) was not significantly different from wild-type levels or the double mutant complemented (PADP14/pDP181). However, biofilm levels decreased with PADP14/pDP181 as compared to PADP14/pDP3 (**Figure 4.13**).

Results found with PADP14 could point to the fact that PA0745 and PA0744 might constitute a heterodimeric protein, as only when both genes are expressed are the phenotypes restored (**Figure 4.11, Figure 4.12, Figure 4.13**). However, the non-polar mutant of PA0745, PADP32, shows wild-type levels of pyocyanin and swarming (**Figure 4.9, Figure 4.10**).

An analysis of different types of interactions between PA0744 and PA0745 is shown in **Figure 4.27**. For this analysis, levels of expression are not taken into account, and it is assumed that the polar effects of PDP135 result in no expression of PA0744. Under those circumstances, all the scenarios analysed present discrepancies with experimental data of this chapter.

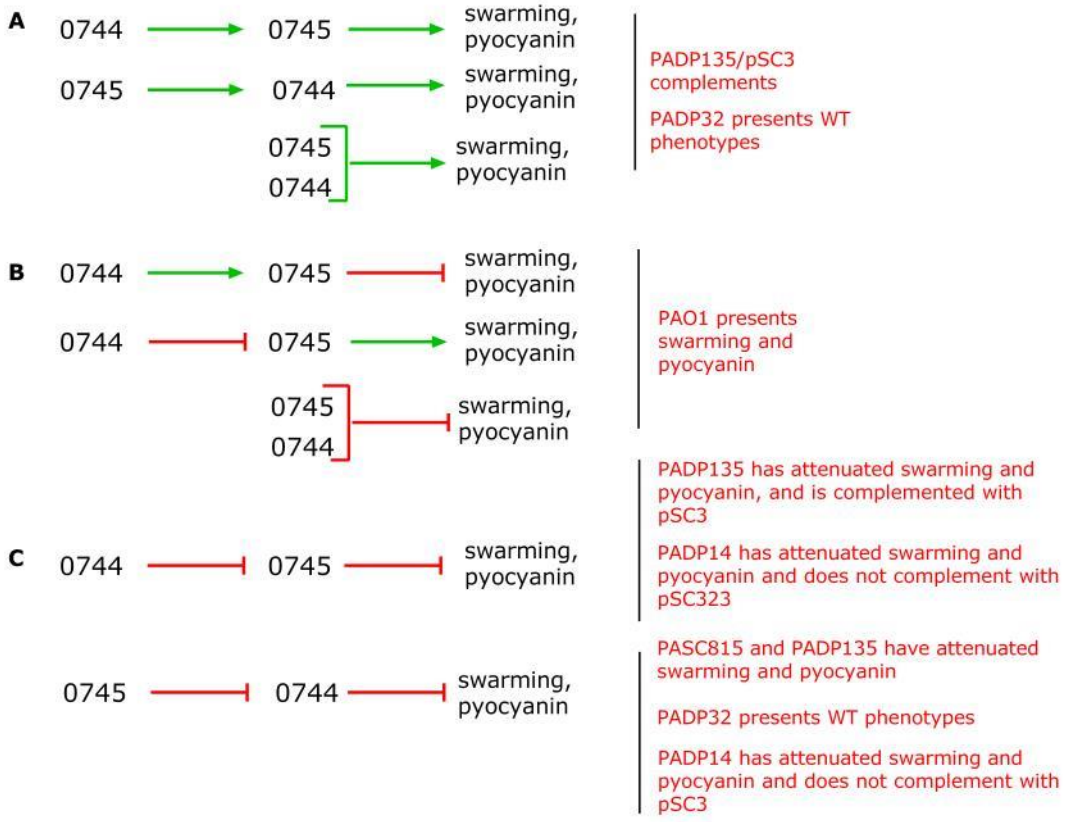


Figure 4.27. Analysis of possible interactions between the ECH PA0744 and PA0745, according to experimental data. Different scenarios are suggested, and reasons against those scenarios are given on the right, in red. All scenarios assume there is no effect of protein expression levels, and that the polar mutant PADP135 has no expression of PA0744. **A,** PA0744 and PA0745 are positive regulators of swarming and pyocyanin, and they either function in a hierarchy (one regulates the other or they are part of the same metabolic pathway) or in parallel (both are needed, e.g. as part of a protein complex). **B,** One of the ECH positively regulates swarming and pyocyanin, the other is a negative regulator; or they are both part of a protein complex which negatively regulates these phenotypes. **C,** Both ECH act negatively towards the attenuation of swarming and pyocyanin, in a hierarchical manner.

Two crucial points were not elucidated during this work: as can be seen in **Table 4.12**, the expression of PA0744 in the absence of PA0745 does not lead to phenotype changes in PADP32, while it shows attenuated pyocyanin and

swarming in PADP14/pSC323. This can be due to the expression levels of both genes; in PADP32, PA0744 is expressed from its native promoter, while in PADP14/pSC323 it relies on P*tac*, which is highly induced in the presence of IPTG. Additionally, the expression of PA0745 only leads to PADP14/pSC3 having attenuated pyocyanin and swarming; while PADP135/pSC3 complements back to wild-type. It is possible that the polar effects from the in-frame deletion of PA0745 still allow for a low level of expression for PA0744, able to complement with a high level of PA0745; while in PADP14 there is no expression of PA0744 whatsoever and therefore no complementation.

Table 4.12. Summary of results with several combinations of PA0744 and PA0745 expression in PAO1. The expected expression levels of PA0744 and PA0745 are shown in brackets. WT, wild-type levels of pyocyanin and swarming; +, protein is expressed; -, protein is not expressed. Highlighted in purple and pink are two combinations of strains that show results in disarray with one another.

Strain	Expression of PA0744	Expression of PA0745	Pyocyanin, swarming
PAO1	+ (native)	+	WT
PADP14/pDP181	+ (P*tac*)	+ (P*tac*)	WT
PASC815	-	+ (native)	-
PADP14/pSC3	-	+ (P*tac*)	-
PADP135	- (polar effect)	-	-
PADP14	-	-	-
PADP135/pSC3	- (polar effect)	+	WT
PADP32	+ (native)	-	WT
PADP14/pSC323	+ (P*tac*)	-	-

The in-frame mutant of PA0744 was complemented with PA0745 and *vice-versa* to assess if these two genes are functional homologues, but pyocyanin was not restored (data not shown), so the two genes do not present overlapping functions.

In summary, the results presented in this chapter show that there are regulatory sequences within PA0745 that might affect the expression of downstream genes such as PA0744, and that PA0744 and PA0745 seem to interact together which allows for wild-type levels of swarming, pyocyanin and biofilm formation. More investigation is needed to better discern the regulation of ECH.

4.3.3 Biological function and regulation of CbsA

CbsA was identified in a screening for ECHs with the aim of identifying potential regulators of CDA synthesis. In line with published positive regulation of motility by DSF-T, the synthase of CDA was expected to enhance swarming motility when overexpressed due to the accumulation of the fatty acid. Overexpression of CbsA from a plasmid vector presented an attenuation of swarming as opposed to the effect of other ECHs, and therefore was chosen for future work [294].

An RNA-seq experiment was performed previous to this work. Therefore, the starting point of this thesis was to analyse the transcriptomic analysis to identify new targets for CbsA and better investigate the global regulations that this putative ECH undertakes. However, despite a large number of statistically significant targets, few were strongly regulated by CbsA (**Figure 4.16**). In addition, functional classification of the targets shows an important number of unknown proteins (**Figure 4.17, Figure 4.18**). In summary, the analysis did not shed light onto new pathways of the downstream effects of CbsA expression, although it showed that this protein might be an important regulator having global effects in *P. aeruginosa* (**Figure 4.17, Figure 4.18**). Investigation then shifted to already known CbsA targets, aiming to deepen previous analyses.

One such result showed that CbsA controls the secretion of total rhamnolipids by the use of the orcinol assay. PASC315 shows an increase of total rhamnolipid production, and PASC315 with IPTG presents a decrease in these surfactants, as compared with the wild-type control [294]. During this thesis, the effect of CbsA in rhamnolipids was further investigated, proving that both mono- and di-rhamnolipids are highly repressed in PASC315 IPTG, both in liquid cultures and in plates (**Figure 4.22, Figure 4.23**). No effect was observed in PASC315 as opposed to the analysis performed previously, probably due to the low sensitivity of TLC plates.

Rhamnolipid defect in PASC315 IPTG partially explains the reduction of swarming motility. However, other elements are affected with the overexpression of CbsA such as flagella and pili, as seen by the attenuation of swimming and twitching motilities under the same conditions (**Figure 4.21**).

Attenuation of swarming, together with an increase in biofilm formation, are representative phenotypes associated with the Rsm/Gac system [80]. In fact, CbsA was shown to activate the expression of RsmY and RsmZ; while RsmA negatively regulates CbsA levels [294]. The involvement of CbsA in biofilm formation was further validated in this thesis, where the effect of CbsA mutation

(in PASC315 without IPTG) is also visible (**Figure 4.25**). This inverse regulation of motility and biofilm also fits with a reduced production of CDA in PASC315 IPTG (see **4.3.2**), however direct regulation of CDA by CbsA has not been proven conclusively to date.

Regarding protease production, results are more complex. A defect in CDA production could result in the reduction of proteases, given the positive regulation of DSF-T reported in the literature [346]. Indeed, results showed that LasA and LasB are attenuated by the overexpression of CbsA (**Figure 4.24**). Results of the AprA assay are not statistically significant but show the same tendency. In contrast, protease IV levels are increased in PASC315 IPTG (**Figure 4.24, D**). The regulation of secreted proteases is highly complex in *P. aeruginosa* which makes it difficult to predict whether the results obtained are consequence of a reduction in CDA levels. The *las* QS system controls all four proteases (LasA, LasB, AprA and PrpL) [28, 195]. Nonetheless, in a closer look these proteases are subjected to different regulations. First, LasA, LasB and AprA are metalloproteases, who depend on zinc to be functionally active, whereas protease IV is a serine protease [317]. It is possible that zinc is less available in PASC315 IPTG; therefore affecting the activity of the metalloproteases. On a different note, protease IV is regulated by PvdS, a sigma factor controlling, amongst others, pyoverdine production [199]. It is possible that CDA production, regulation by CbsA, and other elements such as sigma factors or metal availability result in these mixed results regarding protease production.

4.3.4 Link between enoyl-CoA hydratases and CDA

Both PA0744 and PA0745 have experimentally been linked to the secretion of CDA by *P. aeruginosa* [294, 380]. Indeed, both proteins are homologous to ECH, which in other bacteria regulate the synthesis of DSF-T [244]. CbsA is also a predicted ECH, but presents opposite effects to PA0744 and PA0745, as the overexpression of CbsA results in attenuation of motility and hyperbiofilm formation (**Figure 4.21, Figure 4.25**), so it could presumably be linked to the degradation or catabolism of CDA.

In spite of this, *P. aeruginosa* PAO1 strains expressing different combinations of the ECH and in the presence of CDA (10 µM for biofilm assays, and 100 µM for swarming and pyocyanin) did not restore the phenotypes to wild-type levels (**Figure 4.14, Figure 4.15, Figure 4.26**).

Strikingly, biofilm formation in a PA0745 mutant could be restored by exogenously added CDA in a different study [380]. This research was performed in PA14, in which the production of polysaccharides is markedly different than in PAO1 [105] which could give rise to different results. However, the effects of CDA in UCBPP-PA14 were investigated in **Chapter 3**, where this strain did not show biofilm inhibition in presence of CDA. The discrepancies here could be a result of different experimental procedures, or to the presence of genetic mutations in the strains used.

The addition of DSF-T molecules in μM levels was enough to restore protease production, aberrant biofilm formation and swimming in *S. maltophilia* [246]. However, 118 μM were required to restore *fecA* expression [343]. Therefore, DSF-T seem to present different affinities depending on the target. It is possible that, under the experimental conditions used, CDA can only restore the phenotypes of ECH mutants under a narrow range of concentrations, and that higher or lower amounts have different effects in PAO1 cells that do not allow *P. aeruginosa* to behave as a wild-type.

Regarding swarming assays, it is also possible that CDA is not available to the cells from agar plates, either due to poor solubility or to chemical modifications encountered during the incubation times. This is not likely, as similar experiments show an effect on the addition of other DSF-T, suggesting that the chemically similar CDA is available to *P. aeruginosa* in motility assays (see **Chapter 3, section 3.1.3.2** and [355, 357]).

It is interesting to point out that, although DSF-T networks are similar in terms of the phenotypes that they control, the strategies of regulation differ; such as the sensing and transduction mechanism employed by *Burkholderia sp.* as compared to the one used in xanthomonads. These convergent strategies both result in the regulation of c-di-GMP levels, but this is accomplished with the use of different strategies (**Figure 4.3**). *P. aeruginosa* does not present clear homologues of DSF-T synthases of other organisms (**Table 4.1**) or sensor mechanisms (**Table 4.5, Table 4.6**). Based on the results of this thesis, a link between PA0744, PA0745 or CbsA and CDA metabolism has not been established; and it seems entirely possible that *P. aeruginosa* might have convergent metabolic routes for the synthesis and degradation of DSF-T molecules, using strategies that employ enzymes unrelated to RpfF.

One such strategy is found in *X. fastidiosa.* The phenotypes of *rpfF* mutants of *X. fastidiosa* are not restored by the addition of DSF, which suggests that *rpfF*

has a role in signal transduction. This hypothesis was validated by reconstructing the DSF-T regulation of *X. fastidiosa* in a *rpfFC* mutant of *X. campestris*, and showing that the expression of *rpfF* of *X. fastidiosa* was necessary, alongside *rpfGC* in order to respond to exogenous DSF-T [254]. It is possible that the case of *P. aeruginosa* is similar to this, and that the Δ0745 mutants lose the ability to respond to CDA as well as to produce this signal molecule, under these experimental conditions.

4.4 Conclusion and future directions

Bioinformatic analysis was first used to deepen the understanding of CDA regulatory mechanisms in *P. aeruginosa.* The versatility of *P. aeruginosa*, which contains 15 possible ECH homologues and multiple candidates for sensor proteins, makes it difficult to detect lead regulators of CDA. Despite the high number of candidates, this bacterium does not present clear homologues to either RpfF from *Xcc* or from *B. cenocepacia*; or to RpfC or RpfR. This led us to speculate that *P. aeruginosa* might present an altogether different strategy of CDA synthesis.

The second path that was followed during this chapter was to investigate the functions of PA0744, PA0745 and CbsA, 3 proteins previously linked to the regulation of CDA. Phenotypical assays with ECH mutants show a similar pattern to other species: ECH mutants are affected in motility, biofilm formation and protease production; which raises the question of whether these are really regulating CDA levels, although by different means than in X*anthomonas* or *Burkholderia spp.*

Results showed that PA0744 and PA0745 interact, and are possibly part of the same operon. Expression studies such as qRT-PCR or protein purification would further validate this, alongside isothermal titration calorimetry (ITC) or band shift assays to prove the binding of these two proteins. All 3 ECH homologues participate in global regulatory mechanisms and affect biofilm formation and swarming motility; though the effects of CbsA are opposed to those of PA0744-PA0745. Of special interest for future work is the fact that key phenotypes are involved in Rsm/Gac system as well as in DSF-T. Further investigation could show if these are two systems that intertwine under specific conditions, or if there is a hierarchical relation between them. One of the hypotheses for the lack of phenotypical effects in PAO1 cultures spiked with CDA was that the endogenous production of this fatty acid might hide the effects of exogenously added CDA (see **Chapter 3**). Therefore, the use of potentially CDA null mutants would help investigate CDA targets. However, experiments performed in the presence of CDA in this chapter do not show any effects, either because of the lack of sensing in the ECH mutants, the conditions tested, or yet unknown mechanisms that prevent this from happening.

Regarding ways to study CDA regulation, DSF-T systems of cell-cell communication have not been reported yet in species highly related to *P. aeruginosa*. Therefore, the use of a heterologous system for studying CDA

regulation is not straightforward. Other strategies involve the use of a mutant library to study any genes that respond to exogenous CDA, for example by using promoterless *luxCDABE* constructions. Other omics approaches can also be useful, such as metabolomics to evaluate how the addition of CDA might change the carbon flux.

5 2-TRIDECANONE AS A SIGNALLING MOLECULE IN *P. AERUGINOSA* PAO1

5.1 Introduction

The 2-tridecanone (2TDC), also known as undecyl methyl ketone, is a molecule with pleiotropic effects produced by a wide range of organisms. It mediates defence or competition mechanisms, but the full extent of functions that this molecule undertakes is yet to be investigated. Here, it was hypothesised that 2TDC can act as a signal, altering group behaviour in *Pseudomonas aeruginosa,* in a similar way that it does in other bacterial species [284].

5.1.1 2TDC synthesis and function

Multiple reports have found 2TDC production in the environment. The role of this molecule seems to be regulatory, as it dictates behavioural changes either in the species producing them, or more importantly, in inter-species communication.

2TDC has been detected in various plant structures (twigs, leaves, roots, bark and fruits) and in a variety of plant species (from wild tomato to various rutaceae) [433-435]. The main role of 2TDC in plants is to act as a defence mechanism, as it has potent cidal effects in arthropods, including insects and arachnids [281, 436, 437]

This methyl ketone is also produced by animal glands, and the impact here is somewhat more complex: *Nylanderia fulva*, commonly known as the tawny crazy ant, produces 2TDC which synergises with the activity of formic acid to displace the colonisation of another ant [438, 439]. The male wasp *Philanthus crabroniformis* and the bee *Scaptotrigona depilis* secrete 2TDC in their mandibular glands, though the role of 2TDC here remains to be investigated [440, 441].

The 2TDC molecule is toxic to arthropods, but also signals as a repellent. The genus *Drosophila* produces 2TDC which contributes to the aggregation pheromone blend. However, the effects of 2TDC differ with the species, as in *D. buzzatii* 2TDC inhibits the aggregation behaviour, whereas in *D. repleta* and *D. hydei*, it highly increases aggregation [442, 443]. 2TDC is a promising repellent for mosquitoes [444] and acari [433, 445].

Production of 2TDC in animals is not restricted to arthropods. This ketone is also produced by the *Junco hyemalis* bird, where its levels increase during long days,

correlating with mating periods [446]; and in the interdigital glands of a deer [280].

In addition to being produced by plants, arthropods and animals, 2TDC is a volatile compound secreted by various Gram-positive and Gram-negative bacteria, including species of the genera *Burkholderia, Bacillus, Pseudomonas* (although not *P. aeruginosa*), *Serratia* and even *E. coli* [447, 448].

5.1.2 *P. aeruginosa* and environments with 2TDC

P. aeruginosa is best known for its role in human pathogenesis, but can also colonise plant tissues and a variety of animals. *P. aeruginosa* infects the leaves and roots of many different plant species, notably of *Arabidopsis thaliana* [37, 449]. In fact, this bacterium is found, together with many other potential human pathogens, in the rhizosphere of multiple plant species [34]. *P. aeruginosa* can surely be exposed to the secretion of 2TDC from roots and leaves, and also from other bacteria, during the colonisation of these niches.

Regarding the exposure of *P. aeruginosa* to 2TDC produced by animals, a number of infection models have been used for this bacterium, including rat and mouse, but also organisms in which 2TDC production has been observed, such as *Drosophila* [11]. As *P. aeruginosa* is present in soil and plant leaves, it is also likely that bees and other animals would be exposed to both *P. aeruginosa* and 2TDC.

5.1.3 2TDC in bacteria

Recent research in the group of Dr. Soto at EEC (Granada) with *S. meliloti* shows that a *fadD*- mutant of this bacterium accumulates 2TDC although this module can also be detected in wild-type isolates but at lower levels (personal communication). The *fadD*- mutant shows increased surface motility [283], thus the effects of 2TDC were investigated in *S. meliloti* confirming the increase in swarming caused by this molecule. Swimming was not affected, nor any gene related to flagellar function. Moreover, a much higher number of genes were differentially regulated when 2TDC was added in gas phase and cells were grown in a solid surface, as compared to the 2TDC being added in a liquid culture (88 genes in gas as opposed to 15 genes in liquid). This result shows that 2TDC exerts a modulatory role mainly in gas phase and that the mechanism of modulation might require surface growth [450].

2TDC has shown to impact swarming motility in various bacteria: swarming is enhanced in *P. syringae* and *S. meliloti* with the addition of this molecule, while it is completely abolished in *S. enterica* sv. *typhimurium.* 2TDC also shows reduced biofilm formation in *P. syringae*, as shown in borosilicate tubes stained with crystal violet [284].

Further research in Granada shows the protective role of 2TDC against *Pseudomonas syringae* pv. *tomato*, as tomato plants present less lesions and less cfu/mL when soil or leaves are treated with 2TDC. This ketone also delays and reduces the nodulation of alfalfa by *S. meliloti* [284].

Therefore, it seems that 2TDC alters the multi-cellular behaviour of Gram-negative bacteria; although the nature of this interaction is complex and varies among species. The specific communication network between plants, animals and bacteria mediated through 2TDC also remains to be elucidated, as well as the potential of 2TDC as an anti-bacterial agent.

5.1.4 Aims of the chapter

The general aim of this chapter is to investigate the effects of 2TDC in the biology of PAO1-L and in signalling networks of this organism. More specifically, this work intends to:

- Determine the effect of 2TDC in *P. aeruginosa*
- Unravel the mechanisms underlying the observed phenotypes
- Compare the impact of 2TDC in *P. aeruginosa* with those seen in other bacterial species

5.2 Results

5.2.1 Impact of 2TDC on growth of *P. aeruginosa*

Previous reports have found that 2TDC affects community behaviours in bacteria, and does not show toxicity. With a view to evaluate if this was true for *P. aeruginosa*, the effect of 2TDC on bacterial growth was assessed using the same growth conditions as for the rest of the assays. EtOH was used as the solvent control.

In this thesis, the impact of 2TDC was assessed both in a volatile phase (when added onto the lid of Petri dishes) and in a liquid phase (when added to liquid cultures). Therefore, the impact of this molecule on bacterial growth under both conditions was first assessed. To study the effect of 2TDC in liquid cultures, growth curves were carried measuring OD, whereas to investigate the impact of this molecule when added to the lids of Petri dishes, cells were retrieved from the agar of the plate and both OD and cfu/mL were determined.

Addition of 2TDC to liquid cultures

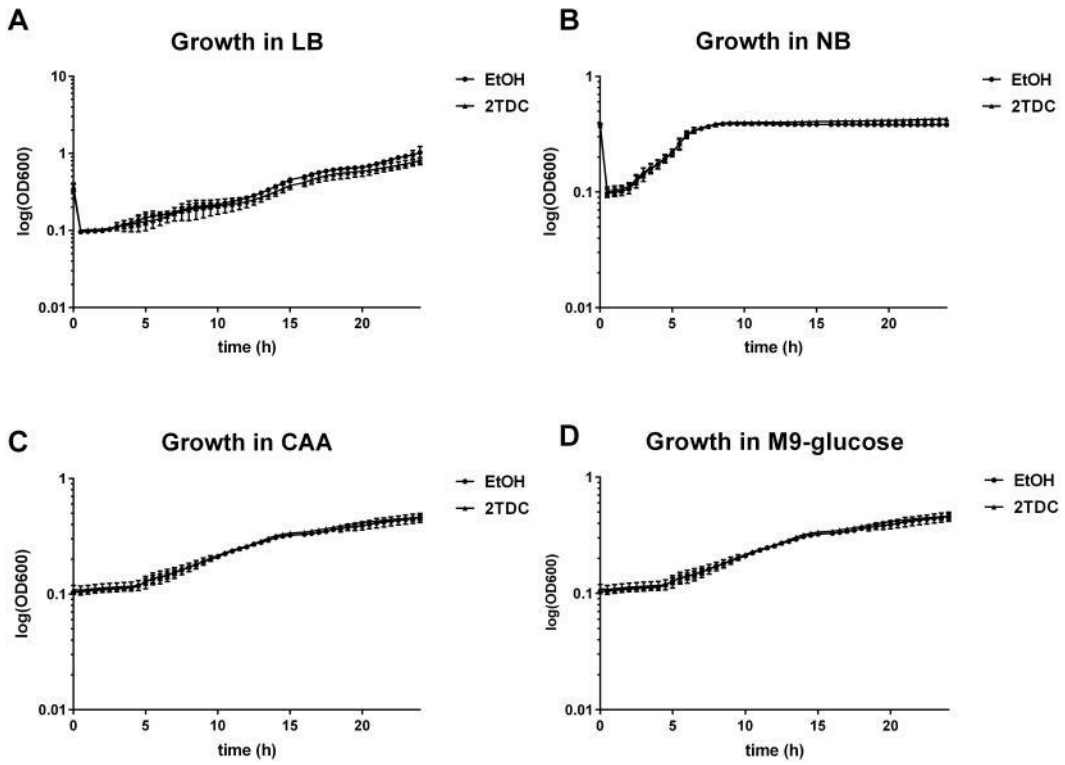


Figure 5.1. Impact of 2TDC on *P. aeruginosa* growth in liquid cultures. Cultures of PAO1-L were incubated at 37 ºC for 24 h in 96-well plates, which were covered with lids to prevent the evaporation of 2TDC. 2TDC was added to a final concentration of 100 µM, and EtOH was used as a solvent control. Results represent the average of three independent replicates. Error bars represent one standard deviation of the means. Results show that 2TDC does not affect growth in liquid, under the tested conditions.

Addition of 2TDC to plate lids

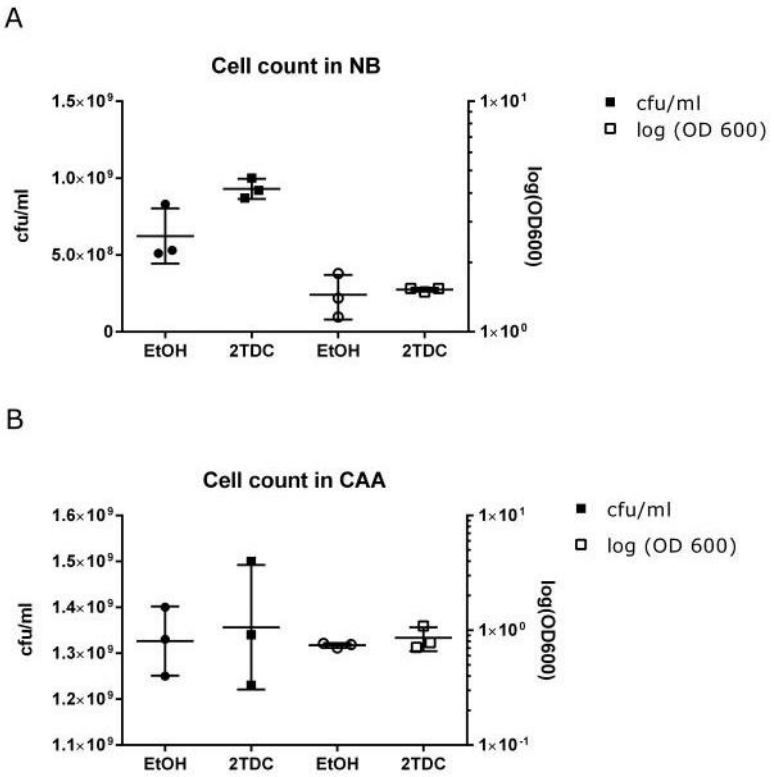


Figure 5.2. Effect of 2TDC on PAO1-L growth in NB (A) and CAA (B). Cells were spread in 0.5 % agar plates, containing 20 µL of a 100 mM stock solution of 2TDC as a volatile compound. Plates were subsequently incubated at 37 ºC for 16 h, cells were recovered from the agar plates and the OD_{600} and cfu/mL were determined. Error bars represent one standard deviation from independent replicates. T-tests were used to assess significance. The addition of 2TDC to plate lids does not affect growth in NB or CAA.

Results do not show significant differences in growth caused by 2TDC, in liquid cultures or during surface growth (**Figure 5.1, Figure 5.2**). This is consistent with reports performed in other bacterial species [284].

5.2.2 Impact of 2TDC on motility in *P. aeruginosa*

The 2TDC molecule has been shown to alter surface motility in a variety of microorganisms, including the plant symbiont *S. meliloti*, where 2TDC increases motility; and the pathogen *Salmonella enterica*, where surface motility is abolished at high concentrations of 2TDC. In all cases swimming was not affected, implying that flagellar function is retained at wild-type levels in the presence of the methyl ketone. To compare the effects of 2TDC in *P. aeruginosa* and other bacteria and evaluate the impact of 2TDC in *P. aeruginosa* motility, swimming, swarming and twitching motilities were next assessed.

5.2.2.1 Swimming

First of all, flagellar activity was checked by swimming assays. Swimming medium consisted of NB supplemented with 0.3 % Bacto Agar (BD). Results show no changes caused by 2TDC when added onto the lid of the plates (**Figure 5.3**).

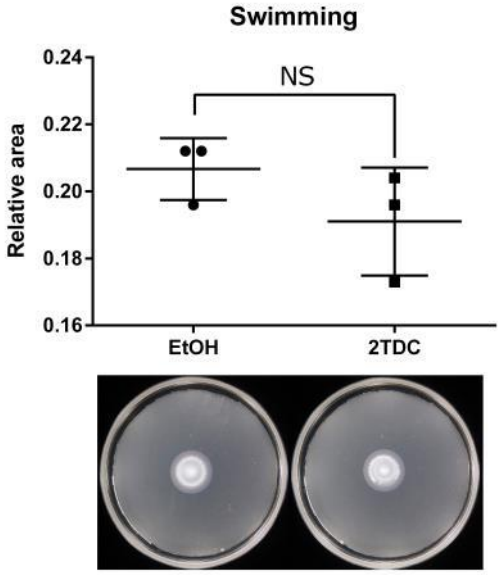
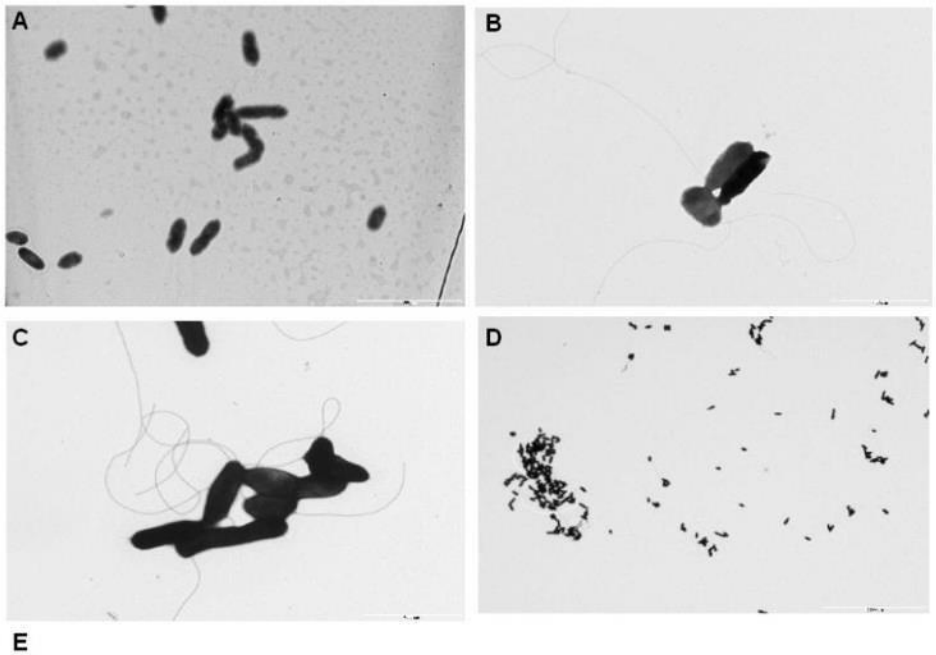


Figure 5.3. Impact of 2TDC on PAO1-L swimming. The lids of swimming plates were supplemented with EtOH **(left)** or 20 µL of a 100 mM stock of 2TDC **(right)** and plates were incubated for 7 h at 37 ºC. This figure shows representative pictures of the swimming results. A t-test was used to compare the area of swimming between conditions; p-value=0.21.

The same assay was repeated in plates containing 0.3 % Bacto Agar (BD), 0.1 % tryptone and 0.5 % NaCl, which did not show any differences either (data not shown). These results are consistent with studies with other bacteria in which 2TDC did not affect swimming, and suggest that flagellar function is not a target of this ketone.

5.2.2.2 Morphology of *P. aeruginosa*

To verify that 2TDC does not affect the cell dimensions or morphology, *P. aeruginosa* PAO1-L cultures were grown in plates under swarming conditions, recovered and visualised with transmission electron microscopy (TEM) (**Figure 5.4**). This figure shows no significant differences between treated and untreated cells.



E

Length of EtOH cells (n=32)	Length of 2TDC cells (n=20)
1.48 µm ± 0.27	1.30 µm ± 0.20

Figure 5.4. Visualisation of PAO1-L swarmer cells with transmission electron microscopy (TEM), in the presence and absence of 2TDC. PAO1-L cells were recovered from swarming plates, fixed with glutaraldehyde in cacodylate buffer, and stained with uranyl acetate, then visualised under a Tecnai G2 12 Biotwin (FEI). **A** and **B,** cells incubated with the EtOH control, magnification x4200 and x9900; respectively. **C** and **D,** cells incubated with 20 µL of a 100 mM stock of 2TDC, as a volatile, and visualised under x9900 and x1050 magnification, respectively. Under these conditions, cells generally presented one flagellum. The average length of the cells is shown in **E**, as measured from all the available images with GIMP v. 2.8.10.

5.2.2.3 Swarming

While swimming is an independent behaviour in which cells move propelled by their flagella, swarming cells coordinate with one another forming highly structured, fractal-like patterns in *P. aeruginosa*. The effect of 2TDC in swarming motility was assessed with a view to understand the impact of this molecule in cell-to-cell communication.

A range of concentrations of 2TDC was used showing a reduction of swarming in a dose-dependent manner. Though, with enough time after inoculation, even the highest concentration tested showed moderate surface translocation, as opposed to *S. enterica* in which swarming could be completely abolished.

The assay was also carried out using a stock of 1 M 2TDC, but at this concentration the molecule seems to crystallise on the surface of the lid and swarming was increased as compared to the 100 mM stock, suggesting that 2TDC was not available to the cells in such high concentration.

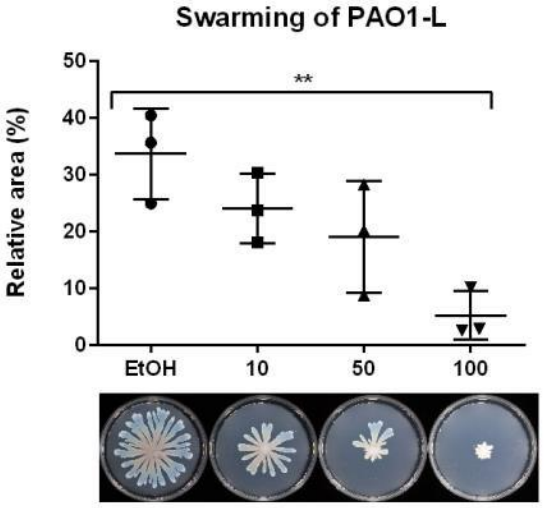


Figure 5.5. Swarming of PAO1-L in presence of various concentrations of 2TDC. Swarming plates were inoculated with PAO1-L in the presence of increasing concentrations of 2TDC and incubated at 37 ºC for 16 h. From left to right, 20 µL of the following stocks were added to the lid of the plates: EtOH, 2TDC 10 mM, 50 mM, 100 mM. Error bars represent one standard deviation from independent triplicates. A one-way ANOVA was used to assess statistical significance; **, p-value=0.0091.

Results show that 2TDC reduces swarming in PAO1-L in NB (**Figure 5.5**). This effect in swarming motility is of special interest as no differences were observed with swimming motility, suggesting that the mechanisms involved in swarming inhibition by 2TDC do not purely involve flagellar activity and are potentially restricted to population behaviours.

5.2.2.4 Twitching

Next, twitching motility was assessed. Twitching is another form of surface translocation involving population behaviour, in which *P. aeruginosa* cells use T4aP to produce cycles of extension and retraction, resulting in a worm-like movement. In this assay, cells move at the bottom of Petri dishes, retrieving nutrients from the solid medium above them.

Results show that, similarly to swarming, 2TDC reduces twitching in a dose-dependent manner (**Figure 5.6**). At the highest concentrations there seems to be a reduction in the effect, which could be due to a lower availability of the methyl ketone in the gas phase.

Twitching was affected to a lesser extent than swarming; though results were highly reproducible, resulting in statistical significance.

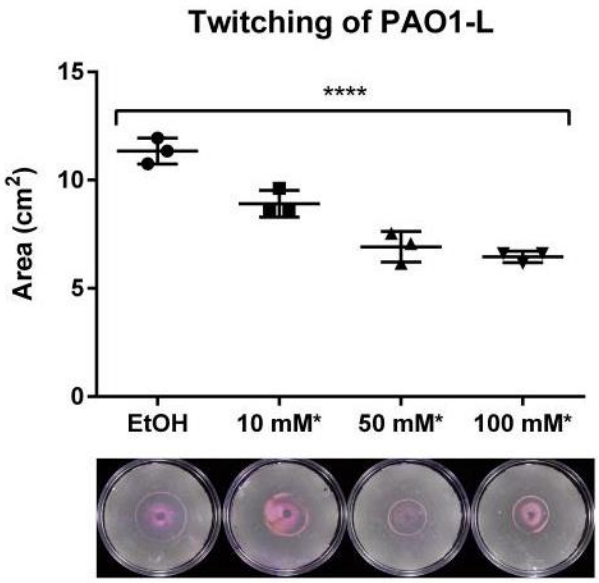


Figure 5.6. Impact of 2TDC on PAO1-L twitching in LB plates. Overnight PAO1-L cultures were inoculated in plates containing 1 % agar, 1 % triptone, 0.5 % yeast extract and 1 % NaCl; and incubated at 37 ºC for 48 h. From left to right, 20 µL of the following stock solutions were added to the lid of the plates: EtOH; 2TDC 10 mM, 50 mM and 100 mM. The agar was removed from the plates and stained with 1 % crystal violet. Error bars represent one standard deviation from independent replicates. A one-way ANOVA was used to assess statistical significance; ****, p-value<0.0001. 2TDC reduces twitching motility in a dose-dependent manner.

The association between T4aP and chemotactic responses has been shown elsewhere [74, 87]. Preliminary chemotactic assays were performed with 2TDC which showed no changes caused by the presence of 2TDC in the agar (see **Appendix, Figure 7.11**). However, due to time restrictions, chemotaxis has not been addressed in detail here. In addition, more work needs to be done to refine the methodology required to study the response to 2TDC in the gas phase.

5.2.3 Impact of 2TDC on biofilms in *P. aeruginosa*

Another population behaviour used by *P. aeruginosa* is biofilm formation. One can classify two broad processes by which sessile cells become planktonic. Biofilm inhibition relates to the inability of motile cells to become sessile, either due to regulatory pathways that disfavour this phenotype or because of physico-chemical properties of the environment which do not allow for bacterial adherence. The other process is biofilm dispersion, when cells detach from the biofilm. Biofilm dispersion is sometimes caused by the presence of molecules either exogenously added or produced by established biofilms. This process generally requires regulatory changes in cells, such as the activation of motility genes or the repression of exopolysaccharide production. Biofilm dispersion is more troublesome to achieve because of the low diffusion rate of secreted compounds through the biofilm matrix and the differentiation that some of these cells have undergone to adapt to a sessile state.

To study the impact of 2TDC in biofilm inhibition, PAO1-L was tagged with GFP, resulting in the PADP44 strain. Two biofilm models were employed: static biofilms grown in chamber slides, and controlled flow biofilms grown in the Bioflux system.

For all the biofilm assays, 2TDC was added at a final concentration of 100 μM, and the same volume of EtOH was added for the control biofilms.

5.2.3.1 Inhibition of biofilm formation

Addition of 2TDC to liquid cultures

Chamber slides with 8-wells were used to examine static biofilm formation in the presence of 2TDC. In order to keep consistent with the growth conditions, both LB and NB were used for this experiment. The chamber slides have lids that prevent the volatilisation of 2TDC. This compound was spiked into liquid cultures normalised to OD_{600}=0.05, to a final concentration of 100 μM. LB cultures were incubated for 15 h, whereas biofilms in NB required at least 48 h of growth. In this case, the medium containing additional compounds (2TDC or the EtOH control) was replaced at 24 h post-inoculation to minimise possible degradation or oxidation of compounds as well as nutrient limitation.

The Bioflux system works as a flow cell. However, the volume of the wells only allows flow for approximately 14.5 h, which limits the time of the experiment. Biofilms were grown in LB but not in NB, as this assay time was too limited to have fully grown biofilms.

Results show that 2TDC inhibits static biofilm development, both in LB and NB (**Figure 5.7**). Surprisingly, biofilms in LB formed under flow did not show any effect caused by 2TDC. The conditions used for both experiments were almost identical except for the presence of flow and the growth state of the cells. This suggests that the inhibition observed depends on very particular growth conditions which were only met under static biofilm growth. Given these contradictory results, biofilm development under 2TDC treatment was further investigated.

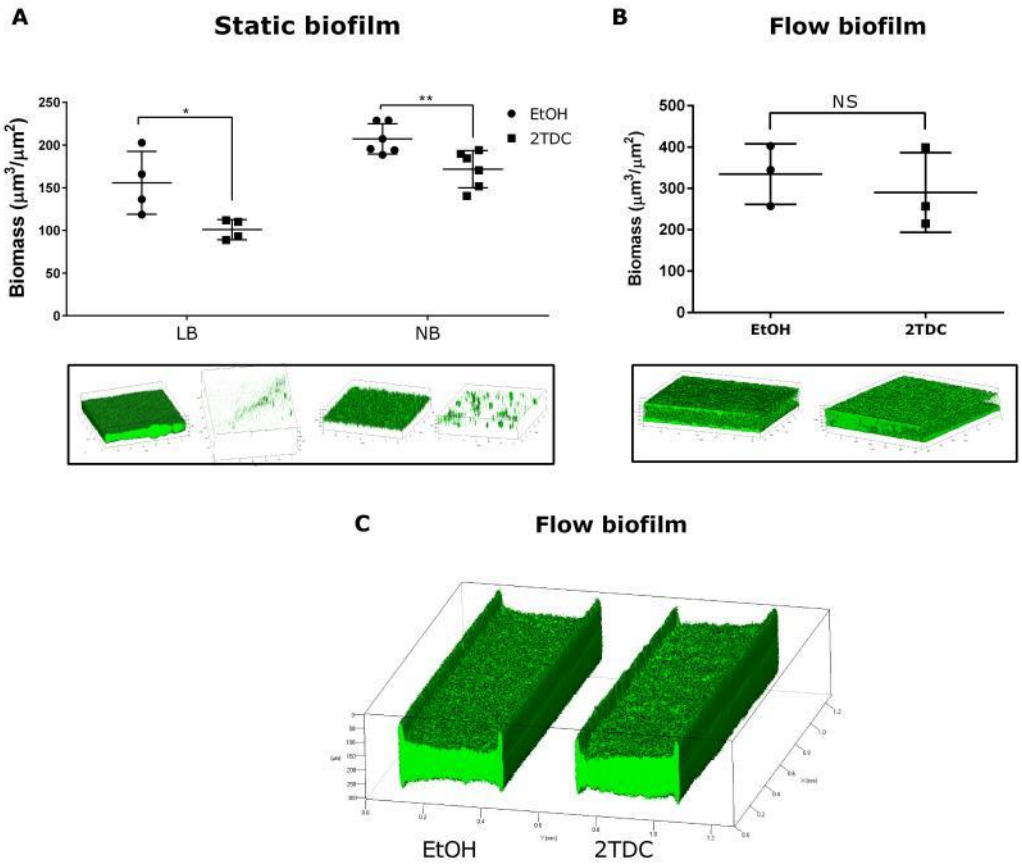


Figure 5.7. Effect of 2TDC on biofilm development under static conditions (A) and controlled flow conditions (B), and detail of growth in flow conditions (C). 100 µM of 2TDC or solvent control EtOH were added to *P. aeruginosa* PAO1-L cells tagged with GFP (PADP44). Biofilms were quantified using Image J and the plugin Comstat2. **A,** Biofilms were grown statically in LB for 15 h and in NB for 48 h. Error bars represent one standard deviation of the means from independent replicates. T-tests were used to assess statistical significance. *, p-value=0.029; **, p-value=0.0055. **B,** Biofilms were grown under 0.5 dyn/cm^2 flow for 14 h. **C,** The image shows a representative pair of EtOH and 2TDC biofilms, at a 5x magnification, which allows for the visualisation of the whole capillary width.

Addition of 2TDC to cells on solid media: colony morphotypes

A distinct biofilm assay involves the formation of wrinkly or smooth colonies by *P. aeruginosa* when grown on rich, solid medium. This assay was chosen as it is complementary to the ones mentioned above, but also because it allows the addition of 2TDC onto the lid of the plates; therefore examining the effects of this molecule when it is available for the cells exclusively from the gas phase.

Colony biofilms were grown in Petri dishes with LB agar containing Coomassie blue and Congo red. Under these conditions, PA14 grows as wrinkly colonies, whereas PAO1 presents a smooth phenotype. The wrinkly/smooth phenotype depends on the redox state of the cells, on the levels of c-di-GMP and on the expression of the Pel exopolysaccharide.

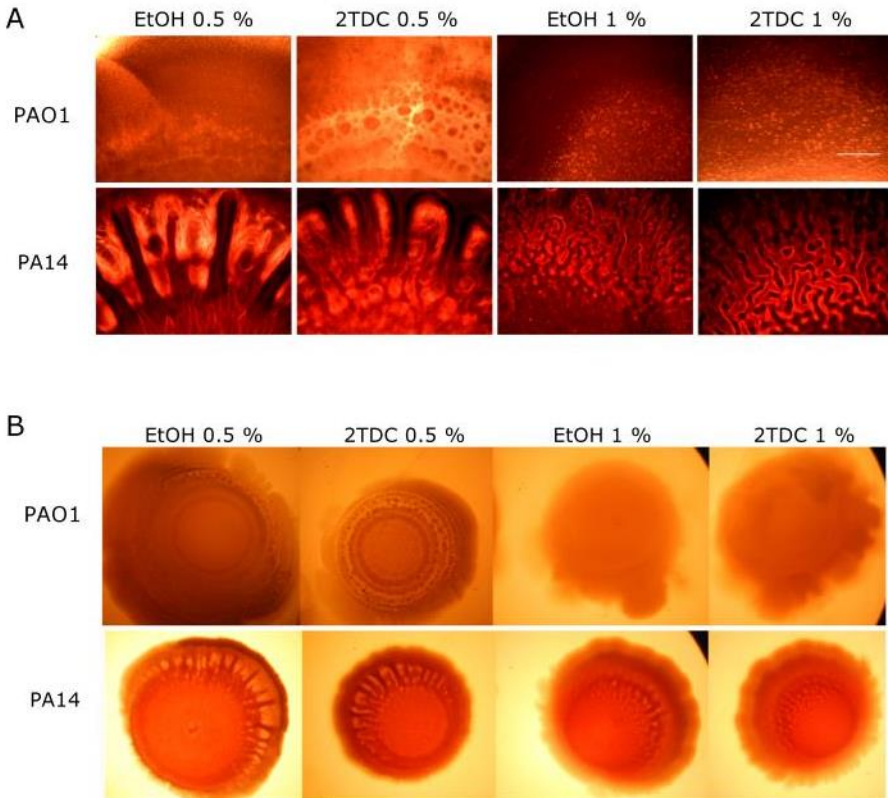


Figure 5.8. Effect of 2TDC on colony morphotypes. Colony morphologies of PAO1-L and UCBPP-PA14 were grown under different agar concentrations (0.5 % and 1 %) in the presence of Congo red and Coomassie blue, with and without 20 µL of a 2TDC 100 mM stock added onto the lid of the Petri dishes. Images were taken by an EVOS optical microscope with a 10x objective **(A)** or a binocular **(B)** and show that 2TDC does not affect the morphotype. The scale bar represents 1 mm.

Results show no differences in colony morphology caused by the exogenous addition of 2TDC (**Figure 5.8**). According to the available literature, 2TDC does not have an impact on the redox state of PA14 cells or impairs the oxygenation of colonies [122]. Additionally, Pel polysaccharide is known to bind to Congo red [109]. No differences in red coloration were observed in biofilms treated with 2TDC (**Figure 5.8**), which suggests that Pel is not differentially expressed with the addition of this molecule.

5.2.3.2 Disruption of mature biofilms

Next, the disruption of established biofilms was investigated using the chamber slides biofilm model. This model permits easy removal and replacement of liquid medium and the visualisation of the biofilm throughout the assay. However, biofilms grown under these conditions can easily be disrupted by aspiration and hence are unable to withstand multiple rounds of pipetting.

Briefly, biofilms were grown overnight in LB or for 2 days in NB. The supernatant was removed and biofilms were visualised by confocal microscopy, resulting in

the imaging before treatment. Then, media containing 2TDC or EtOH was added, and the biofilms were incubated for further 4 h or 8 h. Finally, the supernatant was removed again and biofilms were visualised, giving the data post-treatment. Gain and laser intensity were maintained constant within the same condition.

Biofilms were often found partially disrupted as a result of handling and pipetting as can be observed in **Figure 5.11** (panels **A** and **B**). Under these growth conditions, biofilms of *P. aeruginosa* grow in lawns and show very little heterogeneity. However, after two rounds of pipetting, biofilms often showed high roughness, and the presence of folded films was evident, as seen in **Figure 5.11** (panels **B** and **D**). Consequently, biofilm disruption was not quantified and the analysis was qualitative.

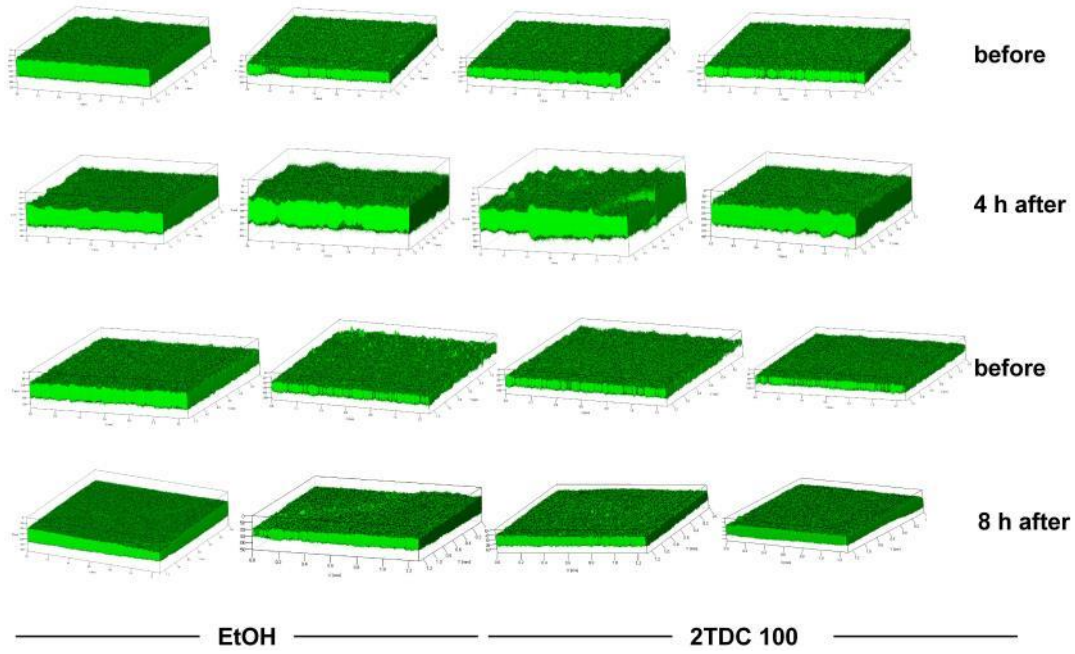


Figure 5.9. Effect of 2TDC on biofilm disruption using the chamber slides in LB. Biofilms of PAO1-L tagged with GFP (PADP44) were visualised pre-treatment and either 4 h or 8 h post-treatment with either 2TDC 100 μM or EtOH as a solvent control. The gain was adjusted to allow for good visualisation and maintained constant within the same condition (i. e. pre-treatment). No effect of 2TDC was observed compared to the control with EtOH.

The same procedure was repeated in NB. In this case, biofilms were less robust, so the following pictures show a certain disruption (**Figure 5.10**). However, this was found with both EtOH and 2TDC and hence most likely a result of shearing forces during pipetting. Detailed pictures of disrupted areas can be found in **Figure 5.11** (panels **C** and **D**). No effect of the 2TDC was observed in established biofilms, in LB (**Figure 5.9**) or NB (**Figure 5.10**).

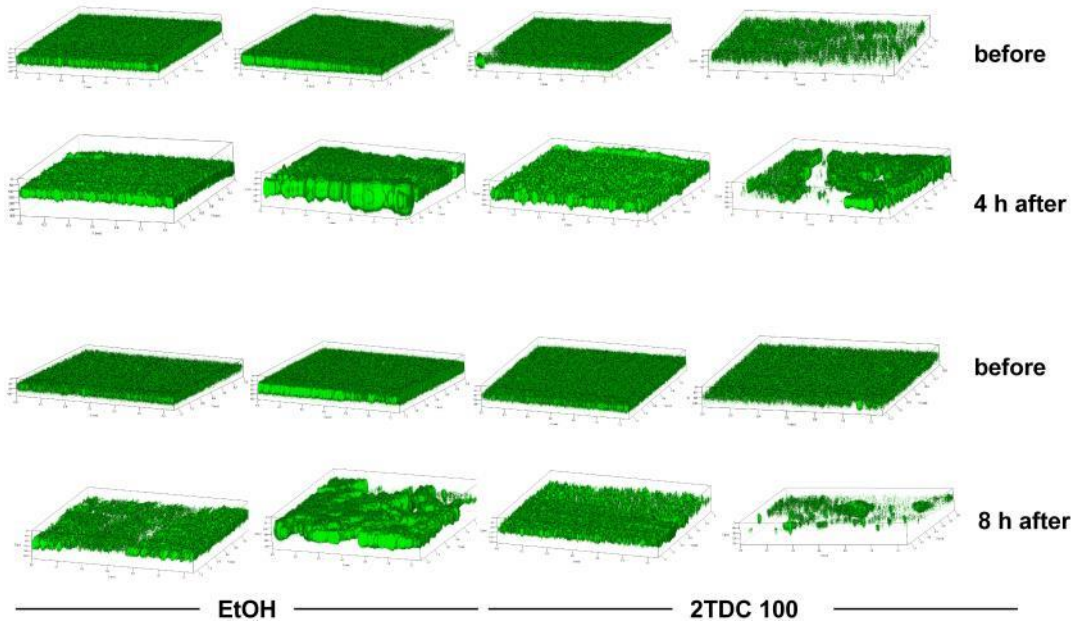


Figure 5.10. Effect of 2TDC on biofilm disruption using the chamber slides in NB. Biofilms of PAO1-L tagged with GFP (PADP44) were visualised pre-treatment (before) and either 4 h or 8 h post-treatment with 2TDC 100 μM or the solvent control EtOH. The gain was adjusted to allow for good visualisation and maintained constant within the same condition (i. e. pre-treatment). Pictures show disruption due to shearing forces, but no effect of 2TDC.

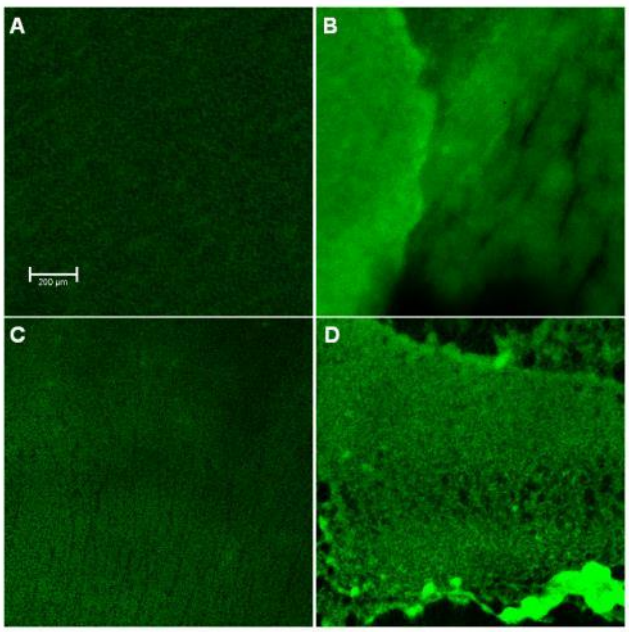


Figure 5.11. Evidence of physical disruption as a result of pipetting in chamber biofilms. This figure shows representative images of disrupted areas in biofilms due to multiple rounds of pipetting. Images were taken at 5x magnification with a Zeiss LSM 700 CLSM. The medium was removed before pre-treatment imaging of biofilms grown in LB **(A)** or NB **(C)**. These same biofilms were then treated with the solvent control EtOH, and the liquid phase was removed previous to imaging. Disrupted areas of biofilms are shown, when grown in LB **(B)** LB or NB **(D)**. The scale bar represents 200 μm.

5.2.3.3 Impact of 2TDC on c-di-GMP levels

Cyclic diguanylate, or c-di-GMP, is a global regulator that controls the switch between acute and chronic infection, including phenotypes such as swarming and biofilm formation. To assess the effect of 2TDC on biofilm formation, the impact of c-di-GMP signalling was studied with the use of a vector carrying a transcriptional fusion responding to this nucleotide named pCdrA::*gfp*^{C} [299]. The *cdrA* gene codes for an adhesin that binds to Psl, promoting auto-aggregation and biofilm formation. The expression of *cdrA* is regulated by c-di-GMP [121].

As a means to explore the impact of 2TDC within biofilms, cells were grown on agar plates prior to the measurement of fluorescence. This experimental approach was chosen because i) it provides versatility for the study of various culture conditions, ii) 2TDC can be added to the lid of the plates, thus the effects of this molecule in the gas phase are studied, iii) conditions are similar to those used for swarming assays and therefore offer a good insight into the mechanism behind swarming reduction in the presence of 2TDC.

P. aeruginosa containing the transcriptional reporter was grown overnight, and cultures were spotted onto agar plates in the presence and absence of 2TDC. After an incubation time or 8 h or 16 h, cells were removed from the place, dissolved in phosphate buffer saline (PBS), and their OD and fluorescence were measured.

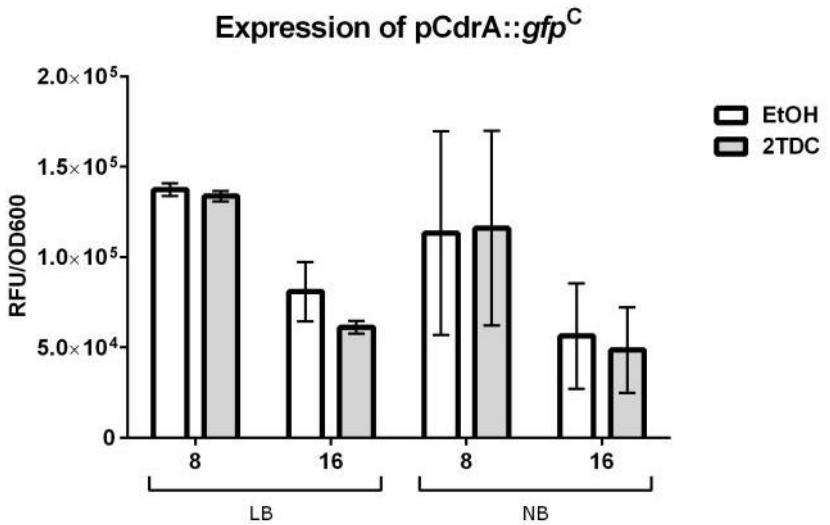


Figure 5.12. Effect of 2TDC on c-di-GMP levels using the P$_{cdrA}$-*gfp* fusion (pCdrA::*gfp*^{c}). Cells were grown on agar plates of either LB or NB and were incubated for 8 h or 16 h at 37 ºC. 2TDC or the solvent control EtOH were added to the lid of the plates prior to incubation. Results show relative fluorescent units (RFU) normalised by the OD_{600} of the samples. Error bars represent one standard deviation of the means. No effect of 2TDC on P$_{cdrA}$-*gfp* expression was observed.

Results show that the expression of *cdrA* is not affected by 2TDC, which suggests that c-di-GMP is not affected by this methyl ketone (**Figure 5.12**).

5.2.3.4 Effect of 2TDC on the expression of *pel* and *psl* genes.

Pel and Psl are two major expolysaccharides involved in the biofilm formation of *P. aeruginosa.* PAO1-L strains carrying the pSC855 and pSC856 translational fusions (for *pelA* and *pslA*, respectively) were also spotted onto agar plates and their expression was assessed with single reads in a combined fluorimeter/spectrophotometer (TECAN). A strain carrying the promoterless reporter backbone vector, pDP275, was used to normalise for the background fluorescence.

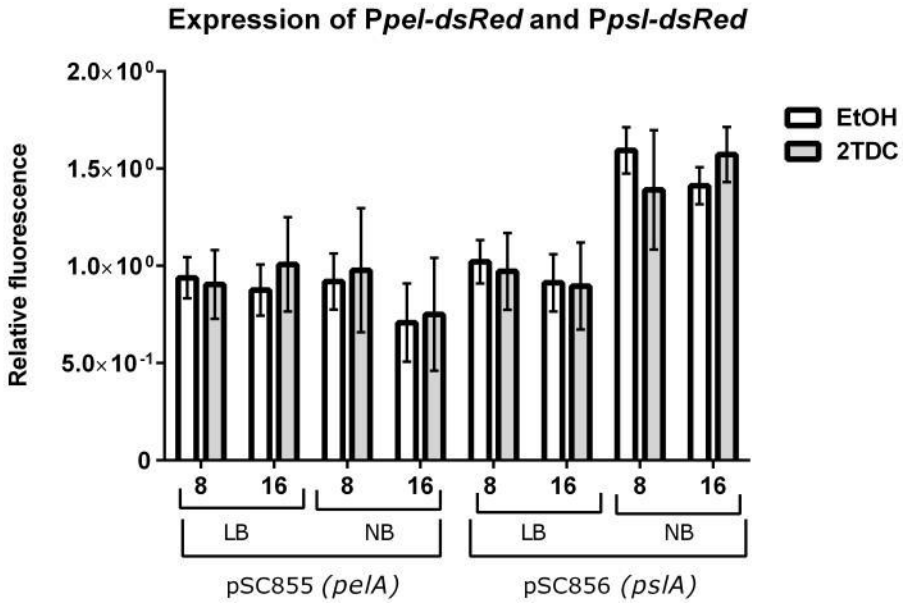


Figure 5.13. Effect of 2TDC on the expression from pSC855 (*pelA)* and pSC856 (*pslA*) translational fusions on agar plates. The pUCP18-based reporters were spotted onto agar LB or NB agar plates and incubated for 8 h or 16 h. Fluorescence was normalised by the OD_{600} and is shown relative to the fluorescence of the background fluorescence of the promoterless construction pDP275. Error bars represent one standard deviation of the means.

The results show that 2TDC does not cause a dramatic effect in the translation of *pelA* or *pslA*, under the two conditions tested (**Figure 5.13**). In line with the data obtained on the expression of *pelA*, Congo red binding did not change as seen in the colony morphotypes assay (**Figure 5.8**).

5.2.4 Impact of 2TDC on Rhamnolipids

One striking difference between swimming cells and swarming cells is that the latter depend on the production of rhamnolipids and their precursors, 3-(3-hydroxyalkanoyloxy) alkanoates (HAA) [76, 169]. Rhamnolipids have also been linked with biofilm formation, where they help maintain biofilm structure [172, 174]. Since 2TDC has a significant impact on swarming motility and potentially in biofilm formation, the effect of this molecule on rhamnolipid production was investigated.

Rhamnolipid levels were measured in both liquid cultures and agar plates. It is worth mentioning that, for the extraction from liquid, 2TDC was added to cultures prior to incubation for 16 h at 37 ºC. For the extraction from swarming plates, 20 µL of a 100 mM 2TDC stock were added to the lid of the plates, which were the same conditions used for swarming assays for consistency.

TLC analysis was used to explore the impact of 2TDC in rhamnolipid production. The detection of rhamnolipids was performed by soaking the TLC plates in an acidic solution of orcinol. One limitation of this technique is that orcinol reacts with products derived of sugar hydrolysis, and therefore this does not allow for the detection of HAAs (see **Experimental procedures, section 2.6.4**).

5.2.4.1 Impact of rhamnolipids in liquid cultures

PAO1-L cells were grown in NB supplemented with EtOH or 2TDC to a final concentration of 100 µM, for 16 h at 37 ºC with 200 rpm shaking. Supernatants were extracted and run in normal phase TLC silica plates. Under these conditions, the retention factor (Rf) of di-rhamnolipids (di-rhm) is lower than that of mono-rhamnolipids (mono-rhm). Results show no apparent differences in the rhamnolipid production in the presence and absence of 2TDC. The highest, green spot corresponds to pyocyanin (**Figure 5.14, Figure 5.15**).

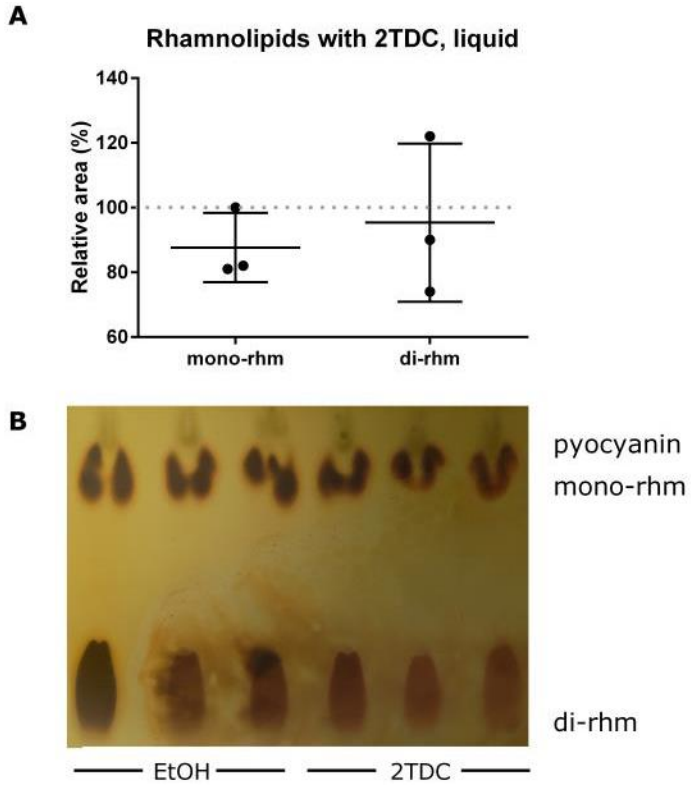


Figure 5.14. TLC analysis of rhamnolipids production from liquid cultures in the presence of 2TDC. A, the area occupied by mono- and di-rhamnolipid (mono-rhm and di-rhm, respectively) with 2TDC was determined by pixel integration analysis and plotted relative to the area of spots from EtOH cultures. Error bars show one standard deviation of the means, from independent triplicates. **B,** Picture of a TLC plate after detection of the spots with an acidic solution of orcinol. The upper spots correspond to mono-rhm, the lower spots correspond to di-rhm. No effect of 2TDC on rhamnolipid production was apparent.

The results indicate that 2TDC does not affect swarming through the modulation of rhamnolipid production, under the tested conditions (**Figure 5.14**). To gain a further insight, a possible role of 2TDC in the regulation of rhamnolipid secretion in solid medium was next investigated.

5.2.4.2 Impact of rhamnolipids on swarming plates

Research conducted in the last decade has shifted our understanding of bacterial gene regulation. One interesting idea is surface sensing, namely the idea that bacterial cells can regulate gene expression upon contact with a surface.

It was hypothesised that 2TDC may only affect *P. aeruginosa* biology upon surface growth, and therefore changes in rhamnolipid production may not be observed in cultures grown in liquid. To test this, the protocol for rhamnolipid detection was adapted to cells grown on semi-solid media. **Figure 5.15** shows that 2TDC has also no effect on rhamnolipid production on semi-solid media.

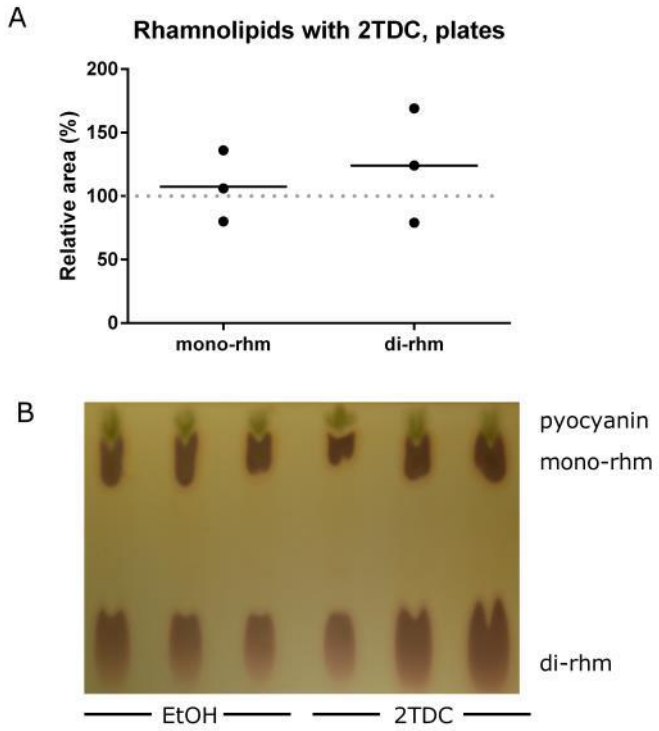


Figure 5.15. TLC analysis of rhamnolipids production from cells grown on NB agar in the presence of 2TDC. A, the area occupied by mono- and di-rhm spots was determined by pixel integration analysis. The percentage of the rhamnolipid area occupied in TLC by 2TDC treated cells is plotted relative to spots from EtOH control plates. **B,** Picture of TLC plate after detection of the spots with an acidic solution of orcinol. The upper spots correspond to mono-rhm, the lower spots correspond to di-rhm. No effect of 2TDC on rhamnolipid production was observed.

The results presented here show that neither mono- nor di- rhamnolipids are affected by 2TDC under the two conditions tested. Further research is needed to investigate the impact on HAAs, as these precursors can also modulate swarming motility but are not detected with this technique.

5.2.5 Impact of 2TDC on pyoverdine production

The addition of 2TDC to *P. aeruginosa* cultures limits the colonisation potential of this bacterium, in terms of reduced motility and, under certain conditions, biofilm formation. Pyoverdine is a siderophore produced by *P. aeruginosa* with high iron binding affinity, which allows for the colonisation of low-iron environments by this bacterium, such as the human host or plant tissues. An interesting regulation of pyoverdine is the fact that cell aggregation, mediated by polysaccharides or other factors, results in the upregulation of pyoverdine through RsmY and RsmZ [150].

It was hypothesised that the inhibition of biofilm observed in chamber slides treated with 2TDC (**Figure 5.7**) could result in the downregulation of pyoverdine due to a lower accumulation of aggregative factors. In addition, this would result in an impaired capacity for survival under low iron conditions, again resulting in

less colonisation capacity for *P. aeruginosa* when treated with 2TDC. For this purpose, the *pvdF* and *pvdS* mutants PAO6382 and PAO6901 were used as negative controls, and pyoverdine production was investigated in both liquid cultures and swarming plates.

5.2.5.1 Impact of pyoverdine in liquid cultures

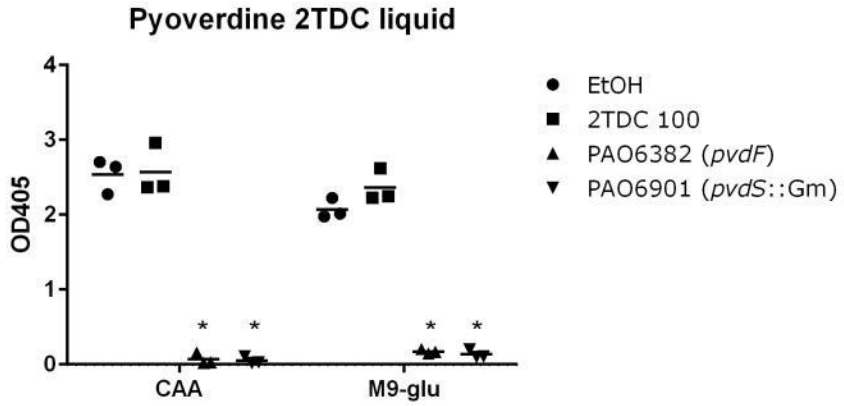


Figure 5.16. Effect of 2TDC on pyoverdine production in ion-depleted liquid media. Cultures were grown in CAA or M9 supplemented with glucose (M9-glu). 2TDC or EtOH were added to cultures of PAO1-L. The PAO1-L *pvdF* mutant strain PAO6382 and the PAO1-L *pvdS* insertional mutant strain PAO6901 were used as negative controls. Multiple t-tests, using a p-value cut off of 0.05 and the Holm-Sidak correction were used to assess significance. PAO6382 vs EtOH, p-value=2.25·10-8 (CAA), p-value=1.77·10-7 (M9-glu). PAO6901 vs EtOH, p-value=2.02·10-8 (CAA), p-value=1.43·10-7 (M9-glu). The results show no impact of 2TDC on pyoverdine production.

The results from **Figure 5.16** indicate that pyoverdine is not affected by 2TDC. OD_{405} values and the colouration of cultures indicated that pyoverdine is being expressed under these conditions and with the addition of 2TDC. As expected, cultures of the pyoverdine-negative strains did not have the characteristic yellow-green fluorescent colouration of pyoverdine.

5.2.5.2 Impact of pyoverdine on swarming plates

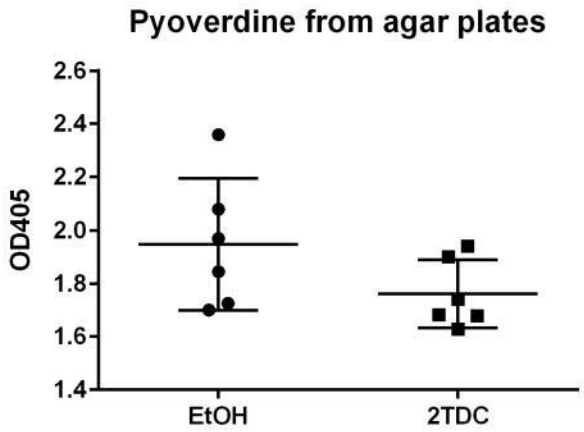


Figure 5.17. Impact of 2TDC on the pyoverdine production of PAO1-L in CAA plates. Plates containing CAA medium were seeded with cultures of PAO1-L and incubated for 16 h at 37 ºC. The agar was mixed with a $KHCO_3$ buffer and removed after 24 h of incubation. The liquid phase was measured for the OD at 405 nm. Error bars represent one standard deviation of the means. A t-test was used to assess statistical differences, p=0.14. Pyoverdine production is not affected under these conditions.

Results show that 2TDC does not affect the production of pyoverdine, under the conditions tested (**Figure 5.17**). The colouration of the plates after incubation was suggestive of pyoverdine production, similarly to the observations from liquid cultures (**Figure 5.16**).

5.2.6 Impact of 2TDC on *P. aeruginosa* regulatory pathways

In order to better understand which regulatory pathways may be involved in effect of 2TDC on motility and biofilms, a number of reporter systems and mutants in the corresponding pathways were used.

5.2.6.1 Involvement of RsmY and RsmZ on 2TDC signalling.

RsmY and RsmZ are small, non-coding RNAs that play regulatory roles in *P. aeruginosa.* They act by sequestering the global regulator RsmA, which is then unable to modulate the post-transcriptional gene expression of the target genes [80, 451]. In broad terms, RsmA activates phenotypes related to acute infection, such as motility, while it inhibits chronic phenotypes, including biofilm formation and type 6 secretion systems (T6SS) [276]. In order to study if 2TDC triggers this signalling pathway, the expression of RsmY and RsmZ was first investigated, using *P. aeruginosa* PAO1-L strains carrying the transcriptional reporter fusions pKR26 (P*rsmY-luxCDABE*) and pKR121 (P*rsmZ-luxCDABE*). Cells containing the reporters were spotted onto LB or NB plates and incubated for 8 h or 16 h in the

presence and absence of 2TDC, at 37 ^{o}C. After that, the spots were recovered, diluted in PBS and their luminescence and OD at λ=600 nm were determined.

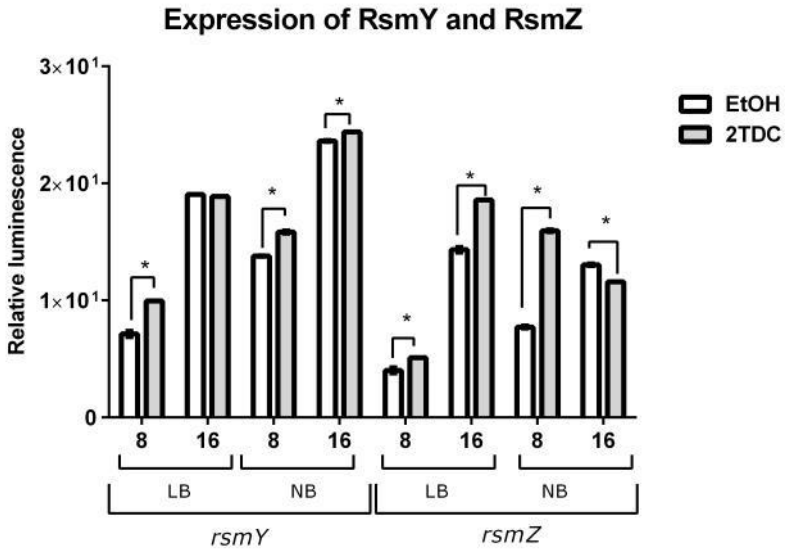


Figure 5.18. Effect of 2TDC on the expression of the small RNAs RsmY and RsmZ. Cells grown on agar plates of either LB or NB show a trend towards activation of transcription of RsmY and RsmZ in the presence of 2TDC. Bioluminescence is presented relative to cell growth (OD_{600}) and background luminescence (from a promoterless pminiCTX-lux). Error bars represent one standard deviation. Multiple t-tests were used to assess statistical significance, with the Holm-Sidak correction and a cut off value of 0.05. *, p-value<0.0001.

With two exceptions, the expression of RsmY and RsmZ was moderately activated in the presence of 2TDC. This suggests a model in which 2TDC somehow triggers the activation of the small RNAs, causing repression of RsmA (and possibly RsmN). In turn, Rsm proteins being repressed would lead to an inhibition of swarming motility. However, these results sit in disarray with the levels of c-di-GMP and the biofilm assays, as the Gac/Rsm pathway controls differentially swarming and biofilm behaviours.

In order to discern if RsmY and RsmZ are the only targets for the control of swarming by 2TDC, a swarming assay was conducted using the strains PASC638 and PASC659 (Δ*rsmY* and Δ*rsmY* Δ*rsmZ* mutants, respectively), and the corresponding isogenic wild-type (PAO1-Nottingham, PAO1-N).

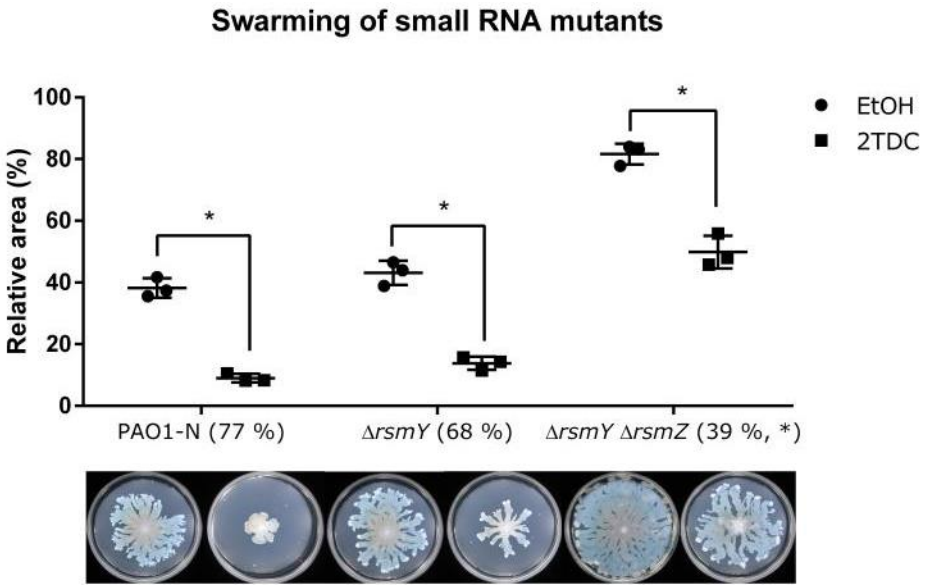


Figure 5.19. Swarming of mutants for RsmY and RsmZ in the presence of 2TDC. Swarming plates were incubated in the presence and absence of 2TDC, at 37 ºC for 16 h. The number of pixels of the swarming areas were normalised by the total pixels of the plates. Percentages indicate the inhibition of swarming relative to the corresponding EtOH control. The inhibition percentage of the double mutant PASC659 was significantly lower than the percentages for the other strains. Multiple t-tests with the Holm-Sidak correction (cut off=0.05) were used to assess statistical significance, *, p-value<0.0001.

As expected, **Figure 5.19** shows that both PASC638 *and* PASC659 display a hyper-motile phenotype. The addition of 2TDC inhibited swarming in all cases. Overall, the inhibition observed for the mutants indicates that RsmY and RsmZ are not the only targets for the action of 2TDC, and that these non-coding RNAs may only have a minor role in 2TDC signalling.

5.2.6.2 Two-component systems

GacS is a SK that phosphorylates GacA, which acts on the expression of the small RNAs RsmY and RsmZ. HptB is another global regulator which controls the expression of RsmY, but not RsmZ. These two proteins are placed upstream the regulatory pathway of RsmY and RsmZ and were therefore chosen for further investigation [277, 452].

To investigate whether the Gac system or HptB have a role in sensing 2TDC, mutants in *hptB* and *gacA* were constructed in the PAO1-L and the impact of this signal molecule in these mutants was tested (**Figure 5.20**).

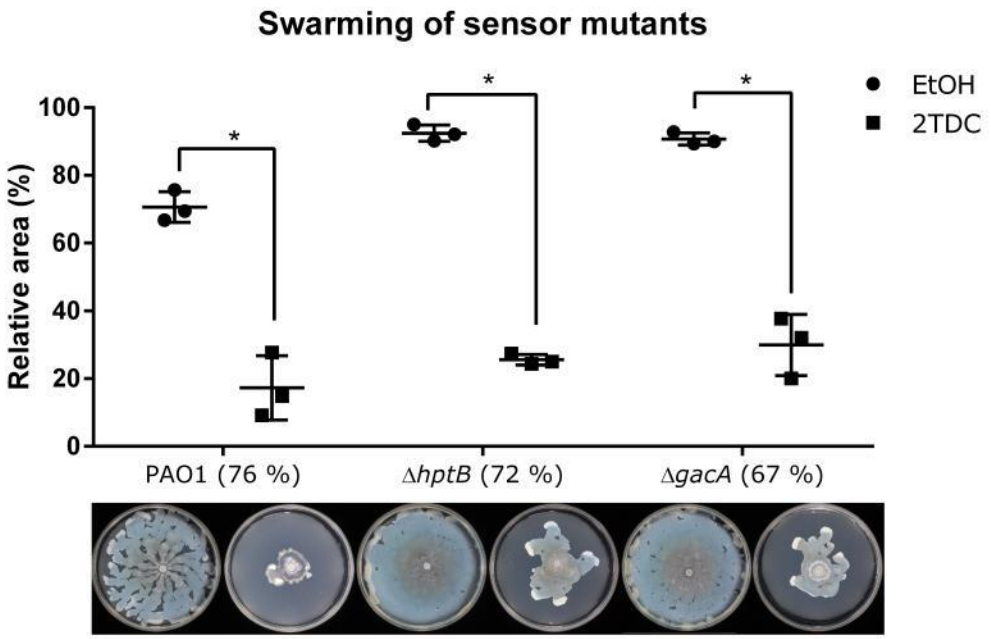


Figure 5.20. Effect of 2TDC on swarming in Δ*htpB* and Δ*gacA* mutants. Swarming plates were incubated in the presence and absence of 2TDC, at 37 ºC for 16 h. The number of pixels of the swarming areas were normalised by the total pixels of the plates. Percentages indicate the inhibition of swarming relative to the corresponding EtOH control. Multiple t-tests with the Holm-Sidak correction (cut off value=0.05) were used to assess statistical significance, *, p-value<0.0001. 2TDC was still able to inhibit swarming in the Δ*hptB* and Δ*gacA* mutants.

5.2.6.3 Quorum sensing

Quorum sensing (QS) has been shown to play an important role in swarming and biofilm formation in *P. aeruginosa* [196, 453]. Therefore, it was hypothesised that 2TDC may be modulating the expression of key QS regulatory genes. To test this hypothesis, the impact of 2TDC on the expression of *lasI, rhlI* and *pqsA* was tested using *lux*-based transcriptional fusions to these genes.

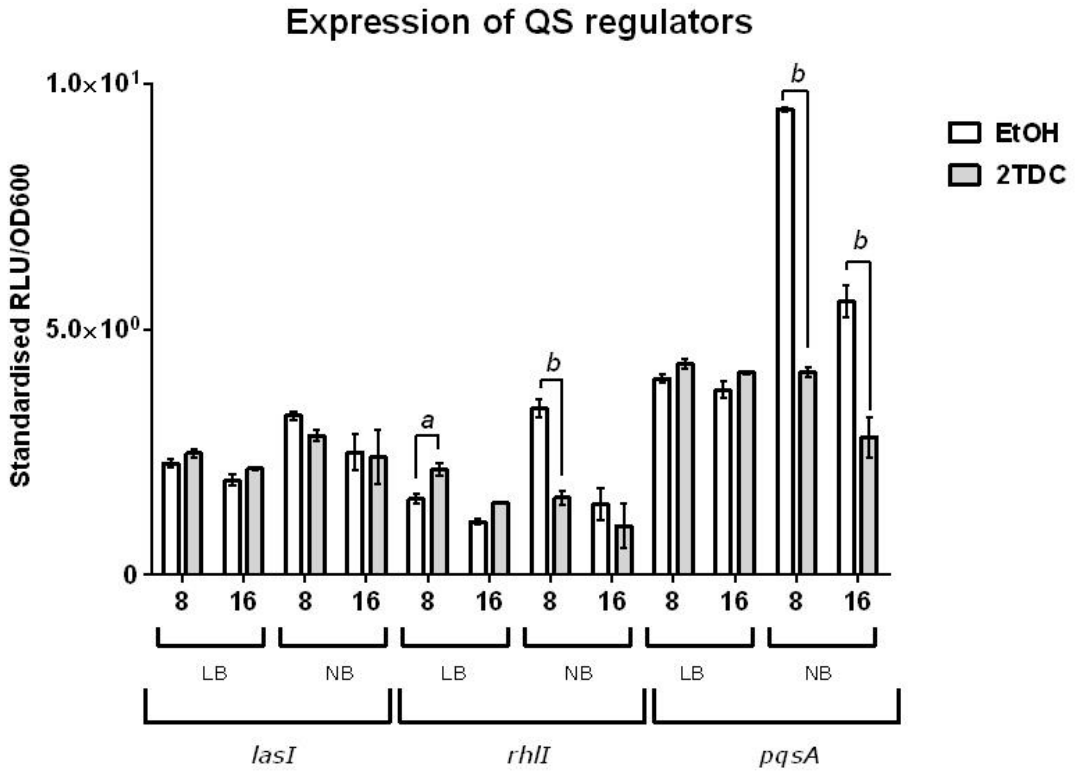


Figure 5.21. Impact of 2TDC on the expression of quorum sensing regulatory genes. Chromosomal transcriptional fusions to the genes *lasI, rhlI* and *pqsA* were spotted onto LB or Nutrient Broth (NB) plates, alongside the corresponding promoterless fusion. Plates were incubated for 8 h or 16 h at 37 ºC. Relative luminescent units (RLU) were divided by the OD_{600}. Results are presented standardised by the RLU/OD and by the background RLU/OD of the promoterless pminiCTX-lux PADP228. Error bars represent one standard deviation of the means. Multiple t-tests, with the Holm-Sidak correction (cut off value=0.05) were performed; a, p-value=0.002; b, p-value<0.0001.

The results suggest an impact of 2TDC in the expression QS genes (**Figure 5.21**). Particularly, the PQS system seems repressed by 2TDC in NB. To validate these results, the production of PQS and HHQ was next explored by analysis with thin layer chromatography (TLC). Molecules were extracted from agar plates with acidified EtOAc, and spotted onto normal phase silica TLC plates (see **Appendix, section 7.4.4**).

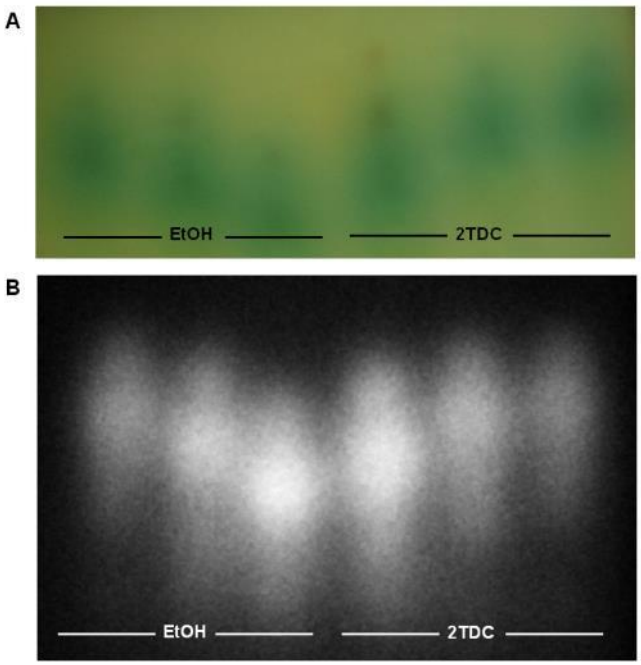


Figure 5.22. 2TDC does not affect the production of PQS or HHQ in NB plates. *P. aeruginosa* cultures were seeded onto agar plates and incubated overnight. PQS and HHQ were extracted with acidified EtOAc and spotted onto normal phase thin layer chromatography (TLC) plates. Plates were then overlaid with soft top agar seeded with the biosensor PAO1-L Δ*pqsA*/CTX::P*pqsA-luxCDABE*. The production of pyocyanin from the biosensor indicates the presence of the signal molecules PQS and HHQ **(A)**, and the production of light from the *pqsA* promoter, also related to the presence of PQS and HHQ **(B)**.

These results show that 2TDC allows for AQ production at wild-type levels (**Figure 5.22**). Although the expression from *pqsA* was repressed, this does not correlate with a reduction in AQ. However, a quantitative analysis of AQs may reveal changes which were not detected by TLC and the use of a biosensor.

The phenazine pyocyanin is one of the targets of the PQS system. To better understand the regulatory effects of 2TDC, the expression of pyocyanin was next investigated. Pyocyanin relies on two operons which only differ in their promoter regions. The transcriptional fusions pA2DA1L and pA1DA2L were used to assess the levels of expression of *phzA1* and *phzA2*, respectively. PAO-L strains containing the reporters were next spotted onto agar plates, and the luminescence and growth were determined.

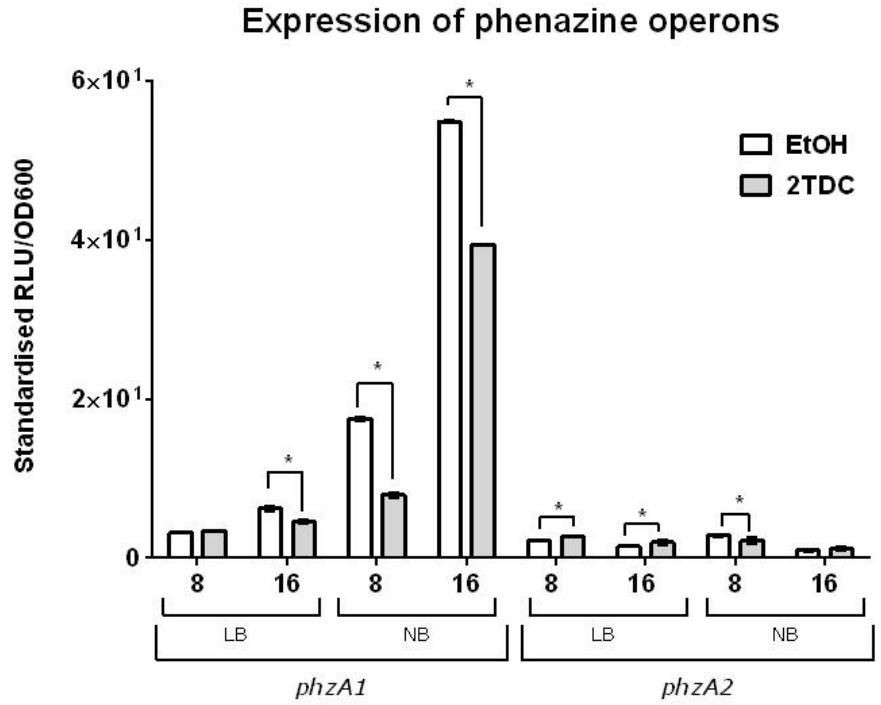


Figure 5.23. Expression of transcriptional reporters pA2DA1L and pA1DA2L in the presence of 2TDC. Biosensors were spotted onto LB or NB agar plates and incubated for 8 h and 16 h at 37 ºC. Relative luminescent units (RLU) were standardised by the OD_{600} and by the background luminescence, with the use of the promoterless pminiCTX-lux PADP228. Error bars represent one standard deviation. Multiple t-tests were performed to assess statistical significance, with the Holm-Sidak method (cut off=0.05). *, p-value<0.05.

The results from **Figure 5.23** show that *phzA1* expression is repressed by 2TDC in NB. The levels of expression of phenazine operons are still high in the presence of 2TDC. It was also observed that expression from the *phzA2B2C2D2E2F2G2* operon is much lower as compared to the empty pminiCTX-lux control.

The repression of *phzA1* expression can be explained by the repression of *pqsA* observed in **Figure 5.21**, but interestingly, production of AQ was similar to wild-type levels, as seen in **Figure 5.22**. This suggests the presence of post-transcriptional regulatory mechanisms which restore the homeostasis of virulence determinants after a transient imbalance caused by 2TDC.

The lack of inhibition in AQ secretion suggests that, although *phz* operons were affected, this may not result in changes of pyocyanin production. To this end, overnight cultures were seeded onto NB plates and allowed to grow for 16 h. After that, pyocyanin was recovered from the plates, extracted with chloroform and quantified. Treatment with 2TDC did not result in differential colouration of the plates, suggesting that 2TDC does not affect pyocyanin production. Further quantification after extraction validates this, showing that either the repression of

pqsA is not dramatic enough to reduce pyocyanin expression, or that 2TDC affects other regulators that, overall, do not allow for a reduction in pyocyanin (**Figure 5.24**).

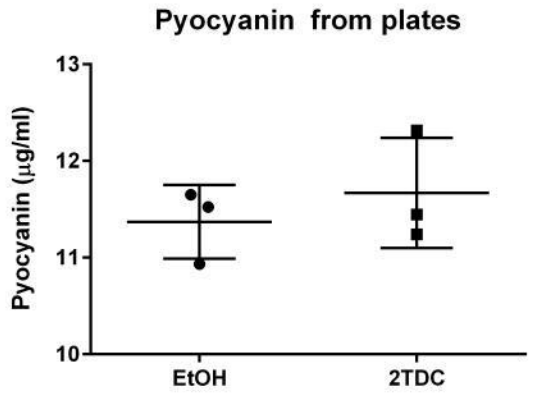


Figure 5.24. 2TDC does not impact pyocyanin production by swarmer cells. *P. aeruginosa* cells were spread onto NB containing 0.5 % agar. The next day, pyocyanin was recovered from the plates with the addition of a $KHCO_3$ buffer, and subsequently extracted with chloroform. Error bars represent one standard deviation of the means from independent triplicates.

All in all, results in QS systems do not offer a strong explanation for the effects in biofilm and motility observed in cultures treated with 2TDC.

5.3 Discussion

The general aim of this chapter was to investigate the impact of 2TDC, a molecule found in environments encountered by *P. aeruginosa*, on the biology of this organism. The study of 2TDC was driven by the fact that this volatile molecule has been shown to affect different phenotypes in other bacteria, in particular biofilm formation and motility. The results presented here constitute initial steps towards a better understanding of the role of volatile compounds in population behaviours.

A major challenge in this work was the handling of a volatile compound in biological assays. Multiple protocols for colonisation factors were adapted to the study of cultures grown on solid medium. Indeed, while classical laboratory methodology has been conducted in liquid, recent investigations show that certain products are differentially regulated between liquid and solid-grown cultures [454]. Proof of concept for the protocol adaptations are found in **Appendix, section 7.4**.

Briefly, after verifying that 2TDC has no impact on growth, this molecule was found to have an impact on biofilm formation and motility and hence a series of assays were performed to unravel the mechanisms behind these effects. Initial studies performed by Wood et al. also did not observe any growth defects in *P. aeruginosa* grown with 2TDC when investigating the role of this molecule in interdigital glands of black-tailed deer [280]. Indeed, the present investigation demonstrates that 2TDC does not show any toxic effect in this bacterium, (**Figure 5.2**). This constitutes an interesting characteristic of 2TDC as a biocontrol agent, as the lack of growth inhibition greatly reduces the emergence of resistance.

It is worth mentioning that the utilisation of 2TDC as a carbon source by various species of pseudomonads, including *P. aeruginosa*, has been described elsewhere [455]. An increase in growth was never observed with 2TDC in this study, suggesting that *P. aeruginosa* cultures were using other carbon sources by catabolite repression. However, the use of 2TDC by *P. aeruginosa* metabolism cannot be discarded, and thus it is possible that part or all of the effects observed were due to the products of 2TDC degradation rather than 2TDC directly affecting *P. aeruginosa* biology.

The motility results presented in this chapter show that, similarly to other bacterial species, 2TDC does not affect swimming motility in *P. aeruginosa* (**Figure 5.3**). In contrast, both swarming and twitching were reduced in the

presence of 2TDC suggesting that 2TDC may require mechanisms of cell-to-cell communication in order to exert its effects (**Figure 5.5, Figure 5.6**). This is consistent with the observation that swarming cells present a vast shift in gene expression, as compared to swimming cells [73, 75]. The hypothesis that 2TDC specifically affects bacterial community behaviours as opposed to independent cell phenotypes is therefore worth considering.

On minimal medium, swarmers in the edge of the tendrils present two flagella and are named hyperswarmers. In addition, this phenotype confers a higher swarming rate without affecting swimming motility [456]. It was hypothesised that 2TDC might reduce or supress the rise of hyperswarmers; therefore only affecting swarming motility. However, under our conditions, no hyperswarmers were observed by electron microscopy, as cells only presented one flagellum (**Figure 3.16**). Therefore this hypothesis was not further explored.

Regarding biofilm formation, results to date do not offer a clear insight on the mechanism behind the effects of 2TDC. When comparing the two assays undertaken with chamber slides (inhibition and disruption), one could argue that 2TDC may only have an important role in the first stages of biofilm formation; namely bacterial adhesion (**Figure 5.7 A, Figure 5.9, Figure 5.10**). Indeed, hydrophobic compounds have shown to limit the adherence of bacteria onto surfaces [457, 458]. However, this argument loses validity when comparing the assays for inhibition of biofilm using chamber slides and the Bioflux system (**Figure 5.7**, **A** and **B**). Both experimental approaches were highly similar: they use glass surfaces for the adherence of cells, and the cells are first allowed to adhere by static incubation. 2TDC was added in both cases from the beginning of the assay. In Bioflux, media supplemented with 2TDC or EtOH was used in the wetting, seeding and flow stages; and therefore impaired attachment caused by 2TDC would affect the subsequent biofilm formation in this model. The effects caused by 2TDC happen therefore after the initial adherence state, and before biofilms are fully developed, possibly during intermediate stages of biofilm formation.

Another possible explanation is that cells were diluted and allowed to grow for 6 h prior to the Bioflux assays, so their growth phase at the time of inoculation would be a late exponential/early stationary, while the overnight cultures used for the static assay were in late stationary phase. The metabolic state of cells could change their capacity to attach and form biofilms.

Consistent with the fact that 2TDC only affects biofilm formation under a narrow set of conditions, colony morphotypes and the expression of reporters for c-di-GMP, Pel and Psl were not affected by 2TDC (**Figure 5.8, Figure 5.12, Figure 5.13**). An important point to make here is that 2TDC was added as a volatile compound in these assays, whereas in chamber slides and Bioflux assays it was added to the liquid cultures (**Figure 5.7**). The partition of 2TDC between the liquid and gas phases, and therefore the availability of 2TDC for the cells, is unknown to date. This difference may explain the lack of results with the morphotypes in Congo red plates and the reporters as compared to the chamber slides. However this does not constitute the full explanation, as the Bioflux assay did not show inhibition of biofilm formation and in both the chamber slides and the Bioflux, 2TDC was added to the liquid phase. Further investigation is required to better understand biofilm formation under 2TDC treatment.

Both biofilm formation and surface translocation rely on a wide range of mechanisms which are tightly regulated. During this work, a series of bioreporters were used to assess the expression of regulatory pathways involved in both biofilm formation and surface motility in the presence of 2TDC, which will be discussed in this section. Various regulators differentially affect swarming and biofilm, including c-di-GMP, QS, Gac/Rsm and cAMP/Vfr [459, 460]. In consequence, it is generally believed that swarming and biofilm formation are opposite phenotypes, so that when cells favour one, they inhibit the other. However, this was not observed during this study, where biofilm formation and swarming motilities are regulated in parallel by the addition of 2TDC (**Figure 5.5, Figure 5.7**).

The cyclic nucleotide c-di-GMP is one major regulator of biofilm expression, with the accumulation of this molecule directly related to biofilm levels. Expression from the pCdrA::*gfp*^{C} reporter is correlated with the general pool of c-di-GMP [121, 299]. The addition of 2TDC to the gas phase did not affect the expression of *cdrA* (**Figure 5.12**), suggesting that 2TDC does not affect swarming or biofilm through the regulation of c-di-GMP.

Another key element driving the transition to sessility is the secretion of exopolysaccharides [105]. In addition, Pel and Psl inhibit swarming motility [461]. Expression from pSC855 and pSC856 is not affected by 2TDC, which discards Pel and Psl polysaccharides as targets of 2TDC. This is further validated by the fact that colonies of PAO1-L treated with 2TDC did not change to a wrinkly

morphotype in agar plates, and the binding of Congo red was not enhanced in the presence of this methyl ketone (**Figure 5.13, Figure 5.8**).

The above-mentioned regulatory pathways are only slightly triggered by the presence of 2TDC, and results from this study suggest the existence of yet unidentified regulators with the same effects in biofilm and cell motility which are affected by the methyl ketone 2TDC. Additionally, general regulators such as Gac/Rsm and QS were also investigated, with similar results (see **5.2.6**).

Another key factor controlling population behaviours is the secretion of rhamnolipids and their precursors, HAAs [71], which was also assessed in this chapter. The differential regulation of rhamnolipids in liquid cultures and swarming plates was detected elsewhere [454]. In consequence, rhamnolipid production was assayed from cultures grown in both liquid and agar plates. Results in this thesis do not show a differential production of either mono- or di-rhamnolipids, albeit HAAs have not been studied yet (**Figure 5.14, Figure 5.15**). Results from the transcriptional reporter for *rhlI* show an increase in activity after 8 h of incubation in LB agar. Instead, in NB agar (medium used for swarming assays), this reporter is repressed after 8 h of incubation and no differential expression is observed after 16 h of incubation (**Figure 5.21**). This puts into manifest the condition-dependent effects of 2TDC. In addition, an early onset repression of *rhlI* in NB was then abrogated with extended incubation times. Together with the lack of effect in rhamnolipid secretion (**Figure 5.14, Figure 5.15**), it seems that the *rhl* system is not greatly triggered by 2TDC.

5.3.1 Impact of 2TDC on key switches of multiple gene expression

A series of pleiotropic pathways were investigated as possible targets for 2TDC. Indeed, phenotypes such as motility or biofilm formation are affected by QS, 2CS and the Gac/Rsm system, amongst others (reviewed in [460]). Data regarding global regulators in this study suggest that their role in 2TDC signalling is, if any, only minor; and other factors might be the major drivers in 2TDC signalling (see **5.3.2**).

While evidence shows that 2TDC could be modulating the levels of RsmY and RsmZ (**Figure 5.18**), results show that the Rsm/Gac system is not greatly influenced by the presence of 2TDC. Results presented in this chapter rather suggest that RsmY and RsmZ levels might be only transiently affected by 2TDC, but that they return to normal levels and do not result in the triggering of an effective signalling cascade. It is possible that other regulators in the

P. aeruginosa network are responsible for the homeostasis or these small RNAs, though they have not been researched during this work.

Firstly, RsmA differentially controls biofilm formation and motility, promoting the switch between acute (motility) and chronic (biofilm) phenotypes [27, 80, 424]. As mentioned before, 2TDC does not differentially regulate these phenotypes.

Secondly, RsmY and RsmZ channel signals from several sensory pathways. Particularly, the GacS/A and HptB 2CS converge with these small RNAs. GacA is the response regulator (RR) of GacS, which is affected by RetS and by LadS and results exclusively in the positive regulation of *rsmZ* and *rsmY* expression [452]. HptB is phosphorylated by PA1611, PA1976 and SagS [278]; affecting RetS and also RsmY, but not RsmZ [277] (see **Introduction, Figure 1.5**). During this work, swarming motility of Δ*gacA* and Δ*hptB* mutants was impaired by the presence of 2TDC, suggesting that the phosphotransfer involving GacA and HptB is not affected by 2TDC (**Figure 5.20**). The lack of swarming in an *hptB* mutant has been previously reported [278]. HptB is a negative regulator of RsmY, and therefore the lack of this sensor protein leads to an inhibition of swarming motility. Surprisingly, PADP159 presents wild-type levels of swarming. Given the complexity of regulators behind the control of swarming motility, it is possible that our PAO1-L present different regulatory networks which would explain these discrepancies.

Thirdly, 2TDC was still able to inhibit swarming motility in PASC638 (Δ*rsmY*) and PASC659 (Δ*rsmY* Δ*rsmZ*)(**Figure 5.19**), supporting the idea that GacA and HptB are not involved in 2TDC signalling.

Finally, RsmA is known to differentially alter the levels of pyocyanin (negatively) and rhamnolipids (positively) [80]. Neither of these two factors was altered by 2TDC (**Figure 5.14, Figure 5.15, Figure 5.24**).

Regarding QS, the most drastic result was found with the transcriptional reporter for *pqsA*, which is greatly repressed with 2TDC, though this is does not result in a differential production of PQS or HHQ according to TLC data (**Figure 5.21, Figure 5.22**), although a a quantitative analysis using LC-MS/MS may reveal small differences. Results suggest that the repression of *pqsA* is a transient effect and that PqsA may reach wild-type levels post-transcriptionally, which is further confirmed by the lack of reduction in pyocyanin, in the presence of 2TDC (**Figure 5.24**). All growth conditions were kept consistent during these assays to ensure good comparison. An alternative hypothesis regarding these results is that the

repression of *pqsA* only causes minor effects on the genes it regulates resulting in a moderate repression of the *phzA1* and possibly *phzA2* reporters (**Figure 5.23**) but maintaining enough levels of PQS and HHQ, and therefore pyocyanin.

Overall, the mechanism behind swarming inhibition by 2TDC was not elucidated, but these data has led us to discard several major regulatory mechanisms as targets for 2TDC.

5.3.2 Possible conserved targets for 2TDC

The impact of 2TDC in other bacteria has been reported elsewhere [284]. This molecule seems to broadly affect motility and biofilm formation in a variety of Gram-negative bacteria. Thus, with an aim to integrate these effects, a search for common targets in *P. syringae*, *S. enterica, S. meliloti* and *P. aeruginosa* was performed, which will be discussed during this section.

The involvement of T4aP in biofilm formation is well described [32, 86, 462], as well as the importance of this type of appendage in surface translocation [83]. Hence, 2TDC affecting T4aP would explain the reduction of swarming, twitching and biofilm in *P. aeruginosa* (albeit under specific conditions for the latter) (**Figure 5.5, Figure 5.6, Figure 5.7**). There are two main ways by which 2TDC may affect T4aP function, i) the modulation in the expression or assembly of T4aP, or ii) the dysregulation of coordinated behaviour between cells. In other words, the presence of 2TDC may result in a lower expression of pili on the cell surface, and/or in cells that are incapable of translocating in a coordinated manner (i. e. twitching and swarming) while retaining wild-type levels of swimming motility. In this sense, tentative chemotactic assays were conducted with 2TDC (see **Appendix, Figure 7.11**); however, no differences were seen under the tested conditions. Further investigation is required to explore the association between T4aP and the impact of 2TDC.

T4aP have long been identified as widespread appendages amongst Gram-negative bacteria [463], and more recently amongst prokaryots in general (for a review, see [90]). In particular, *P. syringae* presents homologues to *pilMNOP* [464] and for *pilABCD*, which was in fact used to complement a *P. aeruginosa pilD* mutant [465]. T4aP in *P. syringae* has been correlated with surface motility, biofilm formation and virulence [466]. Strikingly, effects of 2TDC reported in *P. syringae* show an increase in swarming motility but a decrease in colonisation, which suggests that the signalling cascade triggered by 2TDC is differentially regulated in *P. aeruginosa* and *P. syringae*.

Surface translocation depends on the secretion of biosurfactants (which, in turn, may depend on QS, such as the *rhl* system in *P. aeruginosa*), flagellar rotation and, under certain conditions, T4aP retraction/extension. Reduction of swarming motility by T4aP has been reported [74], which is key in early-stages of biofilm development. The contribution of flagella and T4aP to surface motility might vary between *P. syringae* and *P. aeruginosa* under the conditions tested. In *P. syringae*, a reduction in T4aP could enhance flagellar rotation resulting in higher swarming motility, and impair biofilm formation and thus colonisation. Instead, the conditions employed during this work with *P. aeruginosa* would affect the T4aP signalling to a different degree, resulting in a reduction of swarming motility.

Twitching in *P. aeruginosa* is controlled by the Chp-Pil chemosensory system [467] (see **Introduction, Figure 1.1**). The Chp-Pil system could constitute a target for 2TDC. In line with this, Leech et al. [468] conducted both twitching and swarming assays in mutants of the ChpA protein, which presents a total of eight phosphotransfer domains and one CheY-like REC domain. Mutations in different phosphorylating domains result in various morphologies for these surface motilities. Particularly, mutations in the Hpt domains hpt2 and hpt3 reduce swarming and twitching [468]. To our knowledge, equivalent assays have not been conducted in *P. syringae* and thus further investigation is needed to draw stronger conclusions on common 2TDC targets.

Another possible target for 2TDC is the Che-like chemotaxis system. Homologues of the *E. coli* Che system have been found in *P. aeruginosa* and show an impact in swarming motility without affecting swimming [469, 470]. Furthermore, *P. syringae* also presents homologues for this system, as well as *S. enterica*. This is thus an interesting target for future research. However, there is little knowledge about the role of Che-like proteins in *P. aeruginosa*, or the link between these and biofilm or twitching motilities.

Regarding *S. enterica* and *S. meliloti*, T4aP have not been described, nor twitching motility, but homologues to the Che cluster of *E. coli* have been described as essential for swarming motility. These clusters control flagellar motility, and are in both cases required for swimming [471, 472]. Further investigation is required to identify factors that specifically affect surface motility, but not swimming, and that depend on Che-like proteins.

5.4 Conclusion and future directions

This study has explored various population behaviours and shown that swarming motility and biofilm formation are targets of 2TDC in *P. aeruginosa*. These results are in agreement with similar effects found in *P. syringae, S. meliloti* and *S. enterica*. The mechanisms behind 2TDC control were investigated in *P. aeruginosa* with phenotypical assays and biosensors. Finally, in a search for a model integrating the effects of 2TDC observed in different bacteria, and possible mechanisms behind the impact of 2TDC were reviewed, which resulted in the identification of potential common targets in 2TDC signalling. Two putative targets are suggested: T4aP and Che-like chemotaxis systems (including the Che and Chp systems of *P. aeruginosa*). Chemotaxis systems are of particular interest to pursue this work, particularly with regards to surface motility and colonisation.

The impact that 2TDC would exert on the colonisation of plants by *P. aeruginosa* is yet to be understood. On the one hand, surface motility is generally correlated with the expression of virulence factors [11, 73, 91, 473]. So, in this sense, *P. aeruginosa* would have impaired virulence in environments with 2TDC. However, research has shown that the translocation across solid surfaces of *P. syringae* and *S. meliloti* is enhanced with 2TDC, while the colonisation of plants is reduced in both cases. This challenges the link between motility and colonisation, as shown elsewhere [466]. In consequence, swarming inhibition does not necessarily mean that *P. aeruginosa* infection would be impaired by 2TDC environments and so the effects of 2TDC in *P. aeruginosa* infection require more work.

On a different note, this methyl ketone would only be beneficial for specific plants and conditions, as the reduction of infection by *S. meliloti* would reduce nitrogen fixation and therefore be detrimental; in contrast, a reduction of infection by *P. syringae* or other pathogens would improve plant cultures. Moreover, multiple factors can contribute to the differences observed in infectivity, and the importance of each factor is unknown: the plant host, other organisms colonising the plant, or the bacteria subject of these studies. An area for future investigation is, in consequence, the study of 2TDC from an ecological perspective. Given that *S. meliloti, S. enterica, P. syringae* and *P. aeruginosa* can co-exist in environments such as the rhizosphere and can encounter 2TDC, this methyl ketone may cause great changes in cell-to-cell interactions; both amongst bacteria and also between bacteria and plant host. For example, surface translocation is activated by 2TDC in *P. syringae*, which may allow this pathogen to displace *P. aeruginosa* from the plant host.

Biofilm and swarming are often considered mutually exclusive phenotypes [459]; however research also shows the importance of motility appendages such as flagella and pili in early biofilm establishment [69, 115], and the importance of rhamnolipids in both swarming and biofilm formation [180, 474]. This hints to other pathways regulating both motility and biofilm. The current study is an example of such pathways.

We are just beginning to understand the importance of volatile ketones in inter-species communication and their impact in the environment, but data so far suggests that these molecules might be of paramount importance for the regulation of infection and plant and animal defence against others.

6 GENERAL CONCLUSION AND FUTURE DIRECTIONS

N-acyl-L-homoserine lactones (AHL) and 2-alkyl-4-quinolones (AQ) have long been identified as signalling molecules in *P. aeruginosa* and related organisms. These small molecules are the core of quorum sensing (QS), and are important elements in niche colonisation, including the establishment of an infection in the human host [475]. With the rise of multi-drug resistant bacteria, QS systems have been attractive targets for the development of novel antimicrobial therapies, as the inhibition or attenuation of these regulatory systems would impair the virulence of bacteria. Furthermore, the inhibition of QS does not cause selective pressure for bacteria to develop resistances, which would pose a great improvement to current treatments. In addition, QS inhibition could be used alongside current antibiotics to boost their activity. Various approaches to QS inhibition have been investigated in the last decades [476], though there is no doubt that a better understanding of QS systems will help the development of novel strategies to combat bacterial infection.

Amongst the colonisation determinants that *P. aeruginosa* produces, one of the most problematic is the formation of biofilms, which are virtually impossible to eradicate due to the intrinsic resistance of biofilm-associated cells and to the secretion of exopolysaccharides that create a protective layer surrounding the cells. Diffusible signal factor-type (DSF-T) molecules represent another regulatory layer in the QS circuitry, with signalling roles in a variety of bacteria. DSF-T have shown to impact a variety of phenotypes, including motility, iron acquisition, and biofilm formation. The secretion of *cis*-2-decenoic acid (CDA) in *P. aeruginosa* PAO1 cultures was reported a few years ago [255]. CDA is a fatty acid produced by this bacterium which presents the signature feature of DSF-T, a *cis* double bond between the second (α) and the third (β) carbon. This DSF-T has been shown to inhibit biofilm formation and disperse biofilms of *P. aeruginosa* and a range of other organisms. The discovery of this DSF-T molecule is therefore of paramount importance for future research and for the development of treatments based on QS inhibition. Therefore, one aim of this PhD project, reported in **Chapter 3**, was to advance the knowledge on the impact of CDA in *P. aeruginosa*, with special attention to the effects of this fatty acid in the virulence of this bacterium. To this end, two transcriptomic studies performed in the presence and absence of CDA were analysed and compared: an RNA-seq experiment produced by Chen et al. previous to this project [294] and a microarray published recently [364]. A functional database for *P. aeruginosa* genes was developed as a tool for the analysis of these results. Genes for

multiple regulators and secreted factors were differentially regulated by CDA; however only minor effects were observed in phenotypical assays. Due to time constraints, not all the targets identified in the analysis of the transcriptomic studies were investigated, and hence there is scope for future investigations. For instance, several ATP-dependent proteases were identified. In particular, *clpP2* and *clpC* are both down-regulated by CDA in cells grown in LB; while *clpP, clpP2* and *clpX* are up-regulated in the assay in M9. Intracellular, ATP-dependent proteases are emerging as important factors that shape the virulence of *P. aeruginosa* [477] and hence would be of particular interest to continue this study. Another area for future research could be focused on chemotaxis and aerotaxis mediated by CDA, as multiple genes related to these behaviours were identified in both transcriptomic analysis.

The most striking result found during **Chapter 3** was the lack of impact of CDA in the biofilm formation and dispersion of PAO1. The particular pathways triggered by CDA remain to be elucidated and appear to involve c-di-GMP, and thus future work might shed light to the conditions necessary for this effect. Once these conditions are established, the role of c-di-GMP could be studied in detail. Results in this thesis show that the phosphodiesterase (PDE) PA2567 is activated in the presence of CDA, and therefore the use of a mutant for this protein could be a starting point to understand the mechanism behind biofilm dispersion by CDA. Further along, the impact of CDA in *in vivo* models of infection could be studied to consider the use of this molecule as a treatment against the colonisation of *P. aeruginosa* or other bacteria.

With the aim to better understand the regulation of CDA in *P. aeruginosa*, **Chapter 4** sought to analyse potential proteins involved in the sensing and biosynthesis of this molecule. In particular, sequence alignments and domain organisations were used. *P. aeruginosa* presents a myriad of sensor proteins and enoyl-CoA hydratases (ECH) which make this type of analysis difficult. Multiple proteins were identified with a similar domain organisation to the reporter sensor proteins for BDSF and DSF. On the other hand, an in-depth analysis of the amino acid sequences of ECH candidates showed that several of those proteins may have a role in CDA synthesis. These proteins have not been extensively studied, and hence there is a gap of knowledge on their function in the biology of *P. aeruginosa* that would lead to a more informed identification of candidates for CDA synthesis. In addition to functional analyses, crystallography studies could also increase the understanding of ECH in *P. aeruginosa*. **Chapter 4** also focused on the role of the previously characterised ECH PA0744, PA0745 (termed DspI in

PA14, [380]), PA3426 (termed CbsA in a previous study by Chen et al. [294]) and the PA4980/PA4982, predicted as synthase and sensor kinases of CDA, respectively [364]. Evidence suggests that PA0745 and PA0744 may constitute an operon, and hence both these genes should be considered for further studies. Various mutants were constructed and characterised as a first step to unravel the intricacies of the expression of these proteins. A link between PA0744, PA0745 and CDA regulation could not be established; however, these genes have been shown to highly impact the colonisation factors of *P. aeruginosa* and are therefore interesting for future studies. *P. aeruginosa* presents an arsenal of regulatory networks which might become differentially expressed to compensate for the mutation in one particular ECH. A different approach to the study of ECH could involve the use of isothermal titration calorimetry (ITC), with two main goals: to establish possible protein-protein interactions between PA0744 and PA0745, and to investigate the binding of these proteins to CDA. Other techniques such as electrophoretic mobility shift assay (EMSA) could also be considered.

Regarding CbsA, previous work suggested that it might be implicated in the processing of CDA; however, results from this study do not support those findings. A whole transcriptome study performed with an IPTG-inducible, conditional mutant of *cbsA* [294] was analysed here but did not lead to the identification of interesting targets for further research. The overexpression of CbsA causes a major inhibition of rhamnolipid production, swimming, swarming and twitching motilities; but no effects were observed in the absence of IPTG (*cbsA* mutant conditions). Likewise, various effects were observed in the proteolytic activities; but they only comprised the condition for *cbsA* overexpression. Future work should focus on the optimisation of growth conditions in which CbsA would be strongly expressed, especially with regards to those mimicking natural niches of *P. aeruginosa*. This will help elucidate the biological role of this enzyme and the link to colonisation and, perhaps, CDA regulation.

Bacterial populations are not usually found isolated in the environment, but rather share the same niche with multiple species. As a consequence, bacteria have evolved to respond to the presence of other organisms, either by coordinating certain behaviours, or by competing for resources. Research has shown that multiple DSF-T molecules produce similar effects in various species, suggesting that collaboration mediated through these signals may occur. This is the case of BDSF, which can complement a lack of DSF production in

X. campestris. However, this does not exclude the existence of competition promoted by these same signals, under different conditions or towards different species. The present study therefore aimed to set a starting point in unravelling the relationship between *P. aeruginosa* and species producing two DSF-T molecules; namely DSF and BDSF. Both DSF and BDSF were found to cause major impacts on the biology of *P. aeruginosa*, including the reduction of proteolytic activity, swarming area and twitching motility. Some of these effects have been linked to an inhibition of QS and type 3 secretion system (T3SS) [373], but the particular mechanism of action is not fully understood and could be ground for future studies. Specifically, QS has shown to negatively modulate T3SS [478], and therefore it seems counter-intuitive that BDSF would inhibit both systems. This apparent discrepancy can be the result of changes in strains and in growth conditions, but it could also reveal new regulation mechanisms for classical QS systems and T3SS.

As mentioned above, BDSF and DSF produced similar effects in *P. aeruginosa.* This finding correlates with previous reports [260]. In particular, results presented in **Chapter 3** show that both molecules limit the colonisation capacities of *P. aeruginosa,* and therefore *Xanthomonas* or other producers of these molecules might compete with *P. aeruginosa in vivo*. Future research could aim to study the overall impact of DSF-T from an ecological point of view, and elucidate whether the presence of DSF-T impacts the fitness of *P. aeruginosa.* Of particular note is the fact that CDA also affected twitching, while the *trans* isomer, TDA, did not cause differences in twitching patterns, showing that this effect is exclusive of DSF-T molecules and does not act by unspecific, physicochemical pathways. Future work could focus on the mechanism behind this inhibition, including the study of genes involved in pili biosynthesis and in chemotaxis.

In a similar note, CDA has been reported to affect biofilm formation in various species [255]; however, further research is required to fully understand the impact of this molecule in bacterial populations other than *P. aeruginosa.* DSF has been identified in the lung of patients with cystic fibrosis (CF), which shows that this signal is produced *in vivo* and may have an impact in species such as *P. aeruginosa* [369]. Similar studies could be conducted with CDA, for instance this molecule could be detected from various human tissues to determine the conditions in which it is secreted the most and the concentrations in which it can be found. Another approach would be to quantify the production of CDA from different strains of *P. aeruginosa* to try to identify if a particular lifestyle of this

bacterium results in the regulation of CDA levels (e. g. environmental vs clinical; acute vs chronic, etc.) or if the presence of other species results in a differential regulation of this fatty acid.

CDA seems to be innocuous for human cells [479], but the impact of this fatty acid in the human microbiota does not appear to have been investigated yet. The fact that CDA inhibits biofilm establishment in various Gram-positives and Gram-negatives suggests that this molecule might act on a well conserved target in bacteria. This broad spectrum of action raises the concern that CDA could affect the attachment of microbiota and result in more damage than benefit to human patients. Related to potential inter-species effects of CDA, a transcriptional fusion of *bclABC*, coding for a lectin operon in *B. cenocepacia*, has been shown to respond to the presence of multiple DSF-T, including CDA [480]. This might indicate that CDA activates the expression of lectins in *B. cenocepacia*, with possible implications in colonisation. Conversely, transcriptomic analysis revealed that the *P. aeruginosa lecB* is down-regulated by CDA, hence a closer look at the link between CDA and lectins (in both *P. aeruginosa* and *B. cenocepacia*) could be an interesting area for further investigation.

Following the theme of inter-species communication, the effects of 2TDC in the physiology of *P. aeruginosa* PAO1-L were investigated. 2TDC is a ketone produced by multiple species including plants, animals and bacteria; and work performed elsewhere has shown that this molecule modulates swarming and biofilm formation in various bacterial species [284]. Interestingly, the effects of this ketone seem to be restricted to surface-associated cells. The scientific community has now recognised the importance of cell attachment, as opposed to planktonic growth, as the default lifestyle for most microorganisms [481]. Microorganisms have developed strategies to sense the properties of surfaces and respond accordingly, in a phenomenon termed "surface sensing". Sensing of surface and surface properties occurs in multiple species. Examples include fungi that sense surface rigidity and hydrophobicity [482] and bacteria (including *P. aeruginosa*) that use motility appendages to sense and respond to surfaces [483]. In order to study the effects in attached cells, various protocols for the determination of virulence factors in *P. aeruginosa* were adapted to study cells in agar plates, rather than growing in liquid cultures. Another feature of 2TDC is that it is a volatile molecule, and the effects in gene expression mostly occur when this molecule is present in the gas phase rather than dissolved in an aqueous liquid [450]. However, the solubility and the partition coefficient of this

molecule has not been determined yet, and as a consequence the exact concentration available to the cells from the gas phase is not known, which would represent one major focus for future directions.

Findings reported in **Chapter 5** show that 2TDC inhibits swarming and twitching motility in a dose-dependent manner and does not affect swimming. The mechanism behind motility inhibition was not elucidated and could be an area for future work. In this sense, results reported here have established that rhamnolipids are not affected by the presence of 2TDC. Strikingly, biofilm was also inhibited by 2TDC, which does not follow the classical conception of biofilm and motility being differentially regulated [424, 460]. 2TDC therefore presents enormous potential for the control of bacterial infections, and in particular for the inhibition of colonisation by *P. aeruginosa*. The results from this chapter correlated well with previous findings in other bacteria [284], such as the fact that growth and swimming motility are not affected by 2TDC. In light of the results shown in this thesis, T4aP are suggested as possible targets for this 2TDC, given that their presence is widespread in the bacterial kingdom and for their role in motility and biofilm formation. The determination of the element(s) directly involved in the impact of 2TDC in bacterial motility represents scope for future research.

Fatty acids and their derivatives can present signalling roles in *P. aeruginosa,* constituting an additional layer of phenotypical regulation to the classical cell-cell communication systems. The compounds tested in this study affect bacterial community behaviours and colonisation determinants such as swarming, twitching, biofilm formation and proteolytic activity. Although the relevance of these findings is still not well understood, various producers of DSF-T and 2TDC are encountered by *P. aeruginosa* in the environment, such as *Burkholderia sp.*, *S. maltophilia*, *Xanthomonas sp.* and *S. meliloti*. In consequence, it is likely that *P. aeruginosa* encounters these molecules in environmental settings, and therefore the findings reported in this thesis constitute additional examples of cooperation and competition mediated by small molecules in the bacterial world. Knowledge acquired on these sophisticated systems could potentially lead to the development of new ways of controlling bacterial activities in contexts of clinical, agronomical and industrial relevance.

7 APPENDIX

7.1 Additional general information

7.1.1 Functional database

A functional annotation database was created from combined information in the COG database (http://www.ncbi.nlm.nih.gov/COG/) and the *Pseudomonas* Genome Database (http://www.pseudomonas.com/, [315]), so that PA numbers were categorised according to the COG database. The following tables specify the genes that were assigned additional categories of special interest for this study.

Table 7.1. List of the genes assigned the additional category "O: Biofilm extracellular polymeric substances, formation and regulation". The genes listed below were chosen for their involvement in biofilm formation or regulation, according to the available literature.

PA number	Gene name	PA number	Gene name	PA number	Gene name
PA0762	*algU*	PA2244	*pslN*	PA3545	*algG*
PA0764	*mucB*	PA2245	*pslO*	PA3546	*algX*
PA0765	*mucC*	PA2663	*ppyR*	PA3547	*algL*
PA1097	*fleQ*	PA3058	*pelG*	PA3548	*algI*
PA2231	*pslA*	PA3059	*pelF*	PA3549	*algJ*
PA2232	*pslB*	PA3060	*pelE*	PA3550	*algF*
PA2233	*pslC*	PA3061	*pelD*	PA3551	*algA*
PA2234	*pslD*	PA3062	*pelC*	PA3622	*rpoS*
PA2235	*pslE*	PA3063	*pelB*	PA4033	*mucE*
PA2236	*pslF*	PA3064	*pelA*	PA4446	*algW*
PA2237	*pslG*	PA3385	*amrZ*	PA5253	*algP*
PA2238	*pslH*	PA3540	*algD*	PA5255	*algQ*
PA2239	*pslI*	PA3541	*alg8*	PA5261	*algR*
PA2240	*pslJ*	PA3542	*alg44*	PA5322	*algC*
PA2242	*pslL*	PA3543	*algK*	PA5346	*sadB*
PA2243	*pslM*	PA3544	*algE*	PA5483	*algB*

Table 7.2. Genes assigned with the additional category "i: Two-component systems, probable two-component systems and Hpt proteins".

PA number	Gene name	PA number	Gene name	PA number	Gene name
PA0033	*hptC*	PA1992	*ercS*	PA4032	
PA0034		PA2177		PA4036	
PA0173		PA2479		PA4080	
PA0178		PA2480		PA4101	*bfmR*
PA0179		PA2523	*czcR*	PA4102	*bfmS*
PA0408	*pilG*	PA2524	*czcS*	PA4112	
PA0409	*pilH*	PA2571		PA4117	*bphP*
PA0413	*chpA*	PA2572		PA4196	*bfiR*
PA0414	*chpB*	PA2583		PA4197	*bfiS*
PA0463	*creB*	PA2586	*gacA*	PA4293	*pprA*
PA0464	*creC*	PA2656	*carS*	PA4296	*pprB*
PA0471	*fluR*	PA2657	*carR*	PA4380	*colS*
PA0600	*agtS*	PA2686	*pfeR*	PA4381	*colR*
PA0601	*agtR*	PA2687	*pfeS*	PA4396	
PA0756		PA2798		PA4398	
PA0757		PA2809	*copR*	PA4493	*roxR*
PA0928	*gacS*	PA2810	*copS*	PA4494	*roxS*
PA0929		PA2818	*arr*	PA4546	*pilS*
PA0930		PA2824	*sagS*	PA4547	*pilR*
PA0991	*hptA*	PA2881		PA4725	*cbrA*
PA1098	*fleS*	PA2882		PA4726	*cbrB*
PA1099	*fleR*	PA3044	*rocS2*	PA4776	*pmrA*
PA1157		PA3045	*rocA2*	PA4777	*pmrB*
PA1158		PA3077	*cprR*	PA4843	*gcbA*
PA1179	*phoP*	PA3078	*cprS*	PA4856	*retS*
PA1180	*phoQ*	PA3191	*gtrS*	PA4885	*irlR*
PA1243		PA3192	*gltR*	PA4886	
PA1335	*aauR*	PA3204		PA4982	
PA1336	*aauS*	PA3206		PA4983	
PA1396		PA3271		PA5124	*ntrB*
PA1397		PA3345	*hptB*	PA5125	*ntrC*
PA1437		PA3346		PA5165	*dctB*
PA1438		PA3347		PA5166	*dctD*
PA1456	*cheY*	PA3462		PA5199	*amgS*
PA1458		PA3604	*erdR*	PA5200	*amgR*
PA1459		PA3702	*wspR*	PA5261	*algR*
PA1611		PA3703	*wspF*	PA5262	*algZ*
PA1636	*kdpD*	PA3704	*wspE*	PA5360	*phoB*
PA1637	*kdpE*	PA3714		PA5361	*phoR*
PA1798	*parS*	PA3771		PA5364	
PA1799	*parR*	PA3878	*narX*	PA5483	*algB*

PA1976	*ercS'*	PA3879	*narL*	PA5484	*kinB*
PA1978	*erbR*	PA3946	*rocS1*	PA5511	*mifR*
PA1979	*eraS*	PA3948	*rocA1*	PA5512	*mifS*
PA1980	*eraR*	PA3974	*ladS*		

Regulatory RNAs where already assigned category "O: Post-translational modification, protein turnover, chaperones". They were additionally given a % category sign for "regulatory RNAs".

Table 7.3. Genes encoding small RNAs that were assigned the additional "%: Regulatory RNAs" category.

PA number	Gene name
PA4704.1	*prrF1*
PA4704.2	*prrF2*
PA0527.1	*rsmY*
PA3621.1	*rsmZ*

Genes related to T3SS and that were not were classified in the category "U: Intracellular trafficking, secretion and vesicular transport" are listed in **Table 7.4**. Likewise, genes related to motility were assigned "N: cell motility", and are listed in **Table 7.5.**

Table 7.4. Genes involved in T3SS in *P. aeruginosa* that were assigned category "U: Intracellular trafficking, secretion and vesicular transport"

PA number	Gene name	PA number	Gene name	PA number	Gene name
PA1698	*popN*	PA1707	*pcrH*	PA1720	*pscG*
PA1699	*pcr1*	PA1708	*popB*	PA1721	*pscH*
PA1700	*pcr2*	PA1709	*popD*	PA1722	*pscI*
PA1701	*pcr3*	PA1714	*exsD*	PA1723	*pscJ*
PA1702	*pcr4*	PA1715	*pscB*	PA1724	*pscK*
PA1703	*pcrD*	PA1716	*pscC*	PA1725	*pscL*
PA1704	*pcrR*	PA1717	*pscD*		
PA1705	*pcrG*	PA1718	*pscE*		
PA1706	*pcrV*	PA1719	*pscF*		

Table 7.5. Genes involved in *P. aeruginosa* motility that were assigned category "N: cell motility".

PA number	Gene name	PA number	Gene name	PA number	Gene name
PA1077	*flgB*	PA1092	*fliC*	PA1446	*fliP*
PA1078	*flgC*	PA1094	*fliD*	PA1447	*fliQ*
PA1079	*flgD*	PA1100	*fliE*	PA1448	*fliR*

PA1080	*flgE*	PA1101	*fliF*	PA1449	*flhB*
PA1081	*flgF*	PA1102	*fliG*	PA1450	
PA1082	*flgG*	PA1103		PA1451	
PA1083	*flgH*	PA1104	*fliL*	PA1452	*flhA*
PA1084	*flgI*	PA1105	*fliJ*	PA1453	*flhF*
PA1085	*flgJ*	PA1441	*fliK*	PA1454	*fleN*
PA1086	*flgK*	PA1442	*fliL*	PA1455	*fliA*
PA1087	*flgL*	PA1443	*fliM*	PA1097	*fleQ*
PA3351	*flgM*	PA1444	*fliN*	PA1098	*fleS*
PA1091	*fgtA*	PA1445	*fliO*	PA1099	*fleR*

Genes involved in the regulation of c-di-GMP were assigned an additional category. They are listed in **Table 7.6**.

Table 7.6. Genes containing GGDEF, EAL or HD-GYP motifs, which were assigned the additional category "[a]: c-di-GMP regulation".

PA number	Gene name	PA number	Gene name	PA number	Gene name
PA0169	*siaD*	PA2133		PA4108	
PA0285		PA2200		PA4332	*sadC*
PA0290		PA2567		PA4367	*bifA*
PA0338		PA2572		PA4396	
PA0575		PA2771		PA4601	*morA*
PA0847		PA2818	*arr*	PA4781	
PA0861	*rbdA*	PA2870		PA4843	*gcbA*
PA1107	*roeA*	PA3177		PA4929	
PA1120	*tpbB*	PA3258		PA4959	*fimX*
PA1181		PA3311	*nbdA*	PA5017	*dipA*
PA1433		PA3343		PA5295	
PA1727	*mucR*	PA3702	*wspR*	PA5442	
PA1851		PA3825		PA5487	
PA2072		PA3947	*rocR*		

Overall, 5563 genes from *P. aeruginosa* were annotated. The genes that were not included in this functional database are listed in **Table 7.7**.

Table 7.7. Genes which were not included in the functional annotation database.

PA number	Gene name	PA number	Gene name	PA number	Gene name
PA0026	*plcB*	PA1250	*aprI*	PA3104	*xcpP*
PA0044	*exoT*	PA1324.1	*P9*	PA3154	*wzy*
PA0070	*tagQ1*	PA1431	*rsaL*	PA3164	
PA0162	*opdC*	PA1496		PA3304.1	*P18*
PA0189		PA1525	*alkB2*	PA3305.1	*phrS*
PA0195.1	*pntAB*	PA1615		PA3361	*lecB*
PA0215		PA1632	*kdpF*	PA3366.1	*amiL*
PA0216		PA1682		PA3407	*hasAp*
PA0240		PA1710	*exsC*	PA3484	*tse3*
PA0291	*oprE*	PA1711	*exsE*	PA3547	*algL*
PA0674	*vreA*	PA1712	*exsB*	PA3557	*arnE*
PA0680		PA1714	*exsD*	PA3558	*arnF*
PA0683		PA1774	*crfX*	PA3588	
PA0714.1	*phrD*	PA1781.1	*P11*	PA3701	*prfB*
PA0717		PA1844	*tse1*	PA3719	*armR*
PA0718		PA1848		PA3841	*exoS*
PA0719		PA1985	*pqqA*	PA4033	*mucE*
PA0720		PA1988	*pqqD*	PA4137	
PA0721		PA2068		PA4175	*piv*
PA0722		PA2113	*opdO*	PA4179	
PA0723	*coaB*	PA2140		PA4218	*ampP*
PA0724		PA2191	*exoY*	PA4270.1	*P26*
PA0725		PA2213		PA4272.1	*P27*
PA0727		PA2420		PA4393	*ampG*
PA0748		PA2505	*opdT*	PA4406.1	
PA0755	*opdH*	PA2570	*lecA*	PA4421.1	*rnpB*
PA0826.1		PA2593	*qteE*	PA4451.1	*P35*
PA0826.2	*ssrA*	PA2674		PA4501	*opdD*
PA0836.1	*P5*	PA2700	*opdB*	PA4590	*pra*
PA0843	*plcR*	PA2702	*tse2*	PA4596	*esrC*
PA0887.1	*P7*	PA2703	*tsi2*	PA4661	*pagL*
PA0958	*oprD*	PA2744.1	*P13*	PA4726.1	*P36*
PA0984		PA2760	*oprQ*	PA4726.11	*crcZ*
PA1025		PA2794		PA4726.2	*P30*
PA1030.1	*P8*	PA2832	*tpm*	PA4758.1	*P32*
PA1112.1		PA2853	*oprI*	PA4898	*opdK*
PA1121	*yfiR*	PA2886	*atuA*	PA5181.1	*P34*
PA1122		PA2942.1	*P15*	PA5316.1	
PA1148	*toxA*	PA2958.1	*rgsA*	PA5471.1	
PA1169		PA3038		PA5496	*nrdJb*

PA1245	*aprX*	PA3082	*gbt*	PA5559	*atpE*

7.1.2 Rationale for the assays in agar plates

A lack of cell accumulation was observed under conditions in which swarming motility is impeded, that does not necessarily correlate with growth defects in liquid cultures. Therefore, it was hypothesised that growth may be inhibited in swarming plates under conditions where motility is inhibited, caused by scarce nutrient availability. In other words, cells impaired in their motility stop growing once nutrients in that area are uptaken.

As a preliminary step for the determination of secreted factors from semi-solid media, the growth of cells in swarming plates with and without 2TDC was determined.

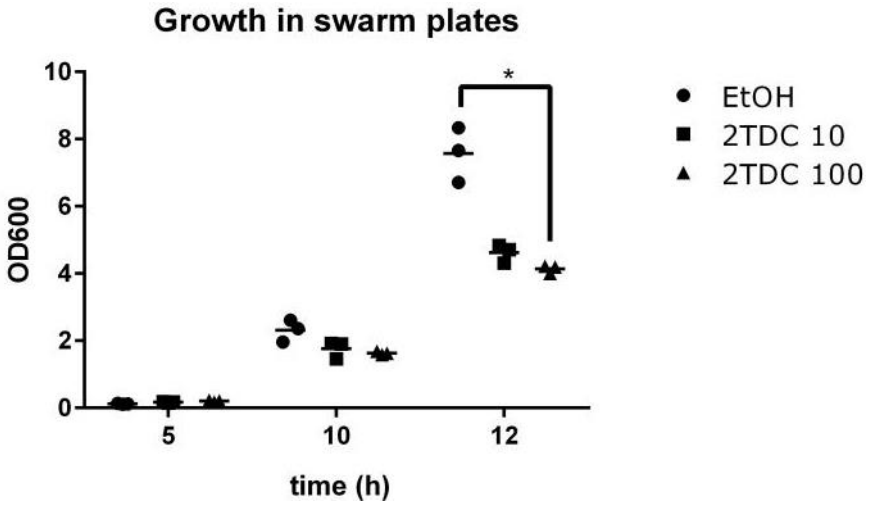


Figure 7.1. Impact on bacterial growth in motility plates. ***P. aeruginosa*** PAO1-L cells were spotted onto swarming plates in the presence of increasing concentrations of 2TDC. After 5 h, 10 h and 12 h of incubation at 37 ºC; cells were recovered from the plates with determined volumes of water and the OD_{600} of the suspensions was measured. Results show that less cells were present in the plates with 2TDC at long incubation times, showing that the inhibition of motility impairs cell growth.

These results prompted to grow cells in the whole area of the Petri dishes in experiments to quantify secreted factors in semi-solid media.

7.1.3 Determination of rhamnolipids by thin layer chromatography

Rhamnolipids were quantified throughout this study using thin layer chromatography (TLC). A proof of concept was performed and can be seen in **Figure 7.2**.

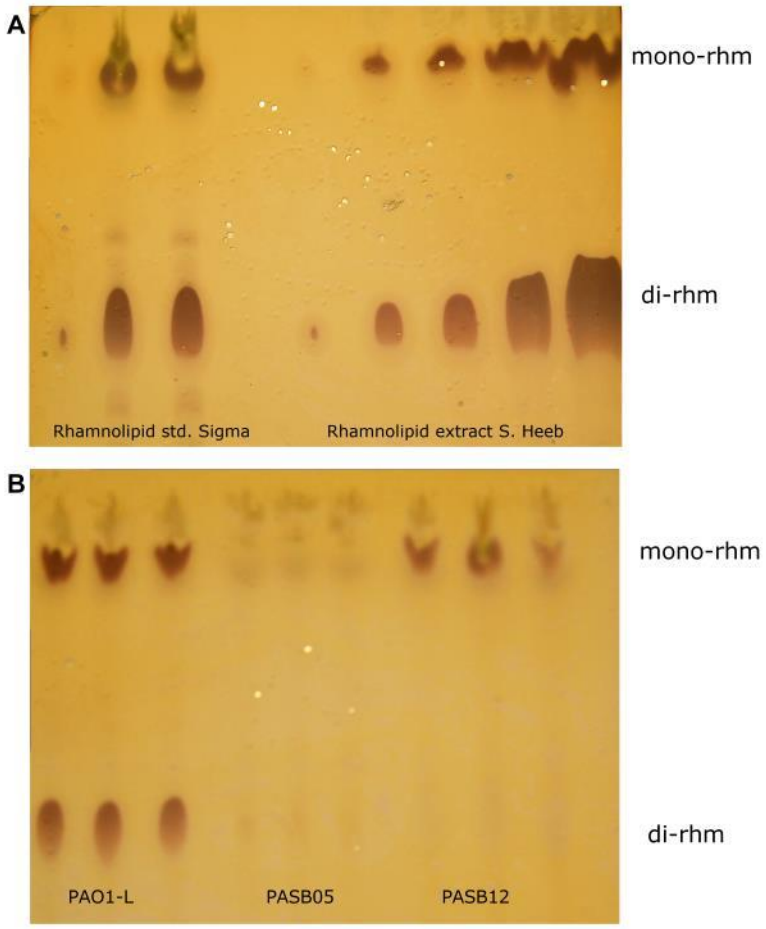


Figure 7.2. Proof of concept for the determination of rhamnolipids by thin layer chromatography (TLC). A, Commercial rhamnolipid standards from Sigma and extracts performed at The University of Nottingham by Stephan Heeb were spotted onto TLC plates. Both mono- and di-rhamnolipids are detected. **B,** Extracts from PAO1-L (wild-type), PASB05 (Δ*rhlA*) and PASB12 (Δ*rhlC*). As expected, the wild-type presents both mono- and di-rhamnolipids; while the *rhlA*- mutant does not produce either rhamnolipid and the *rhlC* mutant presents mono-rhamnolipids but not di-rhamnolipids.

7.2 Additional information on Chapter 3

7.2.1 Summary of RNA-seq data with and without CDA

Table 7.8. Overview of the number of genes differentially expressed according to two statistical tests, in the presence and absence of 100 μM CDA. Numbers in brackets represent those genes which had one of the RPKM being 0. In those genes, the folds are very high as 0 was substituted by 0.000001 for analytic purposes. up, up-regulated by CDA; dw, down-regulated by CDA.

	<2-fold		2-4 fold		>4-fold	
	up	dw	up	dw	up	dw
Baggerly's	174	86	371	128	227 (21)	154 (21)
Intersection	0	0	0	0	20	32 (1)
DESeq	0	0	0	1	20	41 (1)

7.2.2 Biofilm disruption in M9-glucose

Biofilm dispersion in the presence of CDA was assessed in two growth media, LB and M9 supplemented with glucose. Results in M9 are shown in **Figure 7.3**.

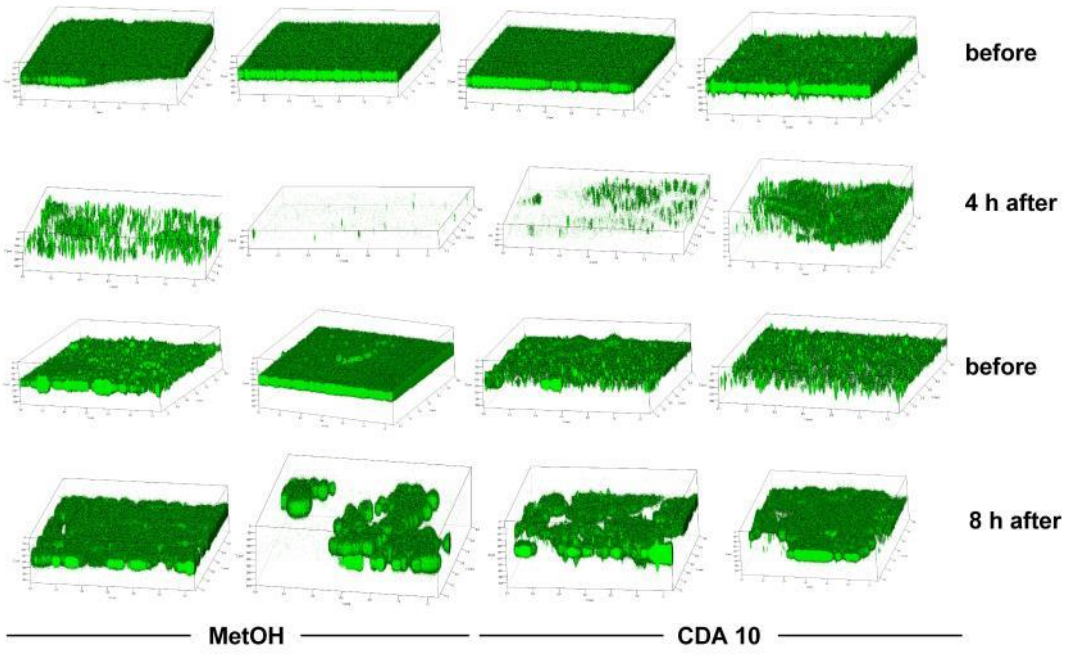


Figure 7.3. Impact of CDA in the dispersion of biofilms of *P. aeruginosa* PAO1-L, in M9 supplemented with glucose. Biofilms were grown overnight, the supernatant was removed and they were subsequently visualised by CLSM ("before"). Then, fresh medium was added, supplemented with 10 μM of CDA or the solvent control, MetOH. Biofilms were allowed to grow under those conditions for either 4 h or 8 h, and were then visualised again ("after"). Results show that CDA does not impact biofilm dispersion, under those conditions.

7.2.3 Detection of rhamnolipids by LC-MS/MS

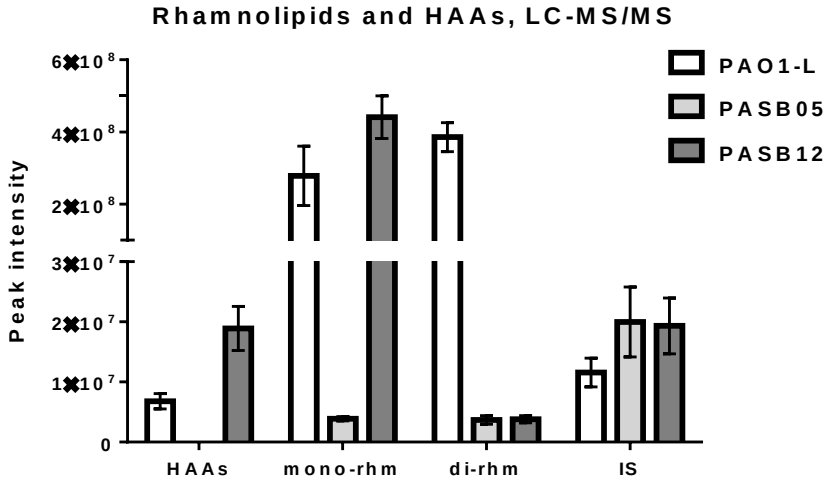


Figure 7.4. Detection of mono- and di-rhamnolipids, and HAAs by LC-MS/MS. Supernatants of a wild-type PAO1, the Δ*rhlA* mutant (PASC05) and the Δ*rhlC* mutant (PASB12) were spiked with the internal standard (IS) and extracted with EtOAc and run in an LC-MS/MS method. As expected, the PAO1-L supernatant contains HAAs, mono-rhamnolipids and di-rhamnolipids. PASB05 only presents small peaks for mono- and di-rhamnolipid which correspond to background noise. PASB12 produced HAAs and mono-rhamnolipids but not di-rhamnolipids. Error bars represent one standard deviation of the means.

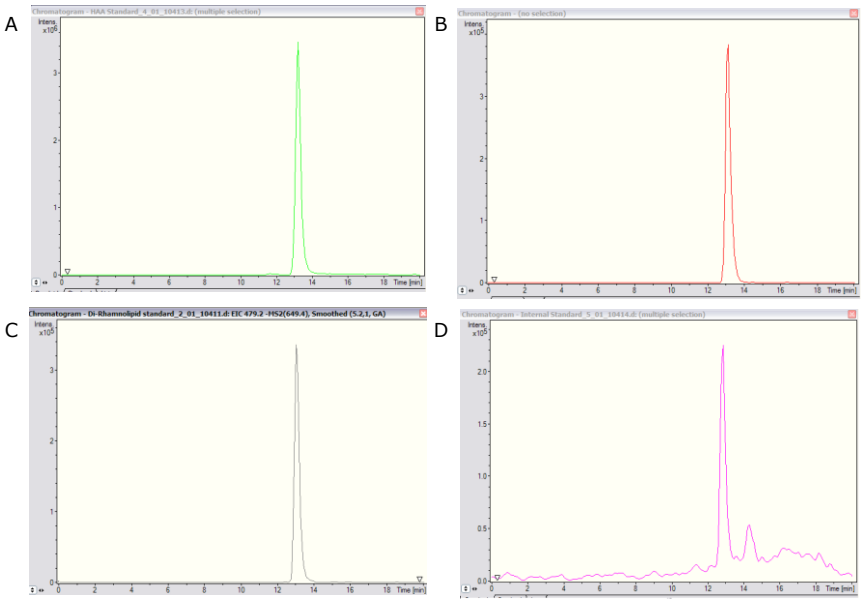


Figure 7.5. Chromatograms of standards for the rhamnolipid detection by LC-MS/MS. A, HAA standard; **B,** mono-rhamnolipid; **C,** di-rhamnolipid; **D,** internal standard.

7.2.4 Phenotypical characterisation of PA4982

PA4982 has been suggested as the SK responsible for the perception of CDA in *P. aeruginosa.* The in-frame deletion mutant for PA4982 was constructed and named PADP127, and a series of assays were performed. Results in **Figure 7.6** and **Figure 7.7** show that this mutant is not impaired in swarming, twitching or biofilm formation.

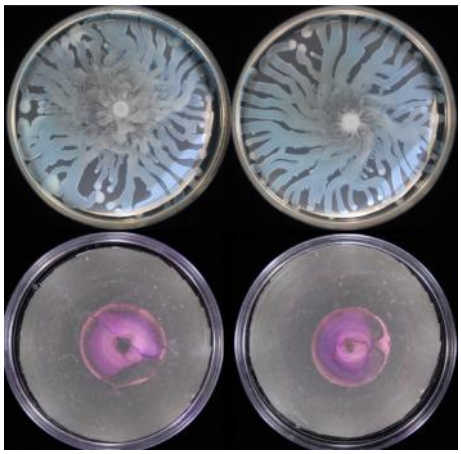


Figure 7.6. Swarming and twitching motilities of PADP127 (Δ4982) as compared to PAO1-L. Cultures of PAO1-L or the isogenic mutant PADP127 were spotted in swarming **(upper row)** or twitching plates **(lower row)**, which were then incubated at 37 ºC for 16 h. The agar was removed from the twitching plates and the cells were stained with crystal violet 1 %. Pictures on the left shows representative results for the PAO1-L wild-type; while pictures on the right correspond to PADP127. Three independent assays were performed for each motility.

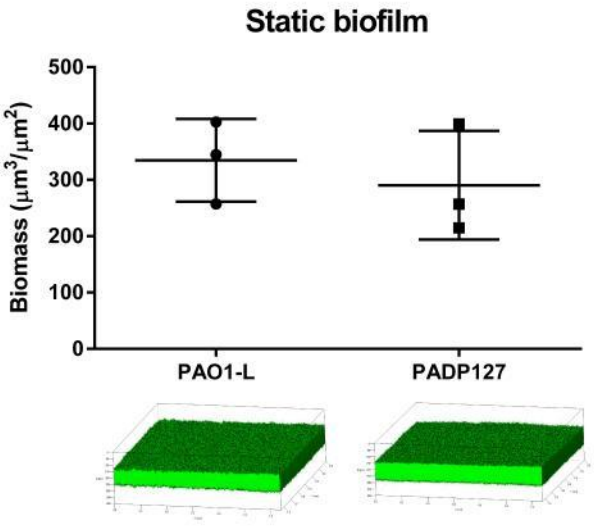


Figure 7.7. Biofilm formation of PADP127 (Δ4982) as compared to PAO1-L. Biofilms were grown statically in chamber slides, for 16 h at 37 ºC, in LB. The supernatant was removed and the biofilms were visualised by CLSM. The biomass was quantified with Image J and the plugin Comstat2. Error bars represent one standard deviation of the means, from independent replicates.

7.3 Additional information on Chapter 4

7.3.1 Analysis of RNA-seq data CbsA

RNA-seq results were statistically assessed with two tests: the Baggerly's and the DESeq test**. Table 7.9** shows the number of genes that were differentially expressed according to each test, and the intersection between both tests.

Table 7.9. Overview of the number of genes differentially expressed in the RNA-seq of CbsA. Statistical significance was assessed with 2 statistical tests, in the conditional mutant for CbsA in the presence (induced condition) and absence (repressed condition) of 1 mM IPTG. up, up-regulated upon CbsA overexpression; dw, down-regulated by CbsA overexpression.

	<2-fold		**2-4 fold**		**>4-fold**	
	up	dw	up	dw	up	dw
Baggerly's	397	2119	15	58	3	3
Intersection	260	94	39	6	0	1
DESeq	260	94	39	6	0	1

7.3.2 Interaction of PA0744 and PA0745

The String Database (http://string-db.org/, [484]) was used to find proteins interacting with PA0744. Homologues for both PA0745 and PA0744 are found in multiple genomes and are often found together, which suggests a possible interaction between these genes or the proteins that they encode (**Figure 7.8**).

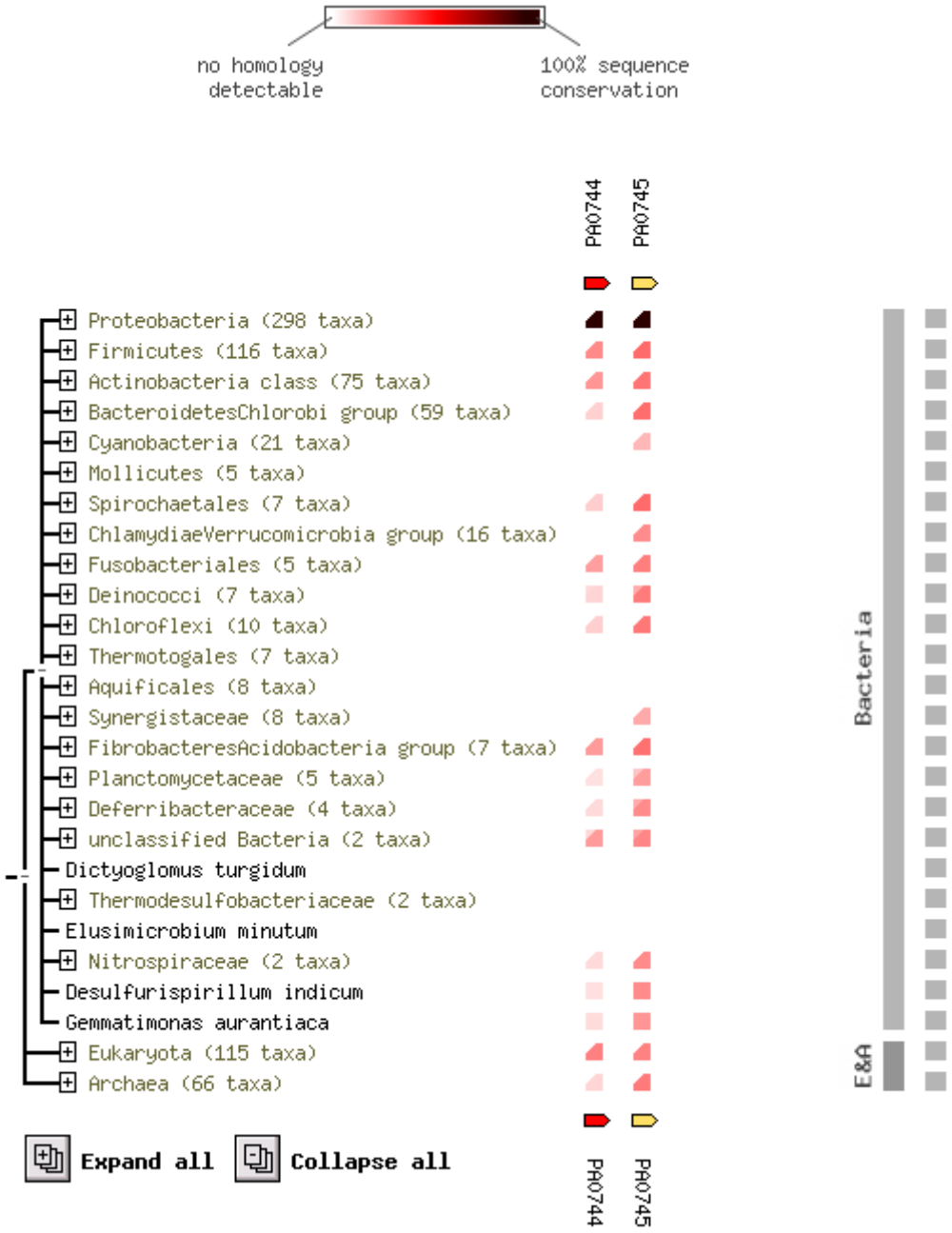


Figure 7.8. Occurrence of PA0744 and PA0745 in genomes, as seen by the String database (consulted 10th May 2016).

The Gene Expression Omnibus (GEO) database was used to find expression profiles of PA0744, and then to ascertain if other neighbouring genes were regulated in a similar manner. As can be seen in **Table 7.10**, PA0744 and PA0745 are frequently co-regulated; as well as the rest of the genes presented, albeit to a lesser extent.

Table 7.10. Gene expression profiles of various enoyl-CoA hydratases relevant to this thesis. The Gene Expression Omnibus (GEO) database was used to find possible co-regulations in the PA0743-PA0747 genes. AZM, azythromicin.

Expression conditions	PA0747	PA0746	PA0745	PA0744	PA0743
Repressed by protoanemonin	-	-	+	+	+
Induced by H_2O_2	+	+	+	+	-
Repressed by AZM	-	+	+	+	-
Induced in planktonic vs biofilm	+	+	+	+	+
Induced by airway epithelia	+	+	+	+	+
Repressed in Δ*kinB* Δ*rpoN* vs Δ*kinB*	-	-	-	+	-

7.3.3 Pyoverdine in PA0744 and PA0745 mutants

Pyoverdine expression was measured in various mutants for PA0744 and PA0745. Results from **Figure 7.9** show that pyoverdine is not affected by the mutations of these ECH in M9-glucose; while there is a small difference in the pyoverdine production in CAA.

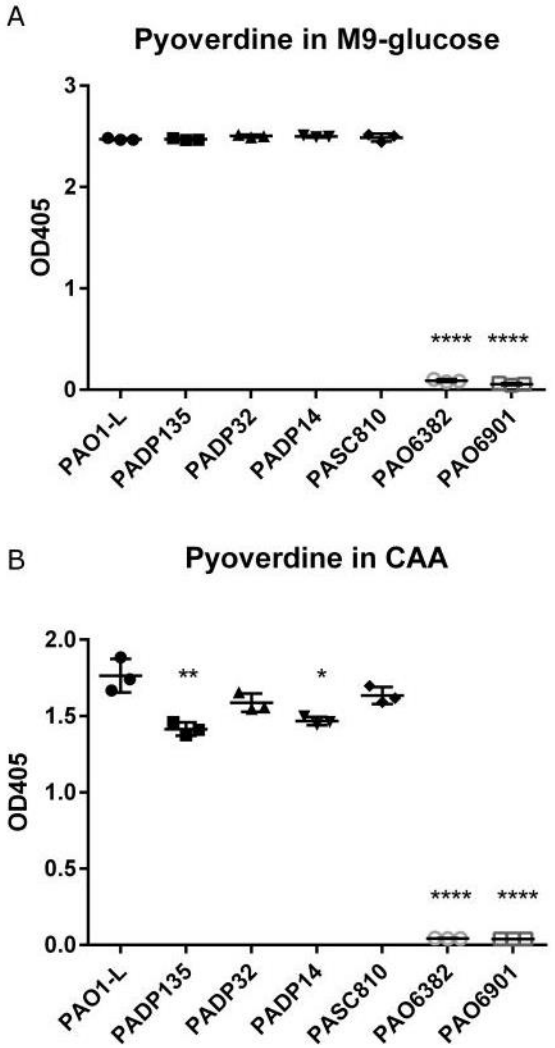


Figure 7.9. Pyoverdine production from selected enoyl-CoA hydratase (ECH) mutants. PAO1-L (wild-type), PADP135 (Δ0745), PADP32 (non-polar PA0745 mutant, aka 0745*), PADP14 (Δ0744 Δ0745), PASC810 (Δ0744), PAO6382 (Δ*pvdF*) and PAO6901 (*pvdS::*Gm) were grown in M9-glucose **(A)** or CAA **(B)**, and the OD_{405} of the filtered supernatants was determined, corresponding to the levels of pyoverdine being produced. Error bars represent one standard deviation from the means. T-tests were performed to assess statistical significance. ****, p-value<0.0001.

7.3.4 IPTG does not affect rhamnolipid expression

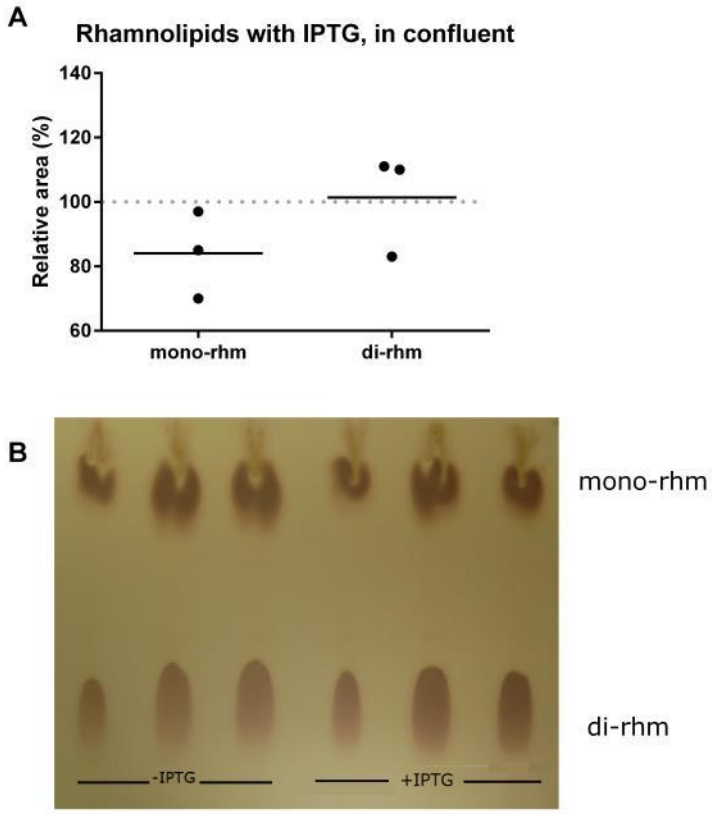


Figure 7.10. Impact of IPTG on the rhamnolipid production of PAO1. Cultures of PAO1-L were incubated in agar plates, in the presence and absence of 1 mM IPTG. Rhamnolipids were extracted with EtOAc and run in normal phase TLC. Results show that IPTG does not affect mono- or di-rhamnolipid production.

7.4 Additional information on Chapter 5

7.4.1 Impact of 2TDC in *P. aeruginosa* chemotaxis

Results with 2TDC suggest that this molecule affects community behaviours, possibly related to pili. A preliminary chemotaxis assay was performed, and results in **Figure 7.11** and show that the 2TDC does not repel *P. aeruginosa* cells. A small reduction in swarming motility was observed, but this is likely the result of the 2TDC acting in the gas phase.

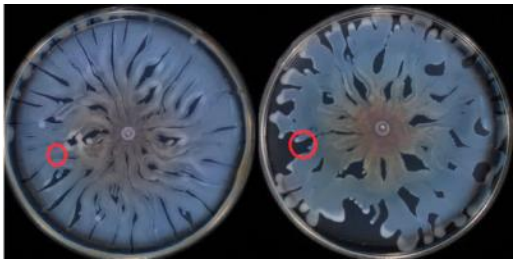


Figure 7.11. Chemotaxis assay of *P. aeruginosa* PAO1-L in the absence and presence of 2TDC. A swarming assay was performed with PAO1-L, and adding a drop of MetOH **(left)** or 2TDC 100 mM **(right)**. The red circles represent the area where the compounds were added.

7.4.2 Determination of pyoverdine production from plates

The pyoverdine production of *P. aeruginosa* PAO1-L was determined in the presence and absence of 2TDC. Prior to that, a proof of concept was performed to ensure the consistency of the method. Results in **Figure 7.12** show that the pyoverdine mutants present a marked reduction in the OD_{405} as compared to the PAO1-L wild-type, related to the secretion of this pigment.

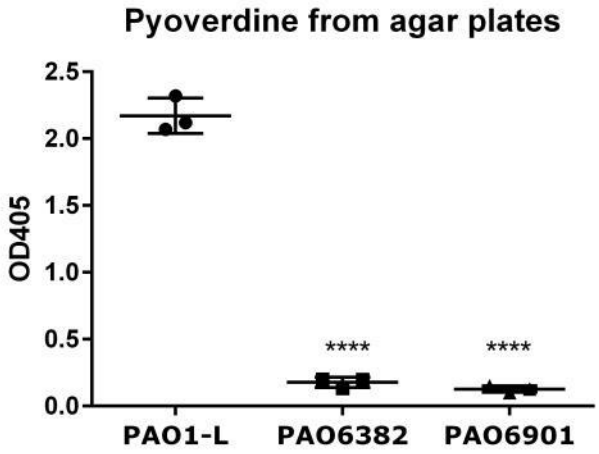


Figure 7.12. Determination of pyoverdine production on agar plates. The wild-type PAO1-L, PAO6382 (Δ*pvdF*) and PAO6901 (*pvdS*::Gm) were grown in agar plates of CAA. After 16 h incubation at 37 ºC, pyoverdine was recovered from the plates and the resulting suspension was filtered, following the determination of OD_{405}. Error bars represent one standard deviation of the means. T-tests were used to assess for statistical significance. ****, $p<0.0001$.

7.4.3 Determination of pyocyanin from agar plates

The production of pyocyanin from *P. aeruginosa* grown in agar plates was assessed, as a previous step for the determination of the impact of 2TDC in this phenotype. Results in **Figure 7.13** show that the Δ*pqsA* mutant presents a marked reduction on pyocyanin production as compared with the isogenic wild-type PAO1-L.

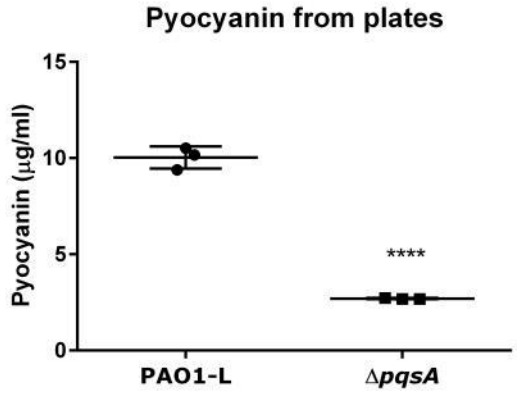


Figure 7.13. Determination of pyocyanin production on agar plates. The ΔpqsA-L strain was grown in swarming plates, pyocyanin was recovered from the agar after incubation at 37 ºC for 16 h and the resulting filtered supernatants were extracted with chloroform. Error bars represent one standard deviation of the means. A t-test was used to assess for statistical significance. ****, p-value<0.0001.

7.4.4 Determination of AQ in *P. aeruginosa* cultures grown on agar plates

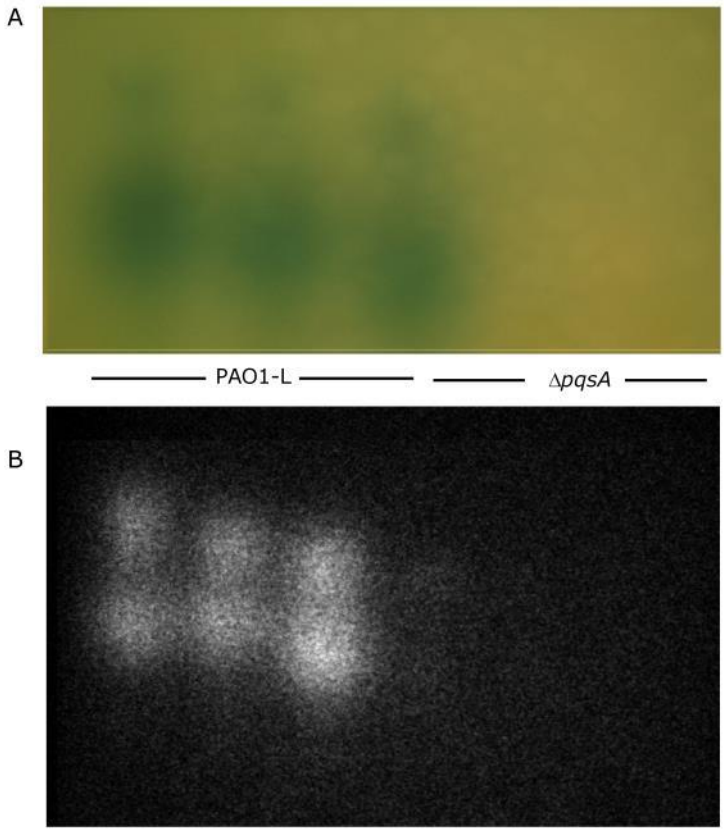


Figure 7.14. Determination of PQS and HHQ from *P. aeruginosa* grown on agar plates. Swarming plates were inoculated with *P. aeruginosa* PAO1-L or the isogenic Δ*pqsA* mutant. Secreted factors were recovered after 16 h incubation at 37 ºC, the resulting suspension was filtered and extracted with EtOAc. Extractions were subsequently spotted on thin layer chromatography plates, run and overlaid with the biosensor strain PAO1-L Δ*pqsA,* CTX::P*pqsA-luxCDABE.* **A,** photography showing the production of pyocyanin by the biosensor as a result of PQS and HHQ being present in the extracts. **B,** luminescence produced by the contact of the biosensor with PQS and HHQ.

BIBLIOGRAPHY

[1] Trunk K, Benkert B, Quack N, Munch R, Scheer M, Garbe J, et al. Anaerobic adaptation in *Pseudomonas aeruginosa*: definition of the Anr and Dnr regulons. Environ Microbiol 2010;12:1719-33.

[2] Colwell RR. A study of features used in the diagnosis of *Pseudomonas aeruginosa*. J Gen Microbiol 1964;37:181-94.

[3] Haynes WC. *Pseudomonas aeruginosa*-its characterization and identification. J Gen Microbiol 1951;5:939-50.

[4] Hilker R, Munder A, Klockgether J, Losada PM, Chouvarine P, Cramer N, et al. Interclonal gradient of virulence in the *Pseudomonas aeruginosa* pangenome from disease and environment. Environ Microbiol 2015;17:29-46.

[5] Ozer EA, Allen JP, Hauser AR. Characterization of the core and accessory genomes of *Pseudomonas aeruginosa* using bioinformatic tools Spine and AGEnt. BMC Genomics 2014;15:737-54.

[6] Pohl S, Klockgether J, Eckweiler D, Khaledi A, Schniederjans M, Chouvarine P, et al. The extensive set of accessory *Pseudomonas aeruginosa* genomic components. FEMS Microbiol Lett 2014;356:235-41.

[7] Goodman AL, Merighi M, Hyodo M, Ventre I, Filloux A, Lory S. Direct interaction between sensor kinase proteins mediates acute and chronic disease phenotypes in a bacterial pathogen. Genes Dev 2009;23:249-59.

[8] Stover CK, Pham XQ, Erwin AL, Mizoguchi SD, Warrener P, Hickey MJ, et al. Complete genome sequence of *Pseudomonas aeruginosa* PAO1, an opportunistic pathogen. Nature 2000;406:959-64.

[9] Matz C, Moreno AM, Alhede M, Manefield M, Hauser AR, Givskov M, et al. *Pseudomonas aeruginosa* uses type III secretion system to kill biofilm-associated amoebae. ISME J 2008;2:843-52.

[10] Scaccabarozzi L, Leoni L, Ballarini A, Barberio A, Locatelli C, Casula A, et al. *Pseudomonas aeruginosa* in dairy goats: genotypic and phenotypic comparison of intramammary and environmental isolates. PloS one 2015;10:10.

[11] D'Argenio DA, Gallagher LA, Berg CA, Manoil C. *Drosophila* as a model host for *Pseudomonas aeruginosa* infection. J Bacteriol 2001;183:1466-71.

[12] Tan MW, Mahajan-Miklos S, Ausubel FM. Killing of *Caenorhabditis elegans* by *Pseudomonas aeruginosa* used to model mammalian bacterial pathogenesis. Proc Natl Acad Sci USA 1999;96:715-20.

[13] Morrison AJ, Wenzel RP. Epidemiology of infections due to *Pseudomonas aeruginosa*. Rev Infect Dis 1984;6:S627-S42.

[14] Sadikot RT, Blackwell TS, Christman JW, Prince AS. Pathogen-host interactions in *Pseudomonas aeruginosa* pneumonia. Am J Respir Crit Care Med 2005;171:1209-23.

[15] Wu CT, Huang JL. Multiple ecthyma gangrenosum in a healthy infant with community-acquired *Pseudomonas aeruginosa* sepsis. Pediatr Emerg Care 2010;26:750-1.

[16] Balasubramanian D, Schneper L, Kumari H, Mathee K. A dynamic and intricate regulatory network determines *Pseudomonas aeruginosa* virulence. Nucleic Acids Res 2013;41:1-20.

[17] Thuong M, Arvaniti K, Ruimy R, de la Salmonière P, Scanvic-Hameg A, Lucet JC, et al. Epidemiology of *Pseudomonas aeruginosa* and risk factors for carriage acquisition in an intensive care unit. J Hosp Infect 2003;53:274-82.

[18] Valles J, Mariscal D, Cortes P, Coll P, Villagra A, Diaz E, et al. Patterns of colonization by *Pseudomonas aeruginosa* in intubated patients: a 3-year prospective study of 1,607 isolates using pulsed-field gel electrophoresis with implications for prevention of ventilator-associated pneumonia. Intens Care Med 2004;30:1768-75.

[19] Chua SL, Liu Y, Yam JK, Chen Y, Vejborg RM, Tan BG, et al. Dispersed cells represent a distinct stage in the transition from bacterial biofilm to planktonic lifestyles. Nat Commun 2014;5:4462.

[20] Cigana C, Lore NI, Bernardini ML, Bragonzi A. Dampening host sensing and avoiding recognition in *Pseudomonas aeruginosa* pneumonia. J Biomed Biotechnol 2011;2011:852513.

[21] Turner KH, Everett J, Trivedi U, Rumbaugh KP, Whiteley M. Requirements for *Pseudomonas aeruginosa* acute burn and chronic surgical wound infection. PLoS Genet 2014;10:e1004518.

[22] Bodey GP, Bolivar R, Fainstein V, Jadeja L. Infections caused by *Pseudomonas aeruginosa*. Rev Infect Dis 1983;5:279-313.

[23] Cornelis P, Dingemans J. *Pseudomonas aeruginosa* adapts its iron uptake strategies in function of the type of infections. Front Cell Infect Microbiol 2013;3:75.

[24] Feldman M, Bryan R, Rajan S, Scheffler L, Brunnert S, Tang H, et al. Role of flagella in pathogenesis of *Pseudomonas aeruginosa* pulmonary infection. Infect Immun 1998;66:43-51.

[25] Williams BJ, Dehnbostel J, Blackwell TS. *Pseudomonas aeruginosa*: host defence in lung diseases. Respirology 2010;15:1037-56.

[26] Engel J, Balachandran P. Role of *Pseudomonas aeruginosa* type III effectors in disease. Curr Opin Microbiol 2009;12:61-6.

[27] Goodman AL, Kulasekara B, Rietsch A, Boyd D, Smith RS, Lory S. A signaling network reciprocally regulates genes associated with acute infection and chronic persistence in *Pseudomonas aeruginosa*. Dev Cell 2004;7:745-54.

[28] Jimenez PN, Koch G, Thompson JA, Xavier KB, Cool RH, Quax WJ. The multiple signaling systems regulating virulence in *Pseudomonas aeruginosa*. Microbiol Mol Biol Rev 2012;76:46-65.

[29] Breidenstein EBM, de la Fuente-Núñez C, Hancock REW. *Pseudomonas aeruginosa*, all roads lead to resistance. Trends Microbiol 2011;19:419-26.

[30] Lopes SP, Ceri H, Azevedo NF, Pereira MO. Antibiotic resistance of mixed biofilms in cystic fibrosis: impact of emerging microorganisms on treatment of infection. Int J Antimicrob Agents 2012;40:260-3.

[31] Mann EE, Wozniak DJ. *Pseudomonas* biofilm matrix composition and niche biology. FEMS Microbiol Rev 2012;36:893-916.

[32] Harmsen M, Yang L, Pamp SJ, Tolker-Nielsen T. An update on *Pseudomonas aeruginosa* biofilm formation, tolerance, and dispersal. FEMS Immunol Med Microbiol 2010;59:253-68.

[33] Voynow JA, Fischer BM, Zheng S. Proteases and cystic fibrosis. Int J Biochem Cell Biol 2008;40:1238-45.

[34] Berg G, Eberl L, Hartmann A. The rhizosphere as a reservoir for opportunistic human pathogenic bacteria. Environ Microbiol 2005;7:1673-85.

[35] Rahme LG, Ausubel FM, Cao H, Drenkard E, Goumnerov BC, Lau GW, et al. Plants and animals share functionally common bacterial virulence factors. Proc Natl Acad Sci U S A 2000;97:8815-21.

[36] Starkey M, Rahme LG. Modeling *Pseudomonas aeruginosa* pathogenesis in plant hosts. Nat Protoc 2009;4:117-24.

[37] Walker TS, Bais HP, Déziel E, Schweizer HP, Rahme LG, Fall R, et al. *Pseudomonas aeruginosa*- plant root interactions. Pathogenicity, biofilm formation, and root exudation. Plant Physiol 2004;134:320-31.

[38] Mendes R, Garbeva P, Raaijmakers JM. The rhizosphere microbiome: significance of plant beneficial, plant pathogenic, and human pathogenic microorganisms. FEMS Microbiol Rev 2013;37:634-63.

[39] Sulochana MB, Jayachandra SY, Kumar SA, Parameshwar AB, Reddy KM, Dayanand A. Siderophore as a potential plant growth-promoting agent produced by *Pseudomonas aeruginosa* JAS-25. Appl Biochem Biotechnol 2014;174:297-308.

[40] Audenaert K, Pattery T, Cornelis P, Höfte M. Induction of systemic resistance to *Botrytis cinerea* in tomato by *Pseudomonas aeruginosa*

7NSK2: role of salicylic acid, pyochelin, and pyocyanin. Mol Plant-Microbe Interact 2002;15:1147-56.

[41] Radhapriya P, Ramachandran A, Anandham R, Mahalingam S. *Pseudomonas aeruginosa* RRALC3 enhances the biomass, nutrient and carbon contents of *Pongamia pinnata* seedlings in degraded forest soil. PloS one 2015;10:e0139881.

[42] Bhakthavatchalu S, Shivakumar S, Sullia S. Characterization of multiple plant growth promotion traits of *Pseudomonas aeruginosa* FP6, a potential stress tolerant biocontrol agent. Ann Biolol Res 2013;4:214-23.

[43] Pal KK, Tilak KV, Saxena AK, Dey R, Singh CS. Antifungal characteristics of a fluorescent *Pseudomonas* strain involved in the biological control of *Rhizoctonia solani*. Microbiol Res 2000;155:233-42.

[44] Kang C, Wu P, Li Y, Ruan B, Li L, Tran L, et al. Understanding the role of clay minerals in the chromium(VI) bioremoval by *Pseudomonas aeruginosa* CCTCC AB93066 under growth condition: microscopic, spectroscopic and kinetic analysis. World J Microbiol Biotechnol 2015;31:1765-79.

[45] Tang S, Yin H, Zhou S, Chen S, Peng H, Liu Z, et al. Simultaneous Cr(VI) removal and 2,2',4,4'-tetrabromodiphenyl ether (BDE-47) biodegradation by *Pseudomonas aeruginosa* in liquid medium. Chemosphere 2016;150:24-32.

[46] Perez Silva RM, Abalos Rodriguez A, Gomez Montes De Oca JM, Cantero Moreno D. Biosorption of chromium, copper, manganese and zinc by *Pseudomonas aeruginosa* AT18 isolated from a site contaminated with petroleum. Bioresour Technol 2009;100:1533-8.

[47] Sakthipriya N, Doble M, Sangwai JS. Systematic investigations on the biodegradation and viscosity reduction of long chain hydrocarbons using *Pseudomonas aeruginosa* and *Pseudomonas fluorescens*. Environ Sci Process Impacts 2016;18:386-97.

[48] Kotresha D, Vidyasagar GM. Isolation and characterisation of phenol-degrading *Pseudomonas aeruginosa* MTCC 4996. World J Microb Biot 2007;24:541-7.

[49] Mukherjee AK, Bordoloi NK. Biodegradation of benzene, toluene, and xylene (BTX) in liquid culture and in soil by *Bacillus subtilis* and *Pseudomonas aeruginosa* strains and a formulated bacterial consortium. Environ Sci Pollut Res Int 2012;19:3380-8.

[50] Shen HB, Yong XY, Chen YL, Liao ZH, Si RW, Zhou J, et al. Enhanced bioelectricity generation by improving pyocyanin production and membrane permeability through sophorolipid addition in *Pseudomonas aeruginosa*-inoculated microbial fuel cells. Bioresour Technol 2014;167:490-4.

[51] Fernández D, Rodríguez E, Bassas M, Viñas M, Solanas AM, Llorens J, et al. Agro-industrial oily wastes as substrates for PHA production by the new strain *Pseudomonas aeruginosa* NCIB 40045: effect of culture conditions. Biochem Eng J 2005;26:159-67.

[52] Singh AK, Mallick N. Exploitation of inexpensive substrates for production of a novel SCL-LCL-PHA co-polymer by *Pseudomonas aeruginosa* MTCC 7925. J Ind Microbiol Biotechnol 2009;36:347-54.

[53] Soberón-Chavez G, Lépine F, Déziel E. Production of rhamnolipids by *Pseudomonas aeruginosa*. Appl Microbiol Biotechnol 2005;68:718-25.

[54] Nitschke M, Costa SGVAO. Biosurfactants in food industry. Trends Food Sci Technol 2007;18:252-9.

[55] Costa SG, Lépine F, Milot S, Déziel E, Nitschke M, Contiero J. Cassava wastewater as a substrate for the simultaneous production of rhamnolipids and polyhydroxyalkanoates by *Pseudomonas aeruginosa*. J Ind Microbiol Biotechnol 2009;36:1063-72.

[56] Marsudi S, Unno H, Hori K. Palm oil utilization for the simultaneous production of polyhydroxyalkanoates and rhamnolipids by *Pseudomonas aeruginosa*. Appl Microbiol Biotechnol 2008;78:955-61.

[57] Hay ID, Ur Rehman Z, Moradali MF, Wang Y, Rehm BH. Microbial alginate production, modification and its applications. Microb Biotechnol 2013;6:637-50.

[58] Ertesvag H, Valla S. Biosynthesis and applications of alginates. Polym Degradation Stab 1998;59:85-91.

[59] Karadzic I, Masui A, Zivkovic LI, Fujiwara N. Purification and characterization of an alkaline lipase from *Pseudomonas aeruginosa* isolated from putrid mineral cutting oil as component of metalworking fluid. J Biosci Bioeng 2006;102:82-9.

[60] Sharon C, Furugoh S, Yamakido T, Ogawa HI, Kato Y. Purification and characterization of a lipase from *Pseudomonas aeruginosa* KKA-5 and its role in castor oil hydrolysis. J Ind Microbiol Biotechnol 1998;20:304-7.

[61] Najafi MF, Deobagkar D, Deobagkar D. Potential application of protease isolated from *Pseudomonas aeruginosa* PD100. Electron J Biotechnol 2005;8:197-203.

[62] Ganesh Kumar A, Swarnalatha S, Sairam B, Sekaran G. Production of alkaline protease by *Pseudomonas aeruginosa* using proteinaceous solid waste generated from leather manufacturing industries. Bioresour Technol 2008;99:1939-44.

[63] Mahanta N, Gupta A, Khare SK. Production of protease and lipase by solvent tolerant *Pseudomonas aeruginosa* PseA in solid-state fermentation using *Jatropha curcas* seed cake as substrate. Bioresour Technol 2008;99:1729-35.

[64] Peterson JW. Bacterial pathogenesis. 4th edition ed: Galveston (TX): University of Texas Medical Branch at Galveston; 1996.

[65] Rohmer L, Hocquet D, Miller SI. Are pathogenic bacteria just looking for food? Metabolism and microbial pathogenesis. Trends Microbiol 2011;19:341-8.

[66] Henrichsen J. Bacterial surface translocation: a survey and a classification. Bacteriol Rev 1972;36:478-503.

[67] Dasgupta N, Arora SK, Ramphal R. The flagellar system of *Pseudomonas aeruginosa*. In: Ramos J-L, editor. *Pseudomonas:* Volume 1 Genomics, lifestyle and molecular architecture. Boston, MA: Springer US; 2004. p. 675-98.

[68] Guttenplan SB, Kearns DB. Regulation of flagellar motility during biofilm formation. FEMS Microbiol Rev 2013:1-23.

[69] Sauer K, Camper AK, Ehrlich GD, Costerton JW, Davies DG. *Pseudomonas aeruginosa* displays multiple phenotypes during development as a biofilm. J Bacteriol 2002;184:1140-54.

[70] Kato J, Kim HE, Takiguchi N, Kuroda A, Ohtake H. *Pseudomonas aeruginosa* as a model microorganism for investigation of chemotactic behaviors in ecosystem. J Biosci Bioeng 2008;106:1-7.

[71] Déziel E. *rhlA* is required for the production of a novel biosurfactant promoting swarming motility in *Pseudomonas aeruginosa*: 3-(3-hydroxyalkanoyloxy) alkanoic acid (HAAs), the precursors of rhamnolipids. Microbiology 2003;149:2005-13.

[72] Kohler T, Curty LK, Barja F. Swarming of *Pseudomonas aeruginosa* is dependent on cell-to-cell signaling and requires flagella and pili. J Bacteriol 2000;182:5990-6.

[73] Overhage J, Bains M, Brazas MD, Hancock RE. Swarming of *Pseudomonas aeruginosa* is a complex adaptation leading to increased production of virulence factors and antibiotic resistance. J Bacteriol 2008;190:2671-9.

[74] Anyan ME, Amiri A, Harvey CW, Tierra G, Morales-Soto N, Driscoll CM, et al. Type IV pili interactions promote intercellular association and moderate swarming of *Pseudomonas aeruginosa*. Proc Natl Acad Sci U S A 2014:18013–18.

[75] Nogales J, Domínguez-Ferreras A, Amaya-Gómez CV, van Dillewijn P, Cuéllar V, Sanjuán J, et al. Transcriptome profiling of a *Sinorhizobium meliloti fadD* mutant reveals the role of rhizobactin 1021 biosynthesis and regulation genes in the control of swarming. BMC Genomics 2010;11:157-74.

[76] Tremblay J, Richardson AP, Lépine F, Déziel E. Self-produced extracellular stimuli modulate the *Pseudomonas aeruginosa* swarming motility behaviour. Environ Microbiol 2007;9:2622-30.

[77] Yeung AT, Torfs EC, Jamshidi F, Bains M, Wiegand I, Hancock RE, et al. Swarming of *Pseudomonas aeruginosa* is controlled by a broad spectrum of transcriptional regulators, including MetR. J Bacteriol 2009;191:5592-602.

[78] Dubern JF, Cigana C, De Simone M, Lazenby J, Juhas M, Schwager S, et al. Integrated whole-genome screening for *Pseudomonas aeruginosa* virulence genes using multiple disease models reveals that pathogenicity is host specific. Environ Microbiol 2015;17:4379-93.

[79] Williams P, Cámara M. Quorum sensing and environmental adaptation in *Pseudomonas aeruginosa*: a tale of regulatory networks and multifunctional signal molecules. Curr Opin Microbiol 2009;12:182-91.

[80] Heurlier K, Williams F, Heeb S, Dormond C, Pessi G, Singer D, et al. Positive control of swarming, rhamnolipid synthesis, and lipase production by the posttranscriptional RsmA/RsmZ system in *Pseudomonas aeruginosa* PAO1. J Bacteriol 2004;184:2936-45.

[81] Beatson SA, Whitchurch CB, Semmler ABT, Mattick JS. Quorum sensing is not required for twitching motility in *Pseudomonas aeruginosa*. J Bacteriol 2002;184:3598-604.

[82] Burrows LL. *Pseudomonas aeruginosa* twitching motility: type IV pili in action. Annu Rev Microbiol 2012;66:493-520.

[83] Bradley DE. A function of *Pseudomonas aeruginosa* PAO polar pili: twitching motility. Can J Microbiol 1980;26:146-54.

[84] Skerker JM, Berg HC. Direct observation of extension and retraction of type IV pili. Proc Natl Acad Sci U S A 2001;98:6901-4.

[85] Beatson SA, Whitchurch CB, Sargent JL, Levesque RC, Mattick JS. Differential regulation of twitching motility and elastase production by Vfr in *Pseudomonas aeruginosa*. J Bacteriol 2002;184:3605-13.

[86] Mattick JS. Type IV pili and twitching motility. Annu Rev Microbiol 2002;56:289-314.

[87] Luo Y, Zhao K, Baker AE, Kuchma SL, Coggan KA, Wolfgang MC, et al. A hierarchical cascade of second messengers regulates *Pseudomonas aeruginosa* surface behaviors. MBio 2015;6:e02456.

[88] Van Gerven N, Waksman G, Remaut H. Pili and flagella biology, structure, and biotechnological applications. Prog Mol Biol Transl Sci 2011;103:21-72.

[89] Kuchma SL, Delalez NJ, Filkins LM, Snavely EA, Armitage JP, O'Toole GA. Cyclic di-GMP-mediated repression of swarming motility by

Pseudomonas aeruginosa PA14 requires the MotAB stator. J Bacteriol 2015;197:420-30.

[90] Maier B, Wong GC. How bacteria use type IV pili machinery on surfaces. Trends Microbiol 2015;23:775-88.

[91] Persat A, Inclan YF, Engel JN, Stone HA, Gitai Z. Type IV pili mechanochemically regulate virulence factors in *Pseudomonas aeruginosa*. Proc Natl Acad Sci U S A 2015;112:7563-8.

[92] Kuchma SL, Ballok AE, Merritt JH, Hammond JH, Lu W, Rabinowitz JD, et al. Cyclic-di-GMP-mediated repression of swarming motility by *Pseudomonas aeruginosa*: the *pilY1* gene and its impact on surface-associated behaviors. J Bacteriol 2010;192:2950-64.

[93] Murray TS, Kazmierczak BI. *Pseudomonas aeruginosa* exhibits sliding motility in the absence of type IV pili and flagella. J Bacteriol 2008;190:2700-8.

[94] Yeung AT, Parayno A, Hancock RE. Mucin promotes rapid surface motility in *Pseudomonas aeruginosa*. MBio 2012;3:e00073.

[95] Costerton JW, Lewandowski Z, Caldwell DE, Korber DR, Lappin-Scott HM. Microbial biofilms. Annu Rev Microbiol 1995;49:711-45.

[96] Adair CG, Gorman SP, Feron BM, Byers LM, Jones DS, Goldsmith CE, et al. Implications of endotracheal tube biofilm for ventilator-associated pneumonia. Intensive Care Med 1999;25:1072-6.

[97] Danhorn T, Fuqua C. Biofilm formation by plant-associated bacteria. Annu Rev Microbiol 2007;61:401-22.

[98] Jennings LK, Storek KM, Ledvina HE, Coulon C, Marmont LS, Sadovskaya I, et al. Pel is a cationic exopolysaccharide that cross-links extracellular DNA in the *Pseudomonas aeruginosa* biofilm matrix. Proc Natl Acad Sci U S A 2015;112:11353-8.

[99] Byrd MS, Sadovskaya I, Vinogradov E, Lu H, Sprinkle AB, Richardson SH, et al. Genetic and biochemical analyses of the *Pseudomonas aeruginosa* Psl exopolysaccharide reveal overlapping roles for polysaccharide synthesis enzymes in Psl and LPS production. Mol Microbiol 2009;73:622-38.

[100] Franklin MJ, Nivens DE, Weadge JT, Howell PL. Biosynthesis of the *Pseudomonas aeruginosa* extracellular polysaccharides, alginate, Pel, and Psl. Front Microbiol 2011;2:167.

[101] Kishioka C, Okamoto K, Hassett DJ, de Mello D, Rubin BK. *Pseudomonas aeruginosa* alginate is a potent secretagogue in the isolated ferret trachea. Pediatr Pulmonol 1999;27:174-9.

[102] Pedersen SS, Kharazmi A, Espersen F, Hoiby N. *Pseudomonas aeruginosa* alginate in cystic fibrosis sputum and the inflammatory response. Infect Immun 1990;58:3363-8.

[103] Hay ID, Wang Y, Moradali MF, Rehman ZU, Rehm BH. Genetics and regulation of bacterial alginate production. Environ Microbiol 2014;16:2997-3011.

[104] Lyczak JB, Cannon CL, Pier GB. Establishment of *Pseudomonas aeruginosa* infection: lessons from a versatile opportunist. Microb Infect 2000;2:1051-60.

[105] Friedman L, Kolter R. Two genetic loci produce distinct carbohydrate-rich structural components of the *Pseudomonas aeruginosa* biofilm matrix. J Bacteriol 2004;186:4457-65.

[106] Mishra M, Byrd MS, Sergeant S, Azad AK, Parsek MR, McPhail L, et al. *Pseudomonas aeruginosa* Psl polysaccharide reduces neutrophil phagocytosis and the oxidative response by limiting complement-mediated opsonization. Cell Microbiol 2012;14:95-106.

[107] Ma L, Wang S, Wang D, Parsek MR, Wozniak DJ. The roles of biofilm matrix polysaccharide Psl in mucoid *Pseudomonas aeruginosa* biofilms. FEMS Immunol Med Microbiol 2012;65:377-80.

[108] Irie Y, Starkey M, Edwards AN, Wozniak DJ, ROmeo T, Parsek MR. *Pseudomonas aeruginosa* biofilm matrix polysaccharide Psl is regulated transcriptionally by RpoS and post-transcriptionally by RsmA. Mol Microbiol 2010;78:158-72.

[109] Friedman L, Kolter R. Genes involved in matrix formation in *Pseudomonas aeruginosa* PA14 biofilms. Mol Microbiol 2004;51:675-90.

[110] Colvin KM, Gordon VD, Murakami K, Borlee BR, Wozniak DJ, Wong GCL, et al. The Pel polysaccharide can serve a structural and protective role in the biofilm matrix of *Pseudomonas aeruginosa*. PLoS Path 2011;7:1-13.

[111] Whitchurch CB, Tolker-Nielsen T, Ragas PC, Mattick JS. Extracellular DNA required for bacterial biofilm formation. Science 2002;295:1487.

[112] Diggle SP, Stacey RE, Dodd C, Cámara M, Williams P, Winzer K. The galactophilic lectin, LecA, contributes to biofilm development in *Pseudomonas aeruginosa*. Environ Microbiol 2006;8:1095-104.

[113] Vallet I, Olson JW, Lory S, Lazdunski A, Filloux A. The chaperone/usher pathways of *Pseudomonas aeruginosa*: identification of fimbrial gene clusters (*cup*) and their involvement in biofilm formation. Proc Natl Acad Sci U S A 2001;98:6911-6.

[114] Ruer S, Stender S, Filloux A, de Bentzmann S. Assembly of fimbrial structures in *Pseudomonas aeruginosa*: functionality and specificity of chaperone-usher machineries. J Bacteriol 2007;189:3547-55.

[115] O'Toole GA, Kolter R. Flagellar and twitching motility are necessary for *Pseudomonas aeruginosa* biofilm development. Mol Microbiol 1998;30:295-304.

[116] Rasamiravaka T, Labtani Q, Duez P, El Jaziri M. The formation of biofilms by *Pseudomonas aeruginosa*: a review of the natural and synthetic compounds interfering with control mechanisms. Biomed Res Int 2015;2015:759348.

[117] Cowles KN, Gitai Z. Surface association and the MreB cytoskeleton regulate pilus production, localization, and function in *Pseudomonas aeruginosa*. Mol Microbiol 2010;76:1411-26.

[118] Li Y, Petrova OE, Su S, Lau GW, Panmanee W, Na R, et al. BdlA, DipA and induced dispersion contribute to acute virulence and chronic persistence of *Pseudomonas aeruginosa*. PLoS Pathog 2014;10:e1004168.

[119] Fazli M, Almblad H, Rybtke ML, Givskov M, Eberl L, Tolker-Nielsen T. Regulation of biofilm formation in *Pseudomonas* and *Burkholderia* species. Environ Microbiol 2014;16:1961-81.

[120] Petrova OE, Sauer K. A novel signaling network essential for regulating *Pseudomonas aeruginosa* biofilm development. PLoS Pathog 2009;5:e1000668.

[121] Borlee BR, Goldman AD, Murakami K, Samudrala R, Wozniak DJ, Parsek MR. *Pseudomonas aeruginosa* uses a cyclic-di-GMP-regulated adhesin to reinforce the biofilm extracellular matrix. Mol Microbiol 2010;75:827-42.

[122] Dietrich LE, Okegbe C, Price-Whelan A, Sakhtah H, Hunter RC, Newman DK. Bacterial community morphogenesis is intimately linked to the intracellular redox state. J Bacteriol 2013;195:1371-80.

[123] Starkey M, Hickman JH, Ma L, Zhang N, De Long S, Hinz A, et al. *Pseudomonas aeruginosa* rugose small-colony variants have adaptations that likely promote persistence in the cystic fibrosis lung. J Bacteriol 2009;191:3492-503.

[124] Briard B, Bomme P, Lechner BE, Mislin GL, Lair V, Prevost MC, et al. *Pseudomonas aeruginosa* manipulates redox and iron homeostasis of its microbiota partner *Aspergillus fumigatus via* phenazines. Sci Rep 2015;5:8220.

[125] Mavrodi DV, Bonsall RF, Delaney SM, Soule MJ, Phillips G, Thomashow LS. Functional analysis of genes for biosynthesis of pyocyanin and phenazine-1-carboxamide from *Pseudomonas aeruginosa* PAO1. J Bacteriol 2001;183:6454-65.

[126] Wang Y, Kern SE, Newman DK. Endogenous phenazine antibiotics promote anaerobic survival of *Pseudomonas aeruginosa* via extracellular electron transfer. J Bacteriol 2010;192:365-9.

[127] Muller M, Merrett ND. Pyocyanin production by *Pseudomonas aeruginosa* confers resistance to ionic silver. Antimicrob Agents Chemother 2014;58:5492-9.

[128] Jeffries JL, Jia J, Choi W, Choe S, Miao J, Xu Y, et al. *Pseudomonas aeruginosa* pyocyanin modulates mucin glycosylation with sialyl-Lewis X to increase binding to airway epithelial cells. Mucosal Immunol 2015:1039-50.

[129] Caci E, Scudieri P, Di Carlo E, Morelli P, Bruno S, De Fino I, et al. Upregulation of TMEM16A protein in bronchial epithelial cells by bacterial pyocyanin. PloS one 2015;10:e0131775.

[130] Manago A, Becker KA, Carpinteiro A, Wilker B, Soddemann M, Seitz AP, et al. *Pseudomonas aeruginosa* pyocyanin induces neutrophil death via mitochondrial reactive oxygen species and mitochondrial acid sphingomyelinase. Antioxid Redox Signal 2015;22:1097-110.

[131] Fothergill JL, Panagea S, Hart CA, Walshaw MJ, Pitt TL, Winstanley C. Widespread pyocyanin over-production among isolates of a cystic fibrosis epidemic strain. BMC Microbiol 2007;7:45.

[132] Mowat E, Paterson S, Fothergill JL, Wright EA, Ledson MJ, Walshaw MJ, et al. *Pseudomonas aeruginosa* population diversity and turnover in cystic fibrosis chronic infections. Am J Respir Crit Care Med 2011;183:1674-9.

[133] Schaber JA, Carty NL, McDonald NA, Graham ED, Cheluvappa R, Griswold JA, et al. Analysis of quorum sensing-deficient clinical isolates of *Pseudomonas aeruginosa*. J Med Microbiol 2004;53:841-53.

[134] Cullen L, Weiser R, Olszak T, Maldonado RF, Moreira AS, Slachmuylders L, et al. Phenotypic characterization of an international *Pseudomonas aeruginosa* reference panel: strains of cystic fibrosis (CF) origin show less in vivo virulence than non-CF strains. Microbiology 2015;161:1961-77.

[135] De Vleesschauwer D, Cornelis P, Hofte M. Redox-active pyocyanin secreted by *Pseudomonas aeruginosa* 7NSK2 triggers systemic resistance to *Magnaporthe grisea* but enhances *Rhizoctonia solani* susceptibility in rice. Mol Plant Microbe Interact 2006;19:1406-19.

[136] Baron SS, Rowe JJ. Antibiotic action of pyocyanin. Antimicrob Agents Chemother 1981;20:814-20.

[137] Ramos I, Dietrich LE, Price-Whelan A, Newman DK. Phenazines affect biofilm formation by *Pseudomonas aeruginosa* in similar ways at various scales. Res Microbiol 2010;161:187-91.

[138] Das T, Kutty SK, Kumar N, Manefield M. Pyocyanin facilitates extracellular DNA binding to *Pseudomonas aeruginosa* influencing cell surface properties and aggregation. PloS one 2013;8:e58299.

[139] Das T, Manefield M. Pyocyanin promotes extracellular DNA release in *Pseudomonas aeruginosa*. PloS one 2012;7:e46718.

[140] Das T, Kutty SK, Tavallaie R, Ibugo AI, Panchompoo J, Sehar S, et al. Phenazine virulence factor binding to extracellular DNA is important for *Pseudomonas aeruginosa* biofilm formation. Sci Rep 2015;5:8398.

[141] Andrews SC, Robinson AK, Rodriguez-Quinones F. Bacterial iron homeostasis. FEMS Microbiol Rev 2003;27:215-37.

[142] Ravel J, Cornelis P. Genomics of pyoverdine-mediated iron uptake in pseudomonads. Trends Microbiol 2003;11:195-200.

[143] Meyer JM, Stintzi A, De Vos D, Cornelis P, Tappe R, Taraz K, et al. Use of siderophores to type pseudomonads: the three *Pseudomonas aeruginosa* pyoverdine systems. Microbiology 1997;143 (Pt 1):35-43.

[144] Dean CR, Poole K. Cloning and characterization of the ferric enterobactin receptor gene (*pfeA*) of *Pseudomonas aeruginosa*. J Bacteriol 1993;175:317-24.

[145] Banin E, Vasil ML, Greenberg EP. Iron and *Pseudomonas aeruginosa* biofilm formation. Proc Natl Acad Sci U S A 2005;102:11076-81.

[146] Stintzi A, Evans K, Meyer JM, Poole K. Quorum-sensing and siderophore biosynthesis in *Pseudomonas aeruginosa: lasR/lasI* mutants exhibit reduced pyoverdine biosynthesis. FEMS Microbiol Lett 1998;166:341-5.

[147] Nguyen AT, O'Neill MJ, Watts AM, Robson CL, Lamont IL, Wilks A, et al. Adaptation of iron homeostasis pathways by a *Pseudomonas aeruginosa* pyoverdine mutant in the cystic fibrosis lung. J Bacteriol 2014;196:2265-76.

[148] Llamas MA, Imperi F, Visca P, Lamont IL. Cell-surface signaling in *Pseudomonas*: stress responses, iron transport, and pathogenicity. FEMS Microbiol Rev 2014;38:569-97.

[149] Chen Y, Yuan M, Mohanty A, Yam JK, Liu Y, Chua SL, et al. Multiple diguanylate cyclase-coordinated regulation of pyoverdine synthesis in *Pseudomonas aeruginosa*. Environ Microbiol Rep 2015;7:498-507.

[150] Visaggio D, Pasqua M, Bonchi C, Kaever V, Visca P, Imperi F. Cell aggregation promotes pyoverdine-dependent iron uptake and virulence in *Pseudomonas aeruginosa*. Front Microbiol 2015;6:902.

[151] Frangipani E, Visaggio D, Heeb S, Kaever V, Cámara M, Visca P, et al. The Gac/Rsm and cyclic-di-GMP signalling networks coordinately

regulate iron uptake in *Pseudomonas aeruginosa*. Environ Microbiol 2014;16:676-88.

[152] Oglesby AG, Farrow JM, 3rd, Lee JH, Tomaras AP, Greenberg EP, Pesci EC, et al. The influence of iron on *Pseudomonas aeruginosa* physiology: a regulatory link between iron and quorum sensing. J Biol Chem 2008;283:15558-67.

[153] Diggle SP, Matthijs S, Wright VJ, Fletcher MP, Chhabra SR, Lamont IL, et al. The *Pseudomonas aeruginosa* 4-quinolone signal molecules HHQ and PQS play multifunctional roles in quorum sensing and iron entrapment. Chem Biol 2007;14:87-96.

[154] Abdel-Mawgoud AM, Hausmann R, Lépine F, Müller MM, Déziel E. Rhamnolipids: detection, analysis, biosynthesis, genetic regulation, and bioengineering of production. In: Soberón-Chávez G, editor. Biosurfactants: Springer-Verlag Berlin Heidelberg; 2011. p. 13-55.

[155] Abdel-Mawgoud AM, Lépine F, Déziel E. Rhamnolipids: diversity of structures, microbial origins and roles. Appl Microbiol Biotechnol 2010;86:1323-36.

[156] Hastie AT, Hingley ST, Higgins ML, Kueppers F. The effect of rhamnolipid hemolysin of *Pseudomonas aeruginosa* on respiratory epithelium. Am Rev Respir Dis 1987;135:513-4.

[157] Zulianello L, Canard C, Kohler T, Caille D, Lacroix JS, Meda P. Rhamnolipids are virulence factors that promote early infiltration of primary human airway epithelia by *Pseudomonas aeruginosa*. Infect Immun 2006;74:3134-47.

[158] Wallace CJ, Medina SH, ElSayed ME. Effect of rhamnolipids on permeability across Caco-2 cell monolayers. Pharm Res 2014;31:887-94.

[159] Cosson P, Zulianello L, Join-Lambert O, Faurisson F, Gebbie L, Benghezal M, et al. *Pseudomonas aeruginosa* virulence analyzed in a *Dictyostelium discoideum* host system. J Bacteriol 2002;184:3027-33.

[160] Haussler S, Rohde M, von Neuhoff N, Nimtz M, Steinmetz I. Structural and functional cellular changes induced by *Burkholderia pseudomallei* rhamnolipid. Infect Immun 2003;71:2970-5.

[161] Van Gennip M, Christensen LD, Alhede M, Phipps R, Jensen PO, Christophersen L, et al. Inactivation of the *rhlA* gene in *Pseudomonas aeruginosa* prevents rhamnolipid production, disabling the protection against polymorphonuclear leukocytes. APMIS 2009;117:537-46.

[162] Jensen PO, Bjarnsholt T, Phipps R, Rasmussen TB, Calum H, Christoffersen L, et al. Rapid necrotic killing of polymorphonuclear leukocytes is caused by quorum-sensing-controlled production of rhamnolipid by *Pseudomonas aeruginosa*. Microbiology 2007;153:1329-38.

[163] Déziel E, Lépine F, Dennie D, Boismenu D, Mamer OA, Villemur R. Liquid chromatography/mass spectrometry analysis of mixtures of rhamnolipids produced by *Pseudomonas aeruginosa* strain 57RP grown on mannitol of naphthalene. Biochim Biophys Acta 1999;1440:244-52.

[164] de Santana-Filho AP, Camilios-Neto D, de Souza LM, Sassaki GL, Mitchell DA, Krieger N. Evaluation of the structural composition and surface properties of rhamnolipid mixtures produced by *Pseudomonas aeruginosa* UFPEDA 614 in different cultivation periods. Appl Biochem Biotechnol 2015;175:988-95.

[165] Moussa TAA, Mohamed MS, Samak N. Production and characterization of di-rhamnolipid produced by *Pseudomonas aeruginosa* TMN. Braz J Chem Eng 2014;31:867-80.

[166] Dubeau D, Déziel E, Woods DE, Lépine F. *Burkholderia thailandensis* harbors two identical *rhl* gene clusters responsible for the biosynthesis of rhamnolipids. BMC Microbiol 2009;9:263.

[167] Rahim R, Ochsner UA, Olvera C, Graninger M, Messner P, Lam JS, et al. Cloning and functional characterization of the *Pseudomonas aeruginosa rhlC* gene that encodes rhamnosyltransferase 2, an enzyme responsible for di-rhamnolipid biosynthesis. Mol Microbiol 2001;40:708-18.

[168] Campos-García J, Caro AD, Nájera R, Miller-Maier RM, Al-Tahhan RA, Soberón-Chávez G. The *Pseudomonas aeruginosa rhlG* gene encodes an NADPH-dependent β-ketoacyl reductase which is specifically involved in rhamnolipid synthesis. J Bacteriol 1998;17:4442-51.

[169] Zhu K, Rock CO. RhlA converts beta-hydroxyacyl-acyl carrier protein intermediates in fatty acid synthesis to the beta-hydroxydecanoyl-beta-hydroxydecanoate component of rhamnolipids in *Pseudomonas aeruginosa*. J Bacteriol 2008;190:3147-54.

[170] Dobler L, Vilela LF, Almeida RV, Neves BC. Rhamnolipids in perspective: gene regulatory pathways, metabolic engineering, production and technological forecasting. N Biotechnol 2016;33:123-35.

[171] Lequette Y, Greenberg EP. Timing and localization of rhamnolipid synthesis gene expression in *Pseudomonas aeruginosa* biofilms. J Bacteriol 2005;187:37-44.

[172] Pamp SJ, Tolker-Nielsen T. Multiple roles of biosurfactants in structural biofilm development by *Pseudomonas aeruginosa*. J Bacteriol 2007;189:2531-9.

[173] Klausen M, Aaes-Jorgensen A, Molin S, Tolker-Nielsen T. Involvement of bacterial migration in the development of complex multicellular structures in *Pseudomonas aeruginosa* biofilms. Mol Microbiol 2003;50:61-8.

[174] Davey ME, Caiazza NC, O'Toole G A. Rhamnolipid surfactant production affects biofilm architecture in *Pseudomonas aeruginosa* PAO1. J Bacteriol 2003;185:1027-36.

[175] Raya A, Sodagari M, Pinzon NM, He X, Zhang Newby BM, Ju LK. Effects of rhamnolipids and shear on initial attachment of *Pseudomonas aeruginosa* PAO1 in glass flow chambers. Environ Sci Pollut Res Int 2010;17:1529-38.

[176] Boles BR, Thoendel M, Singh PK. Rhamnolipids mediate detachment of *Pseudomonas aeruginosa* from biofilms. Mol Microbiol 2005;57:1210-23.

[177] Diaz De Rienzo MA, Stevenson PS, Marchant R, Banat IM. *Pseudomonas aeruginosa* biofilm disruption using microbial surfactants. J Appl Microbiol 2016:868-75.

[178] Kim LH, Jung Y, Yu HW, Chae KJ, Kim IS. Physicochemical interactions between rhamnolipids and *Pseudomonas aeruginosa* biofilm layers. Environ Sci Technol 2015;49:3718-26.

[179] Gerstel U, Czapp M, Bartels J, Schroder JM. Rhamnolipid-induced shedding of flagellin from *Pseudomonas aeruginosa* provokes hBD-2 and IL-8 response in human keratinocytes. Cell Microbiol 2009;11:842-53.

[180] Caiazza NC, Shanks RM, O'Toole GA. Rhamnolipids modulate swarming motility patterns of *Pseudomonas aeruginosa*. J Bacteriol 2005;187:7351-61.

[181] Heck LW, Morihara K, McRae WB, Miller EJ. Specific cleavage of human type III and IV collagens by *Pseudomonas aeruginosa* elastase. Infect Immun 1986;51:115-8.

[182] Heck LW, Morihara K, Abrahamson DR. Degradation of soluble laminin and depletion of tissue-associated basement membrane laminin by *Pseudomonas aeruginosa* elastase and alkaline protease. Infect Immun 1986;54:149-53.

[183] Hong YQ, Ghebrehiwet B. Effect of *Pseudomonas aeruginosa* elastase and alkaline protease on serum complement and isolated components C1q and C3. Clin Immunol Immunopathol 1992;62:133-8.

[184] Schultz DR, Miller KD. Elastase of *Pseudomonas aeruginosa*: inactivation of complement components and complement-derived chemotactic and phagocytic factors. Infect Immun 1974;10:128-35.

[185] Parmely M, Gale A, Clabaugh M, Horvat R, Zhou WW. Proteolytic inactivation of cytokines by *Pseudomonas aeruginosa*. Infect Immun 1990;58:3009-14.

[186] Blackwood LL, Stone RM, Iglewski BH, Pennington JE. Evaluation of *Pseudomonas aeruginosa* exotoxin A and elastase as virulence factors in acute lung infection. Infect Immun 1983;39:198-201.

[187] Woods DE, Cryz SJ, Friedman RL, Iglewski BH. Contribution of toxin A and elastase to virulence of *Pseudomonas aeruginosa* in chronic lung infections of rats. Infect Immun 1982;36:1223-8.

[188] O'Callaghan RJ, Engel LS, Hobden JA, Callegan MC, Green LC, Hill JM. *Pseudomonas* keratitis. The role of an uncharacterized exoprotein, protease IV, in corneal virulence. Invest Ophthalmol Vis Sci 1996;37:534-43.

[189] Engel LS, Hill JM, Caballero AR, Green LC, O'Callaghan RJ. Protease IV, a unique extracellular protease and virulence factors from *Pseudomonas aeruginosa*. J Biol Chem 1998;273:16792-7.

[190] Peters J, Park S, Darzins A, Freck L, Saulnier J, Wallach J, et al. Further studies on *Pseudomonas aeruginosa* LasA: analysis of specificity. Mol Microbiol 1992;6:1155-62.

[191] Kessler E, Safrin M, Abrams WR, Rosenbloom J, Ohman DE. Inhibitors and specificity of *Pseudomonas aeruginosa* LasA. J Biol Chem 1997;272:9884-9.

[192] Kessler E, Safrin M, Olson JC, Ohman DE. Secreted LasA of *Pseudomonas aeruginosa* is a staphylolytic protease. J Biol Chem 1993;268:7503-8.

[193] Laarman AJ, Bardoel BW, Ruyken M, Fernie J, Milder FJ, van Strijp JA, et al. *Pseudomonas aeruginosa* alkaline protease blocks complement activation via the classical and lectin pathways. J Immunol 2012;188:386-93.

[194] Andrejko M, Zdybicka-Barabas A, Janczarek M, Cytrynska M. Three *Pseudomonas aeruginosa* strains with different protease profiles. Acta Biochim Pol 2013;60:83-90.

[195] Conibear TC, Willcox MD, Flanagan JL, Zhu H. Characterization of protease IV expression in *Pseudomonas aeruginosa* clinical isolates. J Med Microbiol 2012;61:180-90.

[196] Pearson JP, Pesci EC, Iglewski BH. Roles of *Pseudomonas aeruginosa las* and *rhl* quorum-sensing systems in control of elastase and rhamnolipid biosynthesis genes. J Bacteriol 1997;179:5756-67.

[197] Toder DS, Gambello MJ, Iglewski BH. *Pseudomonas aeruginosa* LasA: a second elastase under the transcriptional control of *lasR*. Mol Microbiol 1991;5:2003-10.

[198] Gambello MJ, Kaye S, Iglewski BH. LasR of *Pseudomonas aeruginosa* is a transcriptional activator of the alkaline protease gene (*apr*) and an enhancer of exotoxin A expression. Infect Immun 1993;61:1180-4.

[199] Wilderman PJ, Vasil AI, Johnson Z, Wilson MJ, Cunliffe HE, Lamont IL, et al. Characterization of an endoprotease (PrpL) encoded by a PvdS-

regulated gene in *Pseudomonas aeruginosa*. Infect Immun 2001;69:5385-94.

[200] Bleves S, Viarre V, Salacha R, Michel GP, Filloux A, Voulhoux R. Protein secretion systems in *Pseudomonas aeruginosa*: a wealth of pathogenic weapons. Int J Med Microbiol 2010;300:534-43.

[201] Michalska M, Wolf P. *Pseudomonas* exotoxin A: optimized by evolution for effective killing. Front Microbiol 2015;6:963.

[202] Anderson RD, Roddam LF, Bettiol S, Sanderson K, Reid DW. Biosignificance of bacterial cyanogenesis in the CF lung. J Cyst Fibros 2010;9:158-64.

[203] Ostroff RM, Vasil AI, Vasil ML. Molecular comparison of a nonhemolytic and a hemolytic phospholipase C from *Pseudomonas aeruginosa*. J Bacteriol 1990;172:5915-23.

[204] Kalia D, Merey G, Nakayama S, Zheng Y, Zhou J, Luo Y, et al. Nucleotide, c-di-GMP, c-di-AMP, cGMP, cAMP, (p)ppGpp signaling in bacteria and implications in pathogenesis. Chem Soc Rev 2013;42:305-41.

[205] Tamayo R, Pratt JT, Camilli A. Roles of cyclic diguanylate in the regulation of bacterial pathogenesis. Annu Rev Microbiol 2007;61:131-48.

[206] Simm R, Morr M, Kader A, Nimtz M, Römling U. GGDEF and EAL domains inversely regulate cyclic di-GMP levels and trasition from sessility to motility. Mol Microbiol 2004;53:1123-34.

[207] Kulesekara H, Lee V, Brencic A, Liberati N, Urbach J, Miyata S, et al. Analysis of *Pseudomonas aeruginosa* diguanylate cyclases and phosphodiesterases reveales a role for bis-(3'5')-cyclic-GMP in virulence. Proc Natl Acad Sci U S A 2006;103:2839-44.

[208] Hengge R. Principles of c-di-GMP signalling in bacteria. Nat Rev Microbiol 2009;7:263-73.

[209] Merritt JH, Ha DG, Cowles KN, Lu W, Morales DK, Rabinowitz J, et al. Specific control of *Pseudomonas aeruginosa* surface-associated behaviors by two c-di-GMP diguanylate cyclases. MBio 2010;1:e00183.

[210] Malone JG, Jaeger T, Spangler C, Ritz D, Spang A, Arrieumerlou C, et al. YfiBNR mediates cyclic di-GMP dependent small colony variant formation and persistence in *Pseudomonas aeruginosa*. PLoS Pathog 2010;6:e1000804.

[211] Evans TJ. Small colony variants of *Pseudomonas aeruginosa* in chronic bacterial infection of the lung in cystic fibrosis. Future Microbiol 2015;10:231-9.

[212] Gupta K, Liao J, Petrova OE, Cherny KE, Sauer K. Elevated levels of the second messenger c-di-GMP contribute to antimicrobial resistance of *Pseudomonas aeruginosa*. Mol Microbiol 2014;92:488-506.

[213] Baraquet C, Murakami K, Parsek MR, Harwood CS. The FleQ protein from *Pseudomonas aeruginosa* functions as both a repressor and an activator to control gene expression from the *pel* operon promoter in response to c-di-GMP. Nucleic Acids Res 2012;40:7207-18.

[214] Kuchma SL, Brothers KM, Merritt JH, Liberati NT, Ausubel FM, O'Toole GA. BifA, a cyclic-Di-GMP phosphodiesterase, inversely regulates biofilm formation and swarming motility by *Pseudomonas aeruginosa* PA14. J Bacteriol 2007;189:8165-78.

[215] Merritt JH, Brothers KM, Kuchma SL, O'Toole GA. SadC reciprocally influences biofilm formation and swarming motility via modulation of exopolysaccharide production and flagellar function. J Bacteriol 2007;189:8154-64.

[216] Ueda A, Wood TK. Connecting quorum sensing, c-di-GMP, Pel polysaccharide, and biofilm formation in *Pseudomonas aeruginosa* through tyrosine phosphatase TpbA (PA3885). PLoS Pathog 2009;5:e1000483.

[217] Ryan RP, Fouhy Y, Lucey JF, Crossman LC, Spiro S, He YW, et al. Cell-cell signaling in *Xanthomonas campestris* involves an HD-GYP domain protein that functions in cyclic di-GMP turnover. PNAS 2006;103:6712-7.

[218] Ryan RP, McCarthy Y, Andrade M, Farah CS, Armitage JP, Dow JM. Cell-cell signal-dependent dynamic interactions between HD-GYP and GGDEF domain proteins mediate virulence in *Xanthomonas campestris*. Proc Natl Acad Sci U S A 2010;107:5989-94.

[219] Perez-Mendoza D, Aragon IM, Prada-Ramirez HA, Romero-Jimenez L, Ramos C, Gallegos MT, et al. Responses to elevated c-di-GMP levels in mutualistic and pathogenic plant-interacting bacteria. PloS one 2014;9:e91645.

[220] Almblad H, Harrison JJ, Rybtke M, Groizeleau J, Givskov M, Parsek MR, et al. The cyclic AMP-Vfr signaling pathway in *Pseudomonas aeruginosa* is inhibited by cyclic di-GMP. J Bacteriol 2015;197:2190-200.

[221] Albus AM, Pesci EC, Runyen-Janecky LJ, West SE, Iglewski BH. Vfr controls quorum sensing in *Pseudomonas aeruginosa*. J Bacteriol 1997;179:3928-35.

[222] West SE, Sample AK, Runyen-Janecky LJ. The *vfr* gene product, required for *Pseudomonas aeruginosa* exotoxin A and protease production, belongs to the cyclic AMP receptor protein family. J Bacteriol 1994;176:7532-42.

[223] Dasgupta N, Ferrell EP, Kanack KJ, West SE, Ramphal R. *fleQ*, the gene encoding the major flagellar regulator of *Pseudomonas aeruginosa*,

is sigma70 dependent and is downregulated by Vfr, a homolog of Escherichia coli cyclic AMP receptor protein. J Bacteriol 2002;184:5240-50.

[224] Jones AK, Fulcher NB, Balzer GJ, Urbanowski ML, Pritchett CL, Schurr MJ, et al. Activation of the *Pseudomonas aeruginosa* AlgU regulon through *mucA* mutation inhibits cyclic AMP/Vfr signaling. J Bacteriol 2010;192:5709-17.

[225] Fuqua WC, Winans SC, Greenberg EP. Quorum sensing in bacteria: the LuxR-LuxI family of cell density-responsive transcriptional regulators. J Bacteriol 1994;176:269-75.

[226] Swift S, Throup JP, Williams P, Salmond GP, Stewart GS. Quorum sensing: a population-density component in the determination of bacterial phenotype. Trends Biochem Sci 1996;21:214-9.

[227] Winzer K, Hardie KR, Williams P. Bacterial cell-to-cell communication: sorry, can't talk now - gone to lunch! Curr Opin Microbiol 2002;5:216-22.

[228] Henke JM, Bassler BL. Bacterial social engagements. Trends Cell Biol 2004;14:648-56.

[229] Whitehead NA, Barnard AML, Slater H, Simpson NJL, Salmond GPC. Quorum-sensing in Gram-negative bacteria. FEMS Microbiol Rev 2001;25:365-404.

[230] Heeb S, Fletcher MP, Chhabra SR, Diggle SP, Williams P, Cámara M. Quinolones: from antibiotics to autoinducers. FEMS Microbiol Rev 2010;35:247-74.

[231] Garg N, Manchanda G, Kumar A. Bacterial quorum sensing: circuits and applications. Antonie Van Leeuwenhoek 2014;105:289-305.

[232] Reading NC, Sperandio V. Quorum sensing: the many languages of bacteria. FEMS Microbiol Lett 2006;254:1-11.

[233] Atkinson S, Williams P. Quorum sensing and social networking in the microbial world. J R Soc Interface 2009;6:959-78.

[234] Polkade AV, Mantri SS, Patwekar UJ, Jangid K. Quorum sensing: an under-explored phenomenon in the phylum Actinobacteria. Front Microbiol 2016;7:131.

[235] Pesci EC, Milbank JB, Pearson JP, McKnight S, Kende AS, Greenberg EP, et al. Quinolone signaling in the cell-to-cell communication system of *Pseudomonas aeruginosa*. Proc Natl Acad Sci U S A 1999;96:11229-34.

[236] Girard G, Bloemberg GV. Central role of quorum sensing in regulating the production of pathogenicity factors in *Pseudomonas aeruginosa*. Future Microbiol 2008;3:97-106.

[237] Diggle SP, Winzer K, Chhabra SR, Worrall KE, Cámara M, Williams P. The *Pseudomonas aeruginosa* quinolone signal molecule overcomes the cell density-dependency of the quorum sensing hierarchy, regulates *rhl*-dependent genes at the onset of stationary phase and can be produced in the absence of LasR. Mol Microbiol 2003;50:29-43.

[238] Winzer K, Williams P. Quorum sensing and the regulation of virulence gene expression in pathogenic bacteria. Int J Med Microbiol 2001;291:131-43.

[239] Hassett DJ, Ma JF, Elkins JG, McDermott TR, Ochsner UA, West SE, et al. Quorum sensing in *Pseudomonas aeruginosa* controls expression of catalase and superoxide dismutase genes and mediates biofilm susceptibility to hydrogen peroxide. Mol Microbiol 1999;34:1082-93.

[240] Davies DGP, M. R.; Pearson, J. P.; Iglewski, B. H.; Costerton, J. W.; Greenberg, E. P. The involvement of cell-to-cell signals in the development of a bacterial biofilm. Science 1998;280:295-8.

[241] Shrout JD, Chopp DL, Just CL, Hentzer M, Givskov M, Parsek MR. The impact of quorum sensing and swarming motility on *Pseudomonas aeruginosa* biofilm formation is nutritionally conditional. Mol Microbiol 2006;62:1264-77.

[242] Allesen-Holm M, Barken KB, Yang L, Klausen M, Webb JS, Kjelleberg S, et al. A characterization of DNA release in *Pseudomonas aeruginosa* cultures and biofilms. Mol Microbiol 2006;59:1114-28.

[243] Barber CE, Tang JL, Feng JX, Pan MQ, Wilson TJG, Slater H, et al. A novel regulatory system required for pathogenicity of *Xanthomonas campestris* is mediated by a small diffusible signal molecule. Mol Microbiol 1997;24:555–66.

[244] Ryan RP, An SQ, Allan JH, McCarthy Y, Dow JM. The DSF family of cell-cell signals: an expanding class of bacterial virulence regulators. PLoS Pathog 2015;11:e1004986.

[245] Wang LH, He Y, Gao Y, Wu JE, Dong YH, He C, et al. A bacterial cell-cell communication signal with cross-kingdom structural analogues. Mol Microbiol 2004;51:903-12.

[246] Fouhy Y, Scanlon K, Schouest K, Spillane C, Crossman L, Avison MB, et al. Diffusible signal factor-dependent cell-cell signaling and virulence in the nosocomial pathogen *Stenotrophomonas maltophilia*. J Bacteriol 2007;189:4964-8.

[247] Deng Y, Wu J, Eberl L, Zhang LH. Structural and functional characterization of diffusible signal factor family quorum-sensing signals produced by members of the *Burkholderia cepacia* complex. Appl Environ Microbiol 2010;76:4675-83.

[248] He YW, Wu J, Cha JS, Zhang LH. Rice bacterial blight pathogen *Xanthomonas oryzae* pv. *oryzae* produces multiple DSF-family signals in regulation of virulence factor production. BMC Microbiol 2010;10:187.

[249] de Rossi BP, Garcia C, Alcaraz E, Franco M. *Stenotrophomonas maltophilia* interferes via the DSF-mediated quorum sensing system with *Candida albicans* filamentation and its planktonic and biofilm modes of growth. Rev Argent Microbiol 2014;46:288-97.

[250] Deng Y, Liu X, Wu J, Lee J, Chen S, Cheng Y, et al. The host plant metabolite glucose is the precursor of diffusible signal factor (DSF) family signals in *Xanthomonas campestris*. Appl Environ Microbiol 2015;81:2861-8.

[251] Boon C, Deng Y, Wang LH, He Y, Xu JL, Fan Y, et al. A novel DSF-like signal from *Burkholderia cenocepacia* interferes with *Candida albicans* morphological transition. ISME J 2008;2:27-36.

[252] Tian J, Weng LX, Zhang YQ, Wang LH. BDSF inhibits *Candida albicans* adherence to urinary catheters. Microb Pathog 2013;64:33-8.

[253] Beaulieu ED, Ionescu M, Chatterjee S, Yokota K, Trauner D, Lindow S. Characterization of a diffusible signaling factor from *Xylella fastidiosa*. MBio 2013;4:e00539.

[254] Ionescu M, Baccari C, Da Silva AM, Garcia A, Yokota K, Lindow SE. Diffusible signal factor (DSF) synthase RpfF of *Xylella fastidiosa* is a multifunction protein also required for response to DSF. J Bacteriol 2013;195:5273-84.

[255] Davies DG, Marques CN. A fatty acid messenger is responsible for inducing dispersion in microbial biofilms. J Bacteriol 2009;191:1393-403.

[256] Marques CN, Morozov A, Planzos P, Zelaya HM. The fatty acid signaling molecule *cis*-2-decenoic acid increases metabolic activity and reverts persister cells to an antimicrobial susceptible state. Appl Environ Microbiol 2014:6976-91.

[257] Deng Y, Wu J, Tao F, Zhang LH. Listening to a new language: DSF-based quorum sensing in Gram-negative bacteria. Chem Rev 2011;111:160-73.

[258] Vilchez R, Lemme A, Ballhausen B, Thiel V, Schulz S, Jansen R, et al. *Streptococcus mutans* inhibits *Candida albicans* hyphal formation by the fatty acid signaling molecule *trans*-2-decenoic acid (SDSF). ChemBioChem 2010;11:1552-62.

[259] Zhang Y, Cai C, Yang Y, Weng L, Wang L. Blocking of *Candida albicans* biofilm formation by *cis*-2-dodecenoic acid and *trans*-2-dodecenoic acid. J Med Microbiol 2011;60:1643-50.

[260] Ryan RP, Dow JM. Communication with a growing family: diffusible signal factor (DSF) signaling in bacteria. Trends Microbiol 2011;19:145-52.

[261] Kakkar A, Nizampatnam NR, Kondreddy A, Pradhan BB, Chatterjee S. *Xanthomonas campestris* cell-cell signalling molecule DSF (diffusible signal factor) elicits innate immunity in plants and is suppressed by the exopolysaccharide xanthan. J Exp Bot 2015;66:6697-714.

[262] Dean SN, Chung MC, van Hoek ML. *Burkholderia* diffusible signal factor signals to *Francisella novicida* to disperse biofilm and increase siderophore production. Appl Environ Microbiol 2015;81:7057-66.

[263] Slater H, Alvarez-Morales A, Barber CE, Daniels MJ, Dow JM. A two-component system involving an HD-GYP domain protein links cell-cell signalling to pathogenicity gene expression in *Xanthomonas campestris*. Mol Microbiol 2000;38:986-1003.

[264] Ryan RP, Fouhy Y, Garcia BF, Watt SA, Niehaus K, Yang L, et al. Interspecies signalling via the *Stenotrophomonas maltophilia* diffusible signal factor influences biofilm formation and polymyxin tolerance in *Pseudomonas aeruginosa*. Mol Microbiol 2008;68:75-86.

[265] Deng Y, Schmid N, Wang C, Wang J, Pessi G, Wu D, et al. *Cis*-2-dodecenoic acid receptor RpfR links quorum-sensing signal perception with regulation of virulence through cyclic dimeric guanosine monophosphate turnover. Proc Natl Acad Sci U S A 2012;109:15479-84.

[266] Deng Y, Boon C, Eberl L, Zhang LH. Differential modulation of *Burkholderia cenocepacia* virulence and energy metabolism by the quorum-sensing signal BDSF and its synthase. J Bacteriol 2009;191:7270-8.

[267] Huedo P, Yero D, Martinez-Servat S, Ruyra A, Roher N, Daura X, et al. Decoding the genetic and functional diversity of the DSF quorum-sensing system in *Stenotrophomonas maltophilia*. Front Microbiol 2015;6:761.

[268] Rodrigue A, Quentin Y, Lazdunski A, Méjean V, Foglino M. Two-component systems in *Pseudomonas aeruginosa*: why so many? Trends Microbiol 2000;8:498-504.

[269] Casino P, Rubio V, Marina A. The mechanism of signal transduction by two-component systems. Curr Opin Struct Biol 2010;20:763-71.

[270] Gao R, Stock AM. Biological insights from structures of two-component proteins. Annu Rev Microbiol 2009;63:133-54.

[271] Mikkelsen H, Slvaneson M, Filloux A. Key two-component regulatory systems that control biofilm formation in *Pseudomonas aeruginosa*. Environ Microbiol 2011;13:1666-81.

[272] Morris ER, Hall G, Li C, Heeb S, Kulkarni RV, Lovelock L, et al. Structural rearrangement in an RsmA/CsrA ortholog of *Pseudomonas aeruginosa* creates a dimeric RNA-binding protein, RsmN. Structure 2013;21:1659-71.

[273] Kay E, Humair B, Denervaud V, Riedel K, Spahr S, Eberl L, et al. Two GacA-dependent small RNAs modulate the quorum-sensing response in *Pseudomonas aeruginosa*. J Bacteriol 2006;188:6026-33.

[274] Lapouge K, Schubert M, Allain FH, Haas D. Gac/Rsm signal transduction pathway of gamma-Proteobacteria: from RNA recognition to regulation of social behaviour. Mol Microbiol 2008;67:241-53.

[275] Sonnleitner E, Haas D. Small RNAs as regulators of primary and secondary metabolism in *Pseudomonas* species. Appl Microbiol Biotechnol 2011;91:63-79.

[276] Brencic A, Lory S. Determination of the regulon and identification of novel mRNA targets of *Pseudomonas aeruginosa* RsmA. Mol Microbiol 2009;72:612-32.

[277] Bordi C, Lamy MC, Ventre I, Termine E, Hachani A, Fillet S, et al. Regulatory RNAs and the HptB/RetS signalling pathways fine-tune *Pseudomonas aeruginosa* pathogenesis. Mol Microbiol 2010;76:1427-43.

[278] Hsu J, Chen H, Peng H, CHang H. Characterization of the histidine-containing phosphotransfer protein B-mediated multistep phosphorelay system in *Pseudomonas aeruginosa* PAO1. J Biol Chem 2008;283:9933-44.

[279] Antonious GF. 2-undecanone and 2-tridecanone in field-grown onion. J Environ Sci Health B 2013;48:302-7.

[280] Wood WF, Shaffer TB, Kubo A. Volatile ketones from interdigital glands of black-tailed deer, *Odocoileus hemionus columbianus.* J Chem Ecol 1995;21:1401-8.

[281] Braga YF, Grangeiro TB, Freire EA, Lopes HL, Bezerra JN, Andrade-Neto M, et al. Insecticidal activity of 2-tridecanone against the cowpea weevil *Callosobruchus maculatus* (Coleoptera: Bruchidae). An Acad Bras Cienc 2007;79:35-9.

[282] Williams WG, Kennedy GG, Yamamoto RT, Thacker JD, Bordner J. 2-tridecanone: a naturally occurring insecticide from the wild tomato *Lycopersicon hirsutum* f. *glabratum*. Science 1980;207:888-9.

[283] Soto MJ, Fernández-Pascual M, Sanjuan J, Olivares J. A fadD mutant of *Sinorhizobium meliloti* shows multicellular swarming migration and is impaired in nodulation efficiency on alfalfa roots. Mol Microbiol 2002;43:371-82.

[284] Soto Misffut MJ, Nogales Díaz J, Olivares Pascual J, Sanjuan Pinilla J. Método para prevenir y/o controlar infecciones bacterianas. In: CSIC, editor. Spain2014.

[285] Cornelis P, Anjaiah V, Koedam N, Delfosse P, Jacques P, Thonart P, et al. Stability, frequency and multiplicity of transposon insertions in the pyoverdine region in the chromosomes of different fluorescent pseudomonads. J Gen Microbiol 1992;138:1337-43.

[286] Karudugamuwa JL. Media for study of growth kinetics and envelope properties of iron-deprived bacteria. J Clin Microbiol 1987;25:849-55.

[287] Rashid MH, Kornberg A. Inorganic polyphosphate is needed for swimming, swarming and twitching motilities of *Pseudomonas aeruginosa*. Proc Natl Acad Sci U S A 2000;97:4885-90.

[288] Grant SG, Jessee J, Bloom FR, Hanahan D. Differential plasmid rescue from transgenic mouse DNAs into *Escherichia coli* methylation-restriction mutants. Proc Natl Acad Sci U S A 1990;87:4645-9.

[289] Simon R, Priefer U, Pehle A. A broad host range system for in vitro genetic engineering: transposon mutagenesis in Gram-negative bacteria. Nat Biotechnol 1983;1:784-90.

[290] Liu Y-C. Understanding chronic inflammatory diseases in the human lung: the cystic fibrosis and idiopathic pulmonary fibrosis paradigms: The University of Nottingham; 2014.

[291] Holloway BW. Genetic recombination in *Pseudomonas aeruginosa*. J Gen Microbiol 1955;13:572-81.

[292] Hoegy F, Lee X, Noel S, Rognan D, Mislin GL, Reimmann C, et al. Stereospecificity of the siderophore pyochelin outer membrane transporters in fluorescent pseudomonads. J Biol Chem 2009;284:14949-57.

[293] Lopez-Medina E, Fan D, Coughlin LA, Ho EX, Lamont IL, Reimmann C, et al. *Candida albicans* inhibits *Pseudomonas aeruginosa* virulence through suppression of pyochelin and pyoverdine biosynthesis. PLoS Pathog 2015;11:e1005129.

[294] Chen Y. Fatty acid signalling in *Pseudomonas aeruginosa*: The University of Nottingham; 2014.

[295] Rahme LG, Stevens EJ, Wolfort SF, Shao J, Tompkins RG, Ausubel FM. Common virulence factors for bacterial pathogenicity in plants and animals. Science 1995;268:1899-902.

[296] Baba T, Bae T, Schneewind O, Takeuchi F, Hiramatsu K. Genome sequence of *Staphylococcus aureus* strain Newman and comparative analysis of staphylococcal genomes: polymorphism and evolution of two major pathogenicity islands. J Bacteriol 2008;190:300-10.

[297] Higgins S. Regulation of phenazine biosynthesis by quorum sensing in *Pseudomonas aeruginosa*: a systems biology approach: The University of Nottingham; 2014.

[298] Alting-Mees MA, Short JM. pBluescript II: gene mapping vectors. Nucleic Acids Res 1989;17:9494.

[299] Rybtke MT, Borlee BR, Murakami K, Irie Y, Hentzer M, Nielsen TE, et al. Fluorescence-based reporter for gauging cyclic di-GMP levels in *Pseudomonas aeruginosa*. Appl Environ Microbiol 2012;78:5060-9.

[300] Hoang TT, Karkhoff-Schweizer RR, Kutchma AJ, Schweizer HP. A broad-host-range Flp-FRT recombination system for site-specific excision of chromosomally-located DNA sequences: application for isolation of unmarked *Pseudomonas aeruginosa* mutants. Gene 1998;212:77-86.

[301] Voisard C, Bull CT, Keel C, Laville J, Maurhofer M, Schnider U, et al. Biocontrol of root diseases by *Pseudomonas fluorescens* CHA0: current concepts and experimental approaches. In: O'Gara F, Dowling D, Boesten B, editors. Molecular ecology of rhizosphere microorganisms: biotechnology and the release of GMOs. Weinheim, Germany: Wiley-VCH Verlag GmbH; 1994. p. 67-89.

[302] Heeb S, Blumer C, Haas D. Regulatory RNA as mediator in GacA/RsmA-dependent global control of exoproduct formation in *Pseudomonas fluorescens* CHA0. J Bacteriol 2002;184:1046-56.

[303] Hoang TT, Kutchma AJ, Becher A, Schweizer HP. Integration-proficient plasmids for *Pseudomonas aeruginosa*, site-specific integration and use for engineering of reporter and expression strains. Plasmid 2000;43:59-72.

[304] Becher A, Schweizer HP. Integration-proficient *Pseudomonas aeruginosa* vectors for isolation of single-copy chromosomal *lacZ* and *lux* gene fusions. BioTechniques 2000;29:948-50, 52.

[305] Schweizer HP. *Escherichia-Pseudomonas* shuttle vectors derived from pUC18/19. Gene 1991;97:109-21.

[306] Bao Y, Lies DP, Fu H, Roberts GP. An improved Tn7-based system for the single-copy insertion of cloned genes into chromosomes of Gram-negative bacteria. Gene 1991;109:167-8.

[307] Sambrook J, Fritsch EF, Maniatis T. Molecular cloning: a laboratory manual. 2nd edition ed: Cold Spring Harbor Laboratory Press; 1989.

[308] Fletcher MP, Diggle SP, Crusz SA, Chhabra SR, Cámara M, Williams P. A dual biosensor for 2-alkyl-4-quinolone quorum-sensing signal molecules. Environ Microbiol 2007;9:2683-93.

[309] Gay P, Le Coq D, Steinmetz M, Berkelman T, Kado CI. Positive selection procedure for entrapment of insertion sequence elements in Gram-negative bacteria. J Bacteriol 1985;164:918-21.

[310] Mortazavi A, Williams BA, McCue K, Schaeffer L, Wold B. Mapping and quantifying mammalian transcriptomes by RNA-Seq. Nat Methods 2008;5:621-8.

[311] Anders S, Huber W. Differencial expression analysis for sequence count data. Genome Biology 2010;11:R106.

[312] Baggerly KA, Deng L, Morris JS, Aldaz CM. Differential expression in SAGE: accounting for normal between-library variation. Bioinformatics 2003;19:1477-83.

[313] Fang Z, Martin J, Wang Z. Statistical methods for identifying differentially expressed genes in RNA-Seq experiments. Cell Biosci 2012;2:26.

[314] Oliveros JC. Venny. An interactive tool for comparing lists with Venn's diagrams. http://bioinfogp.cnb.csic.es/tools/venny/index.html. 2007.

[315] Winsor GL, Griffiths EJ, Lo R, Dhillon BK, Shay JA, Brinkman FS. Enhanced annotations and features for comparing thousands of *Pseudomonas* genomes in the *Pseudomonas* Genome Database. Nucleic Acids Res 2016;44:D646-53.

[316] Galperin MY, Makarova KS, Wolf YI, Koonin EV. Expanded microbial genome coverage and improved protein family annotation in the COG database. Nucleic Acids Res 2015;43:D261-9.

[317] Caballero AR, Moreau JM, Engel LS, Marquart ME, Hill JM, O'Callaghan RJ. *Pseudomonas aeruginosa* protease IV enzyme assays and comparison to other *Pseudomonas* proteases. Anal Biochem 2001;290:330-7.

[318] Christensen G, Simpson W, Younger J, Baddour L, Barrett F, Melton D, et al. Adherence of cogaulate-negative staphylococci to plastic tissue culture plates: a quantitative model for the adherence of staphylococci to medical devices. J Clin Microbiol 1985;22:996-1006.

[319] Jurcisek JA, Dickson AC, Bruggeman ME, Bakaletz LO. *In vitro* biofilm formation in an 8-well chamber slide. J Vis Exp 2011.

[320] Conant CG, Schwartz MA, Ionescu-Zanetti C. Well plate-coupled microfluidic devices designed for facile image-based cell adhesion and transmigration assays. J Biomol Screen 2010;15:102-6.

[321] Essar DW, Eberly L, Hadero A, Crawford IP. Identification and characterization of genes for a second anthranilate synthase in *Pseudomonas aeruginosa*: interchangeability of the two anthranilate synthases and evolutionary implications. J Bacteriol 1990;172:884-900.

[322] ACD. ACD/ChemSketch v 2.5. 2.5 ed. Toronto, On, Canada: www.acdlabs.com; 2015.

[323] Wittgens A, Tiso T, Arndt TT, Wenk P, Hemmerich J, Muller C, et al. Growth independent rhamnolipid production from glucose using the non-pathogenic *Pseudomonas putida* KT2440. Microb Cell Fact 2011;10:80.

[324] Fletcher MP, Diggle SP, Cámara M, Williams P. Biosensor-based assays for PQS, HHQ and related 2-alkyl-4-quinolone quorum sensing signal molecules. Nat Protoc 2007;2:1254-62.

[325] Heyd M, Kohnert A, Tan TH, Nusser M, Kirschhofer F, Brenner-Weiss G, et al. Development and trends of biosurfactant analysis and purification using rhamnolipids as an example. Anal Bioanal Chem 2008;391:1579-90.

[326] Lépine F, Déziel E, Milot S, Villemur R. Liquid chromatographic/mass spectrometric detection of the 3-(3-hydroxyalkanoyloxy) alkanoic acid precursors of rhamnolipids in *Pseudomonas aeruginosa* cultures. J Mass Spectrom 2002;37:41-6.

[327] Ochsner UA, Hembach T, Fiechter A. Production of rhamnolipid biosurfactants. Adv Biochem Eng Biotechnol 1996;53:89-118.

[328] Schultz J, Milpetz F, Bork P, Ponting CP. SMART, a simple modular architecture research tool: identification of signaling domains. Proc Natl Acad Sci U S A 1998;95:5857-64.

[329] Letunic I, Doerks T, Bork P. SMART: recent updates, new developments and status in 2015. Nucleic Acids Res 2015;43:D257-60.

[330] Sievers F, Wilm A, Dineen D, Gibson TJ, Karplus K, Li W, et al. Fast, scalable generation of high-quality protein multiple sequence alignments using Clustal Omega. Mol Syst Biol 2011;7:539.

[331] Roy A, Kucukural A, Zhang Y. I-TASSER: a unified platform for automated protein structure and function prediction. Nat Protoc 2010;5:725-38.

[332] Yang J, Yan R, Roy A, Xu D, Poisson J, Zhang Y. The I-TASSER Suite: protein structure and function prediction. Nat Methods 2015;12:7-8.

[333] Zhang Y. I-TASSER server for protein 3D structure prediction. BMC Bioinformatics 2008;9:40.

[334] Schneider CA, Rasband WS, Eliceiri KW. NIH Image to ImageJ: 25 years of image analysis. Nat Methods 2012;9:671-5.

[335] Heydorn A, Nielsen AT, Hentzer M, Sternberg C, Givskov M, Ersboll BK, et al. Quantification of biofilm structures by the novel computer program COMSTAT. Microbiology 2000;146 (Pt 10):2395-407.

[336] Vorregaard M. Comstat2 - a modern 3D image analysis environment for biofilms: Technical University of Denmark; 2008.

[337] Chatterjee S, Sonti RV. *rpfF* mutants of *Xanthomonas oryzae* pv. *oryzae* are deficient for virulence and growth under low iron conditions. Mol Plant Microbe Interact 2002;15:463-71.

[338] Thowthampitak J, Shaffer BT, Prathuangwong S, Loper JE. Role of *rpfF* in virulence and exoenzyme production of *Xanthomonas axonopodis* pv. *glycines*, the causal agent of bacterial pustule of soybean. Phytopathology 2008;98:1252-60.

[339] Barel V, Chalupowicz L, Barash I, Sharabani G, Reuven M, Dror O, et al. Virulence and *in planta* movement of *Xanthomonas hortorum* pv. *pelargonii* are affected by the diffusible signal factor (DSF)-dependent quorum sensing system. Mol Plant Pathol 2015;16:710-23.

[340] Scarpari LM, Lambais MR, Silva DS, Carraro DM, Carrer H. Expression of putative pathogenicity-related genes in *Xylella fastidiosa* grown at low and high cell density conditions *in vitro*. FEMS Microbiol Lett 2003;222:83-92.

[341] Suppiger A, Eshwar AK, Stephan R, Kaever V, Eberl L, Lehner A. The DSF type quorum sensing signalling system RpfF/R regulates diverse phenotypes in the opportunistic pathogen *Cronobacter*. Sci Rep 2016;6:18753.

[342] Zhou L, Wang XY, Sun S, Yang LC, Jiang BL, He YW. Identification and characterization of naturally occurring DSF-family quorum sensing signal turnover system in the phytopathogen *Xanthomonas*. Environ Microbiol 2015:4646-88.

[343] Huang TP, Wong AC. A cyclic AMP receptor protein-regulated cell-cell communication system mediates expression of a FecA homologue in *Stenotrophomonas maltophilia*. Appl Environ Microbiol 2007;73:5034-40.

[344] Zhou L, Yu Y, Chen X, Diab AA, Ruan L, He J, et al. The multiple DSF-family QS signals are synthesized from carbohydrate and branched-chain amino acids via the FAS elongation cycle. Sci Rep 2015;5:13294.

[345] Huang YJ, LiPuma JJ. The microbiome in cystic fibrosis. Clin Chest Med 2016;37:59-67.

[346] Tang JL, Liu YN, Barber CE, Dow JM, Wootton JC, Daniels MJ. Genetic and molecular analysis of a cluster of *rpf* genes involved in positive regulation of synthesis of extracellular enzymes and polysaccharide in *Xanthomonas campestris* pathovar *campestris*. Mol Gen Genet 1991;226:409-17.

[347] He YW, Xu M, Lin K, Ng YJ, Wen CM, Wang LH, et al. Genome scale analysis of diffusible signal factor regulon in *Xanthomonas campestris* pv. *campestris*: identification of novel cell-cell communication-dependent genes and functions. Mol Microbiol 2006;59:610-22.

[348] Crossman L, Dow JM. Biofilm formation and dispersal in *Xanthomonas campestris*. Microbes Infect 2004;6:623-9.

[349] Guo Y, Zhang Y, Li JL, Wang N. Diffusible signal factor-mediated quorum sensing plays a central role in coordinating gene expression of *Xanthomonas citri* subsp. *citri*. Mol Plant Microbe Interact 2012;25:165-79.

[350] Zhao Y, Qian G, Yin F, Fan J, Zhai Z, Liu C, et al. Proteomic analysis of the regulatory function of DSF-dependent quorum sensing in *Xanthomonas oryzae* pv. *oryzicola*. Microb Pathog 2011;50:48-55.

[351] Rott P, Fleites LA, Mensi I, Sheppard L, Daugrois JH, Dow JM, et al. The RpfCG two-component system negatively regulates the colonization of sugar cane stalks by *Xanthomonas albilineans*. Microbiology 2013;159:1149-59.

[352] Tang JL, Feng JX, Li QQ, Wen HX, Zhou DL, Wilson TJ, et al. Cloning and characterization of the *rpfC* gene of *Xanthomonas oryzae* pv. *oryzae:* involvement in exopolysaccharide production and virulence to rice. Mol Plant Microbe Interact 1996;9:664-6.

[353] Gudesblat GE, Torres PS, Vojnov AA. *Xanthomonas campestris* overcomes *Arabidopsis* stomatal innate immunity through a DSF cell-to-cell signal-regulated virulence factor. Plant Physiol 2009;149:1017-27.

[354] Xu J, Zhou L, Venturi V, He YW, Kojima M, Sakakibari H, et al. Phytohormone-mediated interkingdom signaling shapes the outcome of rice-*Xanthomonas oryzae* pv. *oryzae* interactions. BMC Plant Biol 2015;15:236-46.

[355] Ryan RP, McCarthy Y, Watt SA, Niehaus K, Dow JM. Intraspecies signaling involving the diffusible signal factor BDSF (*cis*-2-dodecenoic acid) influences virulence in *Burkholderia cenocepacia*. J Bacteriol 2009;191:5013-9.

[356] McCarthy Y, Yang L, Twomey KB, Sass A, Tolker-Nielsen T, Mahenthiralingam E, et al. A sensor kinase recognizing the cell-cell signal BDSF (*cis*-2-dodecenoic acid) regulates virulence in *Burkholderia cenocepacia*. Mol Microbiol 2010;77:1220-36.

[357] Malamud F, Torres PS, Roeschlin R, Rigano LA, Enrique R, Bonomi HR, et al. The *Xanthomonas axonopodis* pv. *citri* flagellum is required for mature biofilm and canker development. Microbiology 2011;157:819-29.

[358] Dow JM, Crossman L, Findlay K, He Y, Feng J, Tang J. Biofilm dispersal in *Xanthomonas campestris* is controlled by cell-cell signaling an is required for full virulence to plants. PNAS 2003;100:10995-1000.

[359] Tao F, Swarup S, Zhang LH. Quorum sensing modulation of a putative glycosyltransferase gene cluster essential for *Xanthomonas campestris* biofilm formation. Environ Microbiol 2010;12:3159-70.

[360] Mensi I, Daugrois JH, Pieretti I, Gargani D, Fleites LA, Noell J, et al. Surface polysaccharides and quorum-sensing are involved in attachment

and survival of *Xanthomonas albilineans* on sugarcane leaves. Mol Plant Pathol 2015:236-46.

[361] Rai R, Ranjan M, Pradhan BB, Chatterjee S. Atypical regulation of virulence-associated functions by a diffusible signal factor in *Xanthomonas oryzae* pv. *oryzae*. Mol Plant Microbe Interact 2012;25:789-801.

[362] Ionescu M, Zaini PA, Baccari C, Tran S, da Silva AM, Lindow SE. *Xylella fastidiosa* outer membrane vesicles modulate plant colonization by blocking attachment to surfaces. Proc Natl Acad Sci U S A 2014;111:E3910-8.

[363] Rahmani-Badi A, Sepehr S, Mohammadi P, Soudi MR, Babaie-Naiej H, Fallahi H. A combination of *cis*-2-decenoic acid and antibiotics eradicates pre-established catheter-associated biofilms. J Med Microbiol 2014:1655-61.

[364] Rahmani-Badi A, Sepehr S, Fallahi H, Heidari-Keshel S. Dissection of the *cis*-2-decenoic acid signaling network in *Pseudomonas aeruginosa* using microarray technique. Front Microbiol 2015;6:383.

[365] Sepehr S, Rahmani-Badi A, Babaie-Naiej H, Soudi MR. Unsaturated fatty acid, *cis*-2-decenoic acid, in combination with disifectants or antibiotics removes pre-established biofilms formed by food-related bacteria. PloS one 2014;9:e101677.

[366] Villa F, Pitts B, Stewart PS, Giussani B, Roncoroni S, Albanese D, et al. Efficacy of zosteric acid sodium salt on the yeast biofilm model *Candida albicans*. Microb Ecol 2011;62:584-98.

[367] He YW, Ng AY, Xu M, Lin K, Wang LH, Dong YH, et al. *Xanthomonas campestris* cell-cell communication involves a putative nucleotide receptor protein Clp and a hierarchical signalling network. Mol Microbiol 2007;64:281-92.

[368] Rai R, Javvadi S, Chatterjee S. Cell-cell signalling promotes ferric iron uptake in *Xanthomonas oryzae* pv. *oryzicola* that contribute to its virulence and growth inside rice. Mol Microbiol 2015;96:708-27.

[369] Twomey KB, O'Connell OJ, McCarthy Y, Dow JM, O'Toole GA, Plant BJ, et al. Bacterial *cis*-2-unsaturated fatty acids found in the cystic fibrosis airway modulate virulence and persistence of *Pseudomonas aeruginosa*. ISME Journal 2012;6:939-50.

[370] Deng Y, Lim A, Lee J, Chen S, An S, Dong YH, et al. Diffusible signal factor (DSF) quorum sensing signal and structurally related molecules enhance the antimicrobial efficacy of antibiotics against some bacterial pathogens. BMC Microbiol 2014;14:51.

[371] Udine C, Brackman G, Bazzini S, Buroni S, Van Acker H, Pasca MR, et al. Phenotypic and genotypic characterisation of *Burkholderia cenocepacia* J2315 mutants affected in homoserine lactone and diffusible

signal factor-based quorum sensing systems suggests interplay between both types of systems. PloS one 2013;8:e55112.

[372] Deng Y, Lim A, Wang J, Zhou T, Chen S, Lee J, et al. *Cis*-2-dodecenoic acid quorum sensing system modulates *N*-acyl homoserine lactone production through RpfR and cyclic di-GMP turnover in *Burkholderia cenocepacia*. BMC Microbiol 2013;13:148.

[373] Deng Y, Boon C, Chen S, Lim A, Zhang LH. *Cis*-2-dodecenoic acid signal modulates virulence of *Pseudomonas aeruginosa* through interference with quorum sensing systems and T3SS. BMC Microbiol 2013;13:231.

[374] Zhu PL, Zhao S, Tang JL, Feng JX. The *rsmA*-like gene *rsmA*(*Xoo*) of *Xanthomonas oryzae* pv. *oryzae* regulates bacterial virulence and production of diffusible signal factor. Mol Plant Pathol 2011;12:227-37.

[375] Newman KL, Almeida RP, Purcell AH, Lindow SE. Cell-cell signaling controls *Xylella fastidiosa* interactions with both insects and plants. Proc Natl Acad Sci U S A 2004;101:1737-42.

[376] Lindow S, Newman K, Chatterjee S, Baccari C, Lavarone AT, Ionescu M. Production of *Xylella fastidiosa* diffusible signal factor in transgenic grape causes pathogen confusion and reduction in severity of Pierce's disease. Mol Plant Microbe Interact 2014;27:244-54.

[377] Caserta R, Picchi SC, Takita MA, Tomaz JP, Pereira WE, Machado MA, et al. Expression of *Xylella fastidiosa* RpfF in citrus disrupts signaling in *Xanthomonas citri* subsp. *citri* and thereby its virulence. Mol Plant Microbe Interact 2014;27:1241-52.

[378] Alavi P, Muller H, Cardinale M, Zachow C, Sánchez MB, Martínez JL, et al. The DSF quorum sensing system controls the positive influence of *Stenotrophomonas maltophilia* on plants. PloS one 2013;8:e67103.

[379] Platts A, Krawetz S. Tools and approaches for an end-to-end expression array analysis. In: Krawetz S, editor. Bioinformatics for systems biology: Springer Science & Business Media; 2009.

[380] Amari DT, Marques CN, Davies DG. The putative enoyl-coenzyme A hydratase *DspI* is required for production of the *Pseudomonas aeruginosa* biofilm dispersion autoinducer *cis*-2-decenoic acid. J Bacteriol 2013;195:4600-10.

[381] An SQ, Febrer M, McCarthy Y, Tang DJ, Clissold L, Kaithakottil G, et al. High-resolution transcriptional analysis of the regulatory influence of cell-to-cell signalling reveals novel genes that contribute to *Xanthomonas* phytopathogenesis. Mol Microbiol 2013;88:1058-69.

[382] Barbier M, Damron FH, Bielecki P, Suarez-Diez M, Puchalka J, Alberti S, et al. From the environment to the host: re-wiring of the transcriptome of *Pseudomonas aeruginosa* from 22 degrees C to 37 degrees C. PloS one 2014;9:e89941.

[383] Rahmani-Badi A, Sepehr S, Babaie-Naiej H. A combination of *cis*-2-decenoic acid and chlorhexidine removes dental plaque. Arch Oral Biol 2015;60:1655-61.

[384] Newell PD, Yoshioka S, Hvorecny KL, Monds RD, O'Toole GA. Systematic analysis of diguanylate cyclases that promote biofilm formation by *Pseudomonas fluorescens* Pf0-1. J Bacteriol 2011;193:4685-98.

[385] Ritchings BW, Almira EC, Lory S, Ramphal R. Cloning and phenotypic characterization of *fleS* and *fleR*, new response regulators of *Pseudomonas aeruginosa* which regulate motility and adhesion to mucin. Infect Immun 1995;63:4868-75.

[386] Déziel E, Lépine F, Milot S, Villemur R. RhlA is required for the production of a novel biosurfactant promoting swarming motility in *Pseudomonas aeruginosa*: 3-(3-hydroxyalkanoyloxy) alkanoic acids (HAAs), the precursors of rhamnolipids. Microbiology-Sgm 2003;149:2005-13.

[387] Soneson C, Delorenzi M. A comparison of methods for differential expression analysis of RNA-seq data. BMC Bioinformatics 2013;14:91.

[388] Tielker D, Hacker S, Loris R, Strathmann M, Wingender J, Wilhelm S, et al. *Pseudomonas aeruginosa* lectin LecB is located in the outer membrane and is involved in biofilm formation. Microbiology-Sgm 2005;151:1313-23.

[389] Jain M, Ramirez D, Seshadri R, Cullina JF, Powers CA, Schulert GS, et al. Type III secretion phenotypes of *Pseudomonas aeruginosa* strains change during infection of individuals with cystic fibrosis. J Clin Microbiol 2004;42:5229-37.

[390] Whitney JC, Beck CM, Goo YA, Russell AB, Harding BN, De Leon JA, et al. Genetically distinct pathways guide effector export through the type VI secretion system. Mol Microbiol 2014;92:529-42.

[391] Ma L, Conover M, Lu H, Parsek MR, Bayles K, Wozniak DJ. Assembly and development of the *Pseudomonas aeruginosa* biofilm matrix. PLoS Pathog 2009;5:e1000354.

[392] Stoodley P, Dodds I, Boyle JD, Lappin-Scott HM. Influence of hydrodynamics and nutrients on biofilm structure. J Appl Microbiol 1998;85 Suppl 1:19S-28S.

[393] Klausen M, Heydorn A, Ragas P, Lambertsen L, Aaes-Jørgensen A, Molin S, et al. Biofilm formation by *Pseudomonas aeruginosa* wild type, flagella and type IV pili mutants. Mol Microbiol 2003;48:1511-24.

[394] Brandenburg KS, Rodriguez KJ, McAnulty JF, Murphy CJ, Abbott NL, Schurr MJ, et al. Tryptophan inhibits biofilm formation by *Pseudomonas aeruginosa*. Antimicrob Agents Chemother 2013;57:1921-5.

[395] Bernier SP, Ha DG, Khan W, Merritt JH, O'Toole GA. Modulation of *Pseudomonas aeruginosa* surface-associated group behaviors by individual amino acids through c-di-GMP signaling. Res Microbiol 2011;162:680-8.

[396] Banin E, Brady KM, Greenberg EP. Chelator-induced dispersal and killing of *Pseudomonas aeruginosa* cells in a biofilm. Appl Environ Microbiol 2006;72:2064-9.

[397] Ha DG, O'Toole GA. c-di-GMP and its effects on biofilm formation and dispersion: a *Pseudomonas aeruginosa* review. Microbiol Spectr 2015;3:MB-0003-2014.

[398] Son MS, Matthews WJ, Jr., Kang Y, Nguyen DT, Hoang TT. *In vivo* evidence of *Pseudomonas aeruginosa* nutrient acquisition and pathogenesis in the lungs of cystic fibrosis patients. Infect Immun 2007;75:5313-24.

[399] Duan K, Surette MG. Environmental regulation of *Pseudomonas aeruginosa* PAO1 Las and Rhl quorum-sensing systems. J Bacteriol 2007;189:4827-36.

[400] Travis J, Potempa J. Bacterial proteinases as targets for the development of second-generation antibiotics. Biochim Biophys Acta 2000;1477:35-50.

[401] Carty NL, Layland N, Colmer-Hamood JA, Calfee MW, Pesci EC, Hamood AN. PtxR modulates the expression of QS-controlled virulence factors in the *Pseudomonas aeruginosa* strain PAO1. Mol Microbiol 2006;61:782-94.

[402] Hamed RB, Batchelar ET, Clifton IJ, Schofield CJ. Mechanisms and structures of crotonase superfamily enzymes- how nature controls enolate and oxyanion reactivity. Cell Mol Life Sci 2008;65:2507-27.

[403] Bi H, Christensen QH, Feng Y, Wang H, Cronan JE. The *Burkholderia cenocepacia* BDSF quorum sensing fatty acid is synthesized by a bifunctional crotonase homologue having both dehydratase and thioesterase activities. Mol Microbiol 2012;83:840-55.

[404] Dow JM, Daniels MJ. *Xylella* genomics and bacterial pathogenicity to plants. Yeast 2000;17:263-71.

[405] Cheng Z, He YW, Lim SC, Qamra R, Walsh MA, Zhang LH, et al. Structural basis of the sensor-synthase interaction in autoinduction of the quorum sensing signal DSF biosynthesis. Structure 2010;18:1199-209.

[406] Bi H, Yu Y, Dong H, Wang H, Cronan JE. *Xanthomonas campestris* RpfB is a fatty acyl-CoA ligase required to counteract the thioesterase activity of the RpfF diffusible signal factor (DSF) synthase. Mol Microbiol 2014;93:262-75.

[407] Andrade MO, Alegria MC, Guzzo CR, Docena C, Rosa MC, Ramos CH, et al. The HD-GYP domain of RpfG mediates a direct linkage between the Rpf quorum-sensing pathway and a subset of diguanylate cyclase proteins in the phytopathogen *Xanthomonas axonopodis* pv *citri*. Mol Microbiol 2006;62:537-51.

[408] He YW, Wang C, Zhou L, Song H, Dow JM, Zhang LH. Dual signaling functions of the hybrid sensor kinase RpfC of *Xanthomonas campestris* involve either phosphorelay or receiver domain-protein interaction. J Biol Chem 2006;281:33414-21.

[409] Chatterjee S, Wistrom C, Lindow SE. A cell-cell signaling sensor is required for virulence and insect transmission of *Xylella fastidiosa*. Proc Natl Acad Sci U S A 2008;105:2670-5.

[410] Dow M. Diversification of the function of cell-to-cell signaling in regulation of virulence within plant pathogenic xanthomonads. Sci Signal 2008;1:pe23.

[411] An SQ, Allan JH, McCarthy Y, Febrer M, Dow JM, Ryan RP. The PAS domain-containing histidine kinase RpfS is a second sensor for the diffusible signal factor of *Xanthomonas campestris*. Mol Microbiol 2014;92:586-97.

[412] Green LK, La Flamme AC, Ackerley DF. *Pseudomonas aeruginosa* MdaB and WrbA are water-soluble two-electron quinone oxidoreductases with the potential to defend against oxidative stress. J Microbiol 2014;52:771-7.

[413] Yang Z, Lu CD. Functional genomics enables identification of genes of the arginine transaminase pathway in *Pseudomonas aeruginosa*. J Bacteriol 2007;189:3945-53.

[414] Illergard K, Ardell DH, Elofsson A. Structure is three to ten times more conserved than sequence- a study of structural response in protein cores. Proteins 2009;77:499-508.

[415] Thornton JM, Todd AE, Milburn D, Borkakoti N, Orengo CA. From structure to function: approaches and limitations. Nat Struct Biol 2000;7 Suppl:991-4.

[416] Mern DS, Ha SW, Khodaverdi V, Gliese N, Gorisch H. A complex regulatory network controls aerobic ethanol oxidation in *Pseudomonas aeruginosa*: indication of four levels of sensor kinases and response regulators. Microbiology 2010;156:1505-16.

[417] Chrzanowski L, Lawniczak L, Czaczyk K. Why do microorganisms produce rhamnolipids? World J Microbiol Biotechnol 2012;28:401-19.

[418] Pessi G, Williams F, Hindle Z, Heurlier K, Holden MT, Cámara M, et al. The global posttranscriptional regulator RsmA modulates production of virulence determinants and *N*-acylhomoserine lactones in *Pseudomonas aeruginosa*. J Bacteriol 2001;183:6676-83.

[419] Gerstein M, Hegyi H, Lin J, Qian J, Luscombe N, Johnson T, et al. Computational proteomics: genome-scale studies of protein function, structure, and evolution. Talk at Harvard 2011.

[420] Feinbaum RL, Urbach JM, Liberati NT, Djonovic S, Adonizio A, A. C, et al. Virulence-related genes using a *Caenorhabditis elegans* infection model. PLoS Pathog 2012;8:e1002813.

[421] Fetrow JS, Siew N, Di Gennaro JA, Martinez-Yamout M, Dyson HJ, Skolnick J. Genomic-scale comparison of sequence- and structure-based methods of function prediction: does structure provide additional insight? Protein Sci 2001;10:1005-14.

[422] Kulasekara HD, Ventre I, Kulasekara BR, Lazdunski A, Filloux A, Lory S. A novel two-component system controls the expression of *Pseudomonas aeruginosa* fimbrial *cup* genes. Mol Microbiol 2005;55:368-80.

[423] Sivaneson M, Mikkelsen H, Ventre I, Bordi C, Filloux A. Two-component regulatory systems in *Pseudomonas aeruginosa*: an intricate network mediating fimbrial and efflux pump gene expression. Mol Microbiol 2011;79:1353-66.

[424] Ventre I, Goodman AL, Vallet-Gely I, Vasseur P, Soscia C, Molin S, et al. Multiple sensors control reciprocal expression of *Pseudomonas aeruginosa* regulatory RNA and virulence genes. Proc Natl Acad Sci U S A 2006;103:171-6.

[425] Choy WK, Zhou L, Syn CK, Zhang LH, Swarup S. MorA defines a new class of regulators affecting flagellar development and biofilm formation in diverse *Pseudomonas* species. J Bacteriol 2004;186:7221-8.

[426] Hay ID, Remminghorst U, Rehm BH. MucR, a novel membrane-associated regulator of alginate biosynthesis in *Pseudomonas aeruginosa*. Appl Environ Microbiol 2009;75:1110-20.

[427] Roy AB, Petrova OE, Sauer K. The phosphodiesterase DipA (PA5017) is essential for *Pseudomonas aeruginosa* biofilm dispersion. J Bacteriol 2012;194:2904-15.

[428] Li Y, Heine S, Entian M, Sauer K, Frankenberg-Dinkel N. NO-induced biofilm dispersion in *Pseudomonas aeruginosa* is mediated by an MHYT domain-coupled phosphodiesterase. J Bacteriol 2013;195:3531-42.

[429] Wagner VE, Bushnell D, Passador L, Brooks AI, Iglewski BH. Microarray analysis of *Pseudomonas aeruginosa* quorum-sensing regulons: effects of growth phase and environment. J Bacteriol 2003;185:2080-95.

[430] Barrett T, Wilhite SE, Ledoux P, Evangelista C, Kim IF, Tomashevsky M, et al. NCBI GEO: archive for functional genomics data sets -update. Nucleic Acids Res 2013;41:D991-5.

[431] Edgar R. Gene Expression Omnibus: NCBI gene expression and hybridization array data repository. Nucleic Acids Res 2002;30:207-10.

[432] Gallagher LA, Manoil C. *Pseudomonas aeruginosa* PAO1 kills *Caenorhabditis elegans* by cyanide poisoning. J Bacteriol 2001;183:6207-14.

[433] Antonious GF, Snyder JC. Repellency and oviposition deterrence of wild tomato leaf extracts to spider mites, *Tetranychus urticae Koch*. J Environ Sci Health B 2015;50:667-73.

[434] Liu XC, Liu Q, Chen XB, Zhou L, Liu ZL. Larvicidal activity of the essential oil from *Tetradium glabrifolium* fruits and its constituents against *Aedes albopictus*. Pest Manag Sci 2015;71:1582-6.

[435] Agnaniet H, Makani T, Bikanga R, Obame LC, Lebibi J, Menut C. Chemical composition and antimicrobial activity of the essential oils of leaves, roots and bark of *Glossocalyx staudtii*. Nat Prod Commun 2009;4:1127-32.

[436] Antonious GF, Kamminga K, Snyder JC. Wild tomato leaf extracts for spider mite and cowpea aphid control. J Environ Sci Health B 2014;49:527-31.

[437] Kumar V, Reddy SG, Chauhan U, Kumar N, Singh B. Chemical composition and larvicidal activity of *Zanthoxylum armatum* against diamondback moth, *Plutella xylostella*. Nat Prod Res 2015:689-92.

[438] Zhang QH, McDonald DL, Hoover DR, Aldrich JR, Schneidmiller RG. North American invasion of the tawny crazy ant (*Nylanderia fulva*) is enabled by pheromonal synergism from two separate glands. J Chem Ecol 2015;41:853-8.

[439] Chen J, Rashid T, Feng G, Zhao L, Oi D, Drees BB. Defensive chemicals of tawny crazy ants, *Nylanderia fulva* (Hymenoptera: Formicidae) and their toxicity to red imported fire ants, *Solenopsis invicta* (Hymenoptera: Formicidae). Toxicon 2013;76:160-6.

[440] McDaniel CA, Schmidt JO, Howard RW. Mandibular gland secretions of the male beewolves *Philanthus crabroniformis*, *P. barbatus*, and *P. pulcher* (Hymenoptera: Sphecidae). J Chem Ecol 1992;18:27-37.

[441] Schorkopf DL, Hrncir M, Mateus S, Zucchi R, Schmidt VM, Barth FG. Mandibular gland secretions of meliponine worker bees: further evidence for their role in interspecific and intraspecific defence and aggression and against their role in food source signalling. J Exp Biol 2009;212:1153-62.

[442] Moats RA, Bartelt RJ, Jackson LL, Schaner AM. Ester and ketone components of aggregation pheromone of *Drosophila hydei* (Diptera: Drosophilidae). J Chem Ecol 1987;13:451-62.

[443] Schaner AM, Jackson LL. (Z)-10-Heptadecen-2-one and other 2-ketones in the aggregation pheromone blend of *Drosophila martensis*, *D. buzzatii*, and *D. serido*. J Chem Ecol 1992;18:53-64.

[444] Innocent E, Gikonyo NK, Nkunya MH. Repellency property of long chain aliphatic methyl ketones against *Anopheles gambiae* s.s. Tanzan J Health Res 2008;10:50-4.

[445] Kimps NW, Bissinger BW, Apperson CS, Sonenshine DE, Roe RM. First report of the repellency of 2-tridecanone against ticks. Med Vet Entomol 2011;25:202-8.

[446] Soini HA, Schrock SE, Bruce KE, Wiesler D, Ketterson ED, Novotny MV. Seasonal variation in volatile compound profiles of preen gland secretions of the dark-eyed junco (*Junco hyemalis*). J Chem Ecol 2007;33:183-98.

[447] Yu K, Hamilton-Kemp TR, Archbold DD, Collins RW, Newman MC. Volatile compounds from *Escherichia coli* O157:H7 and their absorption by strawberry fruit. J Agric Food Chem 2000;48:413-7.

[448] Blom D, Fabbri C, Connor EC, Schiestl FP, Klauser DR, Boller T, et al. Production of plant growth modulating volatiles is widespread among rhizosphere bacteria and strongly depends on culture conditions. Environ Microbiol 2011;13:3047-58.

[449] Plotnikova JM, Rahme LG, Ausubel FM. Pathogenesis of the human opportunistic pathogen *Pseudomonas aeruginosa* PA14 in *Arabidopsis*. Plant Physiol 2000;124:1766-74.

[450] Bernabéu-Roda. Bases moleculares que gobiernan la movilidad swarming de *Sinorhizobium meliloti*: conexión con la formación de biopelículas y establecimiento de simbiosis: Universidad de Granada; 2014.

[451] Valverde C, Heeb S, Keel C, Haas D. RsmY, a small regulatory RNA, is required in concert with RsmZ for GacA-dependent expression of biocontrol traits in *Pseudomonas fluorescens* CHA0. Mol Microbiol 2003;50:1361-79.

[452] Brencic AM, K. A., McManus HR, Castang S, Mogno M, Dove SL, Lory S. The GacS/GacA signal transduction system of *Pseudomonas aeruginosa* acts exclusively through its control over the transcription of the RsmY and RsmZ regulatory small RNAs. Mol Microbiol 2009;73:434-45.

[453] Kirisits MJ, Parsek MR. Does *Pseudomonas aeruginosa* use intercellular signalling to build biofilm communities? Cell Microbiol 2006;8:1841-9.

[454] Morris JD, Hewitt JL, Wolfe LG, Kamatkar NG, Chapman SM, Diener JM, et al. Imaging and analysis of *Pseudomonas aeruginosa* swarming and rhamnolipid production. Appl Environ Microbiol 2011;77:8310-7.

[455] Forney FW, Markovetz AJ. Oxidative degradation of methyl ketones. II. Chemical pathway for degradation of 2-tridecanone by *Pseudomonas multivorans* and *Pseudomonas aeruginosa*. J Bacteriol 1968;96:1055-64.

[456] Deforet M, van Ditmarsch D, Carmona-Fontaine C, Xavier JB. Hyperswarming adaptations in a bacterium improve collective motility without enhancing single cell motility. Soft Matter 2014;10:2405-13.

[457] Oliveira AS, Kaizer MR, Azevedo MS, Ogliari FA, Cenci MS, Moraes RR. (Super)hydrophobic coating of orthodontic dental devices and reduction of early oral biofilm retention. Biomed Mater 2015;10:065004.

[458] Cheng W, Yang C, Ding X, Engler AC, Hedrick JL, Yang YY. Broad-spectrum antimicrobial/antifouling soft material coatings using poly(ethylenimine) as a tailorable scaffold. Biomacromolecules 2015;16:1967-77.

[459] Caiazza NC, Merritt JH, Brothers KM, O'Toole GA. Inverse regulation of biofilm formation and swarming motility by *Pseudomonas aeruginosa* PA14. J Bacteriol 2007;189:3603-12.

[460] Coggan KA, Wolfgang MC. Global regulatory pathways and cross-talk control *Pseudomonas aeruginosa* environmental lifestyle and virulence phenotype. Curr Issues Mol Biol 2012;14:47-70.

[461] Wang S, Yu S, Zhang Z, Wei Q, Yan L, Ai G, et al. Coordination of swarming motility, biosurfactant synthesis, and biofilm matrix exopolysaccharide production in *Pseudomonas aeruginosa*. Appl Environ Microbiol 2014;80:6724-32.

[462] O'Toole G, Kaplan HB, Kolter R. Biofilm formation as microbial development. Annu Rev Microbiol 2000;54:49-79.

[463] Ottow JC. Ecology, physiology, and genetics of fimbriae and pili. Annu Rev Microbiol 1975;29:79-108.

[464] Roine E, Nunn DN, Paulin L, Romantschuk M. Characterization of genes required for pilus expression in *Pseudomonas syringae* pathovar *phaseolicola*. J Bacteriol 1996;178:410-7.

[465] Roine E, Raineri DM, Romantschuk M, Wilson M, Nunn DN. Characterization of type IV pilus genes in *Pseudomonas syringae* pv. *tomato* DC3000. Mol Plant Microbe Interact 1998;11:1048-56.

[466] Taguchi F, Ichinose Y. Role of type IV pili in virulence of *Pseudomonas syringae* pv. *tabaci* 6605: correlation of motility, multidrug resistance, and HR-inducing activity on a nonhost plant. Mol Plant Microbe Interact 2011;24:1001-11.

[467] Whitchurch CB, Leech AJ, Young MD, Kennedy D, Sargent JL, Bertrand JJ, et al. Characterization of a complex chemosensory signal transduction system which controls twitching motility in *Pseudomonas aeruginosa*. Mol Microbiol 2004;52:873-93.

[468] Leech AJ, Mattick JS. Effect of site-specific mutations in different phosphotransfer domains of the chemosensory protein ChpA on *Pseudomonas aeruginosa* motility. J Bacteriol 2006;188:8479-86.

[469] Masduki A, Nakamura J, Ohga T, Umezaki R, Kato J, Ohtake H. Isolation and characterization of chemotaxis mutants and genes of *Pseudomonas aeruginosa*. J Bacteriol 1995;177:948-52.

[470] Kato J, Nakamura T, Kuroda A, Ohtake H. Cloning and characterization of chemotaxis genes in *Pseudomonas aeruginosa*. Biosci Biotechnol Biochem 1999;63:155-61.

[471] Mariconda S, Wang Q, Harshey RM. A mechanical role for the chemotaxis system in swarming motility. Mol Microbiol 2006;60:1590-602.

[472] Greck M, Platzer J, Sourjik V, Schmitt R. Analysis of a chemotaxis operon in *Rhizobium meliloti*. Mol Microbiol 1995;15:989-1000.

[473] Potvin E, Lehoux DE, Kukavica-Ibrulj I, Richard KL, Sanschagrin F, Lau GW, et al. In vivo functional genomics of *Pseudomonas aeruginosa* for high-throughput screening of new virulence factors and antibacterial targets. Environ Microbiol 2003;5:1294-308.

[474] Espinosa-Urgel M. Resident parking only: rhamnolipids maintain fluid channels in biofilms. J Bacteriol 2003;185:699-700.

[475] Williams P, Winzer K, Chan WC, Cámara M. Look who's talking: communication and quorum sensing in the bacterial world. Philos Trans R Soc Lond B Biol Sci 2007;362:1119-34.

[476] Dong YH, Wang LY, Zhang LH. Quorum-quenching microbial infections: mechanisms and implications. Philos Trans R Soc Lond B Biol Sci 2007;362:1201-11.

[477] Breidenstein EBM, Hancock REW. Armand-Frappier Outstanding Student Award — Role of ATP-dependent proteases in antibiotic resistance and virulence. Can J Microbiol 2012;59:1-8.

[478] Bleves S, Soscia C, Nogueira-Orlandi P, Lazdunski A, Filloux A. Quorum sensing negatively controls type III secretion regulon expression in *Pseudomonas aeruginosa* PAO1. J Bacteriol 2005;187:3898-902.

[479] Jennings JA, Courtney HS, Haggard WO. *Cis*-2-decenoic acid inhibits *S. aureus* growth and biofilm in vitro: a pilot study. Clin Orthop Relat Res 2012;470:2663-70.

[480] Suppiger A, Aguilar C, Eberl L. Evidence for the widespread production of DSF family signal molecules by members of the genus *Burkholderia* by the aid of novel biosensors. Environ Microbiol Rep 2015:38-44.

[481] Bjarnsholt T. The role of bacterial biofilms in chronic infections. APMIS Suppl 2013:1-51.

[482] Kou Y, Naqvi NI. Surface sensing and signaling networks in plant pathogenic fungi. Semin Cell Dev Biol 2016;57:84-92.

[483] O'Toole GA, Wong GC. Sensational biofilms: surface sensing in bacteria. Curr Opin Microbiol 2016;30:139-46.

[484] Franceschini A, Lin J, von Mering C, Jensen LJ. SVD-phy: improved prediction of protein functional associations through singular value decomposition of phylogenetic profiles. Bioinformatics 2016;32:1085-7.